SEISMIC DAMAGE ESTIMATION FOR 3D RC VERTICAL IRREGULAR BUILDINGS

A Thesis submitted to Gujarat Technological University

for the Award of

Doctor of Philosophy

In

Civil Engineering

by

Hemil Manharbhai Chauhan

189999912007

Under supervision of

Dr. Kaushal B. Parikh

GUJARAT TECHNOLOGICAL UNIVERSITY

AHMEDABAD

February - 2024

© Hemil Manharbhai Chauhan

DECLARATION

I declare that the thesis entitled **Seismic Damage Estimation for 3D RC Vertical Irregular Buildings** submitted by me for the degree of Doctor of Philosophy is the record of research work carried out by me during the period from December 2018 to November 2023 under the supervision of **Dr. Kaushal B. Parikh** and this has not formed the basis for the award of any degree, diploma, associate ship, fellowship, titles in this or any other University or other institution of higher learning.

I further declare that the material obtained from other sources has been duly acknowledged in the thesis. I shall be solely responsible for any plagiarism or other irregularities, if noticed in the thesis.

Signature of the Research Scholar: Date: 23- Feb-2024

Name of Research Scholar: **Hemil Manharbhai Chauhan**

Place: **Ahmedabad**

CERTIFICATE

I certify that the Work incorporated in the thesis **Seismic Damage Estimation for 3D RC Vertical Irregular Buildings** submitted by **Mr. Hemil Manharbhai Chauhan** (Enrolment no. 189999912007) was carried out by the candidate under my supervision/guidance.

To the best of my knowledge:

(i) The candidate has not submitted the same research work to any other institution for any degree/diploma, Associate ship, Fellowship or other similar titles

(ii) The thesis submitted is a record of original research work done by the Research Scholar during the period of study under my supervision, and

(iii) The thesis represents independent research work on the part of the Research Scholar.

Signature of Supervisor:  Date: 23- Feb-2024

Name of Supervisor: **Dr. Kaushal B. Parikh**

Place: **Dahod**

Course-work Completion Certificate

This is to certify that **Mr. Hemil Manharbhai Chauhan** enrolment no. is **189999912007** enrolled for PhD program in the Civil Engineering branch of Gujarat Technological University, Ahmedabad.

(Please tick the relevant option(s))

☐ He has been exempted from the course-work (successfully completed during M.Phil Course)

☐ He has been exempted from Research Methodology Course only (successfully completed during M.Phil Course)

☑ He has successfully completed the PhD course work for the partial requirement for the award of PhD Degree. His/ Her performance in the course work is as follows-

Grade Obtained in Research Methodology PH 001	Grade Obtained in Self-Study Course (core subject) PH 002
BC	**AA**

Supervisor's Sign

Dr. Kaushal B. Parikh

Originality Report Certificate

It is certified that PhD Thesis titled **Seismic Damage Estimation for 3D RC Vertical Irregular Buildings** by **Mr. Hemil Manharbhai Chauhan** has been examined by us. We undertake the following:

a) Thesis has significant new work / knowledge as compared already published or are under consideration to be published elsewhere. No sentence, equation, diagram, table, paragraph or section has been copied verbatim from previous Work unless it is placed under quotation marks and duly referenced.

b) The Work presented is original and own Work of the author (i.e., there is no plagiarism). No ideas, processes, results or words of others have been presented as Author own Work.

c) There is no fabrication of data or results which have been compiled / analysed.

d) There is no falsification by manipulating research materials, equipment or processes, or changing or omitting data or results such that the research is not accurately represented in the research record.

e) The thesis has been checked using **DrillBit (copy of originality report attached)** and found within limits as per GTU Plagiarism Policy and instructions issued from time to time (i.e., permitted similarity index <=10%).

Signature of the Research Scholar:  Date: 23- Feb-2024

Name of Research Scholar: **Mr. Hemil Manharbhai Chauhan**

Place: **Ahmedabad**

Signature of Supervisor:  Date: 23- Feb-2024

Name of Supervisor: **Dr. Kaushal B. Parikh**

Place: **Dahod**

DrillBit

DrillBit Similarity Report

4	66	A
SIMILARITY %	MATCHED SOURCES	GRADE

A-Satisfactory (0-10%)
B-Upgrade (11-40%)
C-Poor (41-60%)
D-Unacceptable (61-100%)

LOCATION	MATCHED DOMAIN	%	SOURCE TYPE
1	www.mdpi.com	<1	Internet Data
2	www.mdpi.com	<1	Internet Data
3	ceij.ut.ac.ir	<1	Publication
4	Likelihood Ratios for Glaucoma Diagnosis Using Spectral-Domain Optical Coherence by Lisboa-2013	<1	Publication
5	aanda.org	<1	Internet Data
6	moam.info	<1	Internet Data
7	scholar.sun.ac.za	<1	Publication
8	link.springer.com	<1	Internet Data
9	A Resilience and Robustness Oriented Design of Base-Isolated Structures The New by DallAsta-2020	<1	Publication
10	REPOSITORY - Submitted to Dibrugarh University on 2023-11-18 20-47	<1	Student Paper
11	www.mdpi.com	<1	Internet Data
12	journals.plos.org	<1	Publication
13	qdoc.tips	<1	Internet Data

Ph.D. Thesis Non-Exclusive License to GUJARAT TECHNOLOGICAL UNIVERSITY

In consideration of being a Research Scholar at Gujarat Technological University, and in the interests of the facilitation of research at the University and elsewhere, I, **Mr. Hemil Manharbhai Chauhan** having **189999912007** hereby grant a non- exclusive, royalty free and perpetual license to the University on the following terms:

a. GTU is permitted to archive, reproduce and distribute my thesis, in whole or in part, and/or my abstract, in whole or in part (referred to collectively as the "Work") anywhere in the world, for non-commercial purposes, in all forms of media;
b. GTU is permitted to authorize, sub-lease, sub-contract or procure any of the acts mentioned in paragraph (a);
c. GTU is authorized to submit the Work at any National / International Library, under the authority of their "Thesis Non-Exclusive License";
d. The Universal Copyright Notice (©) shall appear on all copies made under the authority of this license;
e. I undertake to submit my thesis, through my university, to any Library and Archives. Any abstract submitted with the thesis will be considered to form part of the thesis.
f. I represent that my thesis is my original Work, does not infringe any rights of others, including privacy rights, and that I have the right to make the grant conferred by this non-exclusive license.
g. If third party copyrighted material was included in my thesis for which, under the terms of the Copyright Act, written permission from the copyright owners is required, I have obtained such permission from the copyright owners to do the acts mentioned in paragraph (a) above for the full term of copyright protection.
h. I understand that the responsibility for the matter as mentioned in the paragraph (g) rests with the authors / me solely. In no case shall GTU have any liability for any acts / omissions / errors / copyright infringement from the publication of the said thesis or otherwise.
i. I retain copyright ownership and moral rights in my thesis, and may deal with the copyright in my thesis, in any way consistent with rights granted by me to my university in this non-exclusive license.

j. GTU logo shall not be used /printed in the book (in any manner whatsoever) being published or any promotional or marketing materials or any such similar documents.

k. The following statement shall be included appropriately and displayed prominently in the book or any material being published anywhere: “The content of the published work is part of the thesis submitted in partial fulfilment for the award of the degree of Ph.D. in Civil Engineering of the Gujarat Technological University”.

l. I further promise to inform any person to whom I may hereafter assign or license my copyright in my thesis of the rights granted by me to my university in this nonexclusive license. I shall keep GTU indemnified from any and all claims from the Publisher(s) or any third parties at all times resulting or arising from the publishing or use or intended use of the book / such similar document or its contents.

m. I am aware of and agree to accept the conditions and regulations of Ph.D. including all policy matters related to authorship and plagiarism.

Date: 23- Feb- 2024

Place: Ahmedabad

Signature of the Research Scholar

Recommendation of the Supervisor: **RECOMMENDED**

Signature of Supervisor

Thesis Approval Form

The viva-voce of the PhD Thesis submitted by **Shri Hemil Manharbhai Chauhan (189999912007)** entitled **Seismic Damage Estimation for 3D RC Vertical Irregular Buildings** was conducted on **23-February-2024 (Friday)** (Day and date) at Gujarat Technological University.

(Please tick any one of the following options)

☑ The performance of the candidate was satisfactory. We recommend that he/she be awarded the PhD degree.

☐ Any further modifications in research work recommended by the panel after 3 months from the date of first viva-voce upon request of the Supervisor or request of Independent Research Scholar after which viva-voce can be re-conducted by the same panel again.

(Briefly specify the modifications suggested by the panel)

☐ The performance of the candidate was unsatisfactory. We recommend that he/she Should not be awarded the PhD degree.

(The panel must give justifications for rejecting the research work)

Dr. Kaushal B. Parikh

Name and Signature of Supervisor with Seal

Dr. Katta Venkatramana

1) External Examiner

Dr. Manjeet Singh Hora

2) External Examiner

ABSTRACT

The current study introduces methods to estimating seismic damage to the unidirectional and bidirectional setback type of 3D RC irregular buildings across a range of time periods. These methodologies are used to calculate the amount of energy that was absorbed as well as the stiffness that was deteriorate and lateral drift that was increasing during seismic loads are applied. Analyses of characteristics such as height changes, aspect ratio changes in floor designs, and the application of acceleration, IS 1893, and mode, amongst other types of monotonic loads, are taken into account while assessing damage at critical points of structural members in RC buildings. Analyses are performed on critical positions on pushover curves, and damage indices that are based on energy, stiffness and drift have been compared with those that are based on deformation, strength and displacement, respectively. These three methods have offered acceptable and reliable results for estimating the damages to existing and/or prospective complex buildings at any given point on the pushover curve. This is because the pushover curve does not indicate the damage status at any given position on the curve. Every single one of the drift findings for every single one of the cases fits well within the tolerance limits of the criteria, and every single one of the building's performances is up to the level required to ensure the safety of the lives of people. The performance criteria has been achieved while the damage index, which is based on the computed stiffness, displays a value of about fifty percent. As a direct consequence of this, a structure that has a damage index that is higher than 50% will sustain more severe damage. Due to the fact that this study focuses just on irregular buildings with unidirectional setbacks, additional research is required to take into consideration several other types of architectural irregularities. The concept of soil-structure interaction may also be applied to determine the anticipated level of damage to a building's footings. This is done through studying the relationship between the soil and the structure.

Acknowledgement

I am incredibly grateful to everyone who has contributed for completing this PhD thesis on damage estimation in area of earthquake engineering.

First, I would like to give sincere gratitude towards my guide and mentor/supervisor, Dr. Kaushal B. Parikh, sir for his help, support, and motivation that he has given to me while doing the study. Their thoughtful comments and helpful feedback had been very useful to make this work enhanced.

I would also be very thankful to Dr. Devesh P. Soni sir and Dr. Jignesh A. Amin sir, who are on my doctoral progress committee, for their time, advice, and comments on my work. The thoughtful comments and ideas they provided have made this work a lot better.

I would like to thank my friends, Mr. Kamlesh Mehta and Dr. Nirav B. Umravia, for their motivation and anchorage throughout my research work. This list of acknowledgements can only capture a small fraction of the people who supported my work. I send my deepest thanks to all. Their help was invaluable to me as I pursued my doctorate. My wonderful wife Priyanka inspires me to strive for greater things in all areas of my life, and no words could ever adequately express my gratitude for her unwavering love, devotion, and scarification. I'd like to thank her for being as patience with me as I was with my study. I'd like to express my appreciation to my son Parshva, my parents, my elder brother, bhabhi and nephew Shrey, my in-laws, and my extended family for all the unconditional love, unwavering trust, and enthusiastic support they've given me throughout my research work.

A word of sincere thanks to the entire staff of the PhD section of university who provided me guidance and support to complete the documentation and assisted me in the conduct of Research Week, DPCs and Open Seminar.

Above all, I owe it all to Almighty Goddess (Khodiyar Maa) for giving me the positive energy, strength, wisdom and health to carry out and accomplish this research work, without blessing of goddess this study could not possible.

Hemil Manharbhai Chauhan

Table of Contents

List of figures

List of tables

CHAPTER 1 INRODUCTION

1.1 General

The structural system should be designed as a consequence to reduce the loss of lives and property. The main reason for structural damage is a loss of strength, stiffness, or ductility. Currently, buildings are built using the IS (Indian standard) code for force based seismic design approach, which means that forces and displacements within elastic limits are computed. Reinforced concrete buildings in earthquake prone areas stand the risk of being damaged or collapsing as a result of seismic instability during the unexpected event [1].The stiffness of the members at the beginning is used to estimate how the design pressures will be distributed among the different structural elements. No matter what kind of forces were used or what reinforcement details were finalised, the stiffness of a part could not be known until the design process was over. The FBD is based on the idea that the stiffness of the members stays the same, that is the limitation of the FBD methods [2]. A numerical measurement known as a seismic damage index is used to determine the amount of damage an earthquake has done to the buildings. It facilitates in assessing the safety and operation of structures and other engineering systems following an earthquake occurrence by giving a numerical representation of the degree of the damage. The precise formulas used to calculate seismic damage indices are subject to modification based on the locality, the applicable building codes, and technical standards.

In recent years, a variety of damage indices have been developed, and each one makes use of certain parameters to calculate the structural damage such as stiffness, strength, energy and ductility [3]. It's essential to note that seismic damage indices are not individual measures but frequently used in conjunction with engineering analyses, such as structural evaluations, to assess the safety and integrity of buildings after an earthquake disaster. The main principle of seismic damage estimation is to meet the desired performance levels to irregular buildings during its design life under seismic loads. Seismic damage estimation in terms of damage indices have been established for reinforced concrete (RC) buildings to mathematically measure the seismic damage suffered by particular RC elements or entire buildings at predefined critical locations against seismic forces. Seismic damage indices for RC buildings have been subjected of much research, and it appears that all feasible possibilities have at least been partially examined. In comparison to the development of all suggested indices, which result in damage index

(DI) equal to zero when no damage occurs, indicating in elastic limit, and DI equal to one indicates at extreme failure, far less work has been put into developing intermediate damage stages [4]. The seismic damage indices that have been proposed can be categorised in a number of ways, but one of the most important distinctions is between local indices, which quantify the level of damage in individual members or at individual joints, and global indices, which describe the damage state of the entire building. Inelastic deformations are typically linked to damage in RC materials such as steel and concrete.

A quantitative method for determining the degree of earthquake related structural damage is the damage index. The damage index is calculated by measuring the structure's response to an earthquake forces, such as displacements, energy, stiffness, ductility, accelerations, or deformations. Based on particular criteria, it offers a numerical value expressing the extent of damage to the buildings. It’s significant to take into account that depending on the situation, the information at together, and the complexity of the building, the specific approach and parameters used for damage estimation may change. It is crucial for any damage model to specify intermediate damage stages to estimate the condition of the building for any deformation during or after any seismic event. Although it is not practical to build earth quakeproof structures, all buildings must be built to withstand seismic forces. As a result, in the case of an earthquake disaster, engineers are permitted to certain structural damage. It can be challenging to make structural design that are totally earthquake-proof due to the uncertain nature, frequency, and magnitude of earthquakes and economy. Presently, study is being done to create a more reliable seismic design process that accounts for the input energy that an earthquake imparts onto a structure that resulting damage to the structures.

Most of the RC buildings in India since last three decades had been developed and designed for gravity loads with insufficient lateral load resistance [5]. The irregularity in structures’ configurations have been identified as one of the main contributors to structural damage during previous earthquakes. A typical type of vertical discontinuity results from the building's dimensions being reduced throughout its height. Due to architectural considerations like aesthetic view, penthouse requirements etc., this type of elevation irregularity, known as setback, is growing in popularity in modern multi-story building construction. The setback significantly affects how seismically resilient a structure is. The severe earthquakes are caused structural damage, which indicated that this kind of structure's seismic performance is unacceptable [6]. In order to design buildings

that can withstand earthquake forces with acceptable damage (referred to as damage levels in Federal Emergency Management Agency, FEMA 356), structural engineers presently frequently use the seismic design processes outlined in seismic design codes.

Performance based seismic design (PBSD) techniques offer the tools to create buildings that can withstand seismic forces with an acceptable level of damage, despite some restrictions and uncertainties. In comparison to conventional prescribed seismic design methodologies, which primarily work to ensure life safety, PBSD tries to enhance the overall performance of structures by taking into account a number of performance criteria, such functionality, reparability, and economic issues. Since last two decades this PBSD technique become so popular in the area of structural design industry and many developed countries are using this seismic design philosophy [7]. In terms of earthquake design of structures, structural engineers in the field and academics concur that 'one has to construct the structure as per the best practises available and pray that a disaster earthquake wouldn't occur'.

In the current study, the limitations of previous research are thoroughly examined, and damage indices are developed that allow pushover analysis to quantify the effects of stiffness deterioration and energy dissipation and lateral drift after each incremental displacement of vertical irregular buildings. The lateral drift parameter is also used to develop drift based damage index using the results of nonlinear dynamic analysis. The primary purpose of this research is to estimate the seismic damage of low to medium rise RC regular and setback type vertical irregular buildings in between of zero (0 %) to one (100 %) scale. A correlation between absorbed energy and deteriorated stiffness with lateral drift is provided in order to simplify and make the DI estimation technique more comprehensible. For low to medium rise vertical irregular 3D RC buildings are being analysed, these suggested DI approaches may be employed on RC buildings to quickly calculate the global damage index. In order to simplify the seismic damage calculation procedure, the most important engineering demand parameters (EDPs), including absorbed energy, degraded stiffness, and lateral drift, are also taken into consideration.

1.2 Motivation of research work

Structures in earthquake-prone areas suffer the risk of being damaged or collapsing as a result of seismic instability during the un104expected event. The structural system should be designed as a consequence to reduce the loss of lives and property. The main

reason for structural damage is a loss of strength, stiffness, or ductility. In order to determine structural engineers need to control damage against severe earthquakes. Therefore, practising engineers must apply quick, efficient, and more precise empirical formulae for predicting structural damage at critical locations. As a result, before finalizing the structural design, a deterministic technique must be developed to define the performance level. For ease of use, numerous study evaluated the structural behaviour by setting the degree of damage on a zero to one scale. In order to determine damage before finalising the structural design, this investigation was done, in addition the suggested damage index methods are used to predict damage using predetermined performance levels using several EDPs. To evaluate the degree of damage on a zero to one scale, various types of engineering demand characteristics have been employed in terms of energy, stiffness, and drift to estimate the seismic damage at intermediate level.

Several researchers have done their work on safety and structural integrity of structures such as buildings, bridges, and other infrastructures, different structures are assessed using seismic damage estimations. Practicing engineers and decision-makers may identify susceptible regions and take the necessary steps to manage risks by estimating possible damage. This increases occupant safety and decreases the probability of casualties and loss of properties. Estimating seismic damage is an essential aspect of the continuing research and advancement of earthquake engineering. Researchers may improve current theories and provide more precise approaches for future evaluations by examining the behaviour of structures under seismic stresses and contrasting damage estimates with actual post-earthquake observations. The end result of this research is a better knowledge of earthquake behaviour and seismic design approaches.

1.3 Problem formulation

The majority of studies have used symmetrical frames or 2D frames to evaluate seismic performance, which were inadequate for vertical irregular-type buildings where torsion is significantly caused by their configuration. Hence, since most structures have irregular geometry and loads, irregular buildings have been taken into consideration for study to assess behaviour and take higher modes of effect into account as well. Several researchers have used parametric studies, where varied ground motions, variations in the 2D frame, and structure height variations are taken into account when conducting analytical work. In the current work, parametric studies on irregular buildings have been taken into account, such as changing the plan aspect ratio, changing building heights,

varying in vertical irregularity, varying lateral loads, and using plastic hinges to define parameters using energy, stiffness, and drift-based methods using the results of nonlinear analysis.

1.4 Objective of research

1) To carry out non-linear analysis utilising their results in order to estimate energy, stiffness, and drift-based damage index on vertical irregular buildings and to validate their results using methodologies for damage indices that are now accessible.

2) To apply the performance based seismic design concept to the formulation of seismic damage index charts will help to evaluate the degree of seismic damage on vertical irregular buildings by using the nonlinear analysis.

3) To derive drift based damage index on irregular buildings considering the theory of nonlinear regression analysis and to ensure their results with available damage index methods.

4) To relate the energy, stiffness and drift based index with performance based seismic design.

Damage indices have been developed by analysing several buildings in both static and dynamic nonlinear methods, while taking a number of various parameters into account. Buildings with plan aspect ratios of 0.5, 0.75, and 1.00 were taken into account at for the parametric study. Another factor is the building height, which is 18 m for low rises, 26 m for middle rises and 38 m for high rises. There are also considered unidirectional as well as bidirectional setbacks with considering variety of geometrical configuration. Three different monotonic loads, such as acceleration, IS and mode, were applied at during the pushover study. Eight different time histories that are compatible with IS 1893–2016 have been used in nonlinear time history study.

1.5 Scope of the work

1) To develop damage indices utilising multiple engineering demand parameters by performing non-linear static and dynamic analysis on irregular buildings.

2) To perform nonlinear analysis of various irregular buildings of varying heights and its vertical irregular configuration, applying lateral loads, and plastic hinges in accordance with I.S 1893 and FEMA 356 provisions.

3) To carry out nonlinear time history analysis that use various scaled ground motions (GMs) that are consistent with the acceleration spectrum of elastic designs and to satisfy the requirements of the I.S seismic code for the development of drift based damage index.

4) To use of SiesmoMatch software, which provides an application to fit earthquake accelerograms with specific target response spectrum as per IS 1893-2016, and then using these time histories to carry out nonlinear dynamic analysis.

5) To use of SAP-2000 software to precisely and quick assessment for critically evaluation of the non-linear analytical process.

6) Nonlinear regression analysis theory is used to quickly and accurately forecast the drift based damage index utilising the findings of nonlinear static and dynamic analysis.

1.5 Organization of the thesis

Chapter 1 represents the background of seismic damage estimation method and overview of the present study.

Chapter 2 discuss the literature research of performance-based seismic design with regard to damage indices, and emphasize the literature study of seismic damage estimation using various engineering demand factors via nonlinear analysis.

Chapter 3 highlights the nonlinear modelling technique and performance-based seismic design philosophy. A numerical investigation for the validation of nonlinear static and dynamic analysis is also provided through recent literature articles.

Chapter 4 discuss about the nonlinear static and dynamic deterministic damage index estimating methods that have been presented. Nonlinear regression concept is also presented for the development of drift-based damage estimation.

Chapter 5 presents application part on a variety of vertical irregular buildings, all recommended damage indices methodologies are employed by using nonlinear modelling process. Additionally, results and discussion are also presented.

Chapter 6 presents the conclusions of research work and recommendation of further scope of work.

CHAPTER 2 LITERATURE STUDY

2.1 Introduction

The Bhuj earthquake in 2001, the Sikkim earthquake in 2011, the Turkey earthquake in 2022, and many other earthquakes, all of which caused the collapse of reinforced concrete structures in entire or in part, have shown that it is necessary to evaluate the seismic performance of a structure before confirming its design. In order to make such a damage calculation, the simplified linear elastic processes that are used in the seismic code of practice are insufficient. As a direct result of this, the specialized area of structural engineering several researchers, have been developed unique design and seismic methods to estimate the structural damage. These procedures take into account performance-based structures and move away from efficient linear elastic approaches in encouraging the usage of more nonlinear techniques.

Investigation is conducted into the damage and vulnerability indices, in addition to the modelling issues connected to the generation of the capacity curve. According to the results obtained by A. Cinitha et al. (2015) [8], it is recommended that the global damage indices in the hardening and elasto plastic sections of the capacity spectra can be determined by using defined basic formulas. Performance-based seismic design, also known as PBSD, is a relatively novel concept in the field of structural engineering that is gradually gaining acceptance in the profession. The Applied Technology Council (ATC), the Federal Emergency Management Agency (FEMA), the Structural Engineers Association of California (SEAOC), California Universities for Research in Earthquake Engineering (CUREE), and SAC (a joint venture of SEAOC, ATC, and CUREE) have all recently published works that discuss the seismic performance of existing and proposed buildings [9]. These works reflect the growing acceptance of the performance based design approach. This kind of design requires a set of processes that ensuring the behaviour of a structure to be at predetermined performance levels when it is subjected to seismic loading.

A nonlinear analytic tool is required in order to conduct an analysis of seismic demands made at the various performance levels. Pushover analysis is typically utilised as the primary method for this kind of nonlinear analysis due to the fact that it is more straightforward in comparison to dynamic processes [10]. According to the findings of a pushover study, buildings with eccentric bracing in soft storeys have a lower drift demand and a reduced risk of collapsing. These findings were published in terms of storey drift

demand and collapse fragility curve, and the research that led to these findings was conducted in 2016 by D. Khan et al. [11]. In the past, researchers have investigated the reducing factor that influences the flexural stiffness of RC columns and beams in order to account for the cracking and softening effects that are caused by seismic loadings. J. Amin et al. (2019) [12] have conducted research on the seismic assessment of reinforced concrete two-dimensional moment resisting frames using gross and effective cross section's moment of inertia for RC beams and column as per IS 1893-2016 [13]. This study was performed using nonlinear static and dynamic analysis on reinforced concrete. Damage indices are powerful tools that have the potential to be used in upcoming design processes, with the end objective being producing solutions that are both more practical and more affordable. Emerging trends in earthquake-resistant design should focus primarily on mitigating the level of damage caused by earthquakes forces.

The objective of the performance-based seismic design, is to provide an explanation for the safety-related judgements that are made. PBSD focuses its attention on the predictive method of evaluating possible seismic performance. M. Zameeruddin et al. (2016) [1] has been worked out on recent advancements in performance-based seismic design engineering and developed numerous damage indices using nonlinear analysis. Despite this, their study can only be used to regular frames because of the limitations of their research. A generalised design philosophy known as PBSD describes design requirements in terms of attaining given performance goals when the structure is exposed to the specified levels of seismic risk [1], [14]. Methods of static and dynamic analysis that are based on displacement and energy can be utilised in order to determine how earthquake-resistant a structure is utilising either real or simulated earthquake time histories in nonlinear dynamic analysis approaches allows for the production of a variety of nonlinear response values. Although dynamic analysis methods are thought to be more accurate, they are impractical due to the complexity of their conceptual and numerical approaches, the difficulty of simulating the cyclic force deformation relations of reinforced concrete (RC) elements, earthquake scaling, and the time required.

As a consequence of this, nonlinear static analysis methods, which are more advantageous, are now often used as analytical tools in the process of determining whether or not structures are safe from seismic activity. The most current nonlinear static methods use lateral load patterns based on the first mode of vibration. These approaches are used for analysing the response of buildings whose behaviour is determined by the fundamental

vibration mode. For structures like irregular buildings, whose three-dimensional seismic response in the inelastic area is extremely difficult, it is imperative to take into consideration the contribution that comes from every significant mode of vibration. This is particularly relevant for structures that have a larger mode response than considering only first mode of vibration, T. Ucar et al. (2017) [15] have developed an energy-based damage index for the purpose of this investigation. Even though there may be minor, moderate, or major structural damage as a result of seismic occurrences, the most important role of structural engineering is to prevent structures from fully collapsing.

This can be accomplished in a number of ways. When designing new structures, the failure mechanism of existing structures that have been subjected to the effects of earthquakes should be taken into consideration. This will help ensure that irrational failure modes, such as soft-story or local failure mechanisms, be avoided. It is possible to design structures in accordance with an acceptable global failure mechanism, in which it is assumed that inelastic flexural deformations will concentrate in plastic hinge regions at both ends of all beams and base columns, in order to achieve a nearly uniform drift over the height of the structure as well as an admirable structural energy dissipation capacity associated with a high level of ductility. This can be accomplished by designing structures in accordance with an acceptable global failure mechanism. It is possible to regulate the failure mechanism by increasing the seismic capacity of structural systems, and it is recommended that the entire structure be constructed to be stable. This study has offered a global failure mechanism by using derived empirical equations, and it has also worked out the hysteretic response by applying nonlinear time history analysis. Oner Merter et al. (2017) [16] and Y. Wang et.al. (2020) [17] proposed a new methodology for energy-based damage assessment on RC frames.

Deterministic and probabilistic are the two methods that can be utilised in the process of damage estimation. Multiple academics or researchers have developed probabilistic damage estimate models for structures that can be used in the event of an earthquake. In addition, Halder et al. (2016) [18] have made efforts to build simple yet comprehensive nonlinear static methods for producing damage estimation indices and fragility curves. These approaches are now in the development stage. In order to ensure that the performance and capacity fulfil the target requirement of the seismic design guideline, it is also crucial to conduct an evaluation of damage for a proposed or an existing building. The parameters taken into account for traditional damage evaluation are

structural ductility, storey drift, element and connection rotation, dissipated energy, and fatigue of the structure. Numerous local and global damage indices have been presented to evaluate reinforced concrete structures based on the fundamental criteria. Because the integral damage assessment must be realistic and take into account the damage characteristics of local elements, research on the global damage indices is significant. Haoxiang H. et al. (2013) [19] had been proposed the integrated damage of a reinforced concrete structure is evaluated using a global damage index based on numerous linear force-deformation curves using results of pushover analysis.

Deterministic approaches have been proposed by a large number of researchers. In the related research, the structural damage value has been determined using two primary approaches. Both of these approaches are fundamental. The first approach is to maintain an equilibrium between a predetermined level of demand placed on the structure and the capacity that is connected with the structure. The second strategy is one that is based on the degradation of structural parameters. Each operation results in the production of one or more damage parameters, which are incorporated into the DI calculation. M. Zameeruddin et al. (2020) [3] has developed a number of DIs by applying a deterministic method to multi-RC moment-resisting frames and followed up with the results. In this instance of utilising the suggested methodologies, a nonlinear static analysis has been carried out, which has allowed for the use of different engineering demand parameters. A check for seismic damage assessment for RC moment-resisting 2D frames is another application of the performance-based seismic design concept [3].

Some more numerous researchers [20],[21],[22],[4],[8] presented deterministic methods for computing, which are based on a variety of engineering demand parameters (EDP).Although nonlinear dynamic analysis had been utilised by Habibi A. et al. (2009, 2012, 2016) [23],[6],[24], to compute drift-based damage index on 2D setback frames, and Ghobarah A. et al. (1999) [22] investigated stiffness-based damage index, the effects of torsional forces were not taken into consideration in these studies. Damage estimation in terms of stiffness, ductility, and dissipated energy has been addressed by S. Diaz et al. (2017) [25], but torsion or bidirectional moment effects had not been taken into account. A comprehensive analysis of the relevant literature demonstrates that these methods are either extremely complicated, ineffective, or only take into account one or two response factors, which means they fail to capture the particular seismic deterioration characteristics of a structure [21]. The issue with such methods is that they are not very good at

expressing the actual degree to which the structure has deteriorated. Pritam H. et al. (2019) [26] introduced damage estimating methods for horizontal irregular and regular RC multi-storied buildings. These approaches employ joint rotation, inter-storey drift (IDR), and peak roof displacement factors, and they take into consideration nonlinear time history analysis.

In terms of mass and lateral stiffness, variations in plan and elevation (and related eccentricities), shape of the plan configuration, presence of setbacks, in-plan stiffness of the floors (rigid diaphragm condition), and continuity of the structural system from the building's foundation to its top, empirical standards are used to classify structures as regular or irregular. Torsional irregularity is one of the most significant factors that contributes to the severe damage that the structures sustain (and possibly even their collapse) [20]. Ravi Kumar C. M. et al. (2012) [27] conducted research to determine the impact that irregular configurations have on the seismic vulnerability of RC buildings. There are several studies that investigate various aspects of torsional irregularity, such as geometric asymmetry, which has been examined and discussed in the validation of technical requirements by G. Ozmen et al. (2014) [28].

Buildings that have regular geometries and equally distributed mass and stiffness in plan as well as in elevation suffer far less damage than those that have shapes that are not regular. However, due to the needs and demands of the current generation as well as the ever-increasing population, architects and engineers have been promoted to build in unconventional configurations. So, the primary challenges in understanding the role of building layout have become clear in earthquake engineering [29]. The Capacity Design Method (CDM) solution, which was proposed by regulating the structure's damage mechanism based on the nonlinear static pushover analysis, is utilised to select the most appropriate building damage mechanism. Based on the nonlinear static pushover analysis, M. C. et al. (2014) [30] proposed a mathematical formulation and numerical studies for regulating the system damage mechanism, and the capacity Design Method (CDM) solution is used to determine the appropriate building damage mechanism. The following methods are being used to assess the degree of damage, analyse the advancement of the fracture mechanism, and evaluate and analyse the building's collapse in accordance with the PBSD: analytical procedures, simplified analysis, damage index, energy criteria, the calculation of system performances using performance-based plastic design (PBPD), the numerical one-step solution analysis, fragility curves, incremental iterative analysis (IIA),

the nonlinear pushover analysis, the nonlinear dynamic analysis, and the incremental nonlinear dynamic analysis (INDA) [30].

In the late 1970s, researchers started to focus on the seismic response of vertically uneven building frames, which has since been the subject of a large number of scholarly articles. Numerous articles have addressed the topic of plan irregularities causing torsion in structural systems. Vertical irregularities are fundamentally defined by discontinuities in the distribution of mass, stiffness, and strength along the vertical axis. Very few studies have been conducted to investigate the effects of discontinuities in each of these parameters separately, whereas a substantial number of studies have focused on the elastic response. Seismic codes recommend elastic time history analysis or elastic response spectrum analysis for determining the design lateral force distribution and providing criteria for categorising vertically irregular structures [31].

In reinforced concrete (RC) buildings, vertical irregularity can have an impact on the degree to which buildings perform and respond, especially when subjected to seismic ground vibrations. In order to prevent damage concentration on the irregularity section, it is essential to understand the manner in which seismic damage is formed as a result of setbacks. A parametric study was performed by Taufic M. et al. (2021) [32] on thirty five reinforced concrete setback frames, with different setback degrees of stepped and towered setback types. In that study, in order to examine the relationship among the damage index ratio and the irregularity indices under safety level seismic input ground motions, 2D reinforced concrete frame models with twenty stepped and fifteen towered setback frames were performed using nonlinear time history analysis. Two nonlinear regression equations were also suggested as an alternative to the dynamic analysis methods in accordance with the results obtained [32]. Pritam H. et al. (2020) [21] conducted research on the process of seismic damage assessment, which estimates the damage index (DI) of low-rise residential buildings with RC frames that are affected by seismic ground motions. In their study, the Park-Ang technique (1985) [33] has been utilised to estimate many three-dimensional DI for a building that has four stories.

These three-dimensional DI include peak roof displacement, damage index (DI), and inter-storey drift (IDR). The Park-Ang methodology has been the subject of a critical analysis, and an investigation into its limitations has been carried out. A straightforward method was implemented in order to calculate the global damage index (GDI) for both

regularly shaped and irregularly shaped buildings. It has been determined that the bottom level has taken the most amount of damage, while the roof has sustained the least amount of damage overall. Their research also made use of a prediction model that was founded on artificial neural networks [34] in order to cut reduce the amount of error that was introduced when computing the damage index. The study also found that nonlinear dynamic analysis needs a lot of ground motions data and difficult mathematical calculations that take a long time to run. Because of this, pushover analysis, a different type of nonlinear static analysis, has become very popular in the design world because it is faster and easier to use than nonlinear time history analysis [35]. However, Samir Tiachacht et al. (2021–2022) [36], [37] have done a number of studies on estimating damage using different composite materials, frame structures based on inverse analysis, laminated plates with different end conditions, and steel plates using frequency response function (FRF) and inverse analysis. Based on the numerical results of nonlinear static analysis, A. Habibi conducted research (2013) [38] in order to come up with a simple and useful index that would indicate the extent to which the structure was damaged. It is suggested that the static pushover analysis be used to make a precise estimate of the damage that buildings will suffer during earthquakes.

The problems with the earlier research have been addressed by suggesting damage indices that can be used for pushover analyses and nonlinear time history analyses to figure out how the reductions of stiffness, energy, and drift-based damage estimations add up gradually. Three different damage indices have been determined by using pushover analysis on different performance levels of setback types of vertical irregular buildings on the pushover curve. One damage index based on drift was determined by using a nonlinear time history as well pushover analysis using a nonlinear regression concept, which have before unaddressed by earlier researchers. The main goal of this study is to figure out how much damage low- to medium-rise RC regular and setback types of vertical irregular buildings perform in terms of DI. It has been decided that decreasing stiffness is related to lateral drift in order to make the DI estimation process easier to use. These suggested methods have been designed to make the damage estimation process easier while still taking into account the most important EDPs, like lateral drift, absorbed energy, and decreasing stiffness. These methods can be used to quickly find the global damage index for small to large RC buildings with vertical irregular buildings, compared to 2D frame analysis. Therefore, most researchers have only been able to use 2D frames for analysis,

resulting in they are unable to provide accurate damage index estimates for buildings with setbacks.

2.2 Contribution by previous researchers

Over the past few decades, researchers have managed to come to develop a number of numerical and experimental approaches of determining through the DI of structures. Evaluation methods are being improved to get the most accurate results. However, structural damage typically occurs in two stages over the duration of a structure's service life. The first stage is caused by load events like earthquakes, wind, accidents, and weathering. The second stage begins later and causes the material and structural strength to deteriorate down. Several techniques have been used over the past few decades to find out the way the material disregards down. The accuracy of the damage index of structures is unable to be assessed by these technical demand parameters alone. These days, the damage estimation process takes into account the effects of multiple response factors interacting together. However, professionals use this method because it is more accurate and easier to use than other modified methods. From this study of the literature, it is clear that seismic zone-wise damage estimates need to be made for all performance levels when uncertain loads like seismic loads are present. It's important to have a collection of standards for determining towards the extent to which damage has been done. These standards must encompass things like nonlinear analysis, evaluating structural elements, damage from different types of composite materials, damage from different structural configurations, and connecting out the breakdown of buildings over time in different environmental conditions. One of the best aspects about this design theory is that the client may decide advance of time what amount of damage is acceptable to a structure under a certain load.

CHAPTER 3 PERFORMANCE BASED SEISMIC DESIGN & NONLINEAR MODELLING

3.1 Performance based seismic design approach

Performance-based seismic design (PBSD) is a method of building design that takes into account a structure's anticipated response to an earthquake. The life safety aim, which is often referred to as achieving certain code criteria and ensuring that a building does not collapse under the design earthquake, is the emphasis of traditional seismic design methodologies. To accomplish higher performance objectives, such as limiting damage, lowering maintenance costs, reducing interruptions, and assuring occupant safety, PBSD extends above and beyond these fundamental standards. The PBPD technique makes the assumption that the inner work performed by the inelastic strain energy of plastic hinges is equivalent to the work performed by the external lateral forces [39].

There are mainly seven key features of PBSD philosophy. 1) Performance objectives 2) Hazard assessment 3) Structural analysis and Performance evaluation 4) Design process 5) Validation and verification of that iterative design process 6) Execution of construction and maintaining the quality control and 7) Post earthquake assessment. Specific performance levels are set for the building by the design team, which consists of structural engineers, architects, and building owners. Limiting structural damage, managing non-structural damage (such as damage to non-structural members or architectural finishes), promising operational continuity, protecting essential infrastructure, and protecting human life are a few examples of these objectives. Nonlinear static analysis method is one of the efficient methods for execution of performance based design. The pushover analysis is an approximate and does not take into consideration dynamic properties like hysteresis, greater mode involvement, etc.

For regular buildings (without torsional irregularity), it is known to produce positive effects. In these circumstances, the pushover curve may be transformed into an acceleration versus displacement response spectrum, which indicates the structure's "seismic capacity." To determine if the capacity satisfies the demand, the "seismic demand" might be included in the same graphic. A performance point is when seismic demand and capacity meet as shown in Figure 5.1. The response of the Multi Degree of

Freedom (MDOF) system might be described by a similar to single degree of freedom, according to the standard nonlinear static push over analysis. The response is regulated by a single degree of freedom system, and regardless of the degree of deformation, the mode's shape is to be believed to be constant throughout [10].

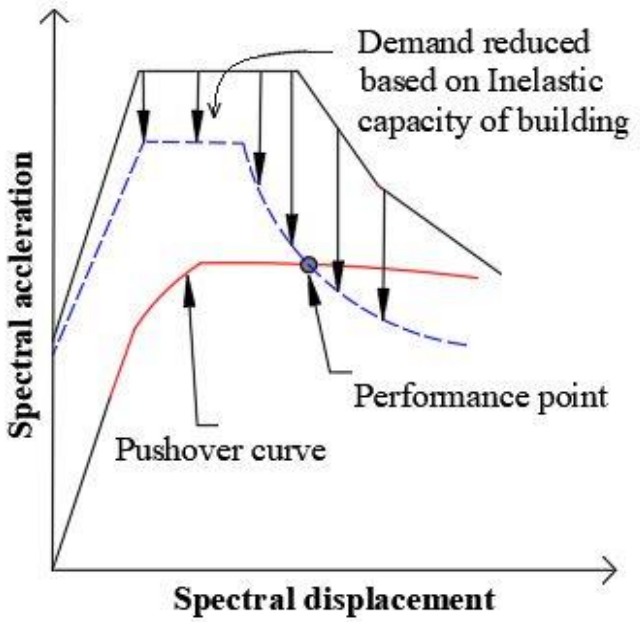

Figure 5.1 Schematic presentation of performance point- [ATC 40]

The evaluation of damage state in a structure's current condition is essential in a performance based design approach because it is linked to the structure's remaining strength, which could be used to make the necessary repairs to improve performance over the structure's extended design life. Under a specific risk level, performance based seismic design (PBSD) allows for the management of structural damage. Such structures sustain modest to substantial damages during strong ground motion (GM), depending on the intensity of the GM. The damage assessment techniques that are now accessible are difficult, time-consuming processes [21], [26]. Hence in present study, the simplified empirical formulae are derived at defined performance levels.

It has been noted that, on an assumption that the structures perform elastically and especially in the first mode of vibration, a linear distribution of lateral design forces has typically been employed in the present seismic design codes. Recent investigations, however, have demonstrated that this distribution may not be relevant in the inelastic range and does not adequately account for the higher mode effects for high-rise buildings. As a result, when affected by earthquake ground movements, building structures built in

accordance with current standards suffer lateral forces that differ from those estimated by the code formula. In order achieve the main aim of performance-based seismic design, it is necessary to directly account for the inelastic behaviour of structures throughout the design process [40].

Nonlinear static analysis provides a solution for performance based seismic design and has been gaining popularity as an approach for seismic evaluation of both new and existing structures, due to its simplicity compared to non-linear time-history analysis [10].The three-dimensional effect of building reactions are now taken into account when using the pushover technique to evaluate seismic damage to buildings. When the first mode is predominate, pushover analysis is an efficient tool for determining the structure's damage [41].

Performance Based Seismic Design is a method of designing buildings that takes into account how they will behave during earthquakes. Performance levels are defined in PBSD to evaluate the anticipated behaviour of a structure under various seismic occurrences. Following typical categories for these performance levels:

The several performance levels in ascending order regarding displacement or lateral load are mentioned here.

1) Operational level (OP): At this performance level, no damage is done to the structure as it is operated up to its elastic limit. The outcomes are essentially the same as those of the linear static or dynamic analysis since they only consider the elastic limit.

2) Immediate occupancy (IO): This performance level exceeds above the structure's elastic limit and causes a nonlinear response. Although it is still regarded as safe after an earthquake, after an earthquake, structures can be used immediately.

2a) Damage Control Range (DCR): This performance level is between IO and LS.

3) Life Safety (LS): This performance level has been reached at the strain hardening stage and belongs within the repairable damage range.

4) Collapse prevention (CP): This performance level is appropriate for gravity loads that result from an earthquake in which a structure partially collapses in the elements but does not completely collapse (serviceable even with significant damage to member).

5) Collapse (C): This performance level is no longer functioning and is unable to provide life protection against gravity loads after a seismic event. Figure 5.2 is shown the defined performance levels on displacement versus base shear curve. Different performance levels

and their divergence from existing standards are shown in Table 5.1 and Table 5.2, respectively.

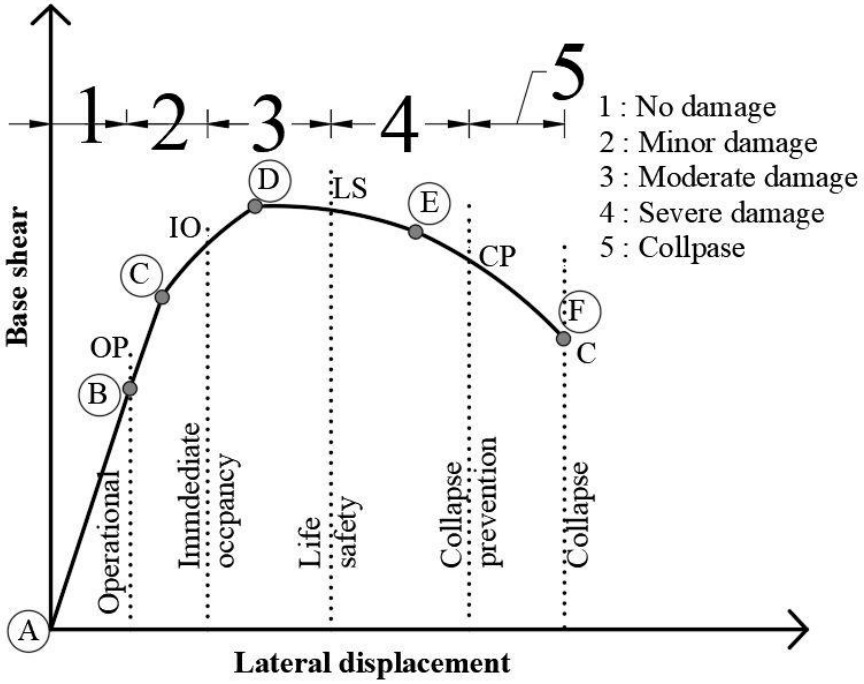

Figure 5.2 Performance levels on pushover curve

Table 5.1 Different performance levels in available standards

FEMA 273/356	ATC 40/58	SEAOC vision 2000
Performance level	Projected damage	Expected performance
Immediate occupancy (IO)	Negligible	Fully operational
Damage control range (DCR)	Light	Operational
Life safety (LS)	Moderate	Life safe
Limited safety range (LSR)	Severe	Near collapse
Collapse prevention (CP)	Complete	Total collapse

Table 5.2 Drift limits at different performance levels [FEMA 273/356, ATC 40/58]

Performance levels	Description	Drift limits
Operational (OP)	Does not undergo any damage	< 0.7 %
Immediate occupancy (IO)	Elements are partially damage	1 %
Life safety (LS)	Remarkably damage of structural and nonstructural elements	2 %
Collapse prevention (CP)	Structural elements are about to collapse	4 %

3.2 Nonlinear modelling

In structural design, nonlinear modelling is essential, especially when dealing with complicated or nonlinear behaviour of materials and structures. Nonlinear modelling approaches are required to provide accurate predictions and ensure structural integrity since linear models often fall short of capturing the entire range of structural response. Concrete, steel, and polymer are just a few of the structural materials that display nonlinear behaviour while under strain. To correctly represent the behaviour of the material, nonlinear material models, such as stress-strain curves or constitutive models, are utilised. These models take into consideration nonlinear processes including creep, strain hardening, and plasticity. Geometric effects and nonlinearities resulting from significant deformations are important considerations in structural design. Predictions made using linear models may be erroneous since they ignore geometric changes and assume minor deformations. Large displacements and rotations are taken into account using nonlinear modelling techniques like finite element analysis (FEA), which allows for a more accurate description of the reaction of the structure [42], [43].

There is a variety of nonlinear modelling literature available for interpreting inelastic behaviour of the structures. Nonlinear building models made of distributed and lumped plastic are often used in investigations. Damage estimation using any of engineering demand parameters is generally mirror image of accuracy of nonlinear modelling. Seismic damage estimation using any engineering demand parameter is often a mirror image of the precision of nonlinear modelling. In order to evaluate the dynamic response of structures subjected to earthquakes, or other dynamic events, nonlinear modelling is essential. The nonlinear behaviour of the structure is taken into account by

nonlinear dynamic analysis techniques including time history analysis and pushover analysis, which offer more accurate forecasts of structural performance under dynamic loads. Complex supports and connections, such as hinges, and joints which behave nonlinearly, are frequently used in structural design. These aspects may be accurately represented using nonlinear modelling, which takes into account things like stiffness deterioration, large deformation and energy loss during load transmission.

The selection of an acceptable nonlinear modelling approach in structural design is influenced by the specifics of the challenge to complexity of the structure's design, the degree of accuracy needed, the computing power at present, and the design guidelines and standards that apply to the analysis process. Modern computational methods and software tools, like as finite element analysis software, are used to carry out nonlinear modelling in structural design. These technologies take into consideration nonlinearities in materials, geometry, and boundary conditions as they solve the equations regulating the behaviour of the structure using numerical techniques. Engineers may acquire precise predictions of the structural response and optimise the design as a result of the iterative process of solving these equations.

3.2.1 Nonlinear static analysis

The computer technique of nonlinear static analysis, referred as pushover analysis is used to study how structures respond to applied loads when nonlinearities exist. It is a key method used in structural engineering and enables evaluation of structures that extend beyond that can be achieved with linear analysis. The relationship between the lateral forces applied and the corresponding displacements or deformations is assumed to be linear in linear static analysis. However, in many situations in reality, the behaviour of structures is nonlinear because of a variety of nonlinearity types, including nonlinear boundary conditions, geometric nonlinearity, and material nonlinearity. These nonlinearities are taken into consideration in nonlinear static analysis to offer a more realistic depiction of the structural response.

Material models that represent the nonlinear behaviour of building materials are included in nonlinear static analysis. Considering concrete as an example, nonlinear behaviour can be seen in the type of nonlinear stress-strain curves, strain softening, and compression or tension failure. These nonlinear material behaviours are represented by material models, such as damage models, elasto-plasticity models, and plasticity models. Large deformations that result from the structure going through considerable shape or

configuration changes are taken into account in nonlinear static analysis. Substantial rotations, significant deflections, and variations in stiffness imposed on by deformation are all taken into consideration as consequences of geometric nonlinearity. The relationship between the applied loads and the resultant displacements is not considered to be linear in nonlinear static analysis. Instead, an iterative method is used to determine the structure's equilibrium condition under the applied stresses.

In order to complete the analysis, a number of nonlinear equilibrium formulas must be solved by applying loads gradually while updating displacements until convergence is reached. It is possible to complete these investigations effectively using specialised software tools. With regard to stress distributions, deformation sequences, and the ability of the structure to sustain applied loads, the findings of nonlinear static analysis offer an understanding of the structural response. Engineers can correctly evaluate the stability of structures, performance, and safety of structures by taking into account nonlinear behaviour, which results in better designs, optimising, and reduction of probable failure modes. It has a number of advantages over conventional linear analysis techniques. The following are some of the primary advantages and limitations of pushover analysis.

Advantages of nonlinear static analysis:

1) Pushover analysis identifies the materials and geometric nonlinearities that contribute to a structure's nonlinear behaviour. It enables the consideration of variables including yielding, plastic deformation, and stiffness/strength deterioration, all of which are essential to correctly anticipating whether structures will react to significant displacements and stresses.

2) Pushover analysis enables the assessment of the structure's load distribution. It gives engineers knowledge of exactly the monotonic lateral loads are distributed between various parts and elements, enabling them to identify problems and adjust the design as necessary. This can be very helpful when designing structural systems with complicated load paths.

3) Pushover analysis offers a thorough knowledge of a structure's general response to lateral stresses. It measures the progressive distribution of loads and deformations through the structure by applying an order of increasing loads until the building reaches its maximum capacity. As a consequence of pushover analysis, it is able to assess the overall structural integrity and find any potential weaknesses at predefined critical locations of buildings.

4) Pushover analysis provides it possible to assess a structure's ductility and ability to dissipate energy. In order reduce the possibility of structural damage and collapse, it helps

assess the structure's capacity for absorbing and dispersing energy during seismic occurrences. Additionally, a significant decrease in stiffness occurs as the lateral load on the structure increases along its height.

5) Pushover analysis enables performance based design methodologies, allowing designers to evaluate a structure's performance beyond conventional code based criteria. Designers can be assessed the safety, usability, and resilience of the building under seismic events by comparing the estimated response of the structure with specified performance targets, such as displacement limits or inter story drift limitations.

Pushover analysis, in general, offers a more thorough and realistic perspective on the manner in which the structure responses to lateral forces, especially seismic loads. It helps in designing more effective more durable structures, assessing repair possibilities, and enhancing overall structural performance.

Although pushover analysis is a useful technique in structural engineering, engineers should be aware of some of its limitations. The following are some of the main limitations of pushover analysis:

1) Simplified models are frequently used in pushover analysis to depict structural behaviour. The findings of the study might be inaccurate since these simplified models might not accurately represent the many details and complexity of the actual structure. The quality of the selected structural model has a significant impact on the analysis's accuracy.

2) Pushover analysis, which assumes that a structure deforms in a quasi-static method, offers an approximation of the structural response. It does not, however, account for the structure's dynamic response, which includes the effects of inertia, damping, and dependent on time behaviour. Additional linear or nonlinear time history analysis of dynamic behaviour should be carried out to provide a more precise evaluation of the behaviour.

3) Typical applications of lateral loads in pushover evaluations include the modal or uniform force distribution. The real distribution of loads and dynamic interactions in the building during an earthquake or other natural disaster may not be fully represented by these load patterns. Designers should use caution when interpreting and estimating the analysis results because they depend on the chosen load pattern.

4) Material models are used in pushover analysis to depict nonlinear behaviour. It can be difficult and unclear to precisely simulate material characteristics such as strain hardening, stress- strain curves, or damage occurrence. The suitability and the accuracy of the selected material models have a significant impact on the accuracy of the analysis outcomes.

5) Pushover analysis uses a number of simplified assumptions, such as assuming that certain element's behaviour rigidly or perfectly plastically or ignoring some secondary effects. Such assumptions could not always hold true in reality, which could lead to restrictions and probable errors in the results of the analysis.

6) Based on the predicted load pattern and nonlinear behaviour, pushover analysis offers an assessment of the structural response. To ensure the accuracy and reliability of the analysis results, they need to be confirmed against experimental data or by using additional methods of analysis.

7) The input parameters for pushover analysis include material characteristics, boundary conditions, and lateral loading factors. Small changes to these factors can have a substantial impact on the results of the analysis. In order to ensure the accuracy and dependability of the study, designers should carefully choose and calibrate these parameters.

In performing pushover analysis, designers should be aware of these constraints and use good technical reasoning. Pushover analysis has combined with other analytical techniques and taking seismic design code suggestions into account can assist to overcome these restrictions and give a more thorough insight of the building behaviour.

3.2.2 Nonlinear dynamic analysis

Nonlinear dynamic analysis is a computer method used to examine the behaviour of structural systems which show nonlinearities with dynamic loading events. It requires using mathematical methods to solve a structural system's equations of motion in order to simulate its response with time duration of an earthquake. The response of the system is assumed to be linearly proportionate to the applied forces or displacements in linear dynamic analysis. But many structural geometries in reality behave in a nonlinear manner, where there is a nonlinear connection between the applied loads and the output response. These nonlinear effects are taken into account by nonlinear dynamic analysis in order to provide an accurate representation of the structural geometry's behaviour.

In order to accomplish this, nonlinear variables in the equations of motion must be solved, such as more complex derivatives, nonlinear forces, or nonlinear structural relationships. Because closed-form analytical solutions are frequently unavailable, these equations are generally solved numerically using iterative processes. In a variety of applications, available finite elements method’s software tools make it easier to simulate and analyse nonlinear dynamic behaviour of buildings [44].It differs from traditional linear analysis methods in a number of ways. Nonlinear dynamic analysis provides a variety of

advantages over linear dynamic analysis for analysing buildings that show nonlinear behaviour. Among the main advantages are as follows.

Advantages of nonlinear dynamic analysis:

1) Nonlinear dynamic analysis offers a more precise assessment of the structure's response. For structural systems with considerable nonlinearities, linear analysis' assumption that forces and displacements have a linear relationship may not hold true. The analysis offers a more precise understanding of the behaviour of the system by taking these nonlinearities into account.

2) Complex events that linear analysis is unable to grasp can be addressed by nonlinear dynamic analysis. Among other factors, nonlinearities can result from boundary conditions, geometric effects, or material behaviour. Large deformations, buckling, snap-through behaviour, material yielding, and hysteresis are a few examples of complex processes. For these events to be correctly modelled and predicted, nonlinear dynamic analysis is required.

3) For the investigation of stability of structural systems and limit states, nonlinear dynamic analysis is giving critical evaluation of structure's behaviour. It's possible that linear analysis won't provide insight on potential instability or failure mechanisms. In order to assess the stability of the system and identify anticipated failure modes, nonlinear analysis may be used to locate critical points in structure's failure modes.

4) Analysing structures that are subjected to extreme loading circumstances, such as earthquakes, explosions, or impact loads, makes use of nonlinear dynamic analysis especially advantageous. Large deformations, nonlinear material behaviour, and intricate interactions are frequently brought on by these occurrences. Nonlinear analysis makes it possible to evaluate the system's functionality and structural reliability under these challenging conditions.

5) Design optimisation is supported by nonlinear dynamic analysis by taking nonlinear influences into account. By locating crucial locations, evaluating structural response, and enhancing the structural system's overall performance and safety, it aids engineers in the refinement and optimization of designs. A design's suitability can also be checked using nonlinear analysis after it has already been evaluated using linear methods, adding another degree of assurance.

6) The establishment and validation of numerical models used for simulation are improved by nonlinear dynamic analysis. Designers may evaluate and enhance their models to make

sure they represent the basic nonlinear behaviour of the system by comparing simulation results with experimental data or analytical solutions for particular scenarios.

In generally, nonlinear dynamic analysis allows for an in depth understanding of the structural behaviour under dynamic loading due to ground vibrations with nonlinearities and offers insightful information for design, analysis, and safety evaluation, especially in cases when linear analysis may produce unreliable or inadequate results.

In structural engineering, nonlinear time history analysis is an effective tool for assessing the dynamic behaviour of structures under substantial earthquake loads. Designers must take into account its limits, like with any analytical technique. The primary drawbacks of nonlinear dynamic analysis are as follows:

1) Comparatively to linear analytic methods, nonlinear time history analysis requires more processing power. For each time step of the analysis, a system of nonlinear equations must be solved, which can take a lot of time and resources, especially for complex and large buildings.

2) Numerical models must be intricate and complex in order to precisely represent the actual behaviour of buildings. These models must take into account a variety of nonlinear phenomena, including boundary condition nonlinearity, geometric nonlinearity, and material nonlinearity. Such models can be difficult to develop and calibrate, and because of their complexity, there is a greater chance that they will introduce errors or uncertainties into the analysis.

3) Nonlinear time history analysis simulates dynamic loads using ground motion data as an input. For precise outcomes, choosing adequate and representative ground motion is essential. However, the number of trustworthy ground motion data that meet the requirements for a specific location can be constrained. Inaccurate forecasts of structure response might result from the improper or inadequate selection of ground motion.

4) In the nonlinear modelling process, various simplifications and assumptions are frequently applied in order to decrease computing complexity. These oversimplifications run with the possibility of degrading the analysis or introducing inaccuracies. For instance, the precision of the overall response prediction may be affected by neglecting certain local or component-level nonlinearities, such as joint behaviour or material variability.

5) Nonlinear time history analysis provides understanding on the way buildings respond to extremely substantial loads. But it might be difficult to predict structural deterioration or collapse before it occurs. As a result, the analysis could make cautious or too optimistic

anticipates since it does not account for all failure modes or the interplay between various failures mechanisms.

6) Adequate characterization of material properties, ranging such as stress-strain correlations, strength parameters, and stiffness properties, is necessary for nonlinear dynamic analysis. These characteristics, however, can be susceptible to unpredictability because of variations in material behaviour, construction quality and workmanships, or testing techniques. The accuracy of the results of the evaluation may be impacted by these issues.

7) The amount of data of the time step employed in the numerical integration method affects the reliability of the analytical results. While selecting a time step that is too small that possibly drastically lengthen calculation time, choosing a time step that is too big that can result in numerical instability and loss of precision.

8) To verify the accuracy of nonlinear time history analysis models, they must be calibrated and tested against experimental data. However, it is expensive and sometimes impracticable to test large-scale structures experimentally under substantial lateral forces. The validation and calibration processes may be complicated by a lack of trustworthy experimental data, adding uncertainty to the results of the study.

Despite these drawbacks, nonlinear dynamic analysis is nevertheless a useful technique for practicing engineers to look into the manner in which structures operate when subjected to dynamic loads along with the way they respond to severe events. It assists in locating probable errors, creating suitable design methods, and enhancing the safety and durability of buildings.

3.3 Validation of nonlinear analysis

The previous study is used as a numerical building example to validate nonlinear models and structural response. As a result, the nonlinear analysis method is validated using two different research papers, one of the research article was published in 2018 and another was in 2016. The SAP2000 version 22 has been used to validate the results of nonlinear analysis.

3.3.1 Nonlinear static analysis validation using research article [45]

One of the study regarding using nonlinear analysis methods, Taner U. et al. (2018) has been carried out their work on the calculation of energy-based base shear force coefficient taking hysteretic behaviour and P-delta effects into consideration. In order to account for P-delta effects and the hysteretic behaviour of reinforced concrete members, a

modified energy balance equation is developed. By combining plastic energy and seismic input energy modification factors, it is possible to easily account for reduced hysteretic characteristics of structural components caused by combined stiffness and strength degradation and pinching effects, as well as hysteretic damping. Pushover analysis and nonlinear time history analysis of numerous 2D RC frames with various numbers of stories are used to verify energy-based base shear coefficients. The time histories of ten scaled ground motions that are in accordance with the elastic design acceleration spectrum and satisfy the duration/amplitude-related requirements are used to perform nonlinear time history analysis frames.

The three-bay moment-resisting frames, which range in height from 3 to 8 stories, are correctly specified and seismically designed in accordance with Turkish seismic design code (2007) criteria. Concrete is assumed to have a typical compression strength of 20 MPa, while steel used for longitudinal and transverse reinforcement has a typical yield strength of 420 MPa. According to TSDC (2007), the site condition is designated as Z3 and the frames are considered in seismic zone 1. According to TSDC (2007), the response reduction factor (Ra) is used to modify the design base shear force based on the structural properties of the system when using the 5 % damped elastic design spectrum. The structural analysis software SAP2000 (2016) were used to design frames while taking into account rectangular beams and square columns. The configuration of the 3 to 8 storey frames utilised for the analysis is shown in. This figure also includes the storey heights (H_i), span lengths of the frame model, evenly distributed dead and live loads (g_i, q_i) in all spans, and concentrated dead and live loads acting on both the interior and exterior beam-column joints (G_{ii}, Q_{ii}) and (G_{ei}, Q_{ei}), respectively.

The magnitude of gravity loads that are distributed and concentrated is shown in Table 5.3. The selection of frame is a 2D model of a 3D internal frame with symmetrical stiffness distribution in all directions and uniform mass distribution on the plan, and gravity loads have been determined in accordance with their magnitudes. Floor weights and associated masses, which are taken into account in seismic calculations, are calculated as a combination of 100 % dead loads and 30 % of live loads using a live load participation factor (n) = 0.30.In pushover analysis, plastic sections are assigned to the ends of beams and columns to model them as nonlinear structural components. A lateral load distribution that is invariant to the first mode form is then utilised. Frames have been increased to a value of $\delta/H_N = 0.02$, where δ indicates lateral displacement and H_N represents total height of frame, which is also taken into account when calculating the base shear force

coefficients based on energy. Figure 5.4 represents pushover curves both with and without the contribution of P-delta effects. Base shear force coefficient (V/W) is the pushover curve's vertical axis, where V represents bas shear and W indicates total seismic weight, while roof drift ratio (δ/H_N) is its horizontal axis. Table 4 presents the pushover based and code-based base shear force coefficients that correspond to a 2% drift ratio [45].

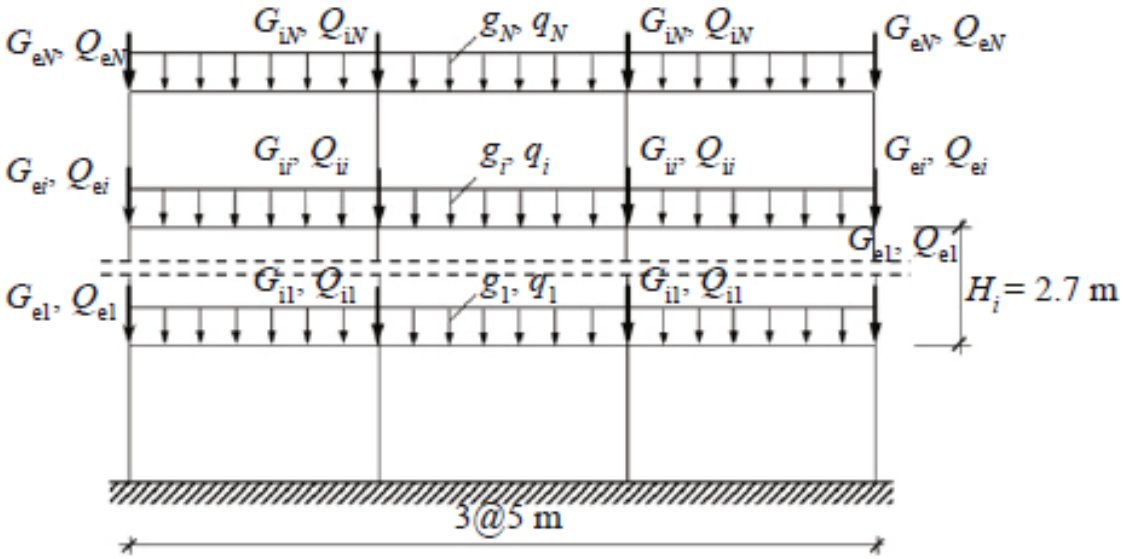

Figure 5.3 Frame models and gravity loads

The author's time period values for the first three modes of the three-story RC frame were 0.607, 0.188, and 0.107; likewise, the current study's time period values for validation were 0.607, 0.207, and 0.134. According to the results shown in

Table ***5.4,*** the base shear co-efficient for a three-story RC frame differences by 5.49 % and 14.85 % for the research article stated above with the validation study that takes into account with and without p-delta effects. It has been noted that the results varied slightly while comparison, since some of the parameters needed for performing the nonlinear static analysis such as plastic hinges, designed reinforcements of beams and columns were not shown in the research article. Hence they are assumed while performing the analysis. The Figure 5.5 and Figure 5.6 are shown the pushover curve obtained from validation model of 3 storey RC frame.

Table 5.3 Magnitude of gravity loads

Uniform loads (kN/m)			
g_i	q_i	g_N	q_N
20.50	6.67	15.50	5.00
Concentrated loads (kN)			

G_{ei}	Q_{ei}	G_u	Q_u	G_{eN}	Q_{eN}	G_{iN}	Q_{iN}
71.00	16.65	102.63	33.33	52.50	12.50	77.45	25.00

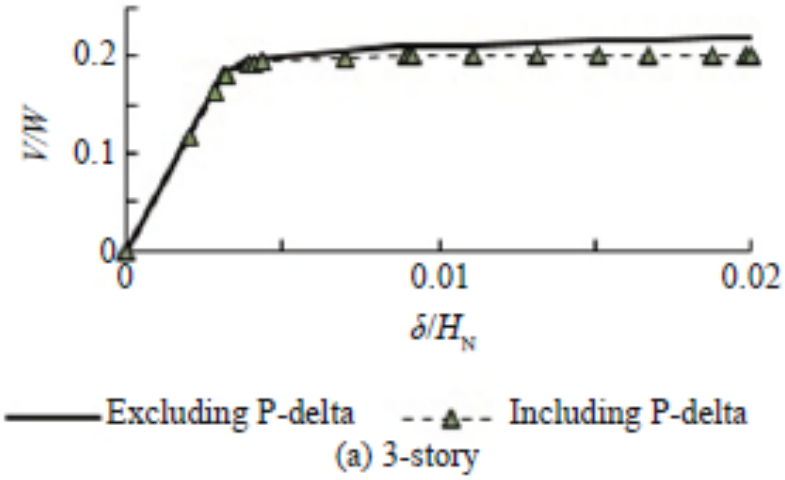

Figure 5.4 Pushover curves of frame of 3 storey RC frame

Table 5.4 Comparison of the base shear co-efficient based on pushover analysis

Frame	(Results without P-delta effect)		(Results with P-delta effect)	
	V_y/W	V_y/W (Validation)	V_y/W	V_y/W (Validation)
3- storey	0.221	0.233	0.202	0.232
Difference	5.49 %		14.85 %	

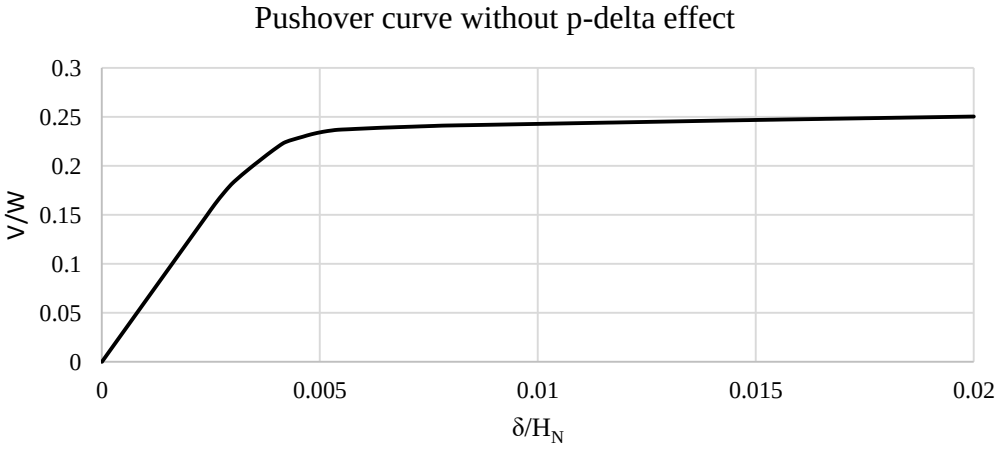

Figure 5.5 Pushover curve of 3- storey RC frame without p- delta effect

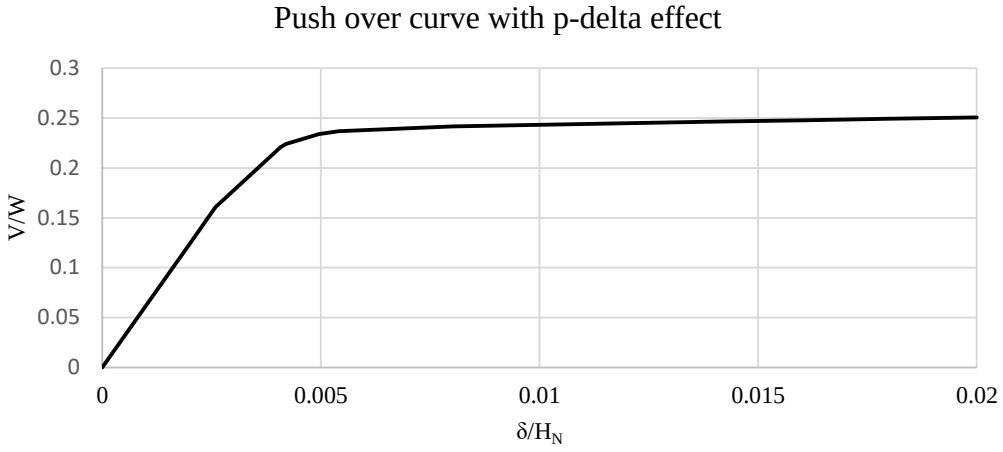

Figure 5.6 Pushover curve of 3- storey RC frame with p- delta effect

3.3.2 Nonlinear dynamic analysis validation using research article [45]

In the research article by Taner U. (2018), According to the magnitude, distance, fault type, and soil professional type information, a total of 10 actual accelerograms are chosen. The PEER NGA strong ground motion database is used as the primary source for obtaining the accelerograms with a magnitude range of 6.5 to 7.5 and source-to-site distances less than 50 km. The site conditions of the accelerograms indicate the characteristics of Z3 soil since it is assumed that all frames belong to the Z3-type site class. Z3 soil profile type definitions are regarded of as the equivalent of the $180 \leq V_{S30} \leq 360$ National Earthquake Hazards Reduction Program (NEHRP) D site class. The chosen ground motions have a strike-slip fault mechanism, and the impacts of nearby faults are not taken into account. Table 5.5 presents the list of available ground motion data as well as the general properties of accelerograms.

Table 5.5 Selected earthquake ground motions and major seismological parameters of records

Record name	Earthquake name	Mw	PGA (g)	PGV (cm/s)	PGD (cm)
IMPVALL.I_I-ELC180	Imperial Valley-02, 1940	6.95	0.281	30.93	8.66
IMPVALL.I_I-ELC270	Imperial Valley-02, 1940	6.95	0.211	31.29	24.18
SUPER.B_B-POE360	Superstition Hills-02,	6.54	0.286	29.02	11.56

	1987				
BIGBEAR_HOS180	Big Bear-01, 1992	6.46	0.101	11.85	3.36
KOBE_KAK000	Kobe, 1995	6.90	0.240	20.80	6.39
KOBE_SHI000	Kobe, 1995	6.90	0.225	31.33	8.38
KOCAELI_DZC180	Kocaeli, 1999	7.51	0.312	58.85	44.05
DUZCE_DZC270	Duzce, 1999	7.14	0.515	84.29	47.99
SIERRA.MEX_CHI090	El Mayor-Cucapah, 2010	7.20	0.197	34.03	31.22
SIERRA.MEX_GEO090	El Mayor-Cucapah, 2010	7.20	0.288	49.54	40.31

The scale factors offering the best match to the elastic design spectrum of the Turkish seismic design code over the study period range (T_A = 0.01 s and T_B = 4.00 s), as well as some relevant variables that may be used to assess the accelerograms' complying with the code requirements to perform nonlinear dynamic analysis. The results of the nonlinear dynamic analysis performed using SAP 2000 software are compared and presented in Table ***5.6*** below.

Table 5.6 Comparison of base shear force coefficient results of nonlinear dynamic analysis

Record name	Result of research article, V/W	Result of validated model, V/W
	3- storey	3- storey
IMPVALL.I_I-ELC180	0.259	0.253
IMPVALL.I_I-ELC270	0.254	0.250
SUPER.B_B-POE360	0.253	0.246
BIGBEAR_HOS180	0.264	0.217
KOBE_KAK000	0.241	0.247

KOBE_SHI000	0.291	0.257
KOCAELI_DZC180	0.250	0.257
DUZCE_DZC270	0.258	0.274
SIERRA.MEX_CHI090	0.260	0.246
SIERRA.MEX_GEO090	0.247	0.256
Average	0.258	0.250

According to the results shown in Table 5.6 the base shear coefficient for a three-story RC frame average value of ten different ground motions is 0.258, and similarly the average value of ten different validated models is 0.250. As a result, there is a difference of approximately 2.85 %, which is nearly the same when performing nonlinear dynamic analysis.

3.3.3 Nonlinear static analysis validation using research article [1]

M. Zameeruddin et. al. (2016) [1] has been worked out in order to account for inelastic behaviour and the impacts of cyclic loading in reinforced concrete structures, force-based seismic design approaches have their limits. Performance-based seismic design was proposed to solve these issues. The recommended approach enables structures to be designed with a realistic and reliable appreciation for risks to life, occupancy, and financial losses that may arise from future seismic events.

An example mid-rise building's moment resisting reinforced concrete frame's (MRF) reaction and damage states were assessed. The example MRF represents a medium rise building with 3-bay and 4-stories. Pushover displacement controlled nonlinear static analysis was performed on the MRF. According to the standards outlined in the first, second, and third generation PBSE processes, the frame's response was evaluated. The sample structures were analytically modelled using SAP 2000V 17.0.The MRF has a bay width of 3 m and a storey height of 3 m. The MRF was set up in accordance with the standards outlined in IS 456:2000 [46], IS 1893-2002 [47], and IS 13920:1993 [48]. For each level, a dead load of 16 kN/m and a live load of 9 kN/m were assigned. Using SAP 2000 V 17.0, the MRF was subjected to the lateral load pattern required by IS 1893 -2002 in order to obtain a pushover curve. Following the guidelines of IS 1893-2002 [47], lateral

loads for seismic zone V (zone factor, z = 0.36) and importance factor 1, which are placed on the hard soil strata, were applied to the frame. Concrete grade M25 and steel grade 415 that were taken into consideration. The sample MRF's layout and elevation are shown in Figure 5.7 and reinforcement details are depicted in Figure 5.8. The reinforcement information for reinforced concrete columns and beams is displayed in Table 5.7 and Table 5.8 respectively.

For validation model prepared in SAP 2000 software has been shown similar reinforcements in beams and columns. Similarly plastic hinges are applied same as indicated in research article. After performing a pushover analysis, a pushover curve was created, as shown in Figure 5.10, which is similar to the curve created from the study paper in Figure 5.9.

Table 5.7 Reinforcements (R/F) details of columns for example MRF

Storey	External column		Interior column	
	Size (mm)	R/F (mm^2)	Size (mm)	R/F (mm^2)
All floors	380 x 380	1155	450 x 450	1620

Table 5.8 Reinforcements (R/F) details of beams for example MRF

Storey	Dimension (mm)	Beam reinforcement (mm^2)								
		Bay 1			Bay 2			Bay 3		
		Top	Bot.	Top	Top	Bot.	Top	Top	Bot.	Top
1st	300 x 300 (mm)	600	261	604	605	261	605	604	261	600
2nd		670	261	651	668	261	668	651	261	670
3rd		552	261	519	545	261	545	519	261	552
4th		330	261	360	372	261	372	360	261	330

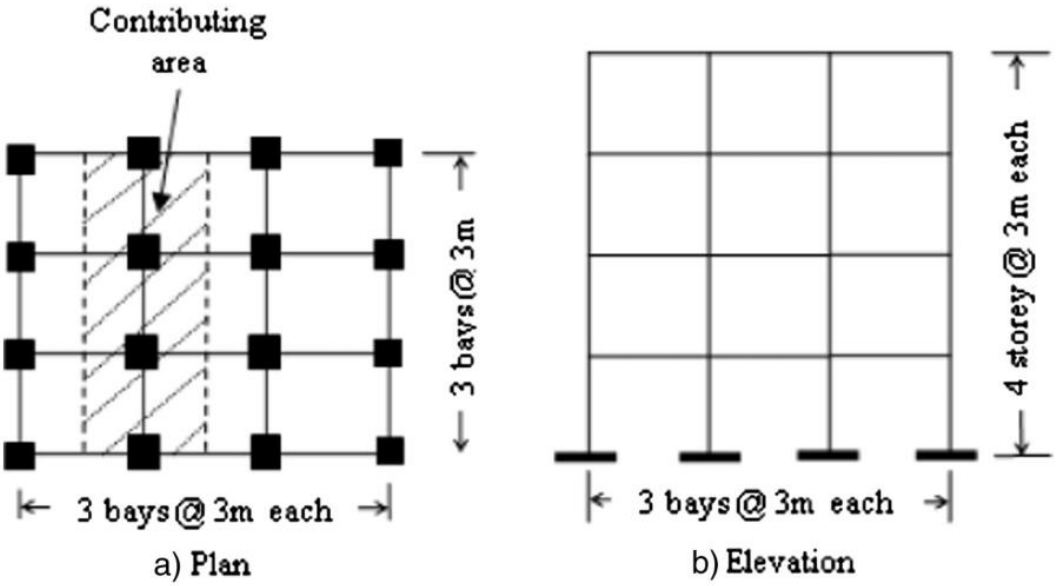

Figure 5.7 Plan and elevation of RC frame

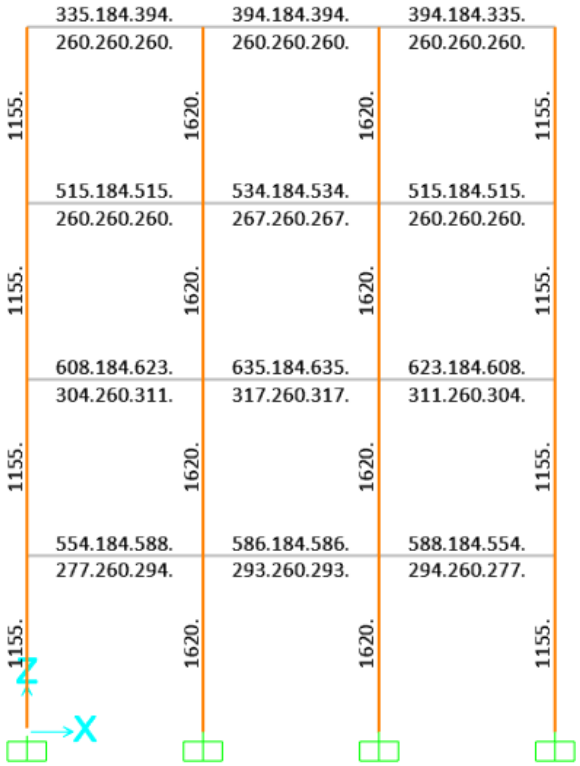

Figure 5.8 Reinforcement details in RC frame of SAP 2000 model

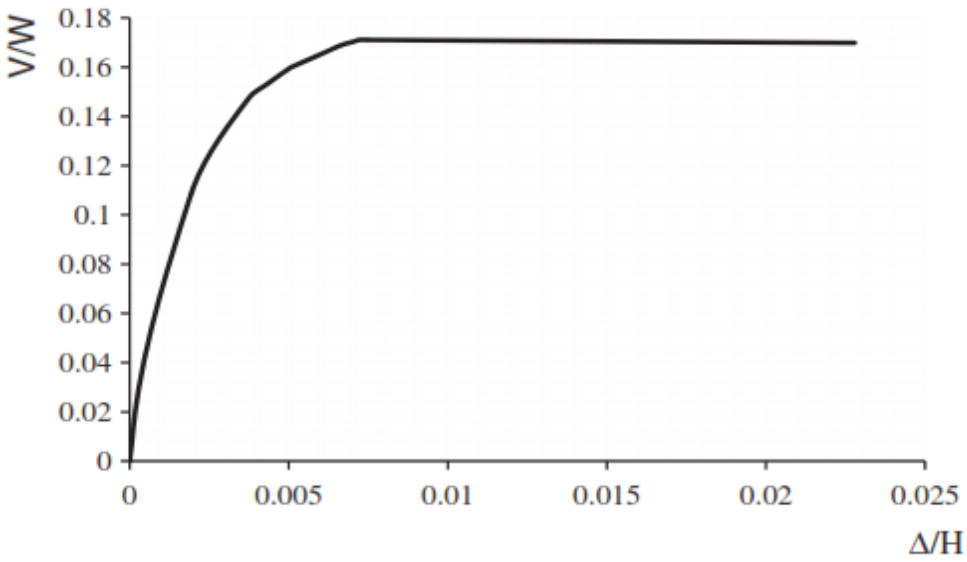

Figure 5.9 Pushover curve for building frame from research article

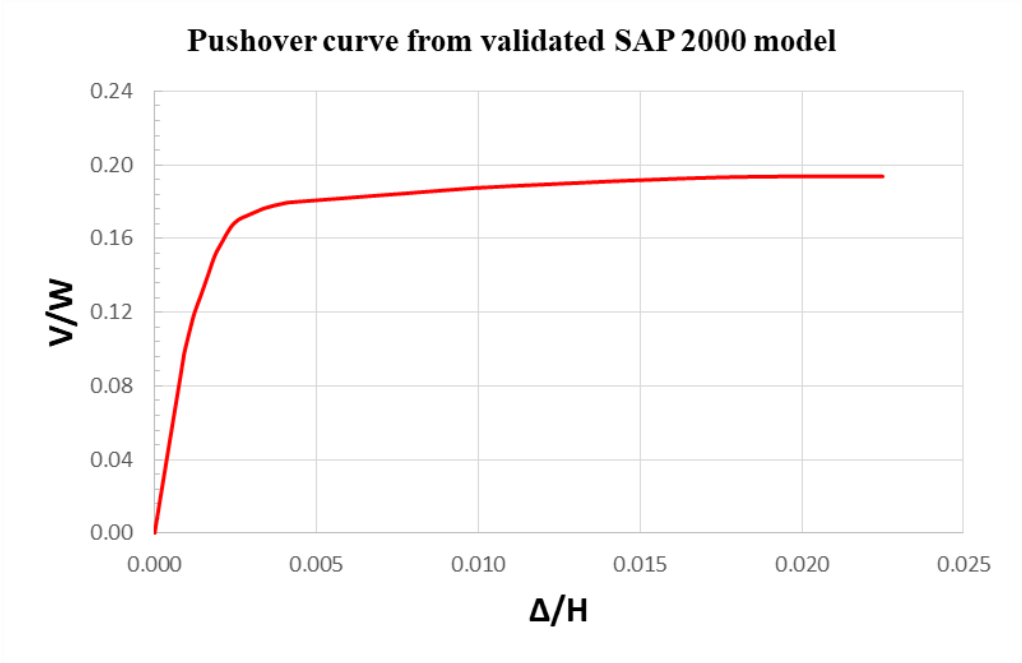

Figure 5.10 Pushover curve for building frame from validation model

3.3.4 Nonlinear dynamic analysis validation using research article [1]

The most precise and reliable analytical technique is known as a time-history analysis. For the example MRF, EL-Centro (1940) and Northridge (1994) were used, with PGA values of 0.319 and 0.968, respectively. For the earthquakes in Northridge (1994) and EL-Centro (1940), maximum displacements of 89.00 mm and 98.00 mm, respectively, were obtained from the research article.

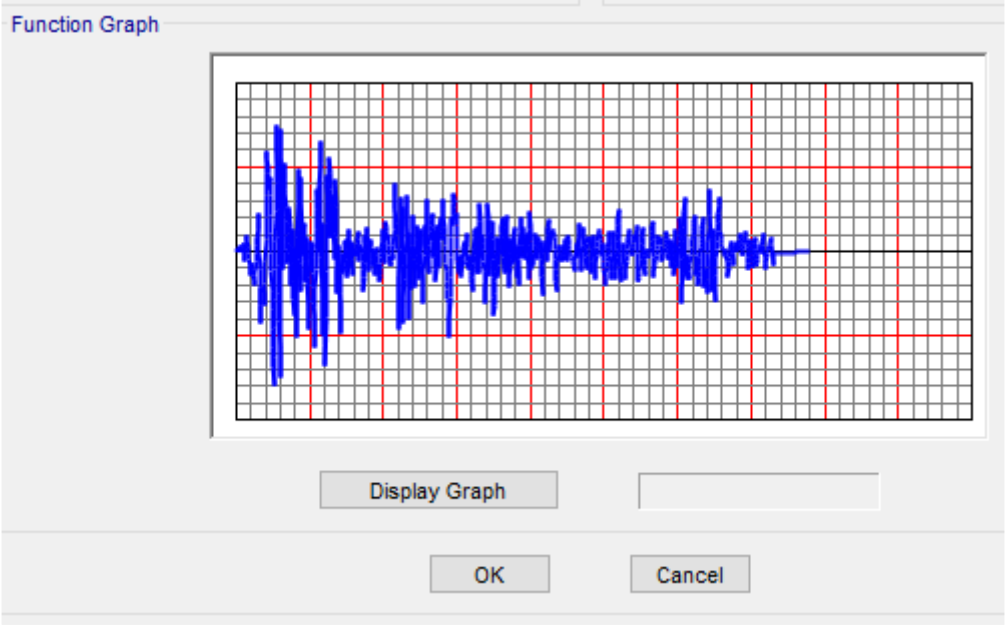

Figure 5.11 Time history of El-Centro earthquake (1940)

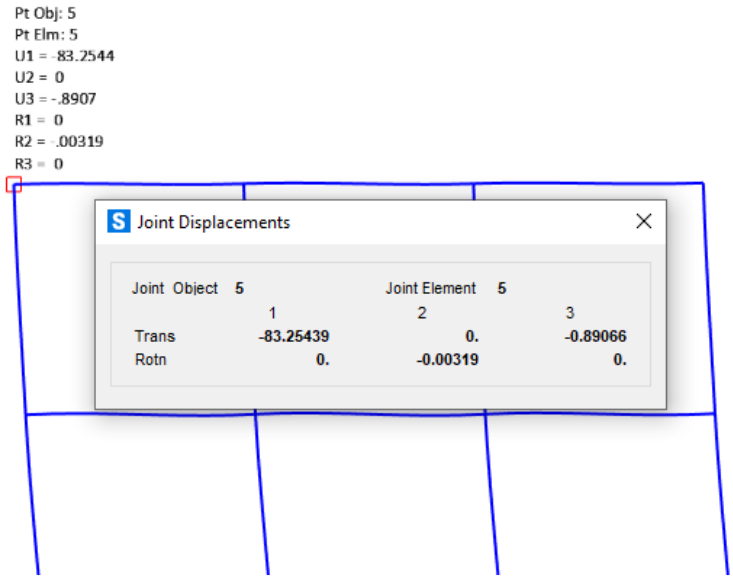

Figure 5.12 Roof displacement using nonlinear time history of El- Centro earthquake

Time history of El-Centro (1940) is used for result of nonlinear time history analysis of research article, which has been shown in Figure 5.11. After performed nonlinear time history analysis of validated model, it has shown around 83.25 mm which is almost same as compare to existing research study, which has been depicted in Figure 5.12.

3.4 Importance of 3D RC vertical irregular buildings as compare to 2D RC frame

A key stage in the process of evaluating the performance of structural systems, such as RC (reinforced concrete) frames, and ensuring that they are safe under a variety of loading circumstances is doing a nonlinear analysis of the system. It is important to keep in consideration that specific variations and analysis methods may change in accordance with the application programme, the modelling assumptions made, and the design codes that are implemented. When doing a comparison between the nonlinear analysis of a vertical irregular RC 2D frame and that of a 3D building, there are a number of critical changes that should be taken into consideration:

1) Complexity: When compared to 2D setback type of frames, 3D vertical irregular buildings typically present a greater degree of complexity. They often consist of irregular geometries, different floor plans, and additional components like as cores, shear walls, and slabs. These elements contribute to a more complicated structural behaviour, which in turn necessitates an analysis method that is more all-encompassing. In general increasing geometric complexity of 3D structures results in the introduction of additional load paths and redistribution mechanisms, which in consequence has an impact on the buildings' overall behaviour.

2) Dimensionality: The dimension of the structures that are being investigated is the primary distinction that may be made. A simplified model is represented by a vertical irregular RC 2D frame. In this model, the structural behaviour is often only studied in two dimensions, specifically the horizontal plane. A 3D building analysis, on the other hand, takes into account the three-dimensional aspect of the structure, taking into account both horizontal and vertical behaviour.

3) Lateral load distribution: In a vertical irregular RC 2D frame, lateral loads, such as wind or earthquake forces, are commonly distributed among the vertical elements (columns and walls) in the plane of analysis. These lateral loads can be caused by a variety of factors, including earthquakes and winds. The distribution of the load is dependent on a number of criteria including the rigidity of each part, the relative placements of the elements, and the rigidity of the floor diaphragms. When designing a structure in three dimensions, the lateral loads are spread across the entire three-dimensional structure. This distribution takes into account the relationships between the vertical and horizontal parts, as well as the diaphragms.

4) Vertical load distribution: The load distribution systems for 2D frames and 3D buildings are very different from one another due to the distinct geometrical arrangements of the two types of structures. Vertical loads are carried almost entirely by the columns and beams of a two-dimensional (2D) frame, which results in very straightforward load courses. A 3D building, on the other hand, distributes loads through a number of different elements that are related to one another, such as columns, walls, slabs, and cores. The load paths of three-dimensional buildings are more complicated and involves significant interactions between the various structural components.

5) Out-of-plane effects: The inability of a 2D frame analysis to capture out-of-plane behaviour is one of the drawbacks of using this type of analysis. Because of the interaction between vertical and horizontal elements in a three-dimensional structure, it is possible to take into account torsional effects, in addition to bending and shear in a number of different directions. These out-of-plane effects can have a considerable impact on the structural response as a whole, and they need to be taken into account in the analysis in the correct manner.

6) Modelling considerations/approach: The modelling process for a 2D frame and the modelling process for a 3D building differ in terms of the level of complexity and the level of detail, respectively. For the purpose of accurately representing the three-dimensional behaviour of a 3D building, a more extensive modelling technique that incorporates elements that can either be solid or shell is required. A 2D frame, on the other hand, can be modelled by employing simplified line elements. In addition, the nonlinearities of the material, such as the cracking of concrete or the yielding of steel, need to be appropriately considered in both of these scenarios. In a two-dimensional frame analysis, the structure is simplified into a two-dimensional plane, and the impacts of out-of-plane behaviour are ignored. It works under the assumption that the structural behaviour in the plane of analysis is primarily determined by the vertical irregularity. An examination of a building in three dimensions takes into account the behaviour of the structure in all three dimensions. It takes into account the in-plane as well as the out-of-plane responses, so capturing the impacts of the vertical irregularity in all directions.

7) Computational effort: Analysing a 3D structure typically demands more processing resources than analysing a 2D frame does. This is due to the complexity of the problem. Longer analysis times and perhaps greater memory requirements are the result of a 3D model's increased complexity, additional degrees of freedom, and higher number of components.

8) Modelling approach: In a two-dimensional frame analysis, the structure is simplified into a two-dimensional plane, and the impacts of out-of-plane behaviour are ignored. It works under the assumption that the structural behaviour in the plane of analysis is primarily determined by the vertical irregularity. An examination of a building in three dimensions takes into account the behaviour of the structure in all three dimensions. It takes into account the in-plane as well as the out-of-plane responses, so capturing the impacts of the vertical irregularity in all directions.

9) Torsional Effects: When compared with 2D frames, the role that torsional effects play in 3D buildings is significantly more substantial. Torsional behaviour is typically constrained in a two-dimensional frame because the structure predominantly deforms along a single plane. However, due to their often asymmetrical layouts or irregular geometry, three-dimensional buildings are susceptible to experiencing substantial torsional moments. These torsional effects have the ability to influence the manner in which the internal forces are distributed and result in complex structural responses.

10) Structural Stability: When comparing 2D frames to 3D buildings, the structural stability factors are different. Vertical irregular RC 2D frames may have stability concerns linked to their planar behaviour, such as sway instability or out-of-plane buckling of parts. These concerns can occur because of the planar behaviour of the frames. The presence of vertical irregularities, as well as the interplay between vertical elements (columns, walls, etc.) and horizontal elements (slabs, floors, etc.), make stability an even more important consideration in 3D buildings.

CHAPTER 4 PROPOSED DAMAGE INDEX

4.1 General

Seismic damage estimation can be done in a number of ways, including analytical methods using computer simulations and mathematical models, empirical methods based on noticeable damage patterns, experimental techniques and other methods. The approach employed depends on the information and resources available as well as the level of estimating accuracy that is were looking for. It's essential to keep in mind that estimating seismic damage is a challenging process which frequently necessitates the skills of structural engineers, seismologists, geotechnical engineers, and other experts with competence in earthquake engineering and risk evaluation. The research that has been done up till now has demonstrated that irregularities in the building configuration produce an unexpected response that results in severe damage when subjected to seismic loads [6].

The process of evaluating and quantifying damages using some computation methods by applying several engineering demand parameters caused to RC irregular buildings, infrastructure, and other real estate as a result of an earthquake or other seismic event is known as seismic damage estimating. The damage estimation of seismic event is important for various purposes, including structural engineering design, emergency response planning, and post-disaster recovery efforts. Seismic damage estimation has involved to evaluate the structural performance and integrity of important infrastructure elements such as dams, bridges, and buildings. In calculating seismic damage of structural members, structural characteristics are taken into account, a structure's vulnerability to seismic forces depends on its analysis methods, design, quality of construction, and material selections.

The height of the building, the structural system (such as reinforced concrete or steel), the lateral load-resisting components (such as shear walls or moment frames), and the type of foundation are all factors that are taken into account when assessing the structural performance. Several researchers had given various damage index formulae to compute the numerical value to identify its damage state. Each method has its own benefits, drawbacks, and application range depending on the exact context and evaluation objectives. Practising engineers have to select the optimal method to estimate seismic damage to the building elements before finalizes the structural design. The methods for

calculating the damage index have been selected after careful consideration of the data, resources, and the degree of accuracy required.

Damage to the building's structural parts, which occurs as a consequence of significant deformation and the concrete becoming nonlinear, is the principal factor that contributes to either the full or partial collapse of irregular reinforced concrete buildings [49].Although there has been an increase in analytical and experimental study on the seismic behaviour of concrete buildings during the past four decades, systematic efforts to quantify the extent of seismic damage to a structure have only been made since about 1980. There are mainly two different damage index approaches that various researches had taken into their study, one is deterministic and second is probabilistic damage indices. A distinction between deterministic and probabilistic indices can be made depending on the mathematical method implemented to calculate the damage index.

The probabilistic method seemed to be the best alternative given the uncertainties related with both the seismic action and the mechanisms of RC components' capacity to withstand reverse cyclic loading applied at high strain rates. This was the case despite the fact that both of these factors were under the control of the researchers. However, deterministic damage indices have received a significant amount of attention so far. This is primarily due to the fact that they are relatively simple to calculate, that they have the potential for direct application in practical circumstances and, most importantly, that the amount of computational effort required to determine them is significantly less than the amount of effort required to determine probabilistic damage indices [50].

Since a consequence of the fact that a number of studies have noted in their published works that vertical irregularities in RC buildings can cause partial or full damage to the structural components, it is necessary to evaluate the damage index of irregular RC buildings due to the unpredictability of building responses. It is possible to accomplish this objective by employing engineering demand parameters (EDPs) such as strength, stiffness, ductility, lateral displacement (drift), and torsion, amongst other important engineering demand factors, to describe the failure process. Before performing damage estimation for RC buildings, the most important things to consider are the factors that have been presented. In particular, the modelling assumptions for nonlinear structural analysis and the selection of seismic lateral load types (static or dynamic loads) are two areas in which there is a large amount of uncertainty in damage computation. It is possible for the actual

strengths of structural components and members to be considerably different from those predicted for study; but, in the majority of instances, these correct strengths will not be recognised [51].

The current study develops and applies enhanced drift-based, stiffness-based and energy-based damage indices for a variety of irregular 3D structures with considerable torsion caused on by the unexpected response carried on by vertical irregularities. Flexural yielding for beams and columns is the main focus of the majority of damage indices. Every type of plastic hinge subjected to nonlinear analysis can use on the recommended methodology. The following is a summary of the advantages and limitations of the new damage indices (DIs) evaluation.

Advantages:

1) The DI is ideal for measuring structural stiffness changes, drift against lateral loads, and absorbed energy associated to the first hysteretic cycle. This may be done regardless of the performance level the DI has been calculating at.

2) Damage may be determined at any loading level on the pushover curve as instead of assuming the most significant displacement or deformation of the buildings near the point of collapse.

3) Damage induced by factors other than flexural yielding can be simulated by using the suggested indices, which can be employed in this way. In this particular scenario, the models are able to account for all of the possible failure modes.

4) Following the application of the lateral load for each incremental pushover analysis step, the stiffness is evaluated, and then the DI is computed while taking into consideration the overall impact of the stiffness degrading. Instead, compute the stiffness by first factoring in the effects of the inertia and damping forces, and then ensuring that the construction frame is in a state of equilibrium.

5) The nonlinear analysis allows for the possibility of computing distinct deteriorating stiffnesses based on the direction of the load at a number of different stated performance levels.

6) Due to the ease with which it may be implemented, the minimal amount of calculations it requires, and the fact that it is effective, it is an ideal substitute to nonlinear time history analysis. It eliminates the need for complicated, time-consuming, and data-intensive

nonlinear time history analysis, which is dependent on a significant amount of ground motion information.

7) Drift-based damage index formulae, which were especially designed for vertical irregular buildings, have the potential to be beneficial for quick evaluation of damage estimation using only a few factors. This is because the formulas were specifically constructed for vertical irregular buildings. The use of nonlinear regression theory contributed to the development of these formulas.

Limitations:

1) The limits of the pushover analysis approach have an impact on the applicability and reliability of the provided damage estimates. This constraint can be overcome by using pushover analysis with other analytical methodologies as well as taking into consideration the suggestions provided by seismic design codes. The behaviour of the vertically irregular RC building will be studied in a more comprehensive manner as a result of this.

2) It necessitates the application of accurate nonlinear modelling; failing to accomplish so would make the nonlinear outcomes unreliable.

This chapter provides three alternate seismic damage computation methodologies to evaluate the overall status of the structure's damage as a result of the various equations. The use of these methods on a 3D irregular RC building has been examined. The first approach is absorbed energy-based damage computation, which is based on the pushover curve and obtained by nonlinear static analysis. A damage index is a type of damage occurrence that takes into account various EDP variants and consists of all of these EDPs. In order to compute the damage index, a number of studies had to be carried out, as can be seen in Table 6.1.A conceptual flowchart is shown in Figure 6.1for the purpose of evaluating the seismic performance of RC buildings in terms of the damage index.

Table 6.1 Summary of damage index

Damage Index	Details to describe (damage index) DI	Proposed empirical formula
A) Local Damage Index		
P. Rajeev, K.K. (2014) Wijesundara [52]	Based on the amount of energy dissipated on concentrically braced steel frame.	$DI = \frac{E_{Dissi.energy}}{E_{Capacity\ energy}}$

Park and Ang (1985) [33]	Based on linear combination of maximum plastic Displacement and plastic dissipated energy.	$DI = \frac{d_m}{d_u} + \beta_e \frac{\int dE}{F_y d_u}$
Powell and Allahabadi (1988) [51]	Based on plastic deformations and ductility	$DI = \frac{U_{max} - U_y}{U_{mon} - U_y}$
Niu and Ren, (1996) [53]	Similar to Park and Ang (1985), but it is formulated with different parameters.	$DI = \frac{\theta_m}{\theta_u} + \alpha \left[\frac{E}{E_u}\right]^{\beta}$
B) Global Damage Index		
Roufaiel and Mayer (1987) [54]	Deformation based DI	$DI = \frac{d_m - d_y}{d_u - d_y}$
Di Pasquale and Cakmak (1988) [55]	Based on time period of an equivalent SDOF system, 1) Max. softening DI	$DI = 1 - \frac{T_{initial}}{T_{final}}$
	2) Plastic based	$DI = 1 - \left[\frac{T_{inital}}{T_{final}}\right]^2$
	3) Final softening	$DI = 1 - \left[\frac{T_{final}}{T_{maxi}}\right]^2$
Ghobarah A., Abou-Elfath H., and Biddah A. (1999) [22]	Based on stiffness of the structure before and after an earthquake	$DI = 1 - \frac{K_{final}}{K_{initial}}$
A. Cinitha, P. K. Umesha, Nagesh R Iyer and N. Lakshmanan (2015) [8]	1) Strain hardening	$DI = \frac{\sqrt{\frac{S_d}{S_a}} - \sqrt{\frac{S_{do}}{S_{ao}}}}{\sqrt{\frac{S_{du}}{S_{au}}} - \sqrt{\frac{S_{do}}{S_{ao}}}}$
	2) Perfectly elasto-plastic curve	$DI = \frac{\sqrt{S_d} - \sqrt{S_{do}}}{\sqrt{S_{du}} - \sqrt{S_{do}}}$

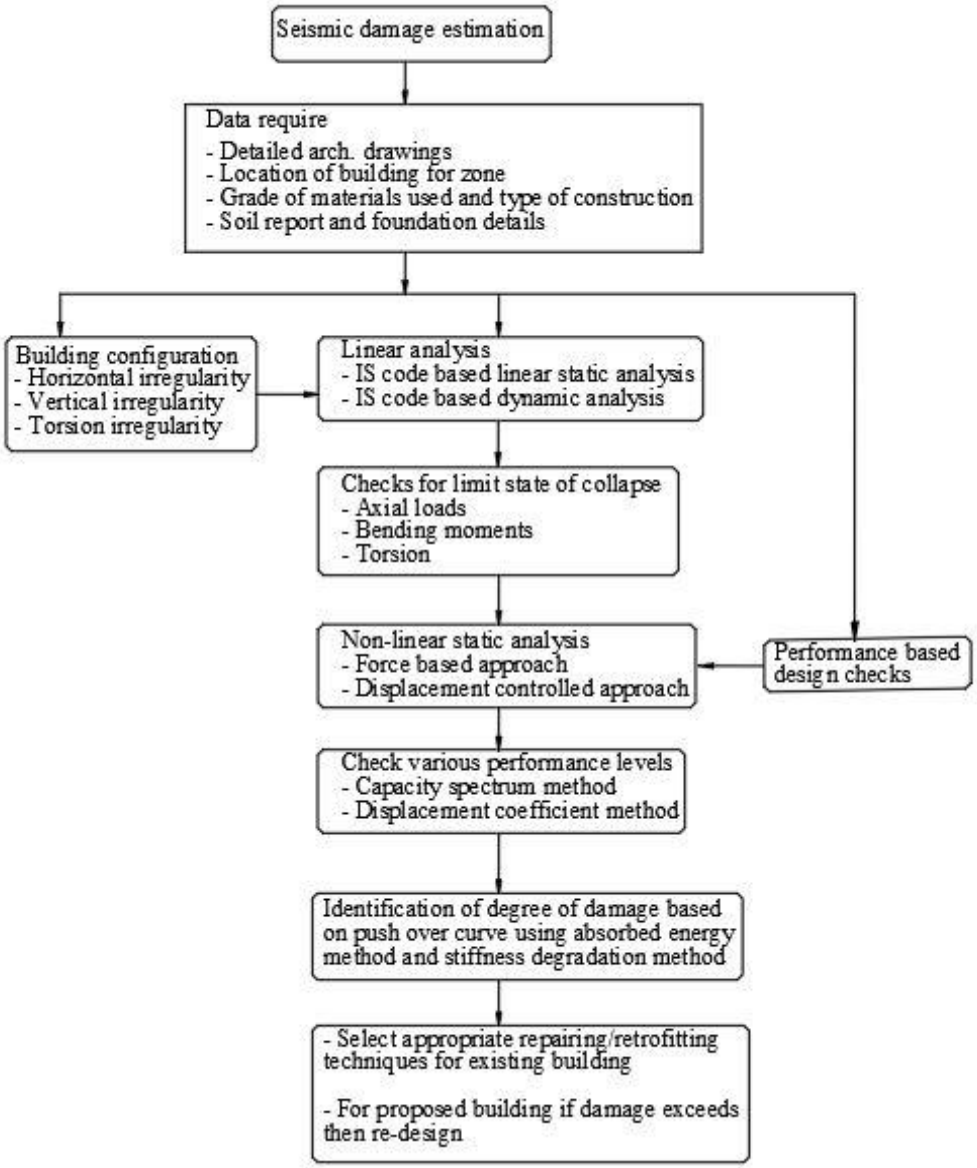

Figure 6.1 Flowchart for seismic damage evaluation in terms of damage index

4.2 Absorbed Energy based damage index

A simple non-linear pushover analysis is used to determine the RC building's energy capacity. The suggested technique is applied on variety of 3D setback type of RC buildings and compared against different available damage computation method. The behaviour of a building when it is subjected to increasing lateral forces is graphically represented by something called the pushover curve. It illustrates the relationship between the load that is applied and the lateral displacement or base shear that is produced as a result. It is usual to make use of the area under the pushover curve for looking to calculate the total dissipated energy that occurred during a seismic event. This can serve as an

indicator of the structure's capacity to withstand seismic stresses. It is important to note that the precise methods and calculations used for energy estimation might differ based on the design codes, analytical techniques, and the specific objectives of the research.

The method that has been offered involves calculating the total amount of inelastic energy that has been used by every buildings throughout the pushover analysis at each incremental load step. In the pushover analysis, the state of the building's damage is determined for each incremental load step at several performance levels using a function that takes into account the amount of energy that has been absorbed by the building. As can be seen in Figure 6.2, pushover curves may be formed in either direction by applying a monotonic load in any one of a number of different patterns. Some of these patterns are applied during analysis include (uniform) acceleration, IS 1893-2016 (an inverted triangle), and mode type (a parabolic). The area under the curve is a representation of the amount of dissipated energy that was taken in by the building itself. This method of area computation avoids the need for nonlinear dynamic analysis by virtue of the fact that it follows the collapse process that begins with the pushover curve. As a result, it makes an attempt to integrate the cumulative cyclic loading effects. The amount of damage incurred as a result of applying dynamic loadings is denoted by the amount of inelastic energy in equation (1). This energy reflects the different energies that are dissipated due to permanent plastic rotations in RC beams and columns, and it provides an indication of the level of damage. Using the first hysteretic cycle as a pushover curve, the area under the curve represents the estimated amount of energy that was absorbed at each of the possible performance levels. At a number of different curve performance levels, the lateral load was able to take up the optimum quantity of the various energies that were being applied. Damage is determined by using equation (2), which states that it is measured as the ratio of the difference between the amount of energy absorbed at the targeted performance level and the amount of energy absorbed at the elastic performance level to the ratio of the amount of energy absorbed at the ultimate displacement point and the amount of energy absorbed at the elastic performance level.

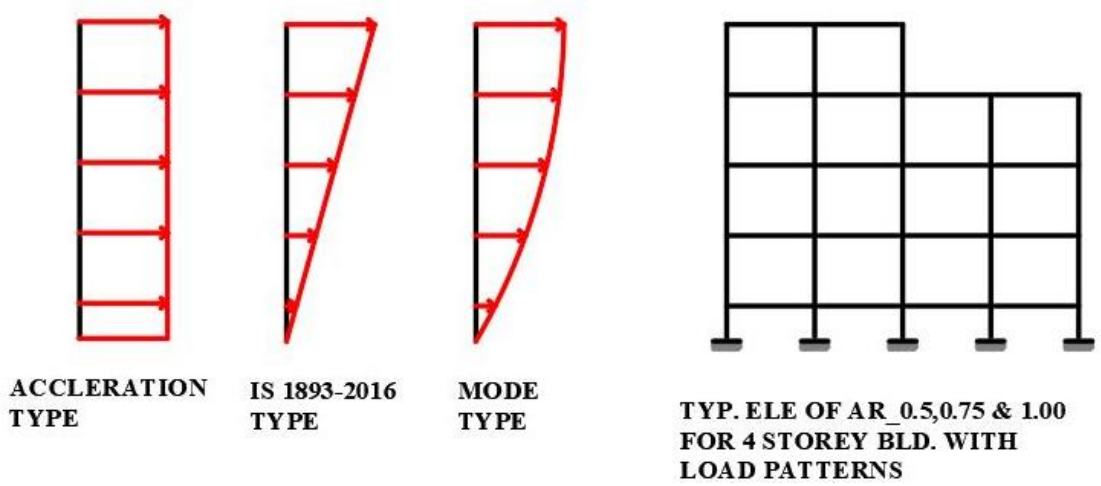

Figure 6.2 Monotonic load patterns

E_i (input energy) = $E_e + E_d$ (1)

Where, E_e (elastic strain energy) = E_k (kinetic energy) + E_s (strain energy) and

E_d (dissipated energy) = E_h (hysteretic energy) + E_ζ (viscous damping energy)

Energy based damage index, $DI_E = \frac{E_{t.p} - E_{op.}}{E_{co.} - E_{op.}}$ (2)

Where $E_{(t.p)}$ targeted point = Absorbed energy at targeted performance level

$E_{op.}$ = Absorbed energy at the operational level, and

$E_{co.}$ = Absorbed energy at collapse level

Energy at targeted point, $E_{t.p} = \int_0^{Sd_{t.p}} ax^6 + bx^5 + \cdots + C$ (3)

$Sd_{t.p.}$ = Spectral displacement at targeted performance level

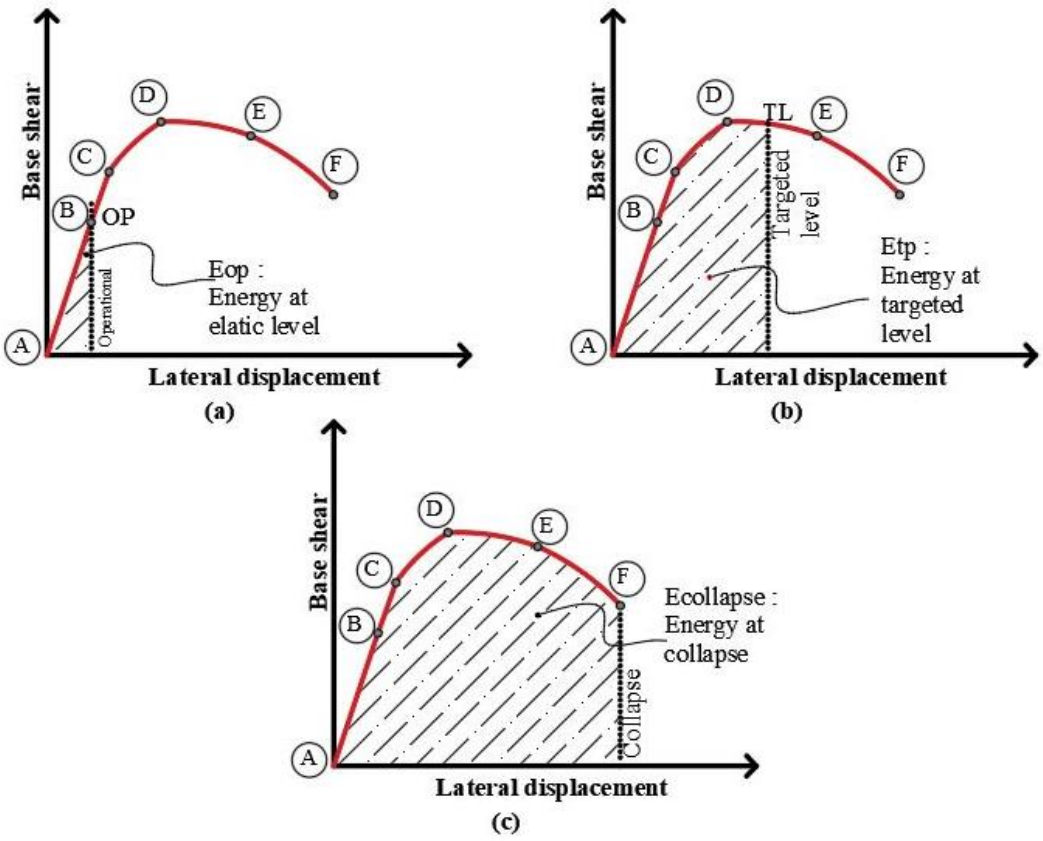

Figure 6.3 (a), (b) & (c) various absorbed energy on critical points

The entire nonlinear energy capacity of the structure is shown in Figure 6.3c (Ecollpase) as the area that is occupied through the point of the building's most ultimate lateral displacement. This area is defined as an area that extends from the point of collapse all the way up to the point of collapse under the curve. Figure 6.3a depicts the area that extends from below the pushover curve all the way to the first yielding point of the curve. This area represents the absorbed energy at the operational level (E_{op}). When the damage is calculated as shown in Figure 6.3b, the energy at the targeted performance point refers to the entire amount of dissipated energy that was taken in by the building prior to any particular performance point that was chosen. The six degree of polynomial equation that represents the fitting curve is displayed in Figure 6.4. Equation (2) is used to calculate an energy-based damage index, and equation (3) is used to calculate the amount of energy that was absorbed at a certain point along the pushover curve.

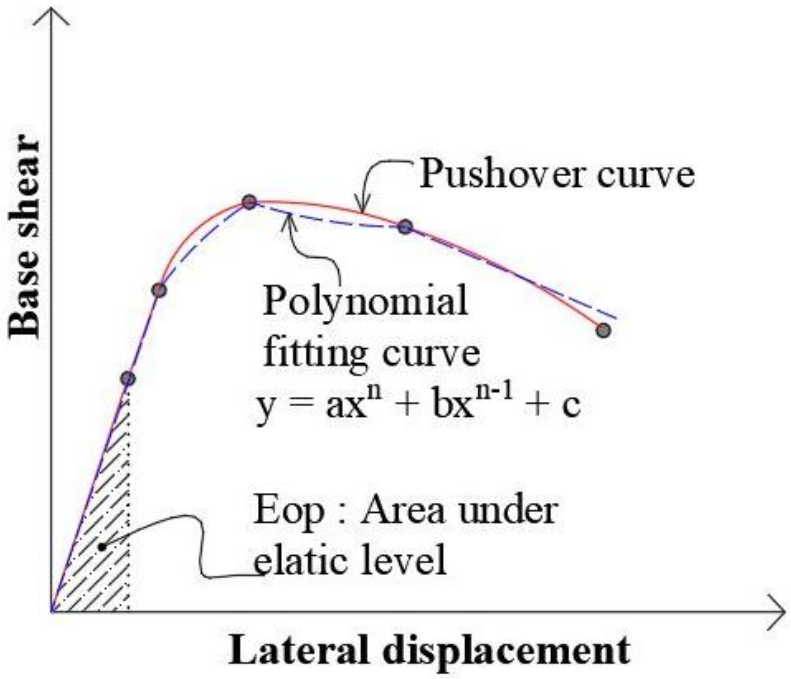

Figure 6.4 Polynomial fitting curve on pushover curve

4.3 Degrading stiffness based damage index

Pushover analysis is a nonlinear method of static analysis that examines the performance of a building under gradually increasing lateral stresses. This type of study is performed via a pushover analysis. It gives extremely helpful information on the capabilities of a building as well as its behaviour during a seismic event. Damage assessment has been the focus of work by a number of researchers in the past, including Bracci J. et al. (1989), H. Banon et al. (1982), and Ghobarah et al. (1999). These researchers focused on stiffness-based damage estimation but had not considered torsion effects in their study. On the other hand, the cumulative effect of cyclic loading has been introduced through the use of nonlinear dynamic analysis[20], which is based on plastic deformation and the dissipation of hysteretic energy. This analysis shows that the stiffness of the structure decreases with each incremental step, and this decrease is dependent on a number of different characteristics. Powell and Allahabadi (1988),[51] were the first researchers to explore the stiffness-based damage index and to carry out a nonlinear time history analysis.

In 1999, Ghobarah et al. [22] created a novel empirical technique based on pushover and nonlinear time history analysis. This technique had some limitations. As a result, M. Zameeruddin et al. (2017) [56] modified the stiffness based damage concept and used nonlinear static analysis to address the cumulative effects of stiffness degradation

parameters. This was done because the initial idea had certain limitations. But given the empirical formula had been used for regular frames only. Hence in current study had modified that method to use of irregular buildings and results of this study show a method for dealing with the decrease in stiffness that results from an increase in the lateral load. When conducting a pushover study, the capacity curve is frequently segmented into numerous components that each represent a different stage of the structural response. This is done so that the stiffness deterioration may be accounted for. Every segment represents a different level of deterioration or damage to the entire structure. It is possible to derive the capacity curve using either computational approaches, experimental tests, or a combination of the two types of data.

The linear elastic behaviour of the structure is represented by the first section of the capacity curve. When there is a significant rise in the load that is being applied, the structure will move into the nonlinear range, which is when there will be a noticeable decrease in its stiffness. This degradation is frequently shown as a descent section on the capacity curve. This section indicates lower stiffness when the structure suffers larger deformations. In pushover analysis, the degree to which there is a degradation in stiffness is dependent on a number of parameters. These elements include the structural system, the material properties, and the design details. Using the new methodology, an investigation of the cumulative effects of each incremental step was carried out. This technique makes the assumption that the stiffness decrease is continuing and that the building does not regain its initial stiffness after the load has been removed from it.

It is frequently employed as a modelling tool for the progressive failure or degradation of structural parts. Deformation of a building results in a decrease in that structure's overall stiffness, which is referred to as "stiffness degradation." This deterioration has been brought on by a number of different parameters, including the yielding of the material, cracking, and damage to structural parts. Deterioration of the building's stiffness has an effect on the response of the structure and can have a substantial impact on its overall performance. When considering about the progressive deterioration of a component's stiffness, there are two changes that need to be taken into account: the first is the position and type of the plastic hinges, and the second is the gradual member stiffness deterioration that occurs between two plastic hinges. When developing plastic hinges, a cross-section stiffness (two-surface) degradation function is applied to bring attention to the progressive yielding influence that is caused by the hinges at order to

calculate the stiffness-based damage index, the initial slope of the pushover curve is measured at multiple critical locations. This slope is employed in the calculation. A structure's level of stiffness has a relationship both directly and inversely with the monotonic lateral load and displacement that is put on it. When determining the level of stiffness for each performance level, the initial slope is employed. Equation (4) is provided as a method for computing a damage index that is based on stiffness at a certain displacement on the pushover curve. The method involves use of nonlinear elements that are dependent on the stiffness of the material, as seen in Figure 6.5.

$$\text{Stiffness based damage index, } \mathrm{DI}_{k\,@\,.tp} = 1 - \frac{\sum V}{\sum K * d} \qquad (4)$$

Where, $\mathrm{DI}_{k\,@\,t.p,}$ targeted point = Stiffness based damage index at targeted performance level

$\Sigma V = V_1 + V_2 + V_3 + \text{---} + V_n$ (Summation of base shear up to targeted performance level)

$\Sigma K = K_1 + K_2 + K_3 + \text{---} + K_n$ (Summation of stiffness up to targeted performance level)

Where 1, 2, 3 -----n are the incremental lateral steps

d = Corresponding lateral displacement at targeted performance level

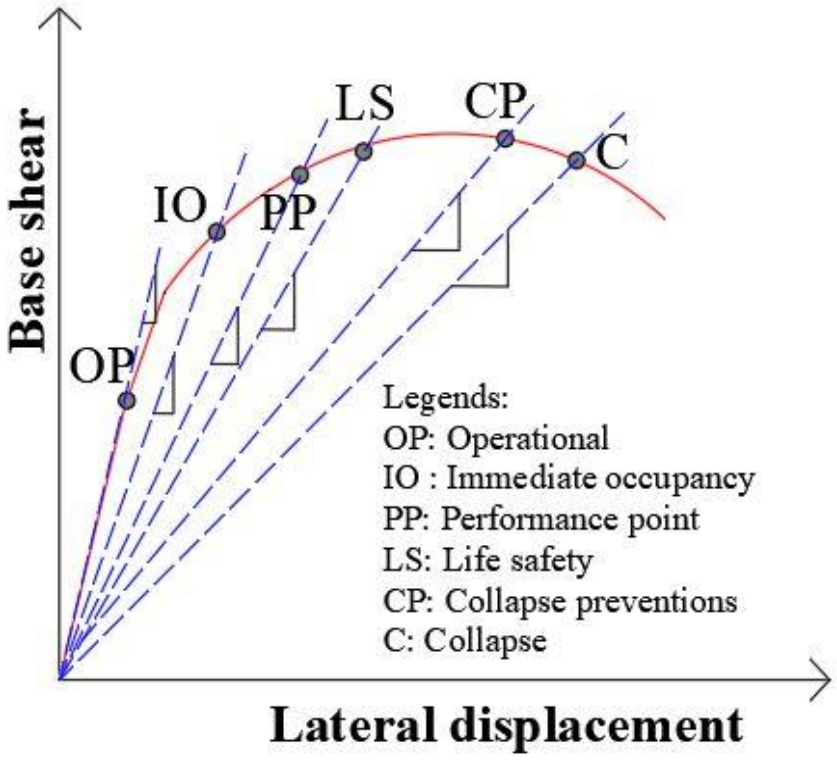

Figure 6.5 Stiffness based nonlinear parameters on pushover curve

4.4 Drift (Displacement) based damage index based on nonlinear static analysis

In this work, the drift criteria has been used to estimate the structural damage that has been done to irregular buildings using the results of pushover analysis. First, the influence of the setback is taken into consideration by employing two irregularity indices that were used by Karavasilis et al. [57]. This work attempts to describe and quantify the irregularity caused by the presence of setbacks through the use of two basic geometrical indices called $Ø_b$ and $Ø_s$. These indices, which are obtained by the following formulae as shown in equation 5 and 6 with reference to Figure 6.6, are mentioned below. The setback irregularity is first quantified using both of the irregularity indices in terms of $Ø_b$ (which is dependent on the number of bays) and $Ø_s$ (which is based on the number of floors), and then the pushover analysis is performed.

In the areas of structural engineering and architecture, a measure called the "irregularity index" is used to quantify the irregularity of a building's setback, which is also referred to as a step-back irregularity or setback irregularity. When evaluating the lateral stiffness and structural behaviour of elevated structures, in particular those with varied setbacks along their height, it is a standard procedure to employ this method. The irregularity index is determined by making a comparison between the actual setback of each level and the average setback of a sequence of floors which occur in quick succession. In most cases, the vertical axis of the building or some other reference point is used to determine where each floor's setback begins and ends. The formula that is used to calculate the irregularity index has based on the particular criteria and that are being applied, but in general, it entails analysing the variation in setbacks that exist between consecutive floors.

A greater degree of irregularity in the setback structure of the building is indicated by an increased irregularity index value. Because of this irregularity, the building's response to lateral loads, such as seismic stresses, may be altered, which may result in greater structural demands and poorer overall stability. This can have an effect on the manner in which the structure performs substantially and could cause for additional design considerations to be made in order to ensure the building's stability and performance. Setback buildings with high irregularity indices may necessitate more complex structural analysis and design procedures than regular or symmetric buildings.

$$Ø_s = \frac{1}{n_s - 1} \sum_{i=1}^{i = n_s - 1} \frac{L_i}{L_{i+1}} \quad (5)$$

$$\emptyset_b = \frac{1}{n_b - 1} \sum_{i=1}^{i=n_b-1} \frac{H_i}{H_{i+1}} \quad (6)$$

Where, n_s represents the number of stories in the frame, n_b the number of bays in the first floor, Hi the height of each level from the base, and Li the width of each bay.

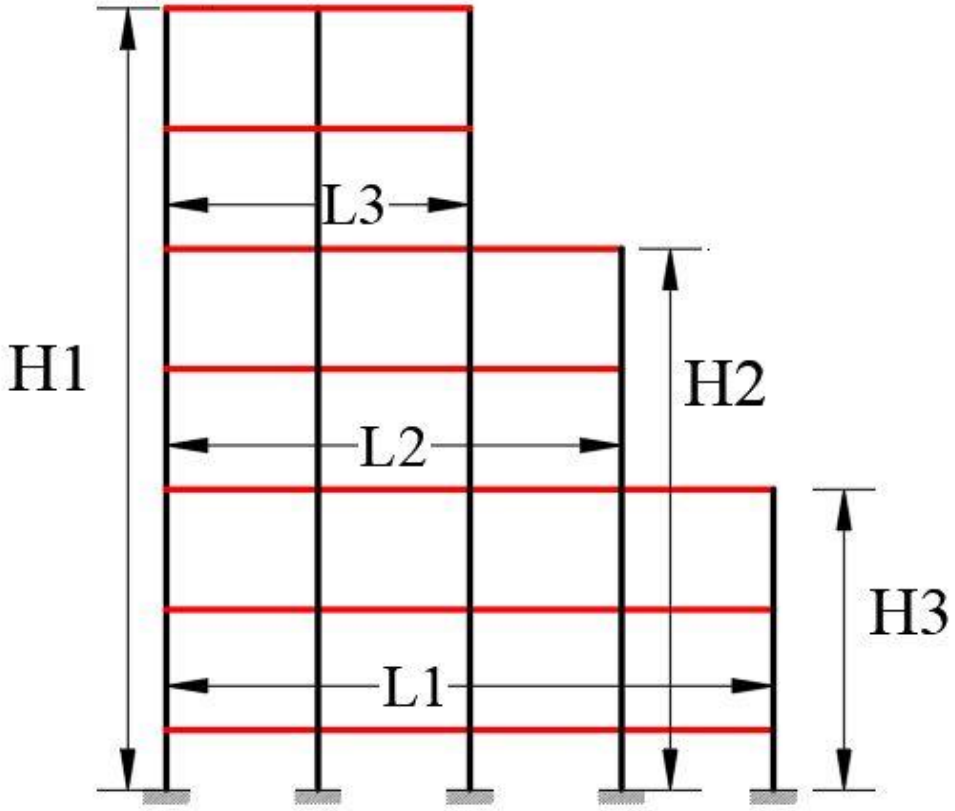

Figure 6.6 Building frame geometry of irregularity indices for definition [T.L Karavasilis et.al 2007]

When developing a drift-based damage index, the modified Park-Ang damage index[33] is generated using the stated in equation 7. In result, by making use of the database that was developed and the multi-variable nonlinear regression analysis, two separate formulas have been proposed in order to evaluate the amount of damage caused to setback types of irregular buildings. A building that is subjected to lateral force can have its overall drift computed using the formula provided in equation 8.

$$DI_{measured\ (P\ \&\ A)} = \frac{d_m - d_y}{d_u - d_y} + \frac{\beta * E_h}{F_y * d_u} \quad (7)$$

Where, d_m and d_y = maximum (targeted level) and yield displacements, respectively

d_u = ultimate displacement, β = constant parameter, which depends on structural characteristics and history of inelastic behaviour and E_h = absorbed hysteretic energy at targeted level. A value of 0.1 for the parameter β has been recommended for nominal strength deterioration [33].

$$OD = \frac{\Delta}{H} \quad (8)$$

Where, OD = overall drift,

Δ = maximum roof displacement and

H = total height of the building.

In order to predict possible damage, a mathematical model based on nonlinear regression analysis is constructed. This application demonstrates the adaptability of nonlinear regression in a variety of domains, especially in situations when linear models are unable to fully capture the relationships between variables. Researchers are able to capture complicated patterns, estimate parameters, make predictions, and get a deeper knowledge of the events that lie below the surface through the use of nonlinear regression. There are a few characteristics that may be easily established for irregular buildings, such as the irregularity indices $Ø_b$ and $Ø_s$ and Ø = product of $Ø_b$ and $Ø_s$ functions, the natural time period (T), and the overall drift of building (OD). A nonlinear regression analysis is performed using the database that is shown in Table 6.2 in order to develop two effective damage equations that may be utilised for the purpose of damage evaluation. By using the findings of the pushover study on 174 sample RC 3D irregular buildings, also Table 6.2 illustrates the association between the variables used in the proposed model and the damage as a function of the design. This was accomplished by using the results of the study. The database was utilised in order to carry out this nonlinear regression study. There are 174 observations displayed in this table. It is possible to derive and evaluate both the power equation and the quadratic polynomial equation, which are two distinct damage measures. Equation 9 and equation 10 respectively show the final mathematical expression of the suggested damage index.

$$DI_{Estimated} = T * 73.0399 + Ø * 134.5440 + OD * 45.4719 + T^2 * (-259.1186) + Ø^2 * (-162.5226) + OD^2 * (-203.9786) + T^3 * 330.6538 + Ø^3 * 80.9829 + OD^3 * 54.5167 + T^4 * (-157.9124) + Ø^4 * (-14.3809) + OD^4 * (-0.0000036) + T * Ø * 7.5548 + Ø * OD * (-0.1482) + T * OD * 1.6685 - 46.4813 \quad (9)$$

The coefficient of determination of regression, or R^2, is a statistical measure that can be used to determine how well the data fit the fitted regression model. In this case, the R^2 value is 0.9346. This demonstrates that the regression equation, when compared to the data, produces accurate results.

$$DI_{Estimated} = 8.395 * T^{0.430} * \emptyset_b{}^{0.813} * \emptyset_s{}^{-1.433} * OD^{-0.091} \quad (10)$$

To formulate the power equation using a fitted regression model, the summation of square deviation was calculated to be 5543.5, which demonstrates that the accuracy of the regression equation is not as good as that of the quadratic equation.

Table 6.2 Database of RC irregular buildings to develop drift based damage index

1	Building designation	Load type	OD @ P.P (%)	$\emptyset_b$	$\emptyset_s$	$\emptyset = \emptyset b * \emptyset s$	DI_ (measured) (P & A-1988)
1	S4_0.50_UD_X	Accl.	0.285	1.10	1.25	1.37	2.765
		IS	0.376				0.000
		Mode	0.328				4.657
2	S4_0.50_UD_Y	Accl.	0.331	1.00	1.00	1.00	4.435
		IS	0.454				0.000
		Mode	0.426				7.572
3	S4_0.75_UD_X	Accl.	0.285	1.10	1.25	1.37	1.864
		IS	0.355				4.988
		Mode	0.327				3.879
4	S4_0.75_UD_Y	Accl.	0.320	1.00	1.00	1.00	3.919
		IS	0.415				8.090
		Mode	0.409				5.916
5	S4_1.00_UD_X	Accl.	0.286	1.10	1.25	1.37	1.862
		IS	0.374				0.000
		Mode	0.327				3.819
6	S4_1.00_UD_Y	Accl.	0.313	1.00	1.00	1.00	3.337
		IS	0.421				0.000

		Mode	0.393				4.512
7	S6_0.50_UD_X	Accl.	0.296	1.06	1.17	1.24	6.417
		IS	0.398				0.000
		Mode	0.337				8.815
8	S6_0.50_UD_Y	Accl.	0.336	1.00	1.00	1.00	7.730
		IS	0.475				0.000
		Mode	0.447				14.460
9	S6_0.75_UD_X	Accl.	0.297	1.06	1.17	1.24	5.361
		IS	0.399				0.000
		Mode	0.364				0.000
10	S6_0.75_UD_Y	Accl.	0.326	1.00	1.00	1.00	7.617
		IS	0.456				0.000
		Mode	0.465				0.000
11	S6_1.00_UD_X	Accl.	0.296	1.06	1.17	1.24	5.028
		IS	0.381				26.413
		Mode	0.336				7.755
12	S6_1.00_UD_Y	Accl.	0.319	1.00	1.00	1.00	6.741
		IS	0.427				27.227
		Mode	0.417				11.906
13	S9_0.50_UD_X	Accl.	0.305	1.04	1.11	1.15	11.152
		IS	0.381				35.134
		Mode	0.345				13.342
14	S9_0.50_UD_Y	Accl.	0.338	1.00	1.00	1.00	12.402
		IS	0.443				32.982
		Mode	0.444				18.772
15	S9_0.75_UD_X	Accl.	0.304	1.04	1.11	1.15	10.521
		IS	0.417				0.000
		Mode	0.343				12.700

16	S9_0.75_UD_Y	Accl.	0.328	1.00	1.00	1.00	12.325
		IS	0.465				0.000
		Mode	0.428				17.642
17	S9_1.00_UD_X	Accl.	0.300	1.04	1.11	1.15	8.105
		IS	0.409				0.000
		Mode	0.338				10.332
18	S9_1.00_UD_Y	Accl.	0.317	1.00	1.00	1.00	10.410
		IS	0.444				0.000
		Mode	0.408				14.971
19	S4_1.00_DF_X_ REG	Accl.	0.200	1.00	1.00	1.00	5.556
		IS	0.200				8.696
		Mode	0.200				8.333
20	S4_1.00_DF_Y_ REG	Accl.	0.240	1.00	1.00	1.00	7.407
		IS	0.200				9.091
		Mode	0.200				8.332
21	S4_1.00_DF_X_ UNI_IR1	Accl.	0.200	1.10	1.25	1.37	4.762
		IS	0.200				8.696
		Mode	0.200				8.333
22	S4_1.00_DF_Y_ UNI_IR1	Accl.	0.200	1.00	1.00	1.00	4.167
		IS	0.200				4.167
		Mode	0.240				8.000
23	S4_1.00_DF_X_ UNI_IR2	Accl.	0.120	1.27	1.25	1.58	13.334
		IS	0.120				7.693
		Mode	0.120				13.334
24	S4_1.00_DF_Y_ UNI_IR2	Accl.	0.160	1.00	1.00	1.00	17.648
		IS	0.160				11.765
		Mode	0.120				5.556
25	S4_1.00_DF_X_ UNI__IR3	Accl.	0.120	1.67	1.25	2.08	14.286
		IS	0.120				10.000

		Mode	0.120				7.693
26	S4_1.00_DF_Y_ UNI_IR3	Accl.	0.120	1.00	1.00	1.00	5.797
		IS	0.160				5.882
		Mode	0.160				7.692
27	S4_1.00_DF_X_ BI_IR2	Accl.	0.120	1.27	1.25	1.58	7.143
		IS	0.080				0.000
		Mode	0.080				12.501
28	S4_1.00_DF_Y_ BI_IR2	Accl.	0.120	1.27	1.25	1.58	0.000
		IS	0.120				0.000
		Mode	0.040				0.000
29	S4_1.00_DF_X_ BI__IR3	Accl.	0.080	1.67	1.25	2.08	8.696
		IS	0.080				9.757
		Mode	0.120				10.001
30	S4_1.00_DF_Y_ BI_IR3	Accl.	0.120	1.67	1.25	2.08	7.018
		IS	0.120				0.000
		Mode	0.040				0.000
31	S6_1.00_DF_X_ REG	Accl.	0.320	1.00	1.00	1.00	4.545
		IS	0.360				6.522
		Mode	0.360				6.383
32	S6_1.00_DF_Y_ REG	Accl.	0.320	1.00	1.00	1.00	4.762
		IS	0.360				6.977
		Mode	0.360				6.667
33	S6_1.00_DF_X_ UNI_IR1	Accl.	0.200	1.06	1.17	1.24	11.765
		IS	0.200				11.765
		Mode	0.200				11.765
34	S6_1.00_DF_Y _UNI_IR1	Accl.	0.200	1.00	1.00	1.00	11.765
		IS	0.200				11.111
		Mode	0.200				11.765

35	S6_1.00_DF_X_ UNI_IR2	Accl.	0.320	1.06	1.17	1.24	0.000
		IS	0.400				0.000
		Mode	0.360				0.000
36	S6_1.00_DF_Y_ UNI_IR2	Accl.	0.360	1.00	1.00	1.00	0.000
		IS	0.440				0.000
		Mode	0.440				0.000
37	S6_1.00_DF_X_ UNI__IR3	Accl.	0.280	1.29	1.17	1.50	2.041
		IS	0.360				6.977
		Mode	0.360				4.348
38	S6_1.00_DF_Y_ UNI_IR3	Accl.	0.320	1.00	1.00	1.00	4.444
		IS	0.400				4.255
		Mode	0.400				4.444
39	S6_1.00_DF_X_ BI_IR1	Accl.	0.200	1.06	1.17	1.24	5.263
		IS	0.240				5.556
		Mode	0.200				5.556
40	S6_1.00_DF_Y _BI_IR1	Accl.	0.200	1.06	1.17	1.24	0.000
		IS	0.200				0.000
		Mode	0.240				5.263
41	S6_1.00_DF_X_ BI_IR2	Accl.	0.120	1.15	1.17	1.34	6.667
		IS	0.120				7.143
		Mode	0.120				7.143
42	S6_1.00_DF_Y_ BI_IR2	Accl.	0.160	1.15	1.17	1.34	11.765
		IS	0.160				11.765
		Mode	0.200				12.500
43	S6_1.00_DF_X_ BI__IR3	Accl.	0.160	1.29	1.17	1.50	5.556
		IS	0.160				11.765
		Mode	0.120				7.143
44	S6_1.00_DF_Y_ BI_IR3	Accl.	0.160	1.29	1.17	1.50	5.263
		IS	0.200				10.000

		Mode	0.240				15.790
45	S9_1.00_DF_X_ REG	Accl.	0.320	1.00	1.00	1.00	7.692
		IS	0.360				6.977
		Mode	0.360				7.317
46	S9_1.00_DF_Y_ REG	Accl.	0.320	1.00	1.00	1.00	8.108
		IS	0.360				7.317
		Mode	0.360				7.895
47	S9_1.00_DF_X_ UNI_IR1	Accl.	0.320	1.04	1.11	1.15	0.000
		IS	0.400				0.000
		Mode	0.360				0.000
48	S9_1.00_DF_Y _UNI_IR1	Accl.	0.360	1.00	1.00	1.00	0.000
		IS	0.440				0.000
		Mode	0.440				0.000
49	S9_1.00_DF_X_ UNI_IR2	Accl.	0.280	1.09	1.11	1.21	4.878
		IS	0.360				6.667
		Mode	0.360				0.000
50	S9_1.00_DF_Y_ UNI_IR2	Accl.	0.320	1.00	1.00	1.00	5.405
		IS	0.400				6.818
		Mode	0.440				0.000
51	S9_1.00_DF_X_ UNI__IR3	Accl.	0.280	1.15	1.11	1.28	4.651
		IS	0.360				4.348
		Mode	0.320				4.348
52	S9_1.00_DF_Y_ UNI_IR3	Accl.	0.320	1.00	1.00	1.00	5.405
		IS	0.400				6.667
		Mode	0.400				7.692
53	S9_1.00_DF_X_ BI_IR1	Accl.	0.280	1.04	1.11	1.15	11.765
		IS	0.360				6.818
		Mode	0.360				10.256

54	S9_1.00_DF_Y _BI_IR1	Accl.	0.320	1.04	1.11	1.15	9.677
		IS	0.360				6.977
		Mode	0.320				6.667
55	S9_1.00_DF_X_ BI_IR2	Accl.	0.280	1.09	1.11	1.15	5.000
		IS	0.360				6.667
		Mode	0.400				13.158
56	S9_1.00_DF_Y_ BI_IR2	Accl.	0.280	1.09	1.11	1.21	5.263
		IS	0.400				6.667
		Mode	0.120				0.000
57	S9_1.00_DF_X_ BI__IR3	Accl.	0.280	1.15	1.11	1.28	4.878
		IS	0.360				6.522
		Mode	0.400				9.756
58	S9_1.00_DF_Y_ BI_IR3	Accl.	0.280	1.15	1.11	1.28	4.878
		IS	0.400				6.122
		Mode	0.040				0.000

4.5 Drift (Displacement) based damage index based on nonlinear dynamic analysis

The extent of damage to a vertical irregular buildings using the nonlinear time history results is determined by a number of different parameters, including the type of structure, dynamic characteristics, plastic displacement, and design variables, amongst others. Taking into account all of these elements is an extremely difficult task. Through the application of nonlinear regression analysis, a mathematical model is developed in this investigation for the purpose of predicting the extent of damage to vertical irregular 3D RC buildings. A few parameters, such as the irregularity indices which defined earlier, the fundamental period (T), and the overall drift (OD), which can be easily determined for buildings, are considered to be the independent variables in order to develop a simple model that is also applicable. The damage (DI) is considered to be the dependent variable. On the basis of the database shown in Table 6.2, a nonlinear regression analysis is carried out in order to create effective damage equations for use in damage estimation. The

quadratic polynomial equation is used in the process of deriving and evaluating the various damage factors.

The selection of time histories is a crucial step in the process of carrying out nonlinear dynamic analysis, as it helps to ensure that the results are correct and representative. In connection to the building that is being analysed, take into consideration the magnitude and the distance to the fault of the earthquakes. The earthquake data need to be scaled suitably so that they correspond to the design criteria and intensity levels that which are aiming for. Make sure the time periods represented by the selected records are consistent with the expected response time of the structure. When trying to account for the inherent variability that is present in seismic events, it is frequently recommended to examine numerous ground motion data.

Choose a sample of earthquake records that is representative of the entire set and that represents a broad spectrum of ground motion properties, such as the various ground motion directions, the frequency content, and the intensities. In this study eight different ground motions data have been used as shown in Table ***6.3***. For the study of nonlinear dynamic analysis, a total of 58 distinct types of RC buildings are taken into consideration. The eight time histories that are described below are used as lateral load characteristics for each building. Because of this, a total of 464 results have been generated after performing the nonlinear dynamic analysis, and the average value of displacement and drift was adopted for the regression analysis. In the process of developing a damage index based on drift, the damage index in terms of power equation developed by Habibi et al. (2016)[6] is utilised as the measured damage index, and its mathematical equation can be found in equation 11.

The building's designation, for example, S4_0.50_UD_X, denotes that it is four stories high with a 0.5 plan aspect ratio and user-defined plastic hinge parameters. The specified empirical accelerograms are scaled in terms of amplitude in time domain to make them fit the code-based seismic hazard level, which is usually described as 5% damped elastic response spectra of acceleration. The scaling method used here is based on eliminating the difference between the scaled acceleration response spectrum and the horizontal elastic design spectrum of the Indian seismic code using the SiesmoMatch 2022 software. The SiesmoMatch 2022 software is generated the response spectra, which is compatible with the IS 1893-2016 [13]. The graph depicted in Figure 6.7 illustrates the

distinct linear-elastic acceleration response spectra of scaled accelerograms. The selected eight original time-histories and matched time histories are shown in Figure 6.8 to Figure 6.23.The parameters used in the research paper of Habibi et al [6] of the power equation to derive the drift-based damage index from measured data are shown in Table 6.4.

Table 6.3 Grounds motion data [45]

TH no.	Record name	Name of Earthquake	Mw	R_{JB} (km)	VS 30 (m/s)	PGA (g)	PGV (cm/s)	PGD (cm)
TH 1	IMPVALL.I_ I-ELC 180	Imperial Valley-02, 1940	6.95	6.09	213.44	0.281	30.93	8.66
TH 2	IMPVALL.I_ I –ELC 270	Imperial Valley-02, 1940	6.95	6.09	213.44	0.211	31.29	24.18
TH 3	SUPER.B_ B-POE 360	Superstition Hills-02, 1987	6.54	11.16	316.64	0.286	29.02	11.56
TH 4	BIGBEAR_ HOS 180	Big Bear-01, 1992	6.46	34.98	296.97	0.101	11.85	3.36
TH 5	KOBE_ KAK 000	Kobe, 1995	6.9	22.50	312	0.24	20.8	6.39
TH 6	KOBE_ SHI 000	Kobe, 1995	6.9	19.40	256	0.225	31.33	8.38
TH 7	KOCAELI_ DZC 180	Kocaeli, 1999	7.51	13.60	281.86	0.312	58.85	44.05
TH 8	DUZCE_ DZC 270	Duzce, 1999	7.14	0.00	281.86	0.515	84.29	47.99

Where, Mw = moment magnitude of earthquake

RJB = Joyner-Boore's distance (Source to site distance less than 50 km)

VS_{30} =Shear-wave velocity to 30 m depth of subsoil,

PGA = Peak ground acceleration, PGV = Peak ground velocity and PGD = Peak ground displacement

In order to make an accurate assessment of the possibility for damage, a mathematical model based on nonlinear regression analysis is developed using the drift of several RC buildings.

$$DI_{measured} = 0.0671 * T^{0.8688} * \emptyset_b{}^{-0.0335} * \emptyset_s{}^{0.5797} * OD^{0.6971} \quad (11)$$

Where, T = Natural time period as per IS 1893-2016, OD = Overall drift in %, $\emptyset_b$ = Bay factor of irregularity index, $\emptyset_s$ = Storey factor of irregularity index

The suggested damage index, expressed mathematically with NLDA results, is shown in Equation 12.One statistical metric for assessing the accuracy of a regression model fit to a set of data is the coefficient of determination of regression (R^2). The R^2 value in this instance is 0.99. This shows that the nonlinear regression equation is reliable when compared to the data.

$$DI_{Estimated} = T * 0.0414 + \emptyset * 0.6379 + OD * 0.1575 + T^2 * (-0.007) + \emptyset^2 * (-0.629) + OD^2 * (-0.254) + T^3 * (-0.014) + \emptyset^3 * 0.2709 + OD^3 * 0.1832 + T^4 * 0.0099 + \emptyset^4 * (-0.043) + OD^4 * (-0.048) + T * \emptyset * (-0.002) + \emptyset * OD * (0.0057) + T * OD * (0.0333) - 0.278 \quad (12)$$

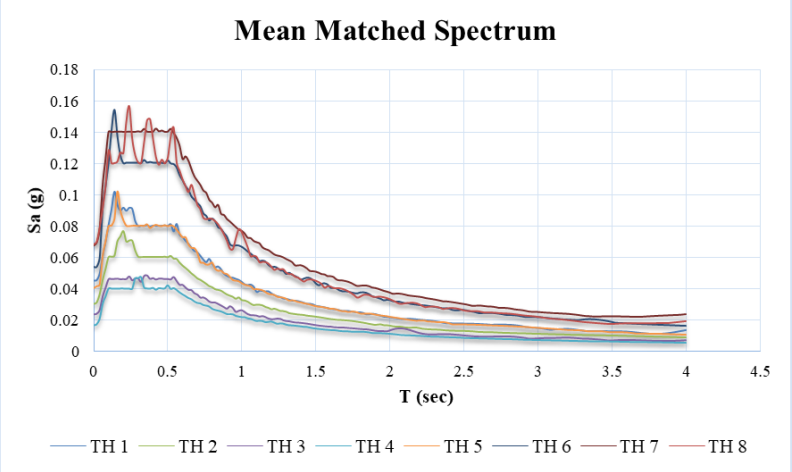

Figure 6.7 Mean Scaled spectra of eight time histories

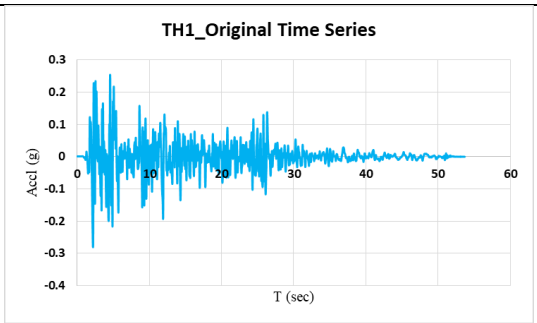

Figure 6.8 Original time history of Imperial Valley-02, 1940_180

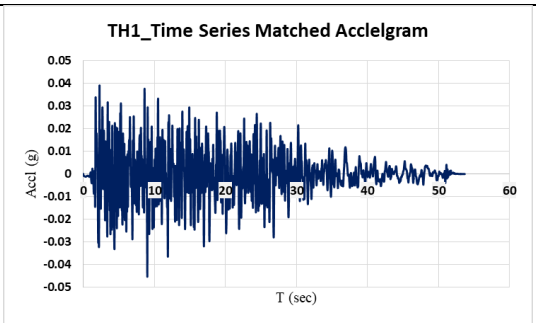

Figure 6.9 Matched time history of Imperial Valley-02, 1940_180

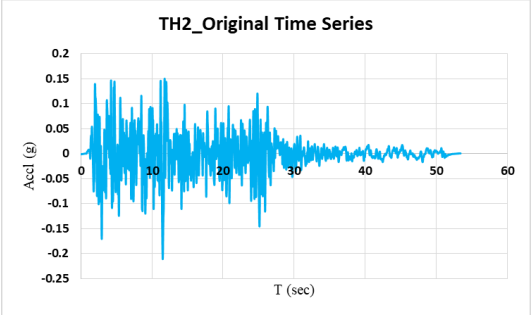

Figure 6.10 Original time history of Imperial Valley-02, 1940_270

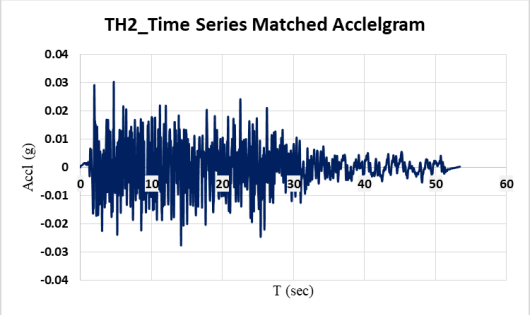

Figure 6.11 Matched time history of Imperial Valley-02, 1940_270

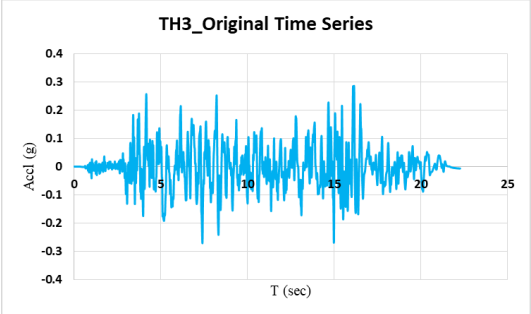

Figure 6.12 Original time history of Superstition Hills-02, 1987

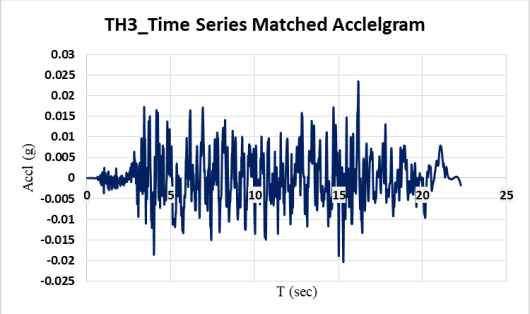

Figure 6.13 Matched time history of Superstition Hills-02, 1987

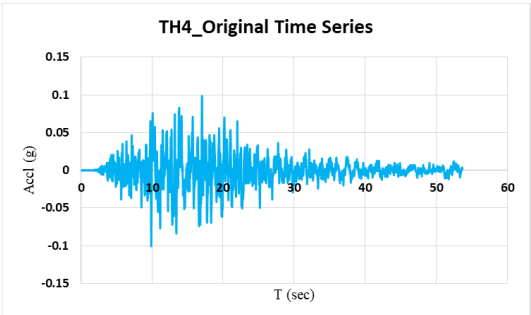

Figure 6.14 Original time history of Big Bear-01, 1992

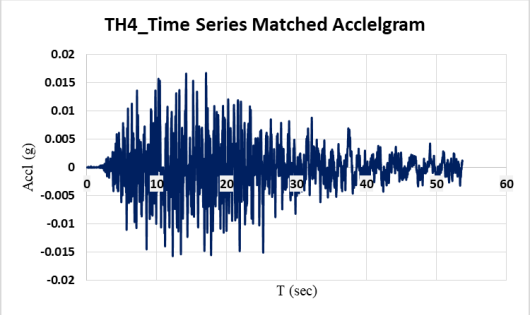

Figure 6.15 Matched time history of Big Bear-01, 1992

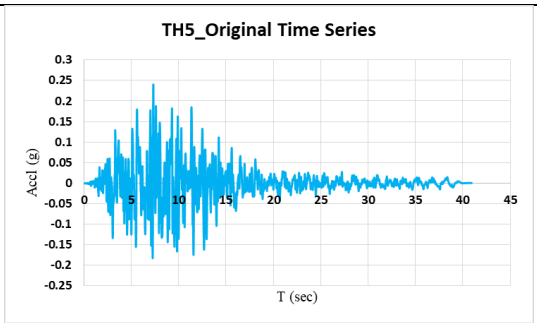

Figure 6.16 Original time history of Kobe, 1995_KAK

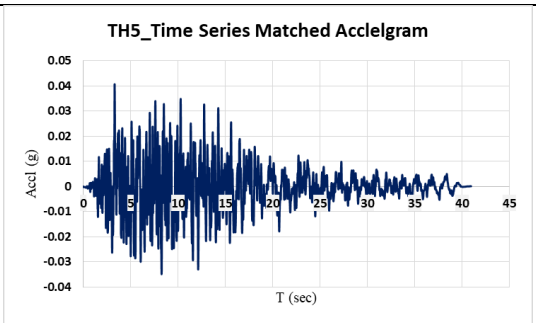

Figure 6.17 Matched time history of Kobe,1995_KAK

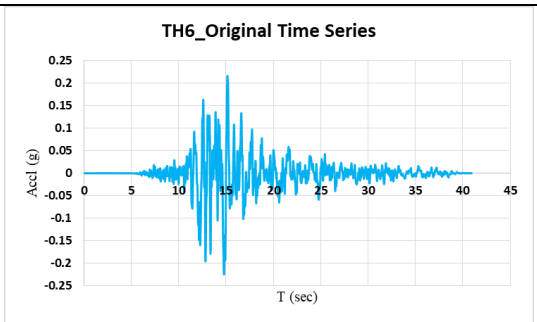

Figure 6.18 Original time history of Kobe, 1995_SHI

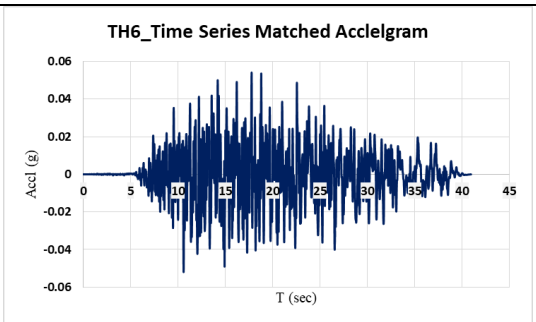

Figure 6.19 Matched time history of Kobe, 1995_SHI

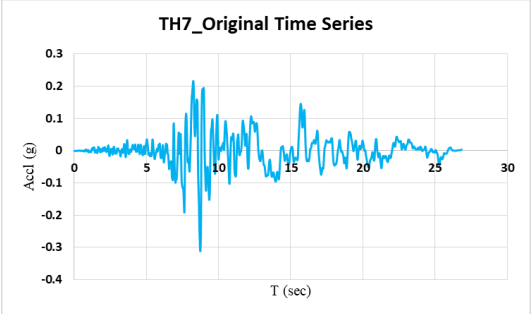

Figure 6.20 Original time history of Kocaeli, 1999

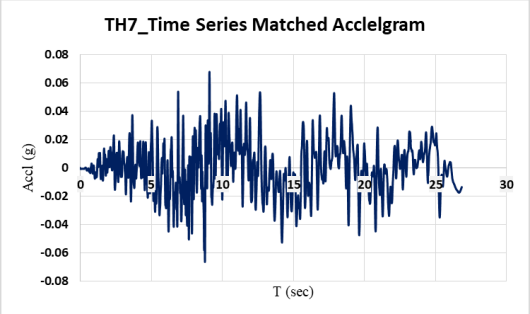

Figure 6.21 Matched time history of Kocaeli, 1999

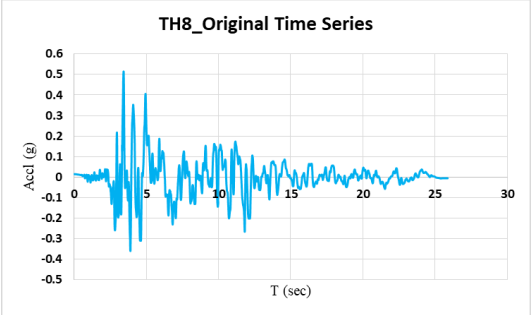

Figure 6.22 Original time history of Duzce, 1999

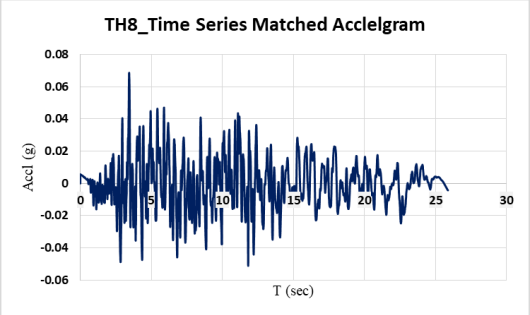

Figure 6.23 Matched time history of Duzce, 1999

Table 6.4 Parameters for calculation of measured drift based damage index using power equation of Habibi et.al.

Sr. No.	Building designation	OD (%)	Time period (sec)	$Ø_b$	$Ø_s$
1	S4_0.50_UD_X	0.82855	0.322	1.10	1.25
2	S4_0.50_UD_Y	0.83524	0.455	1.00	1.00
3	S4_0.75_UD_X	0.82928	0.322	1.10	1.25
4	S4_0.75_UD_Y	0.83201	0.372	1.00	1.00
5	S4_1.00_UD_X	0.82965	0.322	1.10	1.25
6	S4_1.00_UD_Y	0.82947	0.322	1.00	1.00
7	S6_0.50_UD_X	0.59802	0.483	1.06	1.17
8	S6_0.50_UD_Y	0.63311	0.683	1.00	1.00
9	S6_0.75_UD_X	0.59848	0.483	1.06	1.17
10	S6_0.75_UD_Y	0.62579	0.558	1.00	1.00
11	S6_1.00_UD_X	0.59888	0.483	1.06	1.17
12	S6_1.00_UD_Y	0.63061	0.483	1.00	1.00
13	S9_0.50_UD_X	0.48571	0.724	1.04	1.11
14	S9_0.50_UD_Y	0.5582	1.025	1.00	1.00
15	S9_0.75_UD_X	0.4882	0.724	1.04	1.11
16	S9_0.75_UD_Y	0.53308	0.837	1.00	1.00
17	S9_1.00_UD_X	0.4765	0.724	1.04	1.11
18	S9_1.00_UD_Y	0.50323	0.724	1.00	1.00
19	S4_1.00_DF_X_ REG	0.78909	0.322	1.00	1.00
20	S4_1.00_DF_Y_ REG	0.79544	0.322	1.00	1.00

21	S4_1.00_DF_X_ UNI_IR1	0.83958	0.322	1.10	1.25
22	S4_1.00_DF_Y _UNI_IR1	1.54347	0.322	1.00	1.00
23	S4_1.00_DF_X_ UNI_IR2	0.75769	0.322	1.27	1.25
24	S4_1.00_DF_Y__UNI_IR2	0.76403	0.322	1.00	1.00
25	S4_1.00_DF_X_ UNI__IR3	0.75824	0.322	1.67	1.25
26	S4_1.00_DF_Y_ UNI_IR3	0.76533	0.322	1.00	1.00
27	S4_1.00_DF_X_ BI_IR2	0.75565	0.322	1.27	1.25
28	S4_1.00_DF_Y_ BI_IR2	0.75703	0.322	1.27	1.25
29	S4_1.00_DF_X_ BI__IR3	0.75834	0.322	1.67	1.25
30	S4_1.00_DF_Y_ BI_IR3	0.75742	0.322	1.67	1.25
31	S6_1.00_DF_X_ REG	0.6153	0.483	1.00	1.00
32	S6_1.00_DF_Y_ REG	0.61626	0.483	1.00	1.00
33	S6_1.00_DF_X_ UNI_IR1	0.55804	0.483	1.06	1.17
34	S6_1.00_DF_Y _UNI_IR1	1.00125	0.483	1.00	1.00
35	S6_1.00_DF_X_ UNI_IR2	0.59194	0.483	1.06	1.17
36	S6_1.00_DF_Y_ UNI_IR2	0.6084	0.483	1.00	1.00
37	S6_1.00_DF_X_ UNI__IR3	0.59825	0.483	1.29	1.17
38	S6_1.00_DF_Y_ UNI_IR3	0.60496	0.483	1.00	1.00
39	S6_1.00_DF_X_ BI_IR1	0.57433	0.483	1.06	1.17
40	S6_1.00_DF_Y _BI_IR1	0.57044	0.483	1.06	1.17
41	S6_1.00_DF_X_ BI_IR2	0.99851	0.483	1.15	1.17
42	S6_1.00_DF_Y_ BI_IR2	0.69563	0.483	1.15	1.17
43	S6_1.00_DF_X_ BI__IR3	0.56963	0.483	1.29	1.17

44	S6_1.00_DF_Y_ BI_IR3	0.56866	0.483	1.29	1.17
45	S9_1.00_DF_X_ REG	0.5127	0.724	1.00	1.00
46	S9_1.00_DF_Y_ REG	0.51465	0.724	1.00	1.00
47	S9_1.00_DF_X_ UNI_IR1	0.47723	0.724	1.04	1.11
48	S9_1.00_DF_Y _UNI_IR1	0.50417	0.724	1.00	1.00
49	S9_1.00_DF_X_ UNI_IR2	0.46654	0.724	1.09	1.11
50	S9_1.00_DF_Y_ UNI_IR2	0.49174	0.724	1.00	1.00
51	S9_1.00_DF_X_ UNI__IR3	0.46632	0.724	1.15	1.11
52	S9_1.00_DF_Y_ UNI_IR3	0.48326	0.724	1.00	1.00
53	S9_1.00_DF_X_ BI_IR1	0.47336	0.724	1.04	1.11
54	S9_1.00_DF_Y _BI_IR1	0.47885	0.724	1.04	1.11
55	S9_1.00_DF_X_ BI_IR2	0.4769	0.724	1.09	1.11
56	S9_1.00_DF_Y_ BI_IR2	0.47773	0.724	1.09	1.11
57	S9_1.00_DF_X_ BI__IR3	0.46167	0.724	1.15	1.11
58	S9_1.00_DF_Y_ BI_IR3	0.45861	0.724	1.15	1.11

CHAPTER 5 NUMERICAL MODELLING & DISCUSSION OF RESULTS

5.1 Numerical modelling

The proposed DIs have been applied to 4-, 6-, and 9-storey regular and vertically irregular RC buildings with setbacks of unidirectional and bidirectional types, as illustrated in Figure 7.1 and Figure 7.2. In the short, medium, and long periods, there are respective representations of three separate, three-dimensional RC buildings. The heights of the foundation and the remaining floors are, respectively, 2 metres and 4 metres. For example, a building may be marked as S4_0.5_UD_UNI_IR1_X_, which indicates that it has four storeys, with 0.5 plan aspect ratio, is of the unidirectional setback type, considers the user defined plastic hinges parameters and first level to be irregular, and X denotes that it faces horizontally. In order to compute DIs, a series of parametric analyses were carried out, during which time three distinct monotonic loadings, two directions of setback, different types of plastic hinges and the three distinct storey irregularities were taken into consideration. It is estimated that the dimensions of rectangular (outside) columns will be 300 mm X 600 mm for four- and six-storey buildings, and 300 mm X 750 mm for nine-storey buildings.

It is considered that each building has square (internal) columns measuring 600 mm X 600 mm, and that each storey has beams measuring 230 mm X 450 mm. Concrete with a compressive strength of 25 MPa and steel with a yield strength of 415 MPa are typically used in the construction of buildings. Main bars and lateral ties are typically made of steel with same yielding strength. The slab and floor finish each have a set of particular dead loads, which are assigned at 3.75 and 1.00 kN/m^2 respectively. Brick masonry walls with a thickness of 230 mm are used on the outside beams, while brick masonry walls with a thickness of 115 mm are used on the internal beams. All slabs are subjected to a live load of 2 kN/m^2, which is the standard as per IS 875- II provisions. The design of buildings is governed by the regulations IS 456-2000 [58] and IS 1893-2016 [13], both of which include provisions for linear static and dynamic analysis. A linear analysis is carried out using a zone factor of 0.16, an importance factor of 1, a response reduction factor of 5, and a medium soil stratum. This is all done in accordance with IS 1893-2016 [13], which specifies the manner in which the seismic load have to be computed. IS 1893-2016 [13] recommends a reduced moment of inertia for structural elements like beams and columns

than the previous IS 1893- 2002 [47] requires. As a direct consequence of this, the current study takes into account both the strong column and the weak beam conceptions.

The linear static and dynamic analysis is carried out, and the structural design of each RC building is carried out in accordance with the provisions outlined in IS 456-2000 [58]. Reinforcement of each beam and column is provided as required after finalising the linear analysis and as per load combination. For example, whatever reinforcements are required for each RC building; same are provided in the beams and columns for that building. The reinforcement requirements that were provided for a building with four storeys are shown in Figure 7.3 to Figure 7.8, values have been shown in cm^2. The nonlinear analysis was performed once the structural design had been completed before being applied to its final state. It is essential to the efficiency of nonlinear static and dynamic methods that reinforced concrete members be modelled using an inelastic constitutive equation. Plastic hinges are which have been used to give the reinforced concrete members their inelastic characteristics. According to performance-based seismic engineering (PBSE), plastic hinges can either be controlled by deformation (referred to as ductile action) or controlled by force (referred to as brittle action). Limitations on plastic rotation are specified for reinforced concrete beams and columns by the PBSE standards.

The current study assigns beam-column joints a default and user defined deformation-controlled (ductile action) type of plastic hinge characteristic that is 5% apart from beam and column joints for each buildings case. According to ATC 40-1996, the maximum allowable displacement for any RC building was determined to be 4% of the building's height. The ideal force-deformation curve is shown in Figure 7.9, and each feature of each plastic hinge is presented there. The most critical part of the structure is the representation of the building's worst-case scenario when it is subjected to lateral loading. In order to calculate the lateral seismic force distribution for the pushover investigation, acceleration, IS 1893, and mode types of loading patterns are applied. Figure 7.9 also represents a simplified version of the load-deformation relationship.

This version depicts a linear reaction from point A to point B, which is followed by a linear response from point B to point C at a decreased level of stiffness. Ignoring the effects of vertical loads operating through lateral displacements, the slope that is expected to exist from point B to point C in the absence of any definite experiment value can be considered to be between 0 and 10 percent of the slope that was present at the beginning.

The highest amount of the member's strength is represented by the ordinate of point C, whereas the deflection at which a significant amount of that strength deteriorates is shown by the coordinate of point D. The remaining strength of the structure is shown by the line DE.

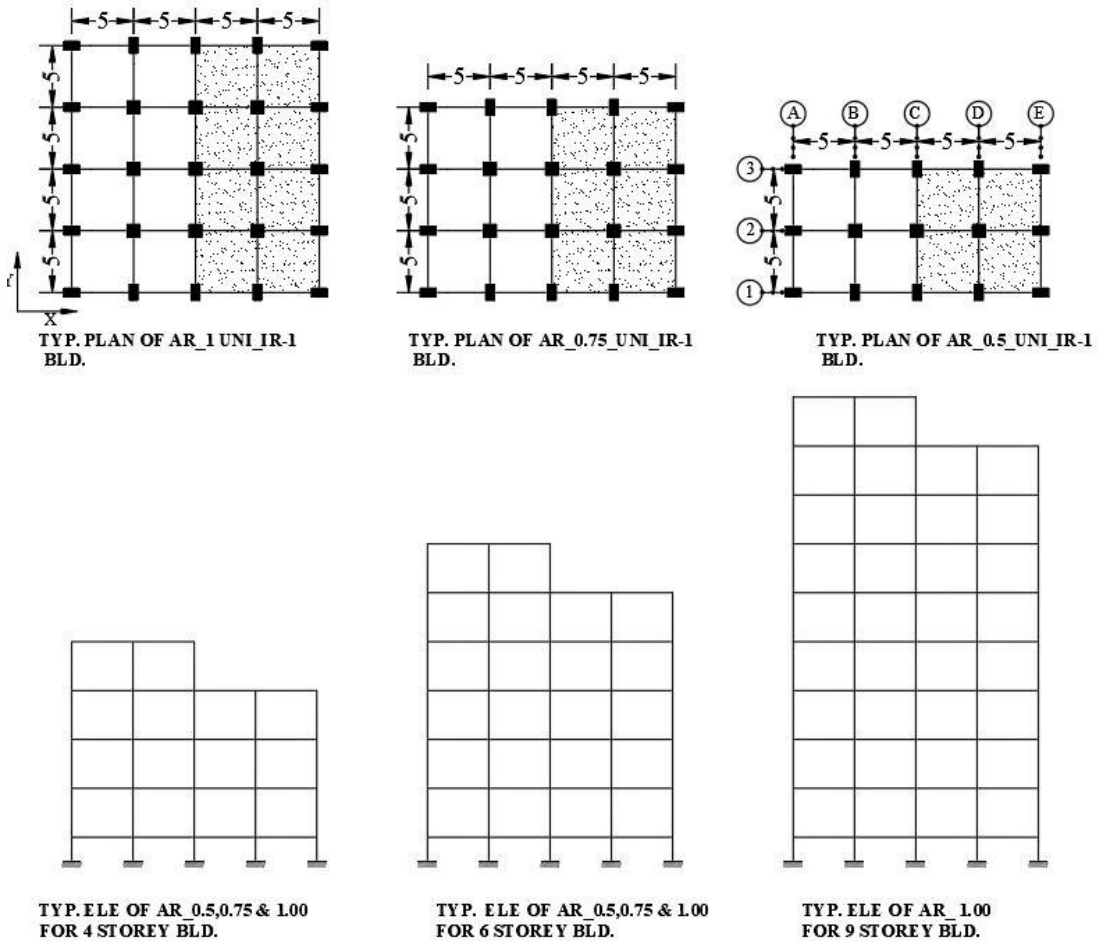

Figure 7.1 Typical plans and elevation for RC irregular buildings with various AR

The torsion in the present study is caused by a vertical irregularity in the building, which creates unanticipated reactions during analysis. Standard 174 pushover curves have been employed in the process of damage assessment at a variety of the curve's performance levels. For the purpose of analysing the general behaviour in terms of pushover curves of the various buildings shown in Figure 7.10 to Figure 7.183, a total of 58 graphs of drift in relation to energy-based DI and 58 graphs of drift in relation to stiffness-based DI have been formed. The pushover curves of these RC buildings which are shown in Figure 7.1,

were made by using user-defined plastic hinges with different plan aspect ratios, as shown in

Figure 7.10 to Figure 7.63. For the purpose of estimating damage, the first hysteretic cycle is taken into account for an extensive spectrum of energies, together with initial and secant stiffness at a variety of performance levels. The pushover curves of these RC buildings are shown in accordance with Figure 7.2,were analysed by utilising the default type of plastic hinges with various types of setbacks and vertical irregularities, as illustrated in Figure 7.64 to Figure 7.183.

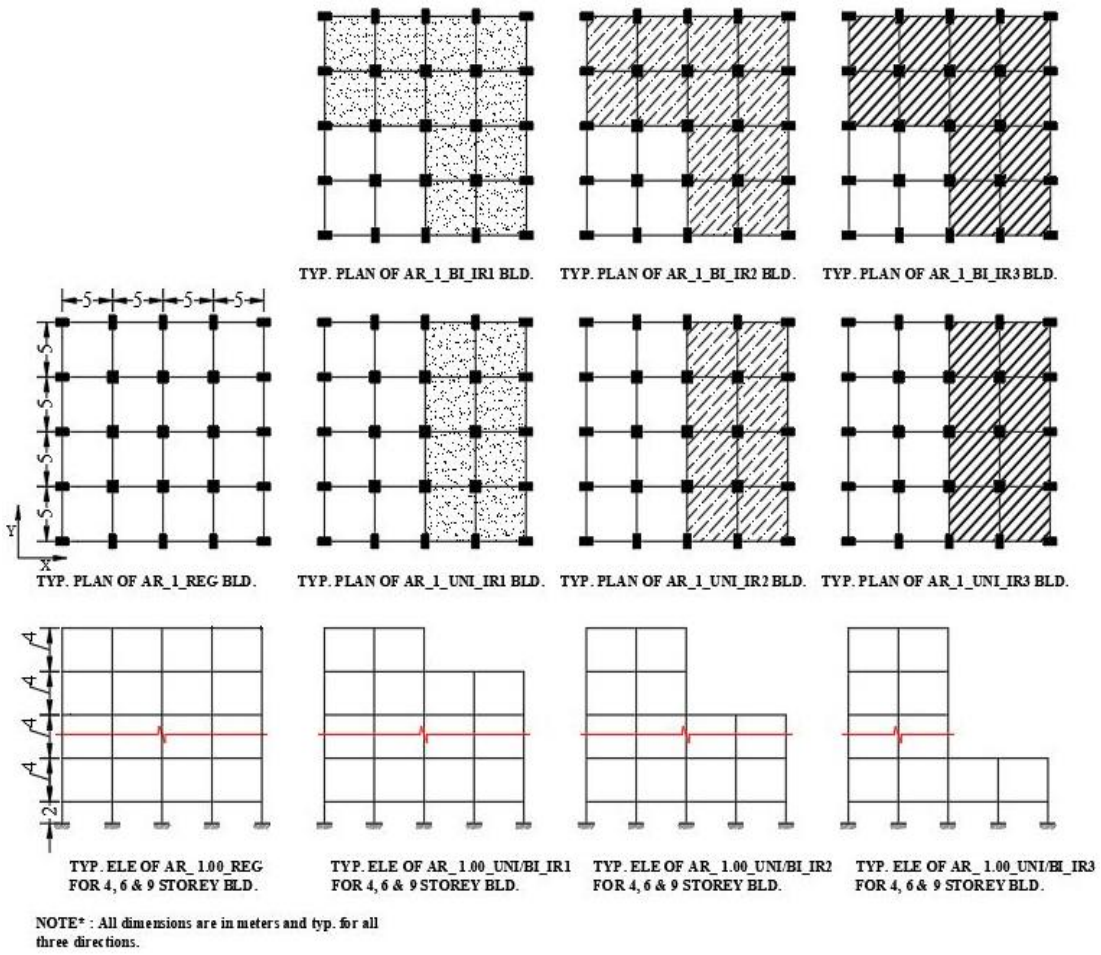

Figure 7.2 Typical plans and elevation with unidirectional and bidirectional setback

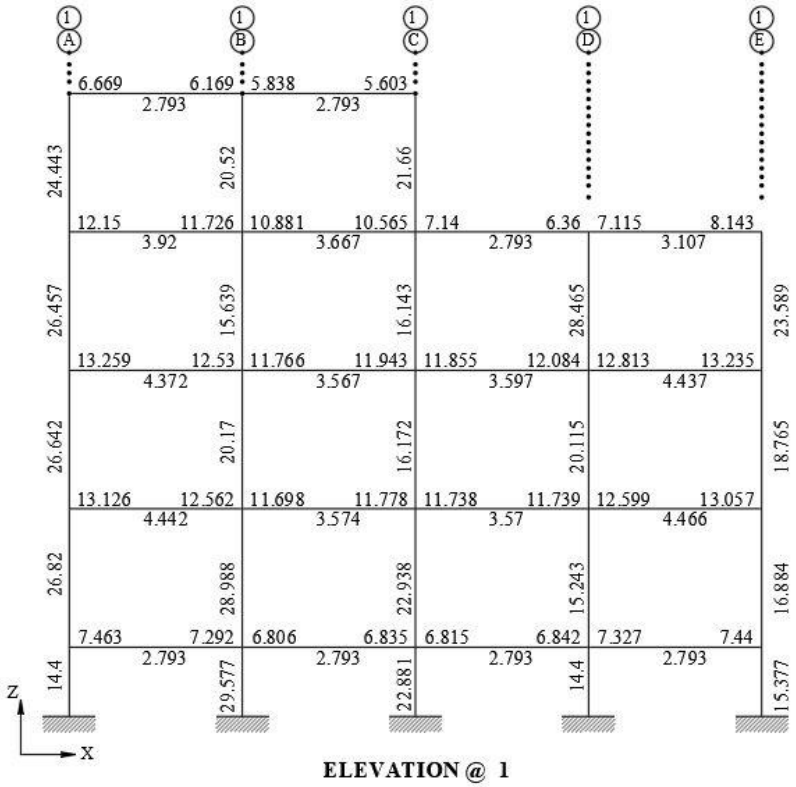

Figure 7.3 Reinforcement details for 4 storey building for grid -1

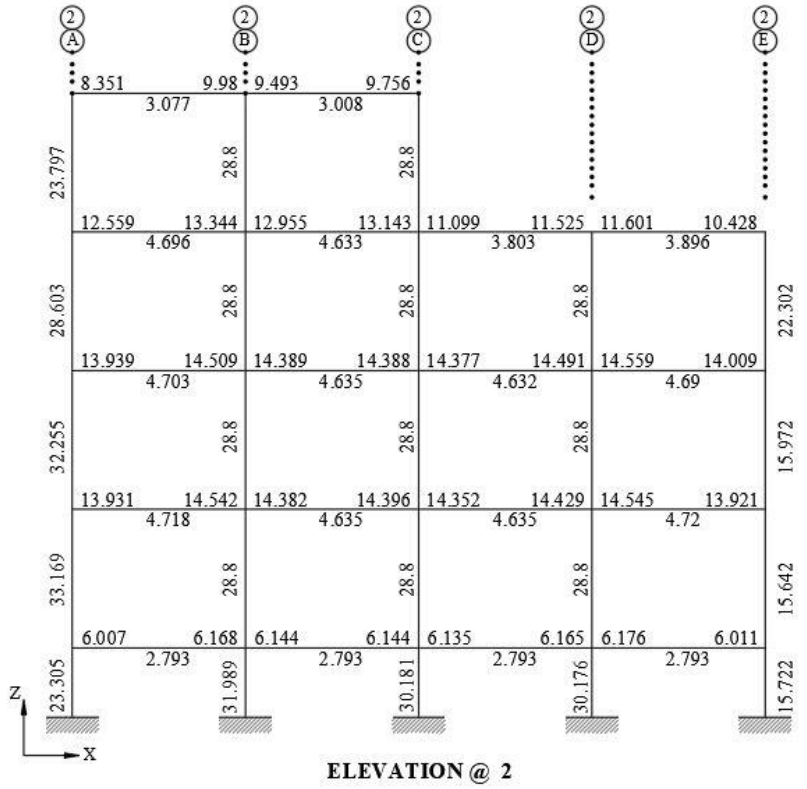

Figure 7.4 Reinforcement details for 4 storey building for grid -2

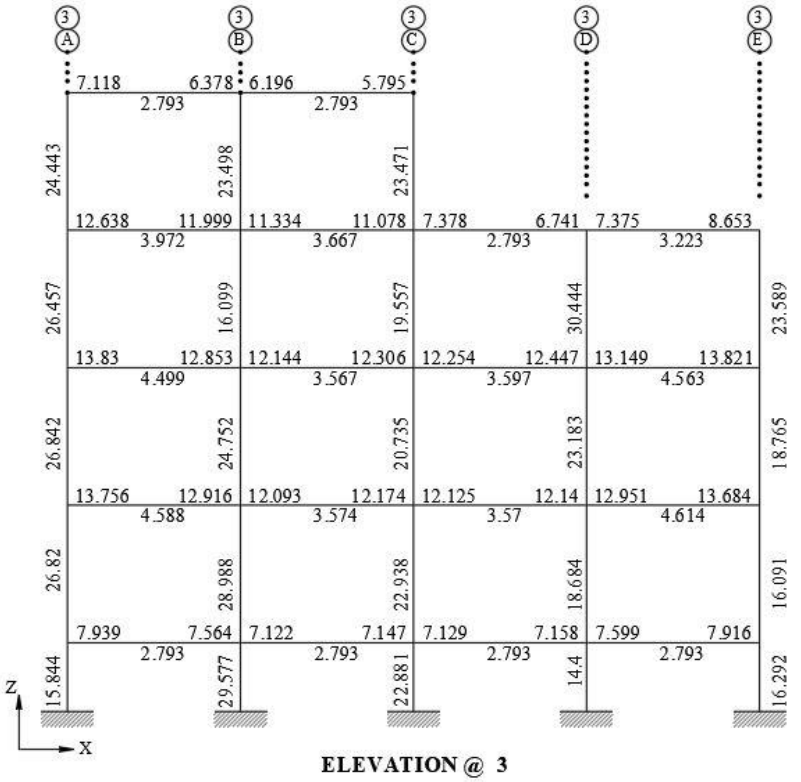

Figure 7.5 Reinforcement details for 4 storey building for grid -3

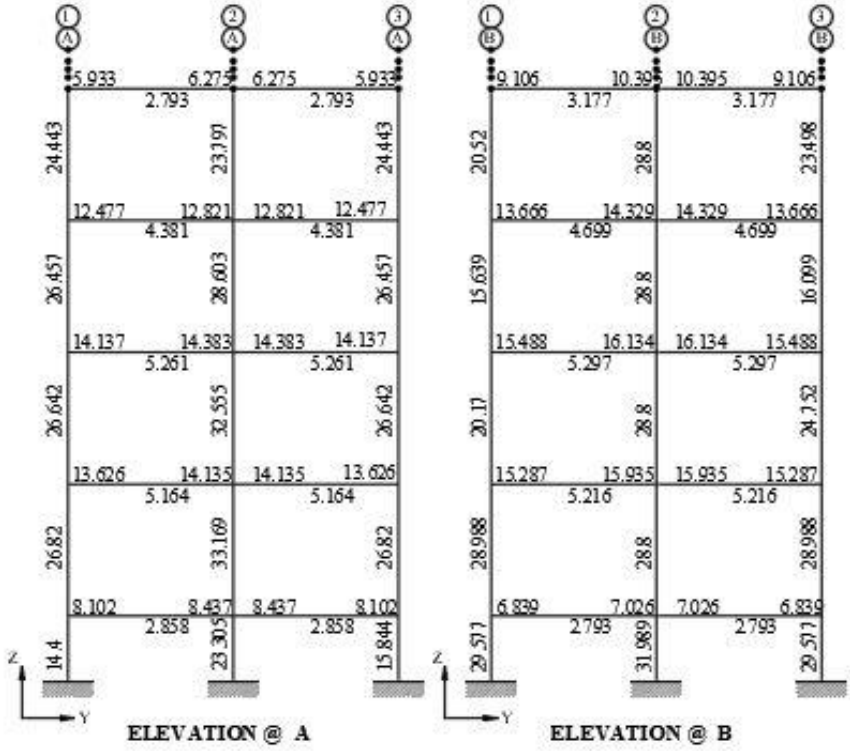

Figure 7.6 Reinforcement details for 4 storey building for grid A & B

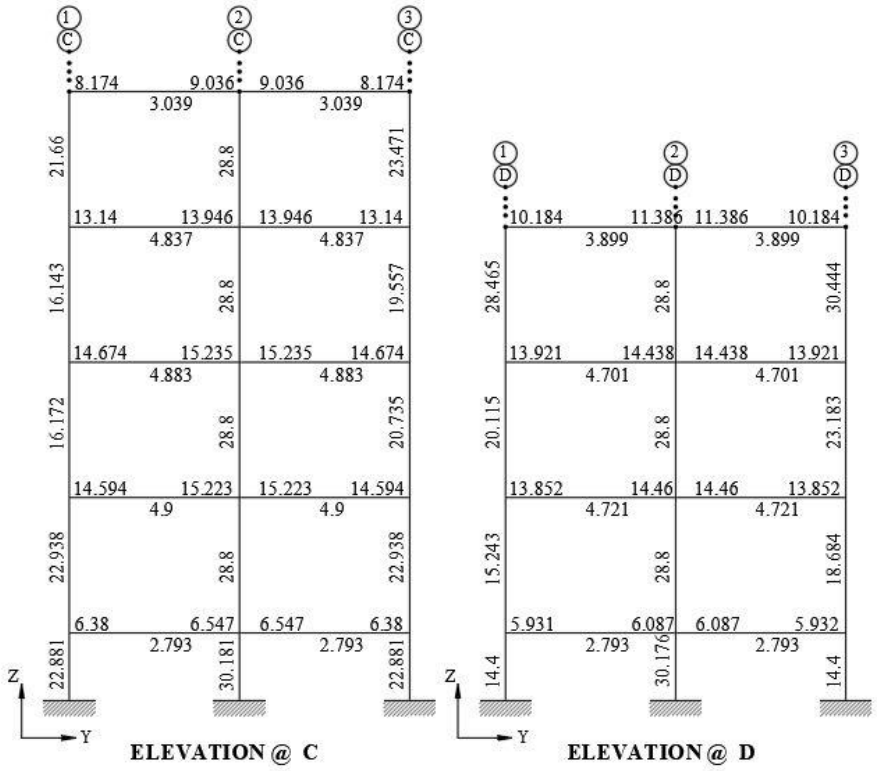

Figure 7.7 Reinforcement details for 4 storey building for grid C & D

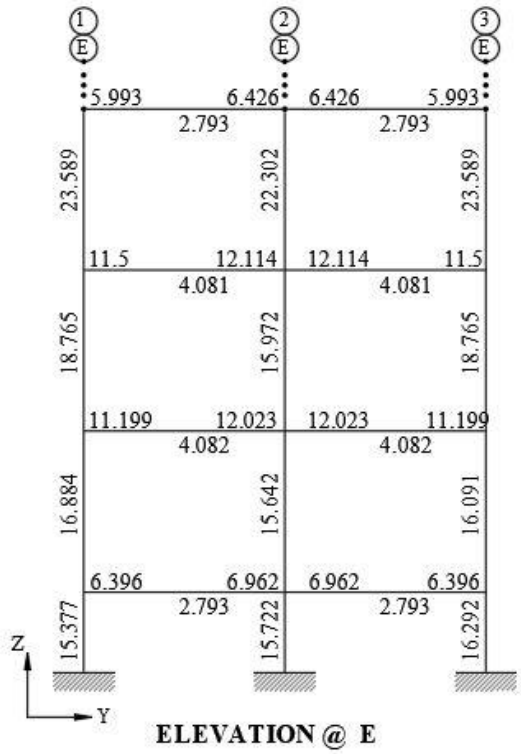

Figure 7.8 Reinforcement details for 4 storey building for grid -E

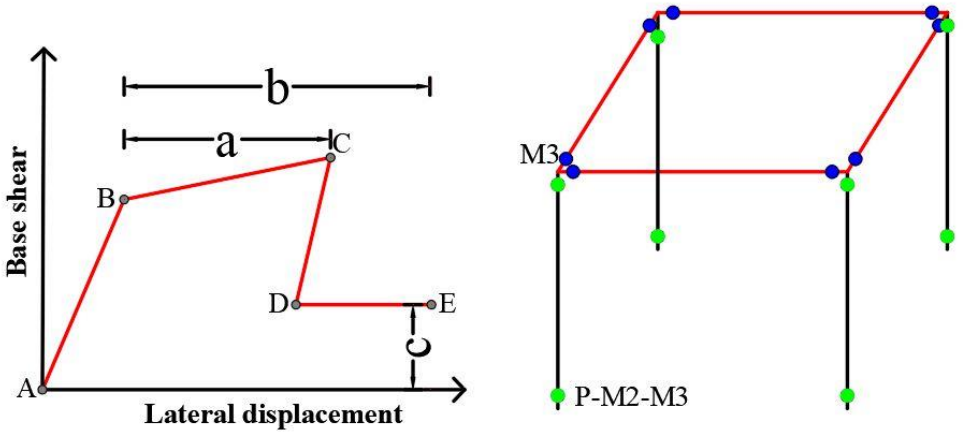

Figure 7.9 Typical force-deformation curve and hinges details

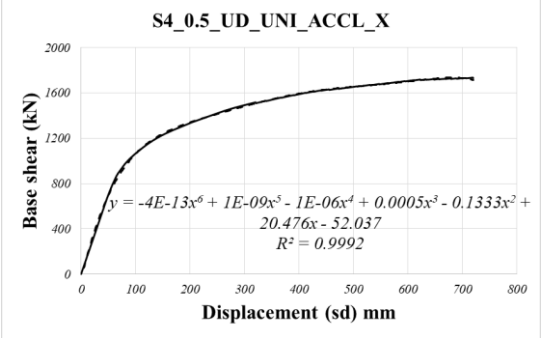

Figure 7.10 Pushover curve of building S4_0.5_UD_UNI_IR1_ACCL_X

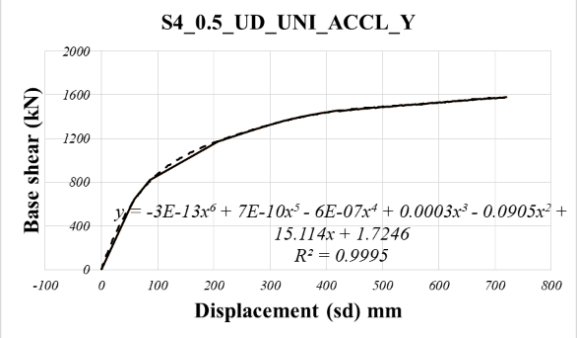

Figure 7.11 Pushover curve of building S4_0.5_UD_UNI_IR1_ACCL_Y

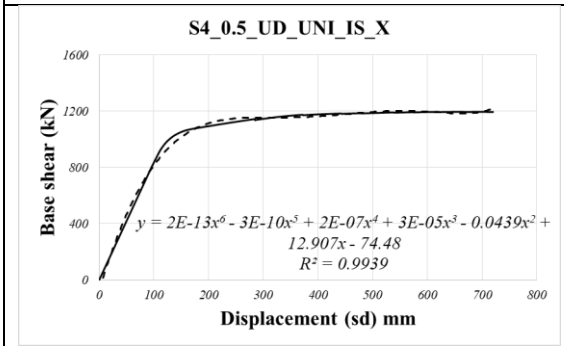

Figure 7.12 Pushover curve of building S4_0.5_UD_UNI_IR1_IS_X

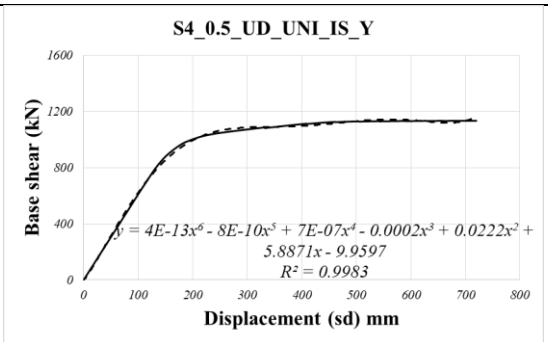

Figure 7.13 Pushover curve of building S4_0.5_UD_UNI_IR1_IS_Y

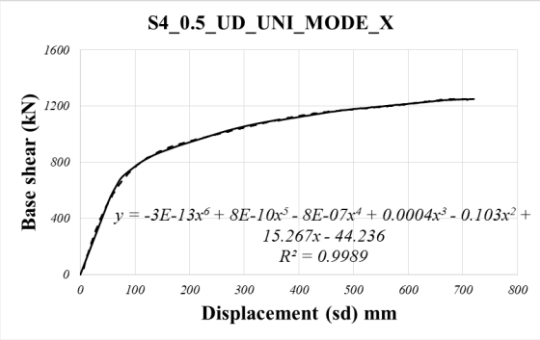

Figure 7.14 Pushover curve of building S4_0.5_UD_UNI_IR1_MODE_X

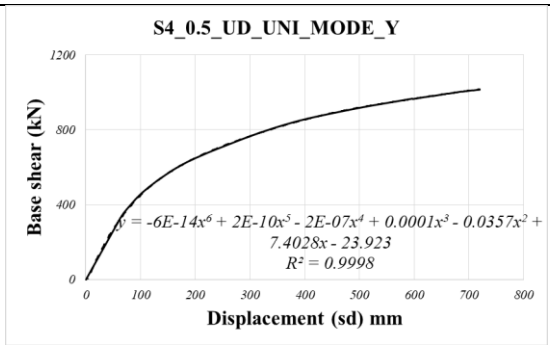

Figure 7.15 Pushover curve of building S4_0.5_UD_UNI_IR1_MODE_Y

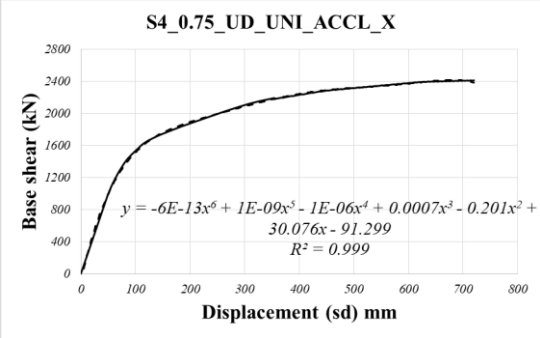

Figure 7.16 Pushover curve of building S4_0.75_UD_UNI_IR1_ACCL_X

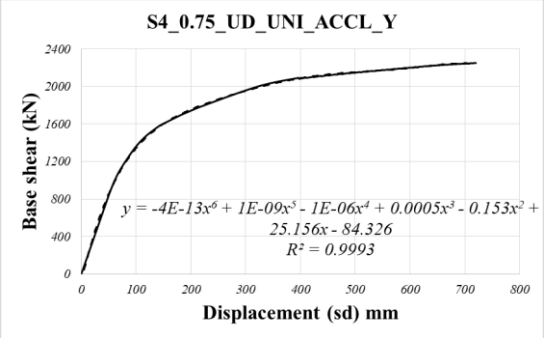

Figure 7.17 Pushover curve of building S4_0.75_UD_UNI_IR1_ACCL_Y

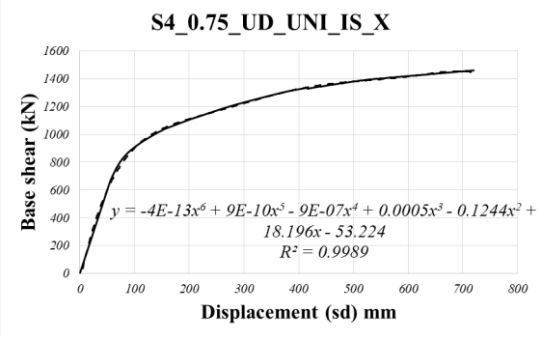

Figure 7.18 Pushover curve of building S4_0.75_UD_UNI_IR1_IS_X

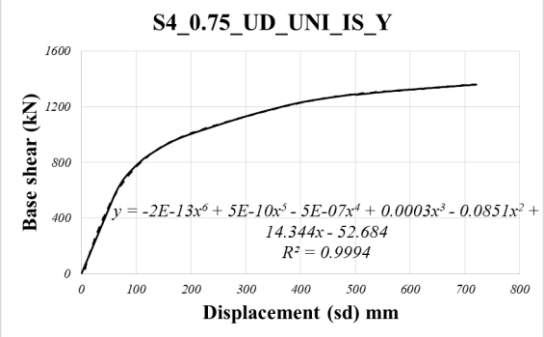

Figure 7.19 Pushover curve of building S4_0.75_UD_UNI_IR1_IS_Y

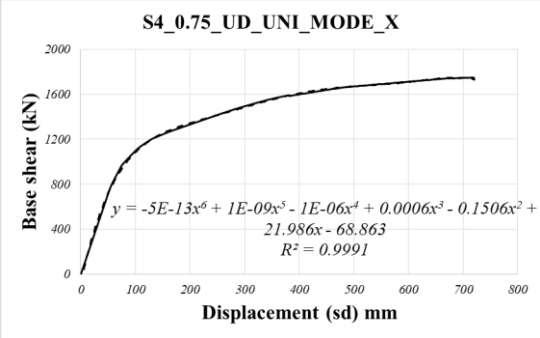

Figure 7.20 Pushover curve of building S4_0.75_UD_UNI_IR1_MODE_X

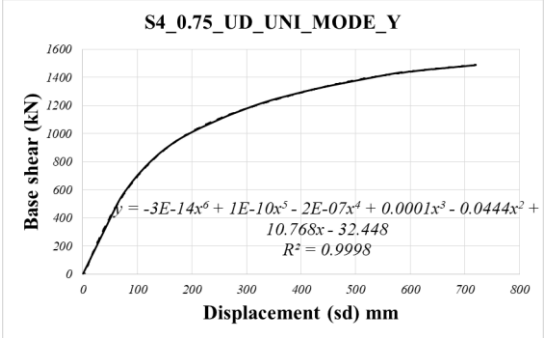

Figure 7.21 Pushover curve of building S4_0.75_UD_UNI_IR1_MODE_Y

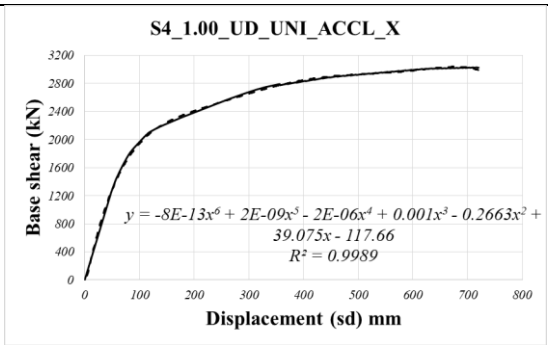

Figure 7.22 Pushover curve of building S4_1.00_UD_UNI_IR1_ACCL_X

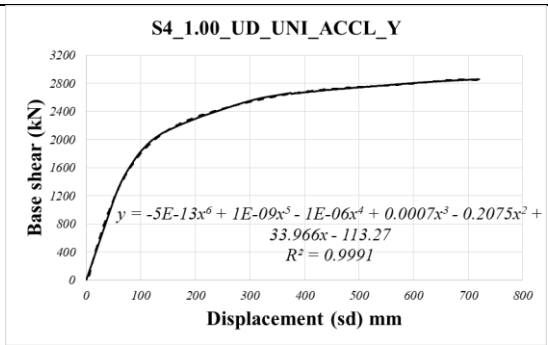

Figure 7.23 Pushover curve of building S4_1.00_UD_UNI_IR1_ACCL_Y

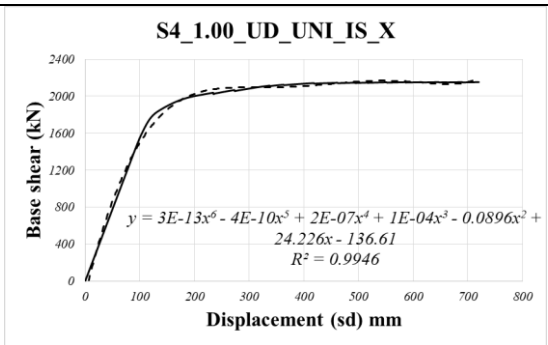

Figure 7.24 Pushover curve of building S4_1.00_UD_UNI_IR1_IS_X

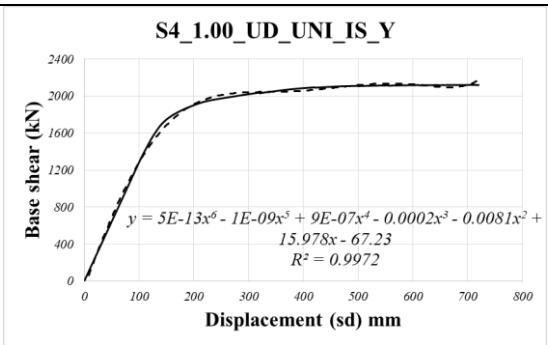

Figure 7.25 Pushover curve of building S4_1.00_UD_UNI_IR1_IS_Y

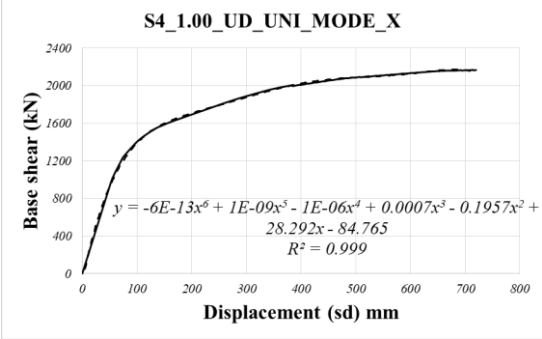

Figure 7.26 Pushover curve of building S4_1.00_UD_UNI_IR1_MODE_X

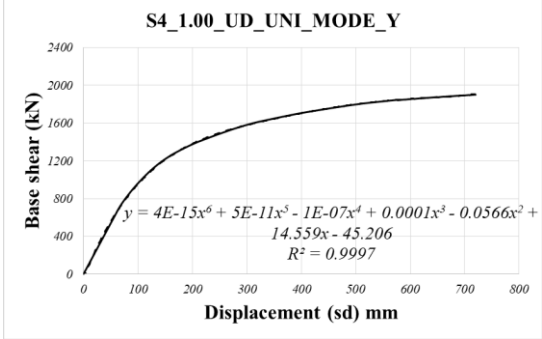

Figure 7.27 Pushover curve of building S4_1.00_UD_UNI_IR1_MODE_Y

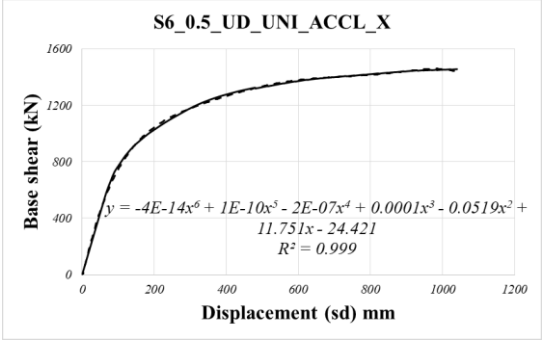

Figure 7.28 Pushover curve of building S6_0.5_UD_UNI_IR1_ACCL_X

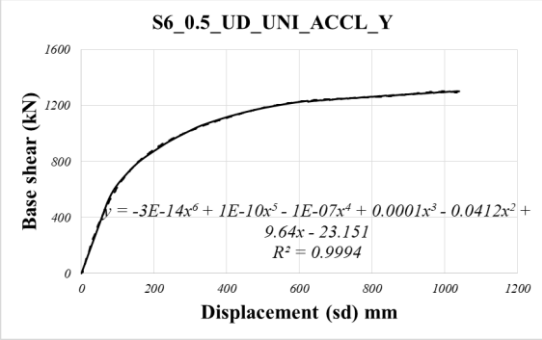

Figure 7.29 Pushover curve of building S6_0.5_UD_UNI_IR1_ACCL_Y

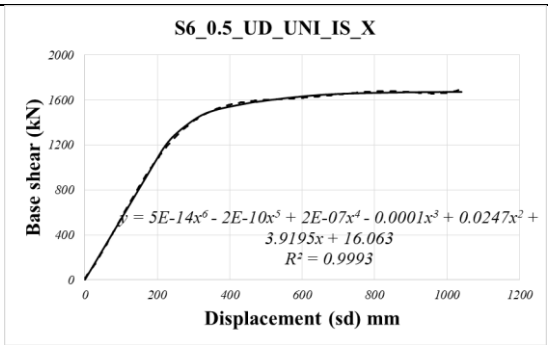

Figure 7.30 Pushover curve of building S6_0.5_UD_UNI_IR1_IS_X

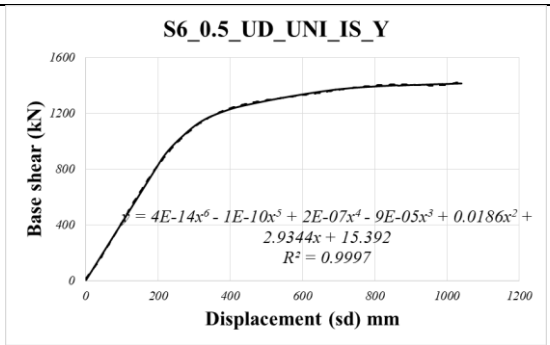

Figure 7.31 Pushover curve of building S6_0.5_UD_UNI_IR1_IS_Y

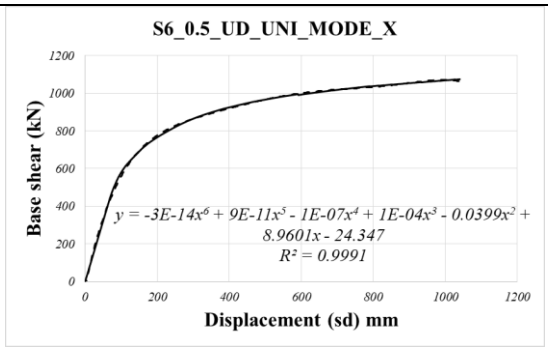

Figure 7.32 Pushover curve of building S6_0.5_UD_UNI_IR1_MODE_X

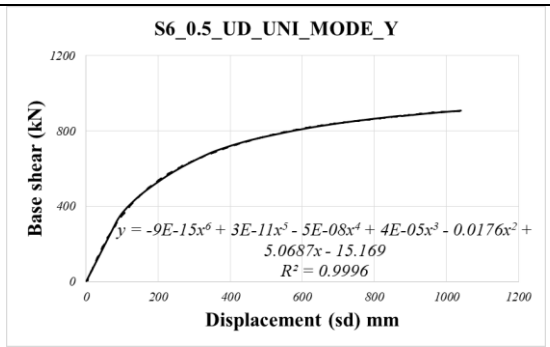

Figure 7.33 Pushover curve of building S6_0.5_UD_UNI_IR1_MODE_Y

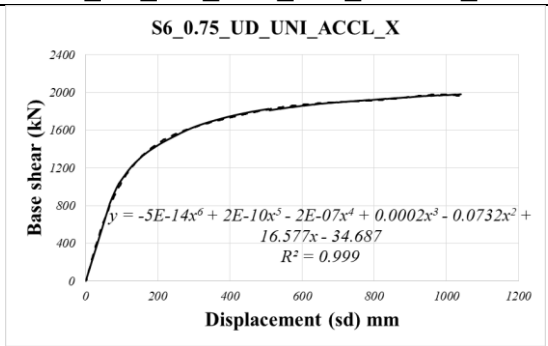

Figure 7.34 Pushover curve of building S6_0.75_UD_UNI_IR1_ACCL_X

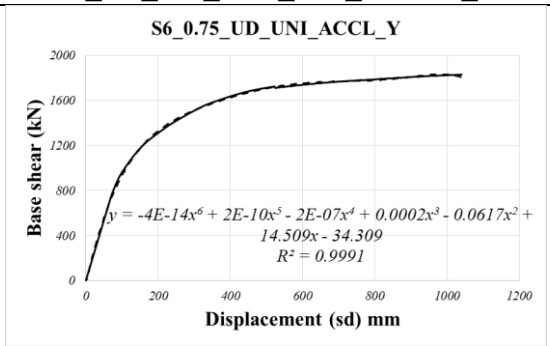

Figure 7.35 Pushover curve of building S6_0.75_UD_UNI_IR1_ACCL_Y

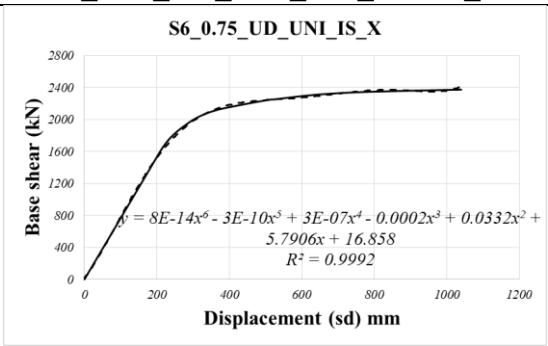

Figure 7.36 Pushover curve of building S6_0.75_UD_UNI_IR1_IS_X

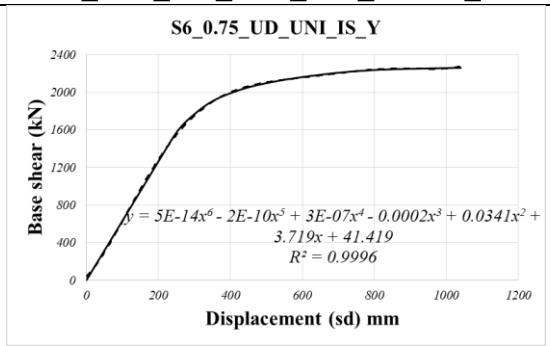

Figure 7.37 Pushover curve of building S6_0.75_UD_UNI_IR1_IS_Y

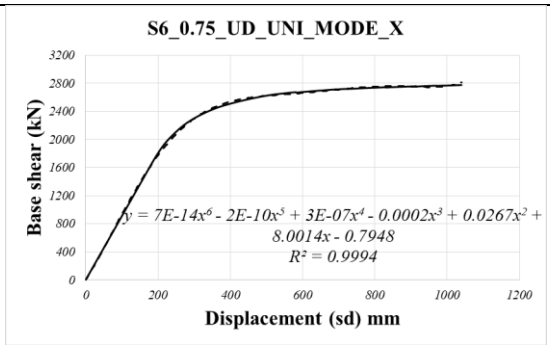

Figure 7.38 Pushover curve of building S6_0.75_UD_UNI_IR1_MODE_X

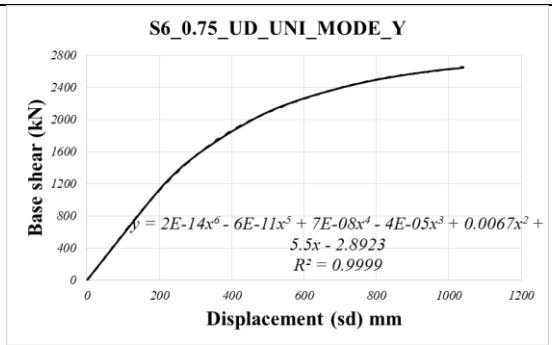

Figure 7.39 Pushover curve of building S6_0.75_UD_UNI_IR1_MODE_Y

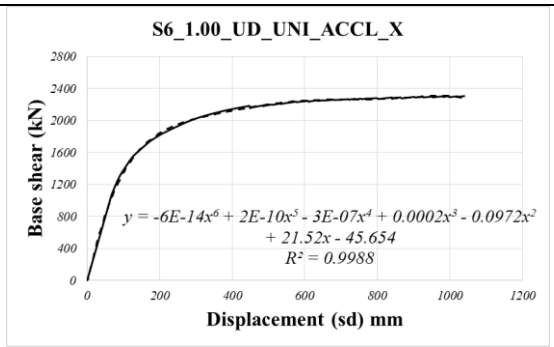

Figure 7.40 Pushover curve of building S6_1.00_UD_UNI_IR1_ACCL_X

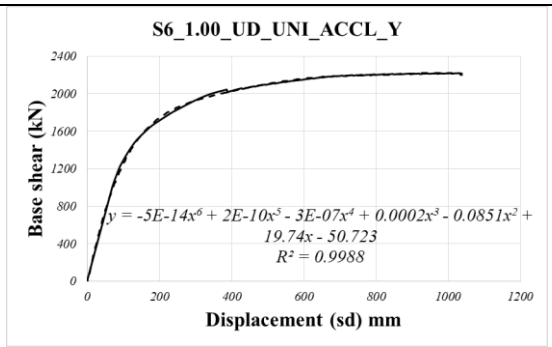

Figure 7.41 Pushover curve of building S6_1.00_UD_UNI_IR1_ACCL_Y

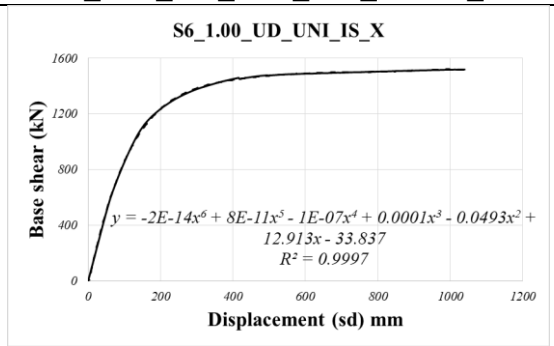

Figure 7.42 Pushover curve of building S6_1.00_UD_UNI_IR1_IS_X

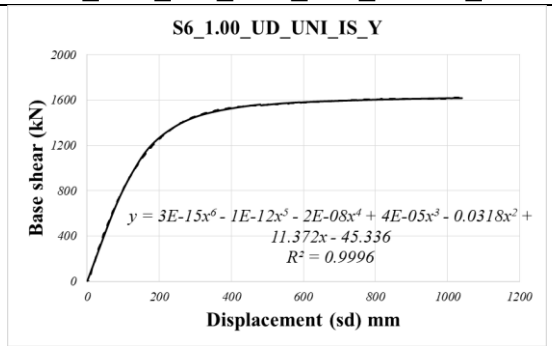

Figure 7.43 Pushover curve of building S6_1.00_UD_UNI_IR1_IS_Y

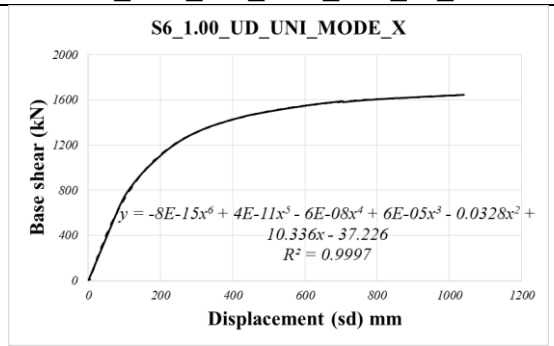

Figure 7.44 Pushover curve of building S6_1.00_UD_UNI_IR1_MODE_X

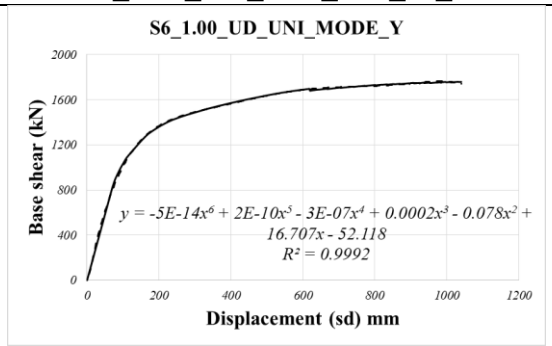

Figure 7.45 Pushover curve of building S6_1.00_UD_UNI_IR1_MODE_Y

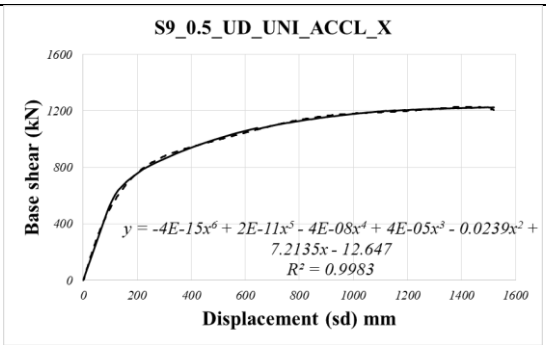

Figure 7.46 Pushover curve of building S9_0.5_UD_UNI_IR1_ACCL_X

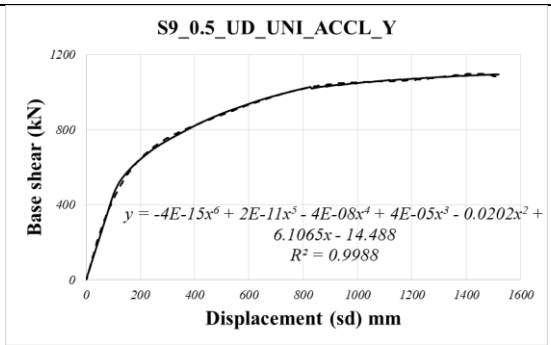

Figure 7.47 Pushover curve of building S9_0.5_UD_UNI_IR1_ACCL_Y

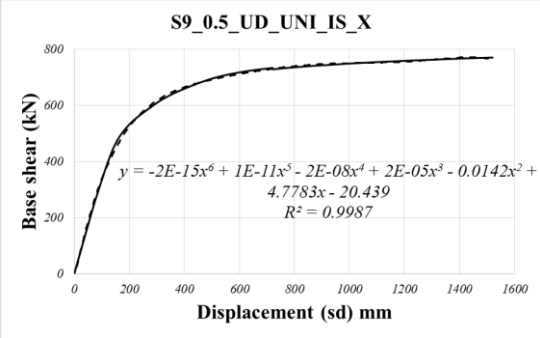

Figure 7.48 Pushover curve of building S9_0.5_UD_UNI_IR1_IS_X

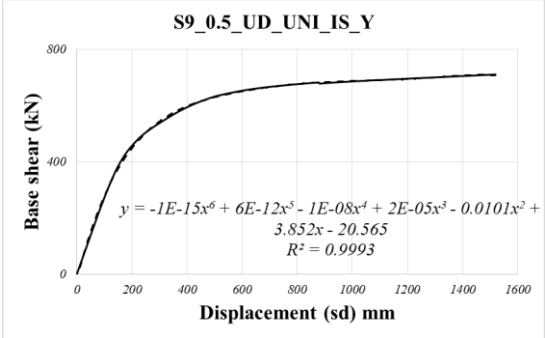

Figure 7.49 Pushover curve of building S9_0.5_UD_UNI_IR1_IS_Y

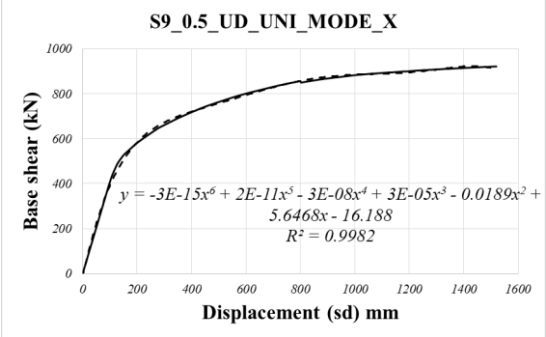

Figure 7.50 Pushover curve of building S9_0.5_UD_UNI_IR1_MODE_X

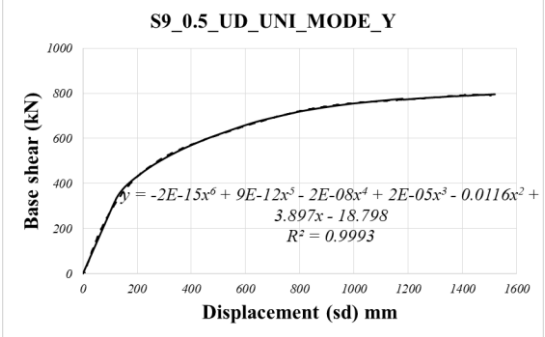

Figure 7.51 Pushover curve of building S9_0.5_UD_UNI_IR1_MODE_Y

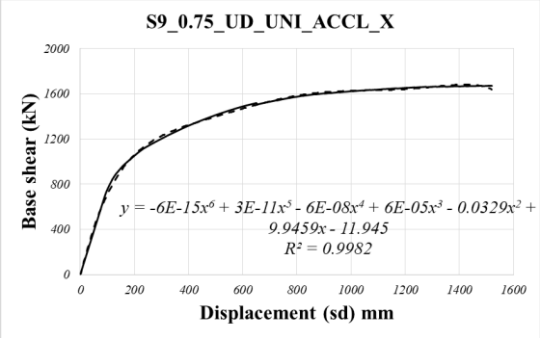

Figure 7.52 Pushover curve of building S9_0.75_UD_UNI_IR1_ACCL_X

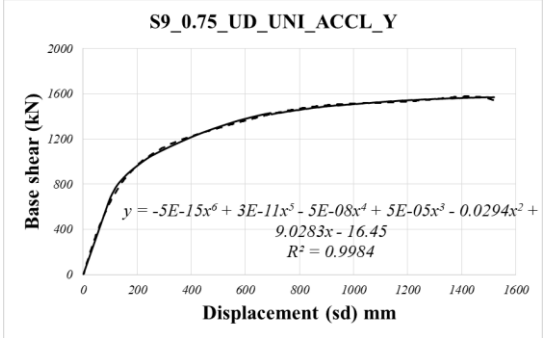

Figure 7.53 Pushover curve of building S9_0.75_UD_UNI_IR1_ACCL_Y

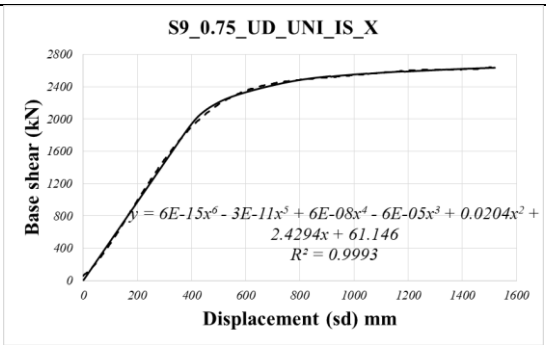

Figure 7.54 Pushover curve of building S9_0.75_UD_UNI_IR1_IS_X

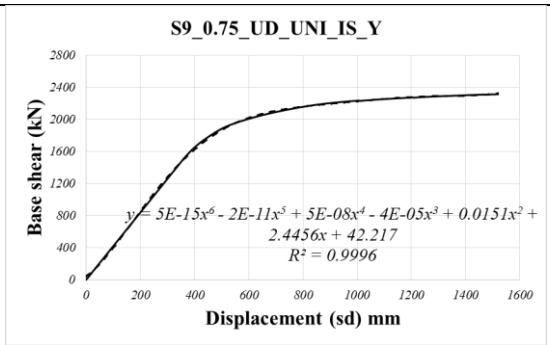

Figure 7.55 Pushover curve of building S9_0.75_UD_UNI_IR1_IS_Y

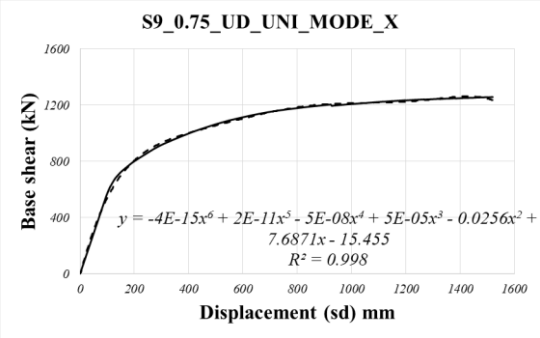

Figure 7.56 Pushover curve of building S9_0.75_UD_UNI_IR1_MODE_X

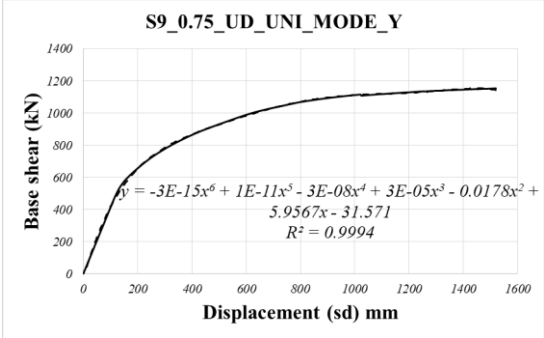

Figure 7.57 Pushover curve of building S9_0.75_UD_UNI_IR1_MODE_Y

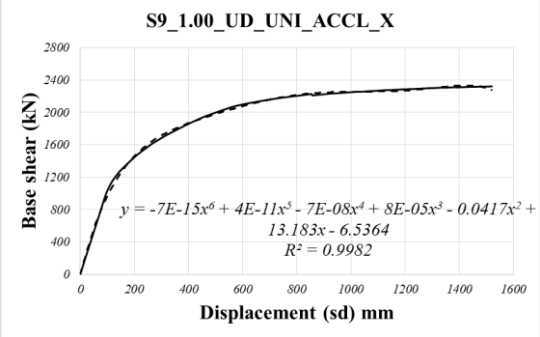

Figure 7.58 Pushover curve of building S9_1.00_UD_UNI_IR1_ACCL_X

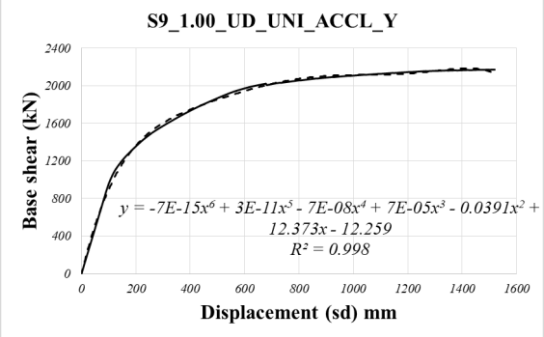

Figure 7.59 Pushover curve of building S9_1.00_UD_UNI_IR1_ACCL_Y

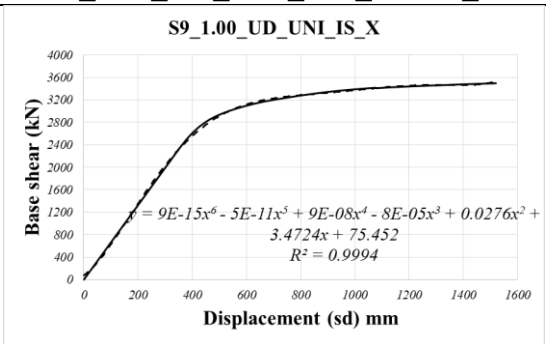

Figure 7.60 Pushover curve of building S9_1.00_UD_UNI_IR1_IS_X

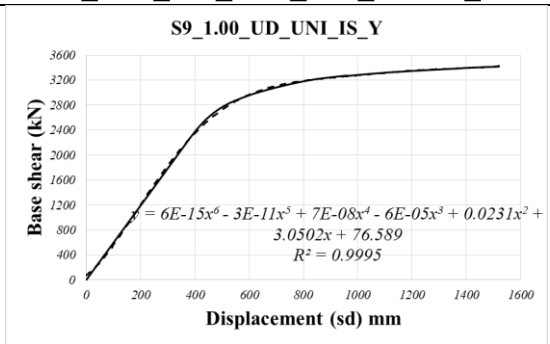

Figure 7.61 Pushover curve of building S9_1.00_UD_UNI_IR1_IS_Y

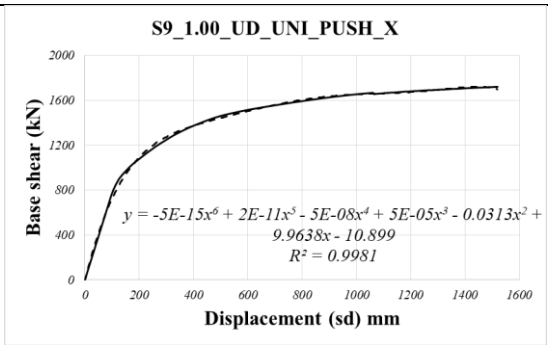

Figure 7.62 Pushover curve of building S9_1.00_UD_UNI_IR1_MODE_X

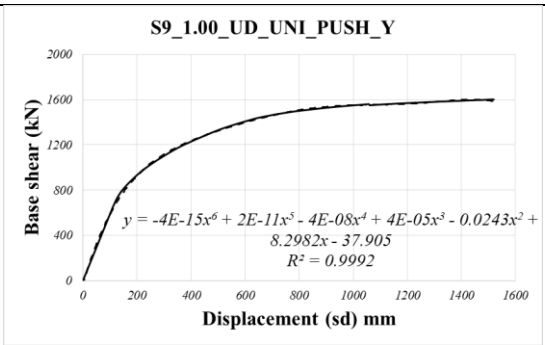

Figure 7.63 Pushover curve of building S9_1.00_UD_UNI_IR1_MODE_Y

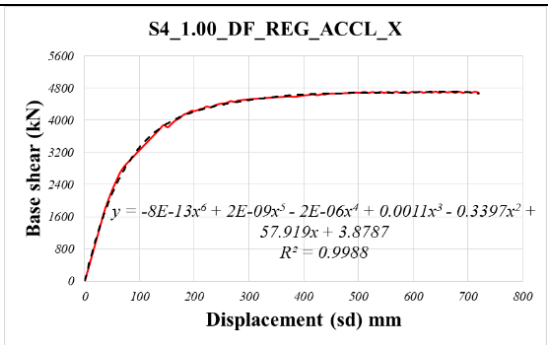

Figure 7.64 Pushover curve of building S4_1.00_DF_REG_ACCL_X

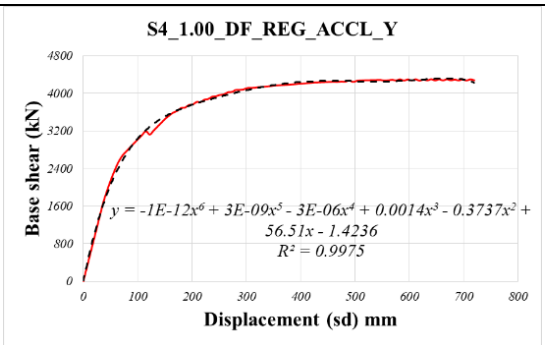

Figure 7.65 Pushover curve of building S4_1.00_DF_REG_ACCL_Y

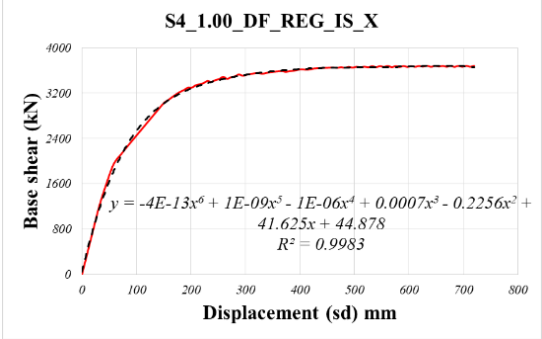

Figure 7.66 Pushover curve of building S4_1.00_DF_REG_IS_X

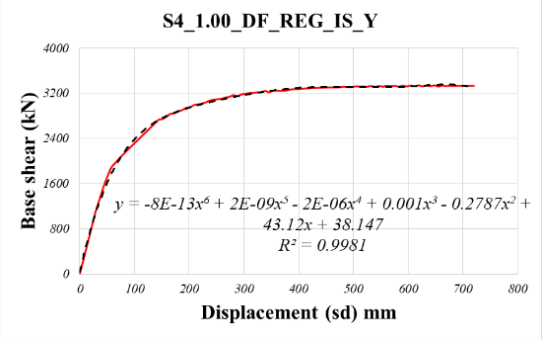

Figure 7.67 Pushover curve of building S4_1.00_DF_REG_IS_Y

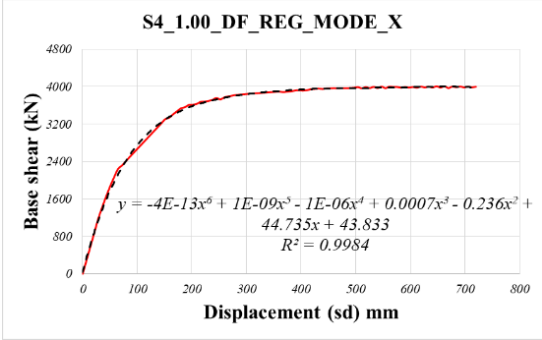

Figure 7.68 Pushover curve of building S4_1.00_DF_REG_MODE_X

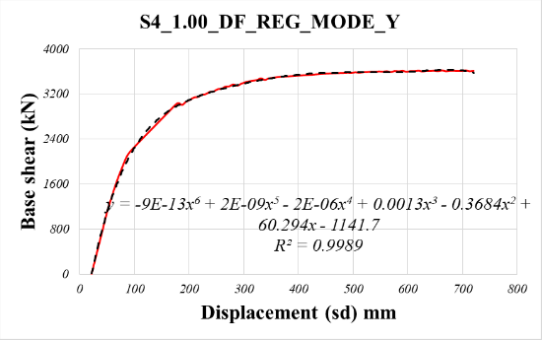

Figure 7.69 Pushover curve of building S4_1.00_DF_REG_MODE_Y

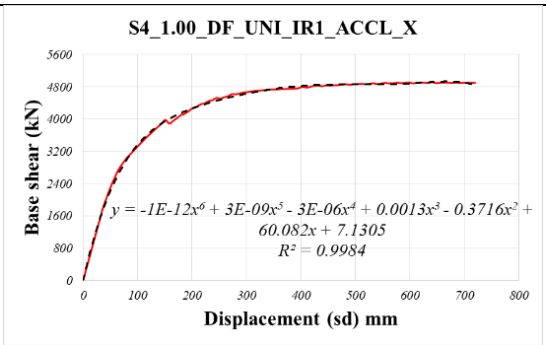

Figure 7.70 Pushover curve of building S4_1.00_DF_UNI_IR1_ACCL_X

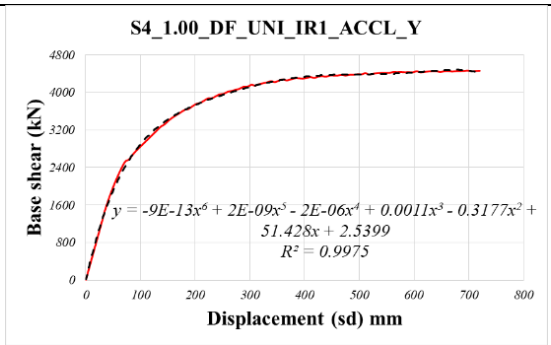

Figure 7.71 Pushover curve of building S4_1.00_DF_UNI_IR1_ACCL_Y

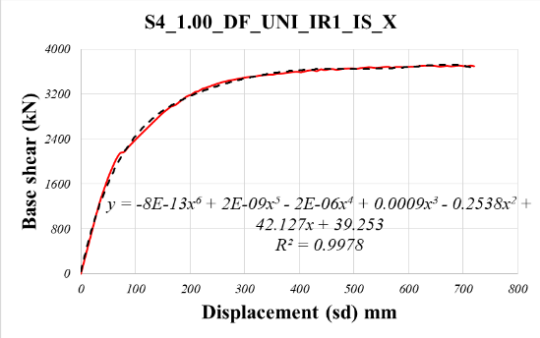

Figure 7.72 Pushover curve of building S4_1.00_DF_UNI_IR1_IS_X

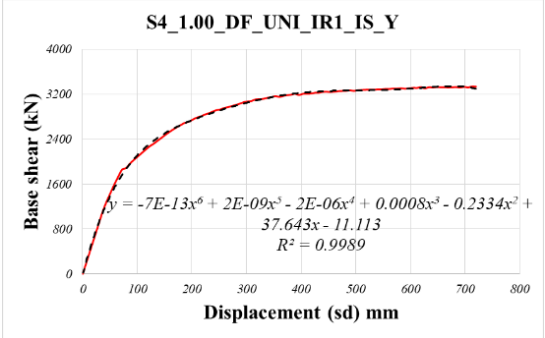

Figure 7.73 Pushover curve of building S4_1.00_DF_UNI_IR1_IS_Y

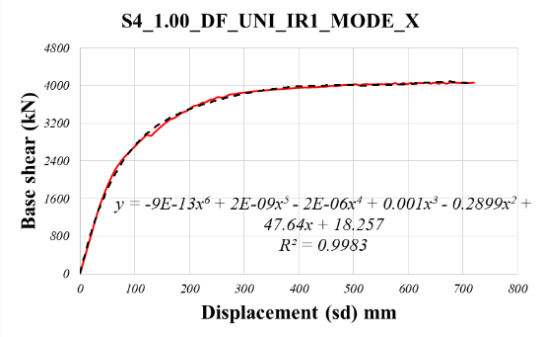

Figure 7.74 Pushover curve of building S4_1.00_DF_UNI_IR1_MODE_X

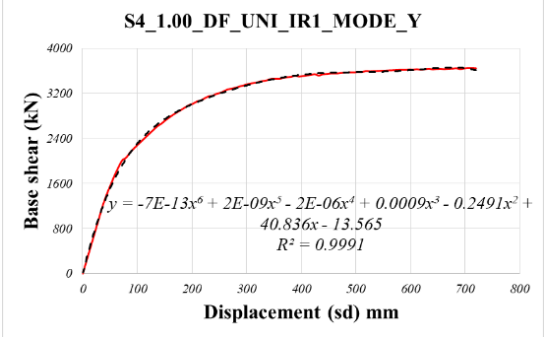

Figure 7.75 Pushover curve of building S4_1.00_DF_UNI_IR1_MODE_Y

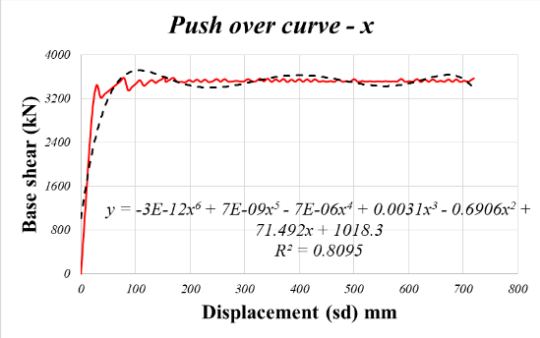

Figure 7.76 Pushover curve of building S4_1.00_DF_UNI_IR2_ACCL_X

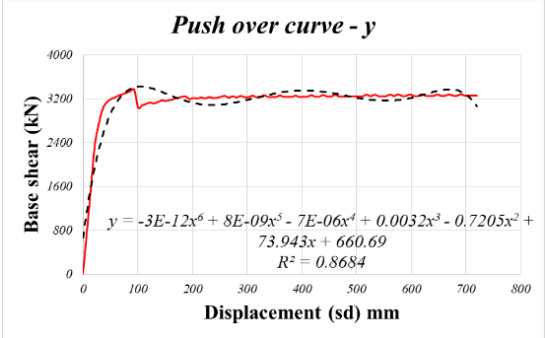

Figure 7.77 Pushover curve of building S4_1.00_DF_UNI_IR2_ACCL_Y

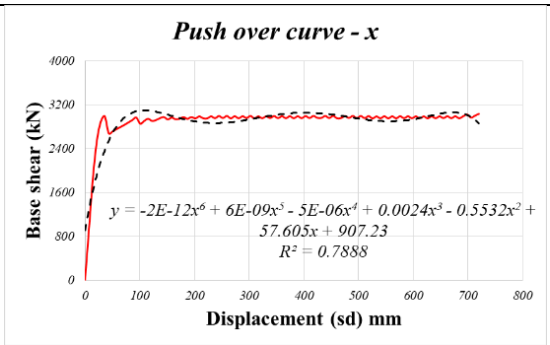

Figure 7.78 Pushover curve of building S4_1.00_DF_UNI_IR2_IS_X

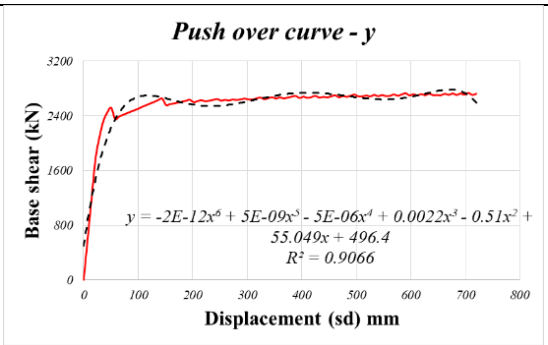

Figure 7.79 Pushover curve of building S4_1.00_DF_UNI_IR2_IS_Y

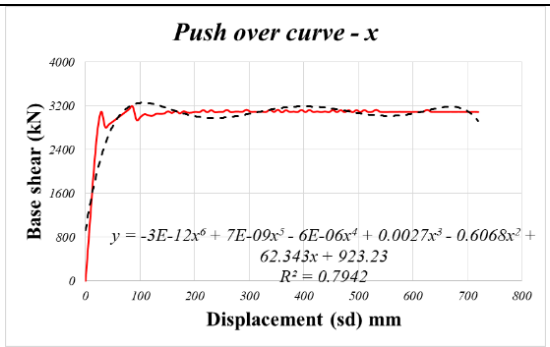

Figure 7.80 Pushover curve of building S4_1.00_DF_UNI_IR2_MODE_X

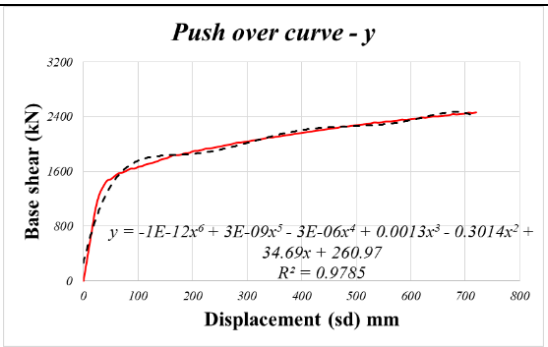

Figure 7.81 Pushover curve of building S4_1.00_DF_UNI_IR2_MODE_Y

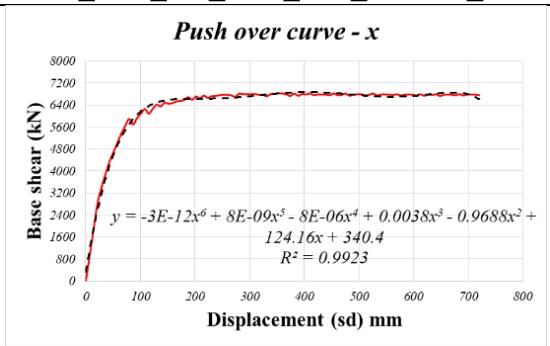

Figure 7.82 Pushover curve of building S4_1.00_DF_UNI_IR3_ACCL_X

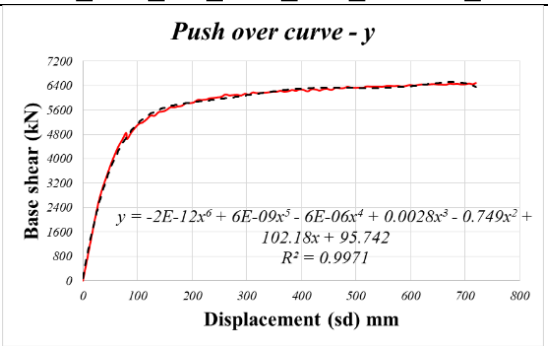

Figure 7.83 Pushover curve of building S4_1.00_DF_UNI_IR3_ACCL_Y

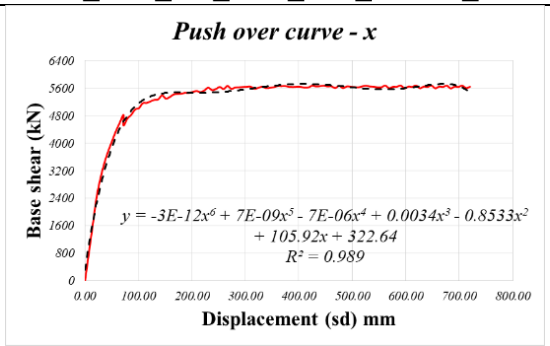

Figure 7.84 Pushover curve of building S4_1.00_DF_UNI_IR3_IS_X

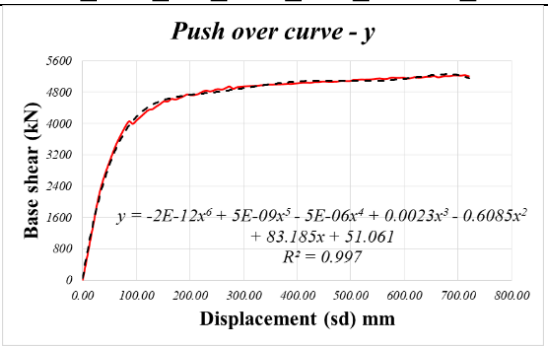

Figure 7.85 Pushover curve of building S4_1.00_DF_UNI_IR3_IS_Y

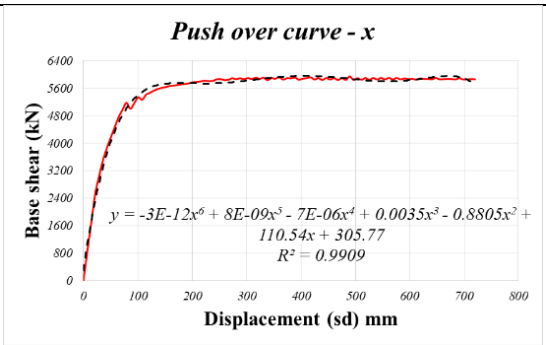

Figure 7.86 Pushover curve of building S4_1.00_DF_UNI_IR3_MODE_X

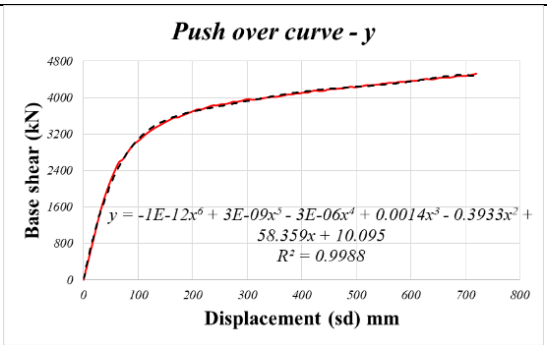

Figure 7.87 Pushover curve of building S4_1.00_DF_UNI_IR3_MODE_Y

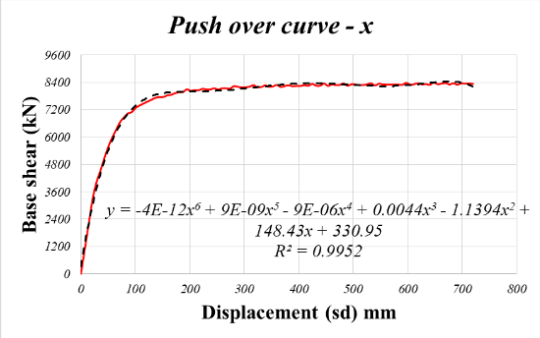

Figure 7.88 Pushover curve of building S4_1.00_DF_BI_IR2_ACCL_X

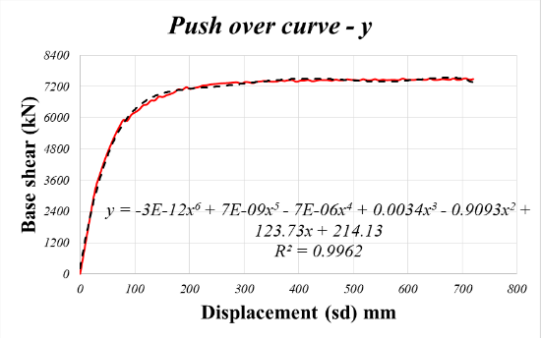

Figure 7.89 Pushover curve of building S4_1.00_DF_BI_IR2_ACCL_Y

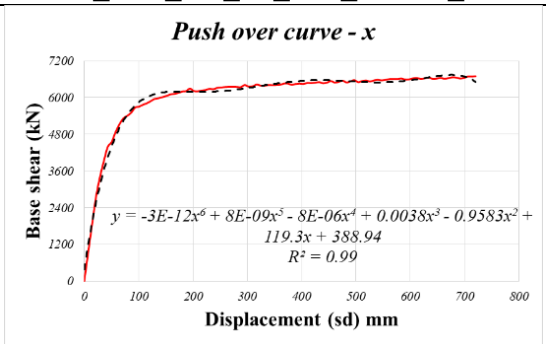

Figure 7.90 Pushover curve of building S4_1.00_DF_BI_IR2_IS_X

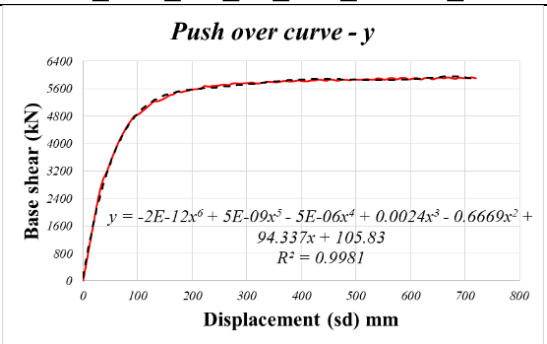

Figure 7.91 Pushover curve of building S4_1.00_DF_BI_IR2_IS_Y

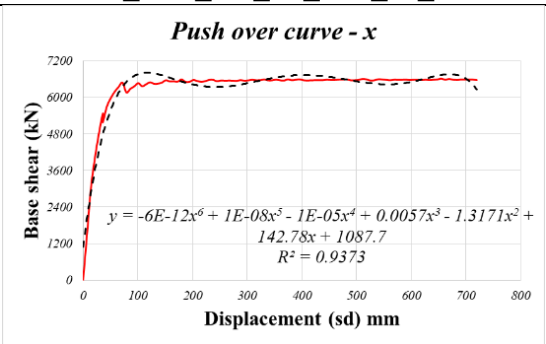

Figure 7.92 Pushover curve of building S4_1.00_DF_BI_IR2_MODE_X

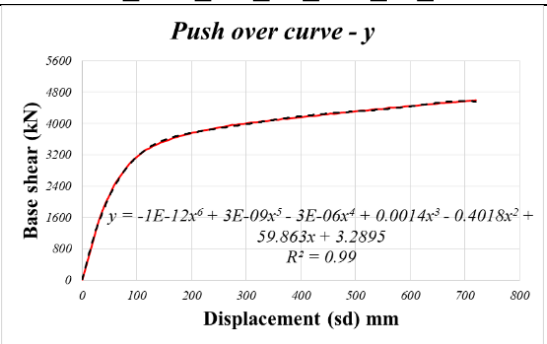

Figure 7.93 Pushover curve of building S4_1.00_DF_BI_IR2_MODE_Y

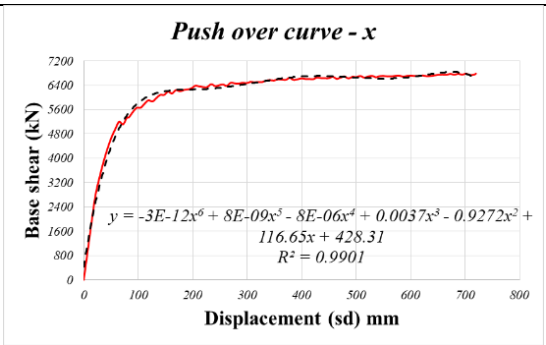

Figure 7.94 Pushover curve of building S4_1.00_DF_BI_IR3_ACCL_X

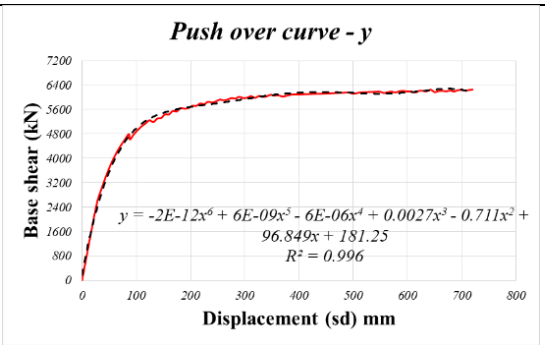

Figure 7.95 Pushover curve of building S4_1.00_DF_BI_IR3_ACCL_Y

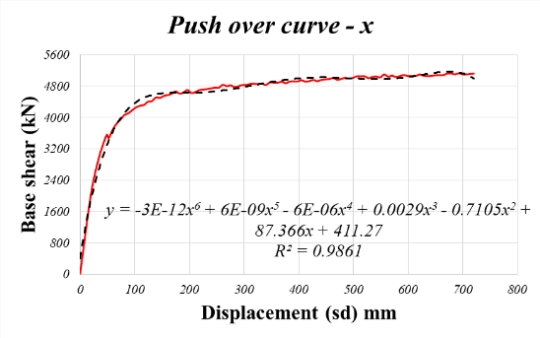

Figure 7.96 Pushover curve of building S4_1.00_DF_BI_IR3_IS_X

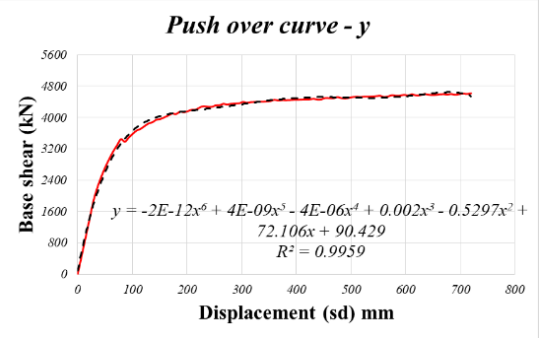

Figure 7.97 Pushover curve of building S4_1.00_DF_BI_IR3_IS_Y

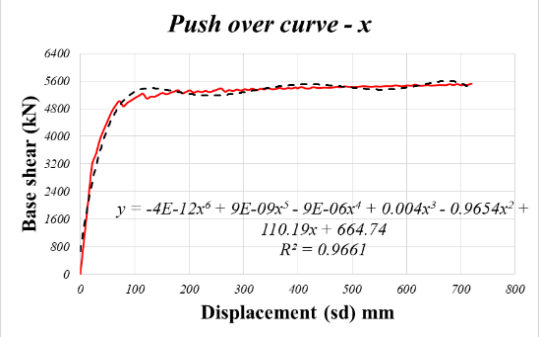

Figure 7.98 Pushover curve of building S4_1.00_DF_BI_IR3_MODE_X

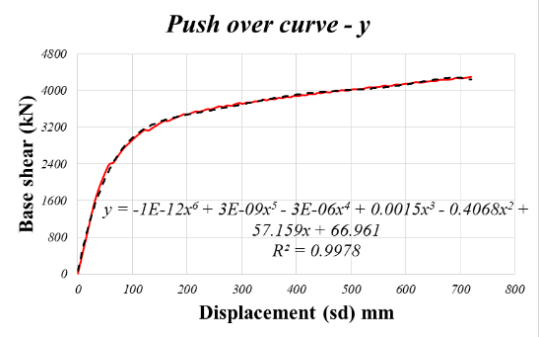

Figure 7.99 Pushover curve of building S4_1.00_DF_BI_IR3_MODE_Y

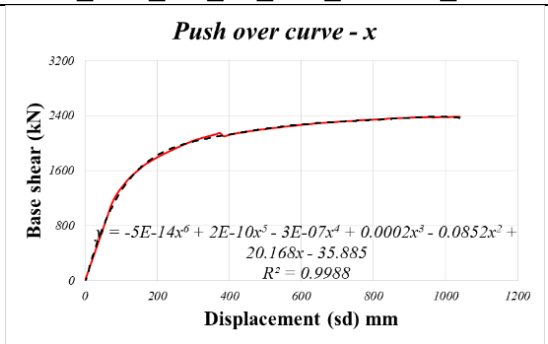

Figure 7.100 Pushover curve of building S6_1.00_DF_REG_ACCL_X

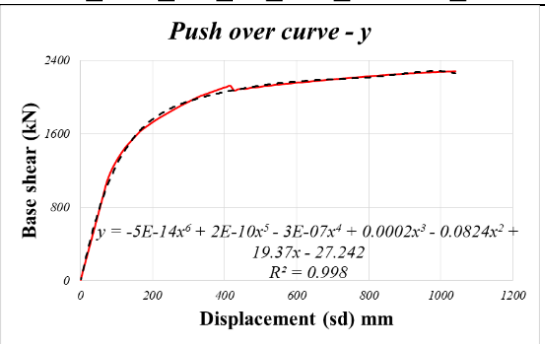

Figure 7.101 Pushover curve of building S6_1.00_DF_REG_ACCL_Y

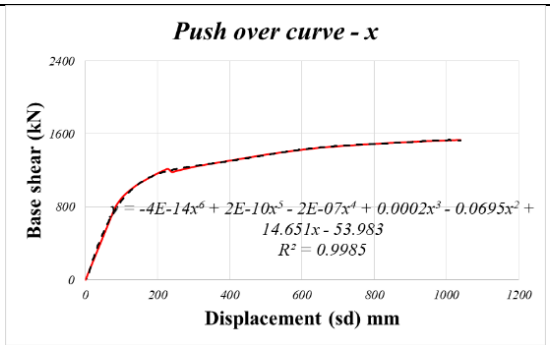

Figure 7.102 Pushover curve of building S6_1.00_DF_REG_IS_X

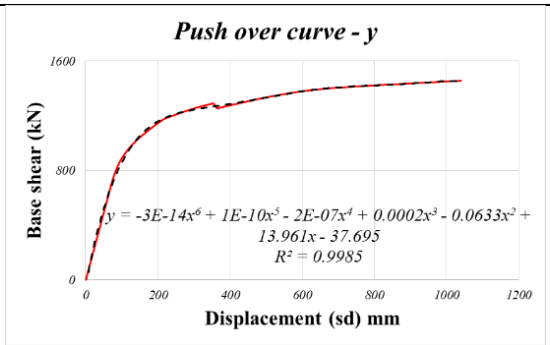

Figure 7.103 Pushover curve of building S6_1.00_DF_REG_IS_Y

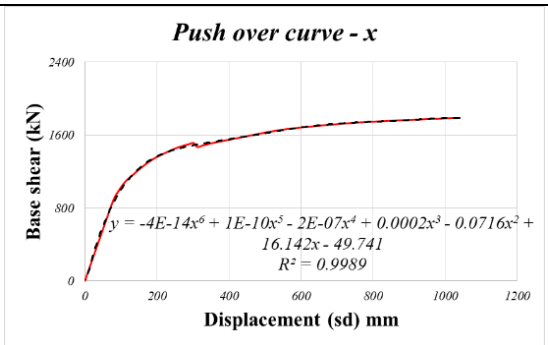

Figure 7.104 Pushover curve of building S6_1.00_DF_REG_MODE_X

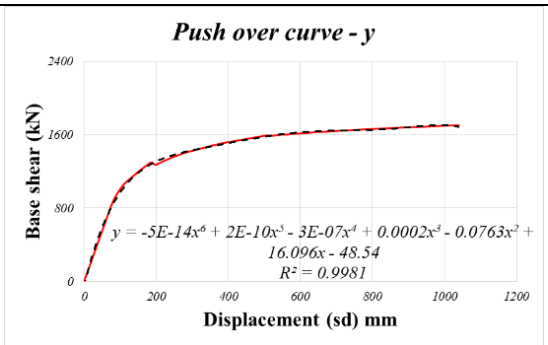

Figure 7.105 Pushover curve of building S6_1.00_DF_REG_MODE_Y

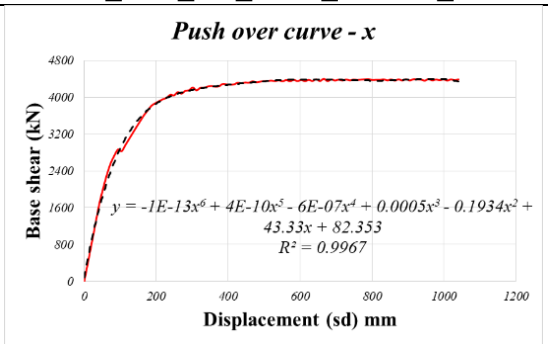

Figure 7.106 Pushover curve of building S6_1.00_DF_UNI_IR1_ACCL_X

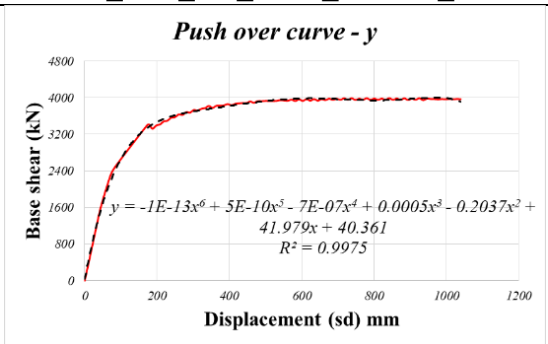

Figure 7.107 Pushover curve of building S6_1.00_DF_UNI_IR1_ACCL_Y

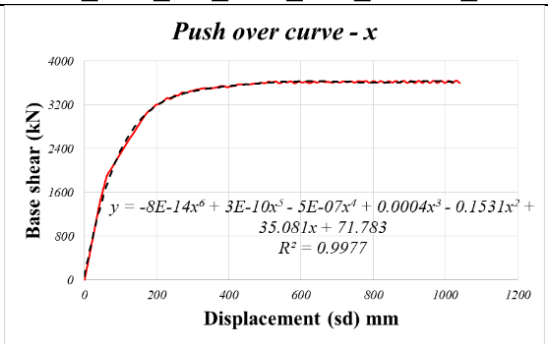

Figure 7.108 Pushover curve of building S6_1.00_DF_UNI_IR1_IS_X

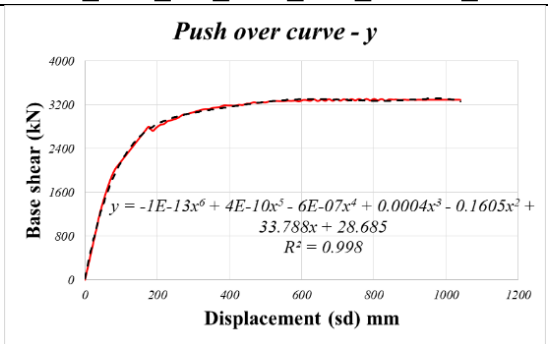

Figure 7.109 Pushover curve of building S6_1.00_DF_UNI_IR1_IS_Y

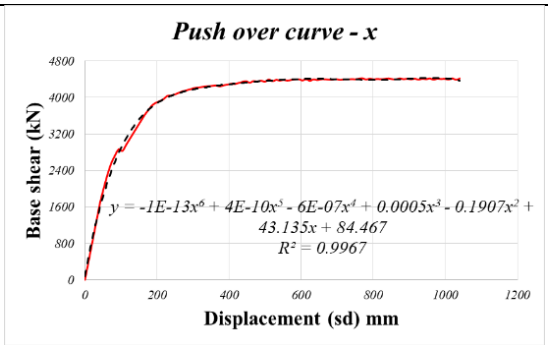

Figure 7.110 Pushover curve of building S6_1.00_DF_UNI_IR1_MODE_X

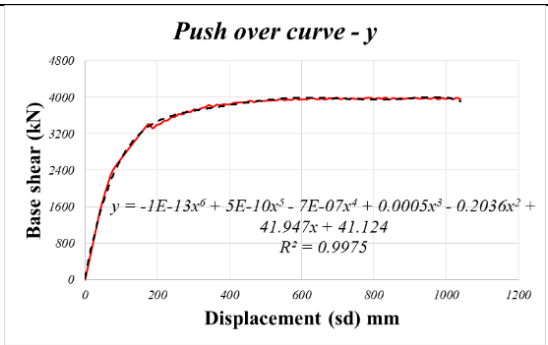

Figure 7.111 Pushover curve of building S6_1.00_DF_UNI_IR1_MODE_Y

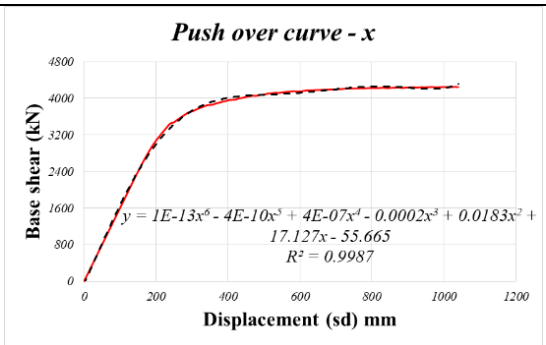

Figure 7.112 Pushover curve of building S6_1.00_DF_UNI_IR2_ACCL_X

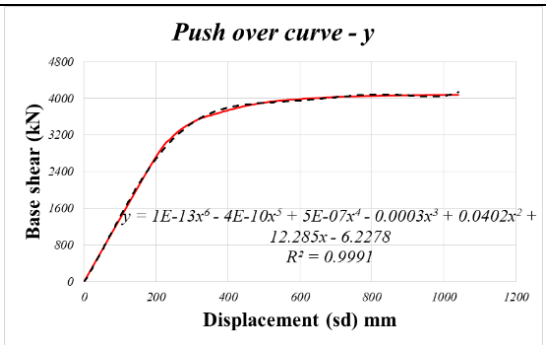

Figure 7.113 Pushover curve of building S6_1.00_DF_UNI_IR2_ACCL_Y

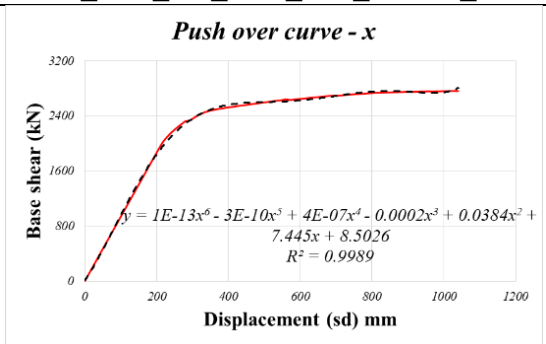

Figure 7.114 Pushover curve of building S6_1.00_DF_UNI_IR2_IS_X

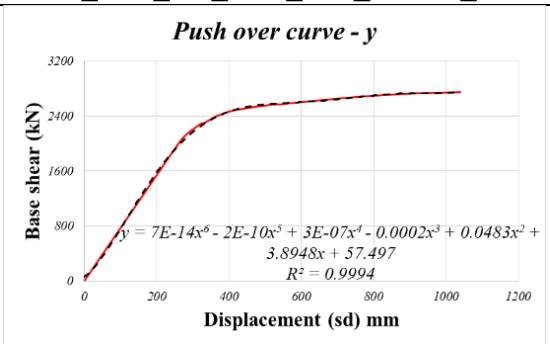

Figure 7.115 Pushover curve of building S6_1.00_DF_UNI_IR2_IS_Y

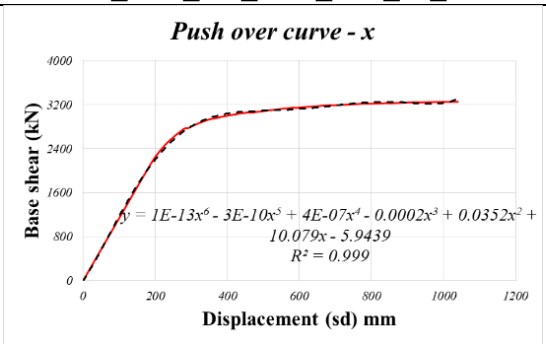

Figure 7.116 Pushover curve of building S6_1.00_DF_UNI_IR2_MODE_X

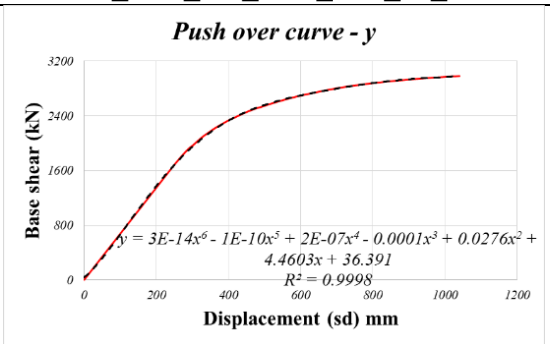

Figure 7.117 Pushover curve of building S6_1.00_DF_UNI_IR2_MODE_Y

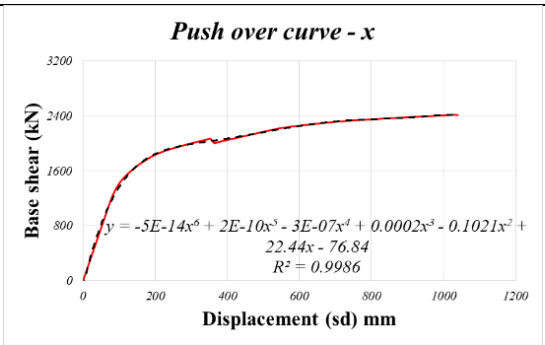

Figure 7.118 Pushover curve of building S6_1.00_DF_UNI_IR3_ACCL_X

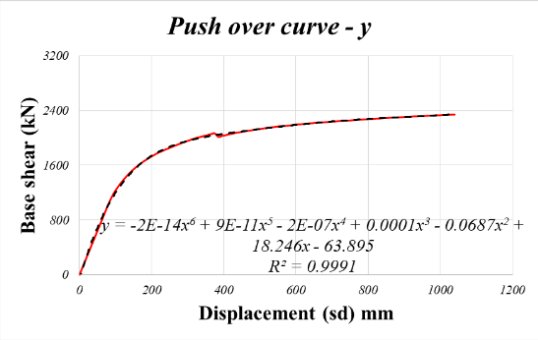

Figure 7.119 Pushover curve of building S6_1.00_DF_UNI_IR3_ACCL_Y

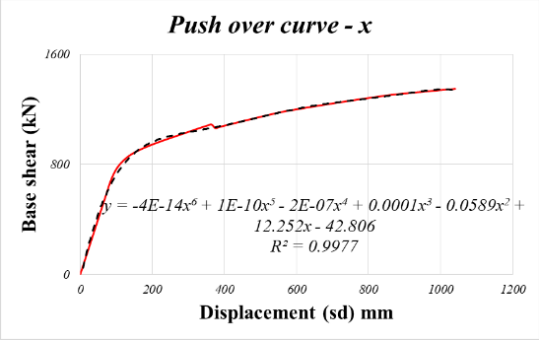

Figure 7.120 Pushover curve of building S6_1.00_DF_UNI_IR3_IS_X

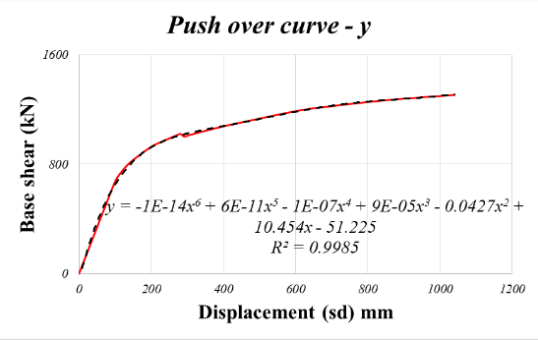

Figure 7.121 Pushover curve of building S6_1.00_DF_UNI_IR3_IS_Y

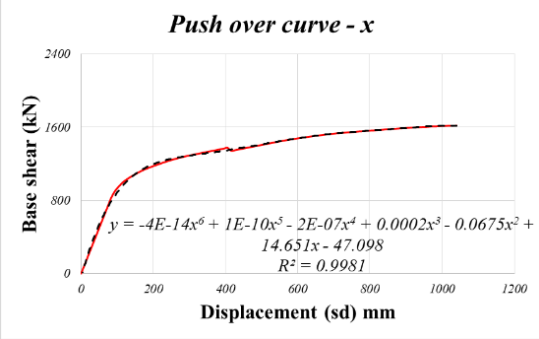

Figure 7.122 Pushover curve of building S6_1.00_DF_UNI_IR3_MODE_X

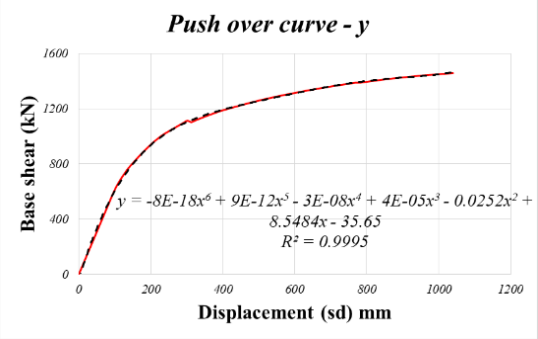

Figure 7.123 Pushover curve of building S6_1.00_DF_UNI_IR3_MODE_Y

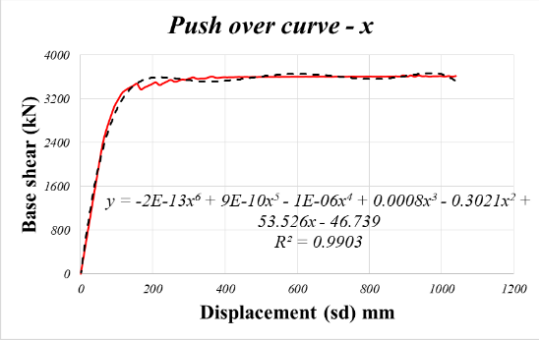

Figure 7.124 Pushover curve of building S6_1.00_DF_BI_IR1_ACCL_X

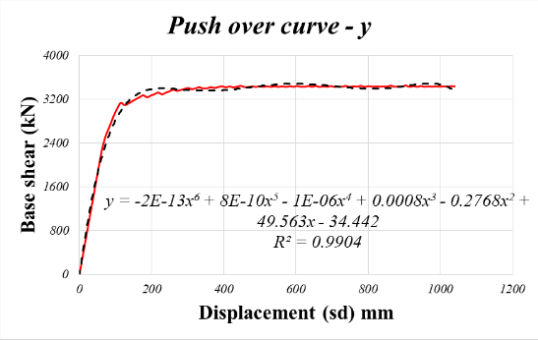

Figure 7.125 Pushover curve of building S6_1.00_DF_BI_IR1_ACCL_Y

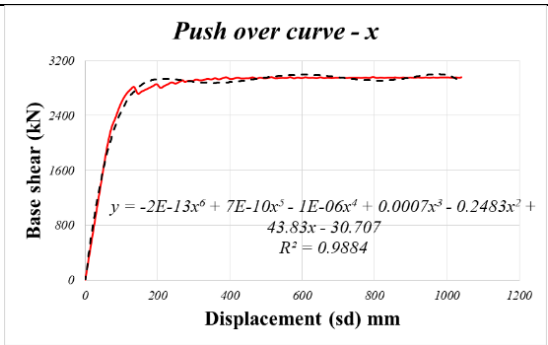

Figure 7.126 Pushover curve of building S6_1.00_DF_BI_IR1_IS_X

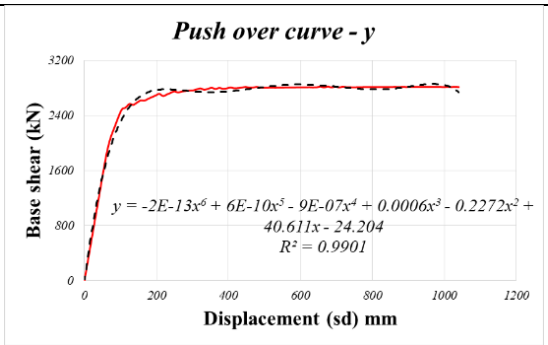

Figure 7.127 Pushover curve of building S6_1.00_DF_BI_IR1_IS_Y

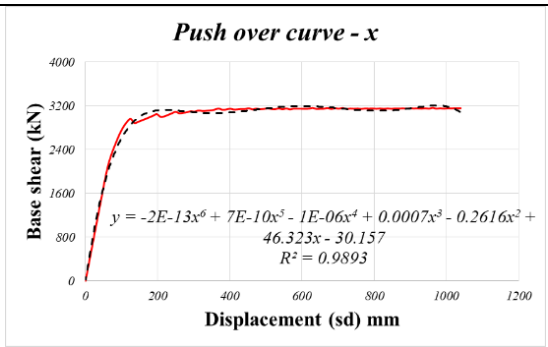

Figure 7.128 Pushover curve of building S6_1.00_DF_BI_IR1_MODE_X

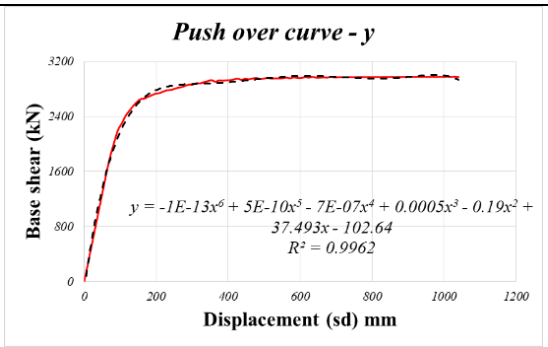

Figure 7.129 Pushover curve of building S6_1.00_DF_BI_IR1_MODE_Y

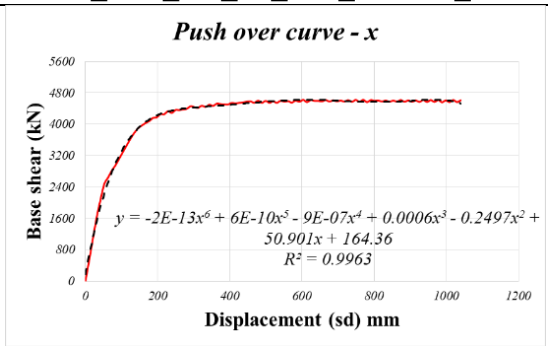

Figure 7.130 Pushover curve of building S6_1.00_DF_BI_IR2_ACCL_X

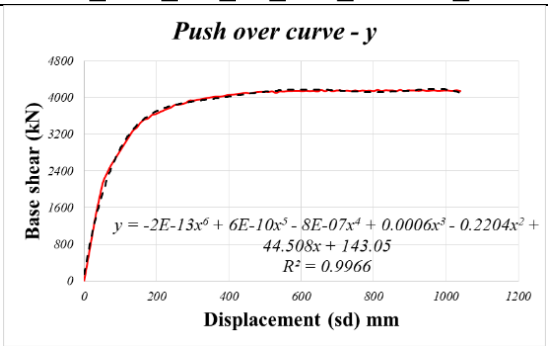

Figure 7.131 Pushover curve of building S6_1.00_DF_BI_IR2_ACCL_Y

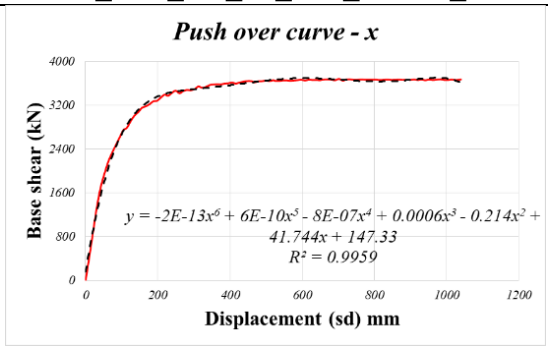

Figure 7.132 Pushover curve of building S6_1.00_DF_BI_IR2_IS_X

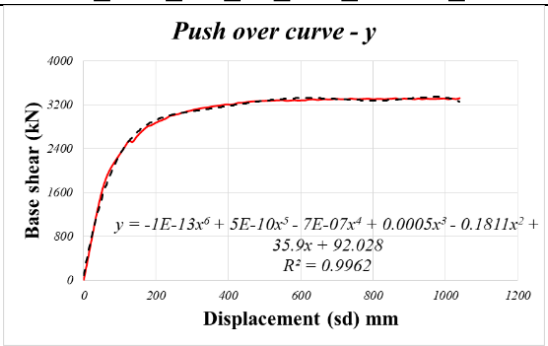

Figure 7.133 Pushover curve of building S6_1.00_DF_BI_IR2_IS_Y

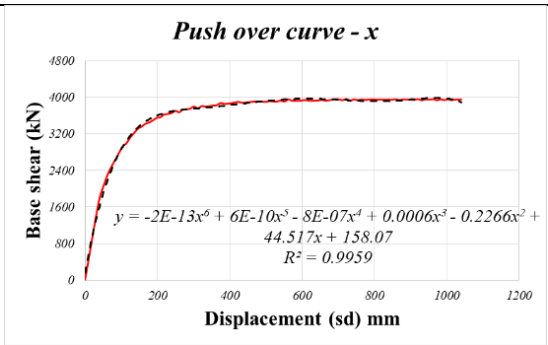

Figure 7.134 Pushover curve of building S6_1.00_DF_BI_IR2_MODE_X

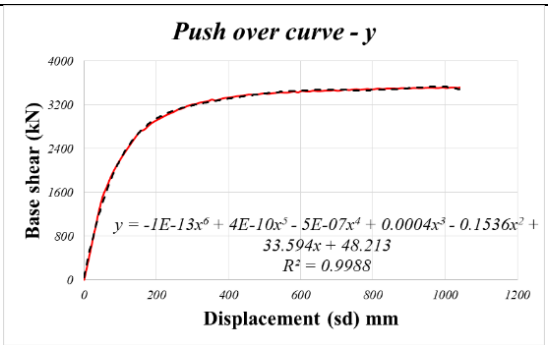

Figure 7.135 Pushover curve of building S6_1.00_DF_BI_IR2_MODE_Y

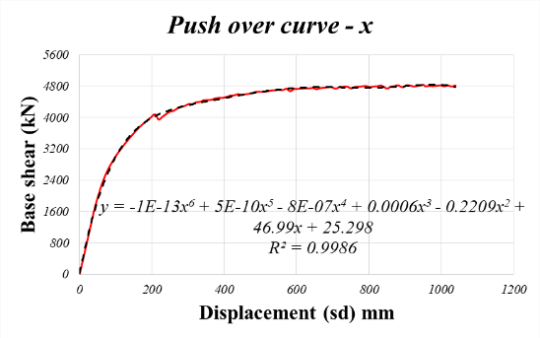

Figure 7.136 Pushover curve of building S6_1.00_DF_BI_IR3_ACCL_X

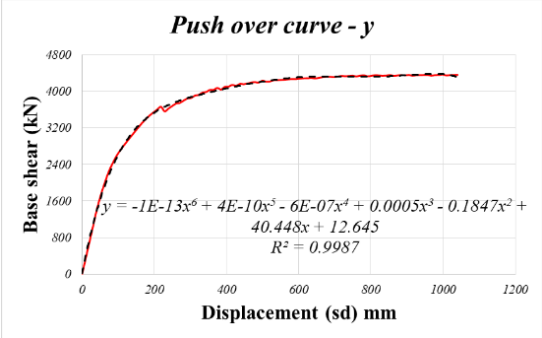

Figure 7.137 Pushover curve of building S6_1.00_DF_BI_IR3_ACCL_Y

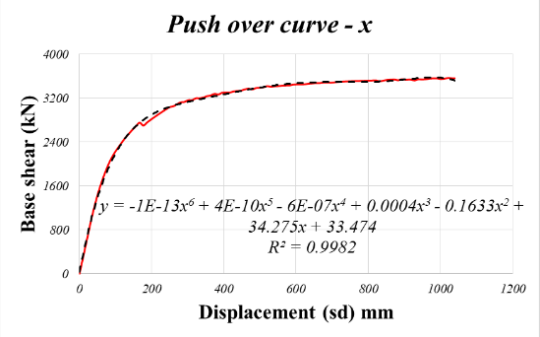

Figure 7.138 Pushover curve of building S6_1.00_DF_BI_IR3_IS_X

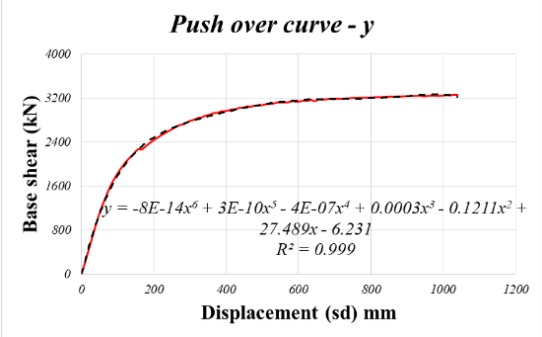

Figure 7.139 Pushover curve of building S6_1.00_DF_BI_IR3_IS_Y

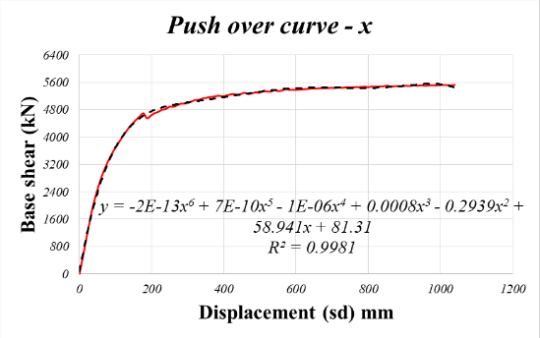

Figure 7.140 Pushover curve of building S6_1.00_DF_BI_IR3_MODE_X

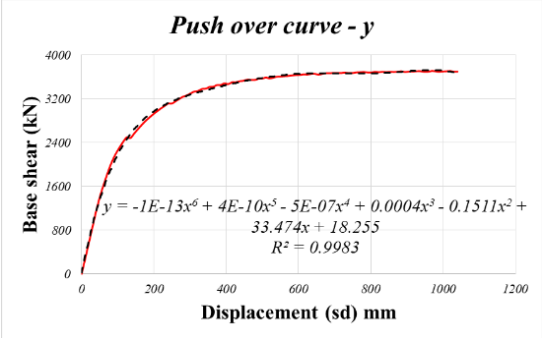

Figure 7.141 Pushover curve of building S6_1.00_DF_BI_IR3_MODE_Y

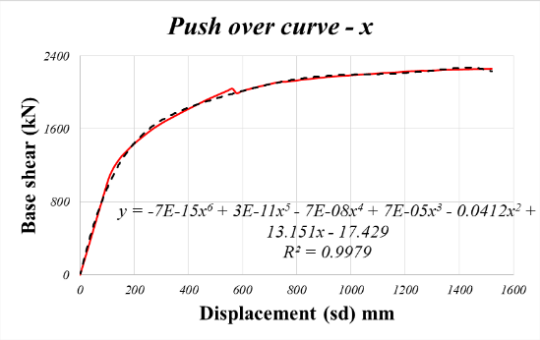

Figure 7.142 Pushover curve of building S9_1.00_DF_REG_ACCL_X

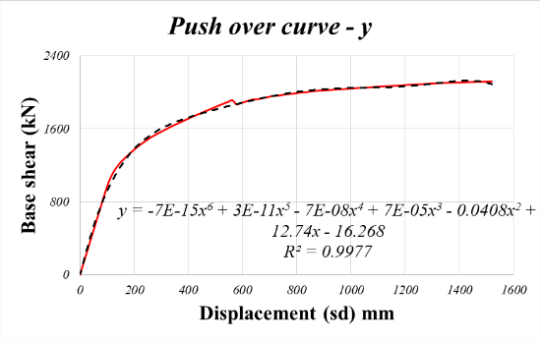

Figure 7.143 Pushover curve of building S9_1.00_DF_REG_ACCL_Y

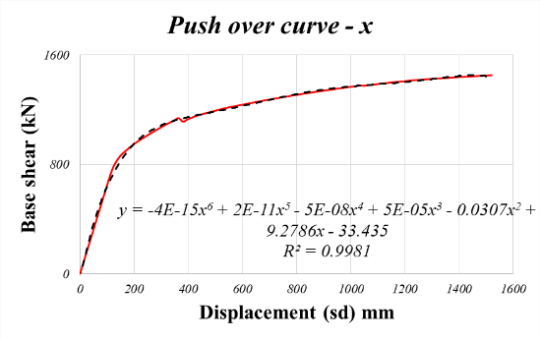

Figure 7.144 Pushover curve of building S9_1.00_DF_REG_IS_X

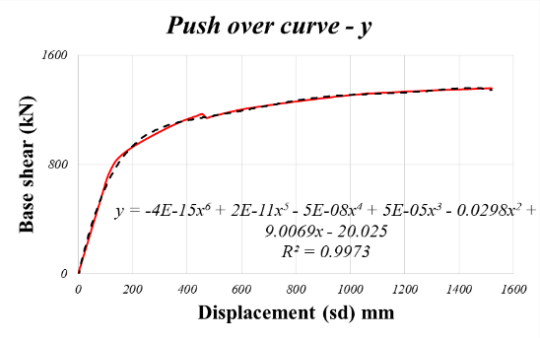

Figure 7.145 Pushover curve of building S9_1.00_DF_REG_IS_Y

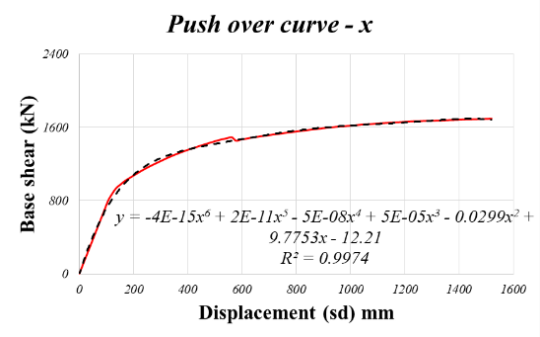

Figure 7.146 Pushover curve of building S9_1.00_DF_REG_MODE_X

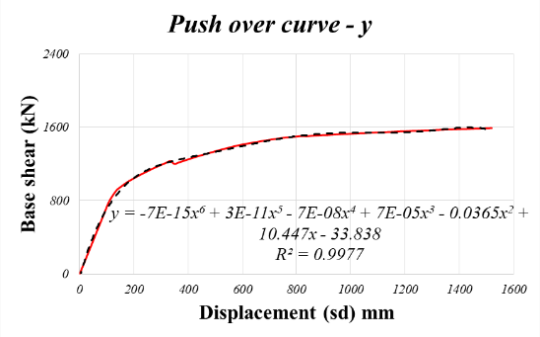

Figure 7.147 Pushover curve of building S9_1.00_DF_REG_MODE_Y

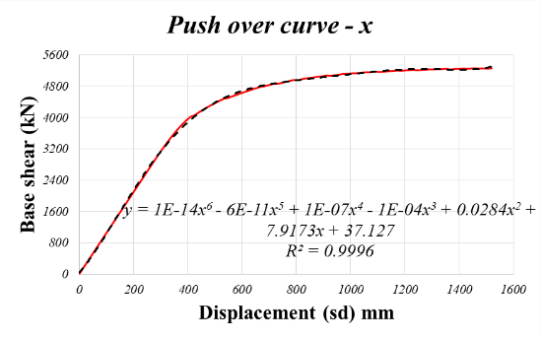

Figure 7.148 Pushover curve of building S9_1.00_DF_UNI_IR1_ACCL_X

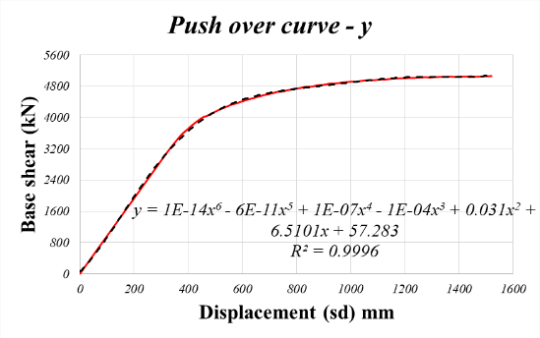

Figure 7.149 Pushover curve of building S9_1.00_DF_UNI_IR1_ACCL_Y

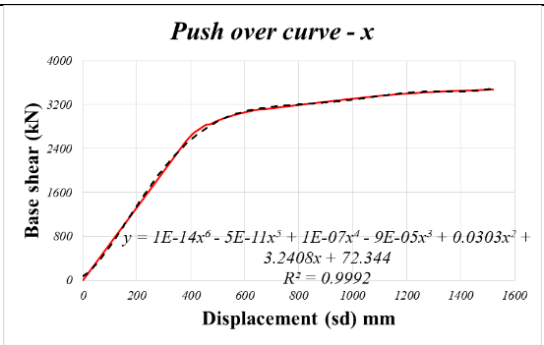

Figure 7.150 Pushover curve of building S9_1.00_DF_UNI_IR1_IS_X

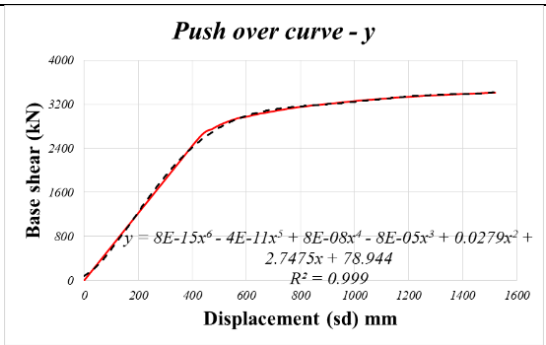

Figure 7.151 Pushover curve of building S9_1.00_DF_UNI_IR1_IS_Y

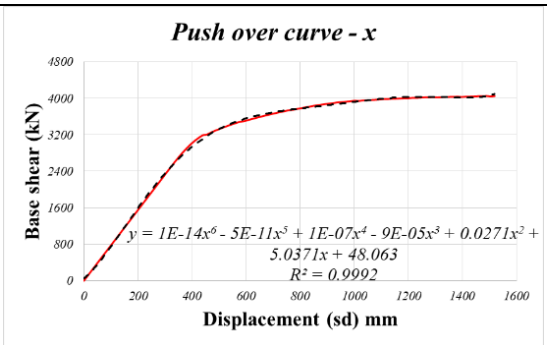

Figure 7.152 Pushover curve of building S9_1.00_DF_UNI_IR1_MODE_X

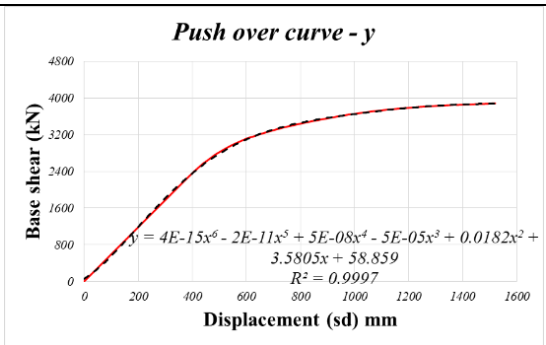

Figure 7.153 Pushover curve of building S9_1.00_DF_UNI_IR1_MODE_Y

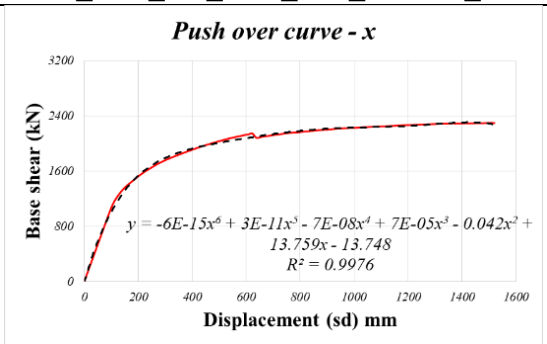

Figure 7.154 Pushover curve of building S9_1.00_DF_UNI_IR2_ACCL_X

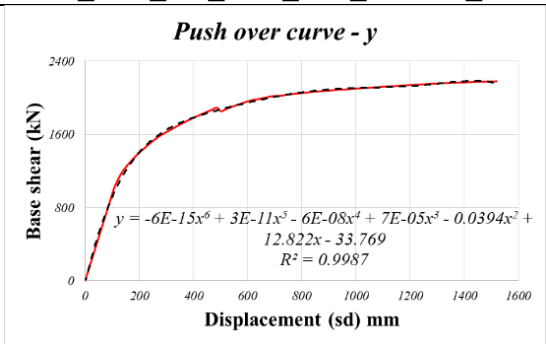

Figure 7.155 Pushover curve of building S9_1.00_DF_UNI_IR2_ACCL_Y

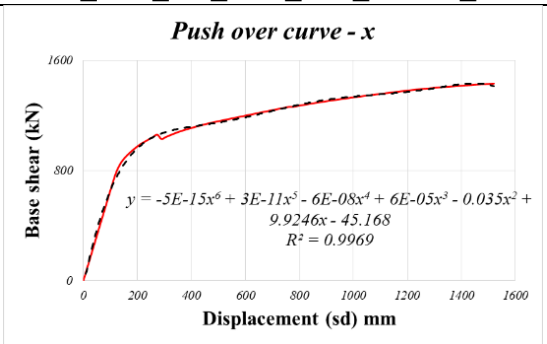

Figure 7.156 Pushover curve of building S9_1.00_DF_UNI_IR2_IS_X

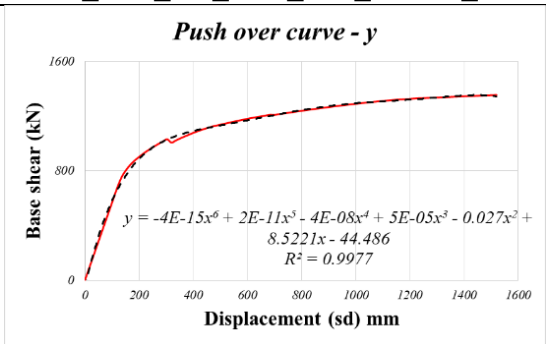

Figure 7.157 Pushover curve of building S9_1.00_DF_UNI_IR2_IS_Y

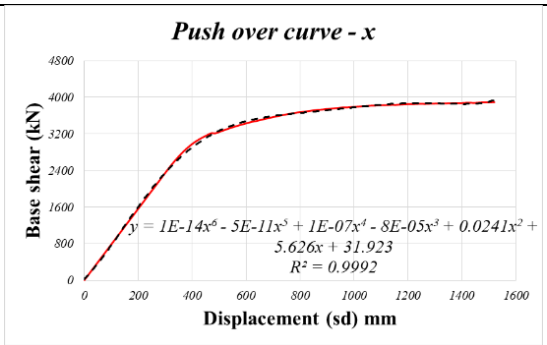

Figure 7.158 Pushover curve of building S9_1.00_DF_UNI_IR2_MODE_X

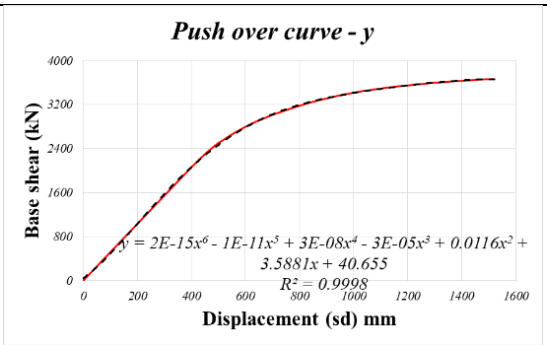

Figure 7.159 Pushover curve of building S9_1.00_DF_UNI_IR2_MODE_Y

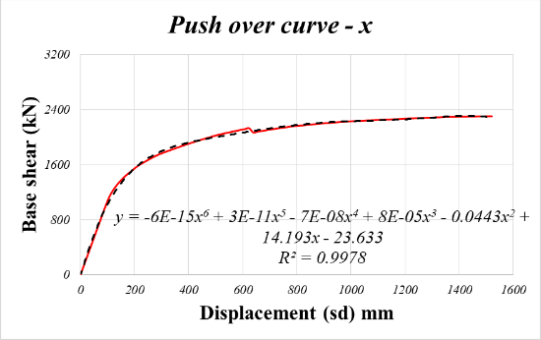

Figure 7.160 Pushover curve of building S9_1.00_DF_UNI_IR3_ACCL_X

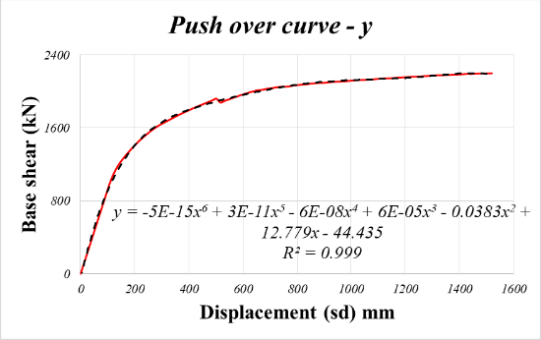

Figure 7.161 Pushover curve of building S9_1.00_DF_UNI_IR3_ACCL_Y

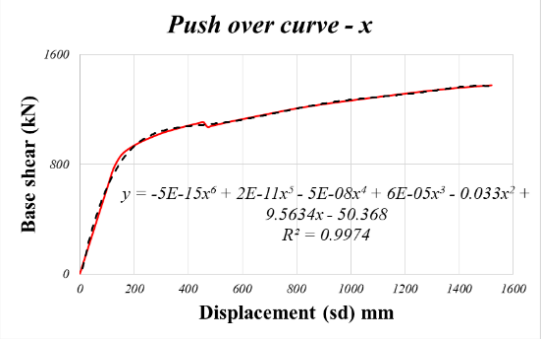

Figure 7.162 Pushover curve of building S9_1.00_DF_UNI_IR3_IS_X

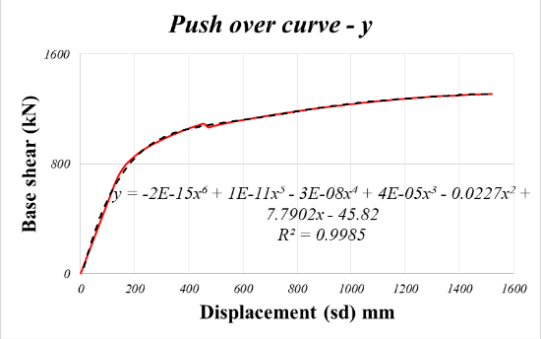

Figure 7.163 Pushover curve of building S9_1.00_DF_UNI_IR3_IS_Y

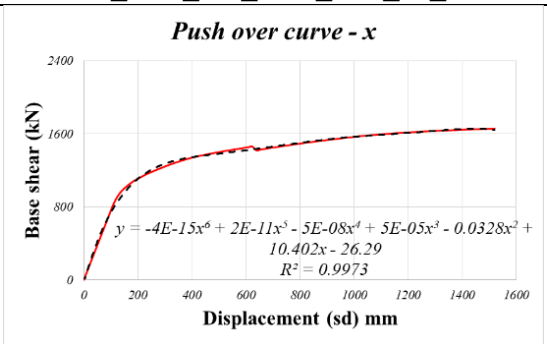

Figure 7.164 Pushover curve of building S9_1.00_DF_UNI_IR3_MODE_X

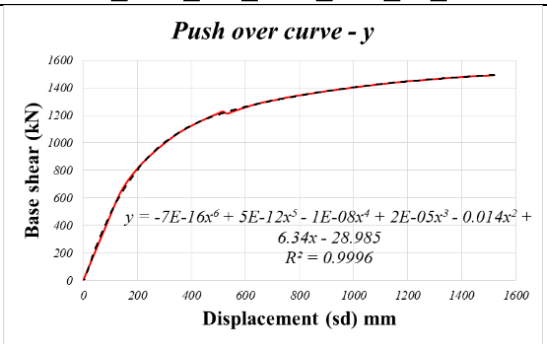

Figure 7.165 Pushover curve of building S9_1.00_DF_UNI_IR3_MODE_Y

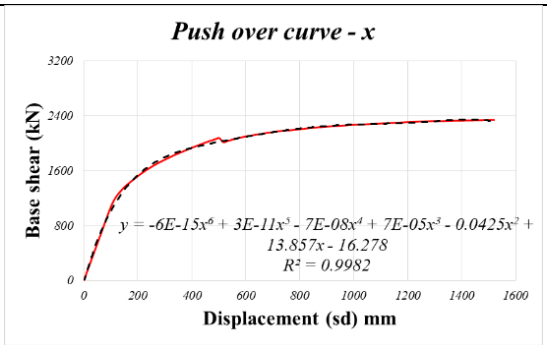

Figure 7.166 Pushover curve of building S9_1.00_DF_BI_IR1_ACCL_X

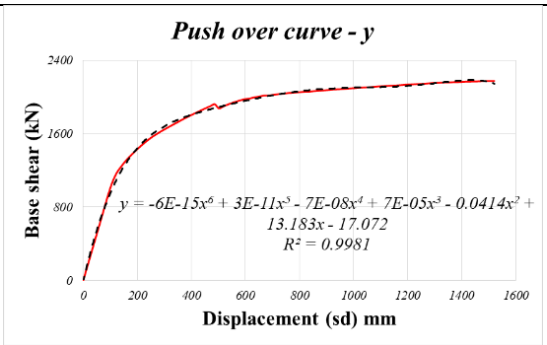

Figure 7.167 Pushover curve of building S9_1.00_DF_BI_IR1_ACCL_Y

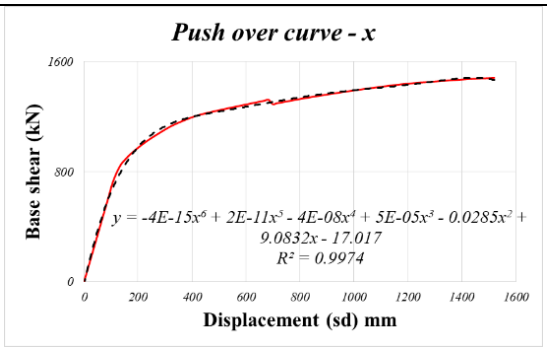

Figure 7.168 Pushover curve of building S6_1.00_DF_BI_IR1_IS_X

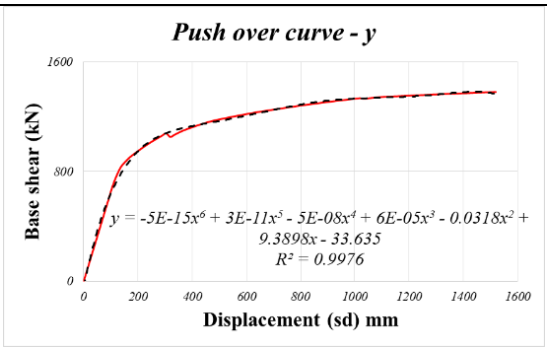

Figure 7.169 Pushover curve of building S6_1.00_DF_BI_IR1_IS_Y

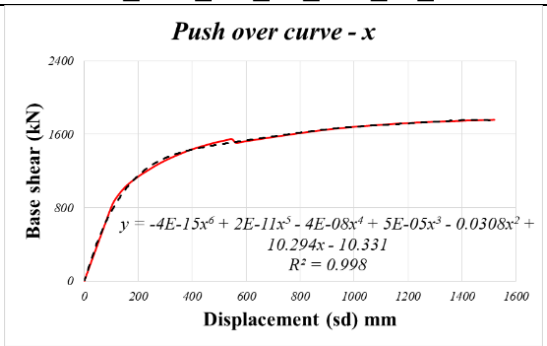

Figure 7.170 Pushover curve of building S6_1.00_DF_BI_IR1_MODE_X

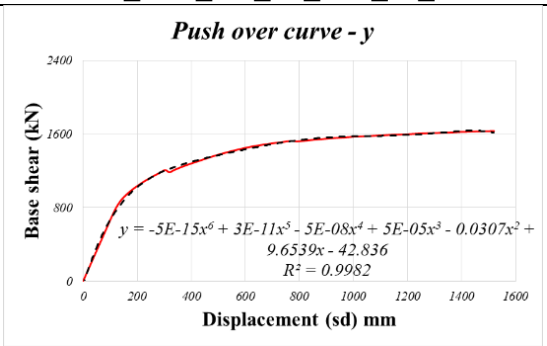

Figure 7.171 Pushover curve of building S6_1.00_DF_BI_IR1_MODE_Y

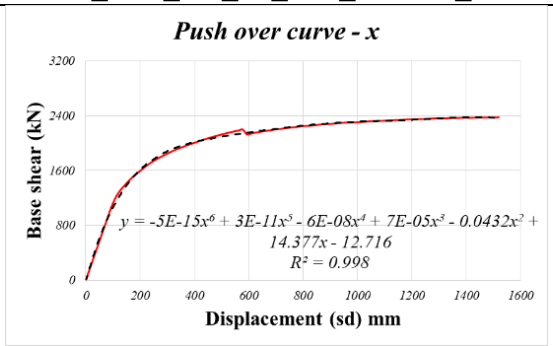

Figure 7.172 Pushover curve of building S6_1.00_DF_BI_IR2_ACCL_X

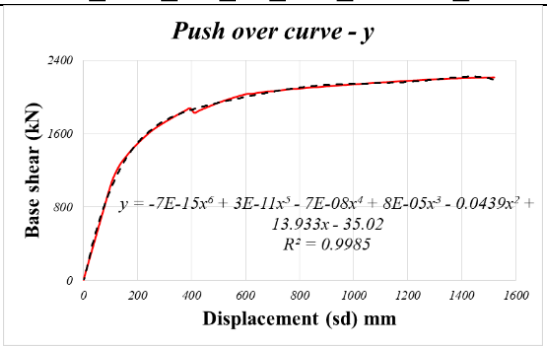

Figure 7.173 Pushover curve of building S6_1.00_DF_BI_IR2_ACCL

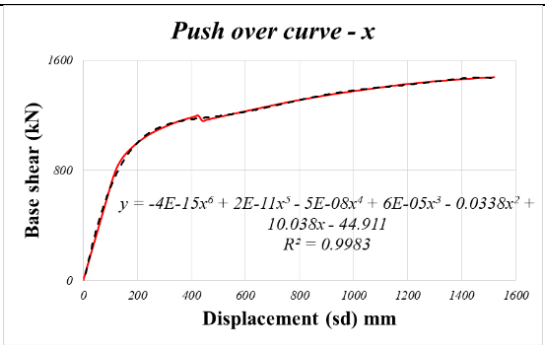

Figure 7.174 Pushover curve of building S6_1.00_DF_BI_IR2_IS_X

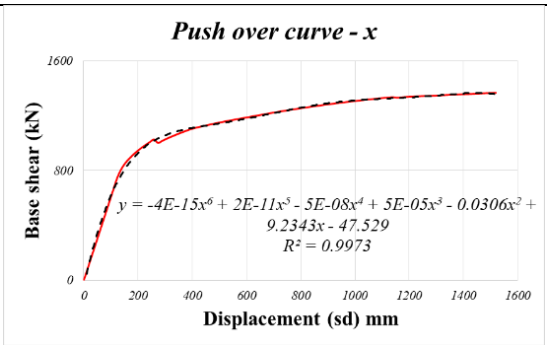

Figure 7.175 Pushover curve of building S6_1.00_DF_BI_IR2_IS_Y

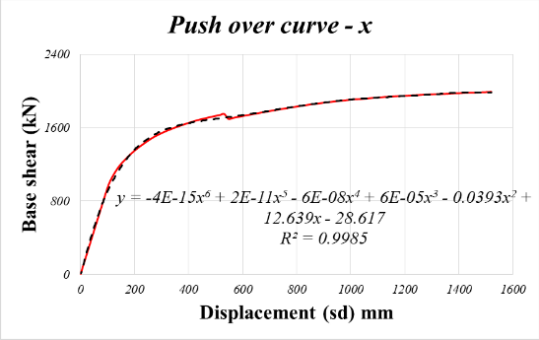

Figure 7.176 Pushover curve of building S6_1.00_DF_BI_IR2_MODE_X

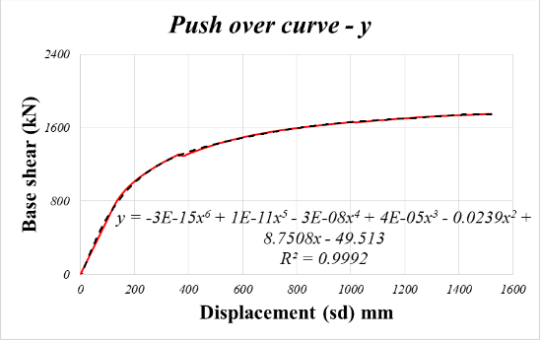

Figure 7.177 Pushover curve of building S6_1.00_DF_BI_IR2_MODE_Y

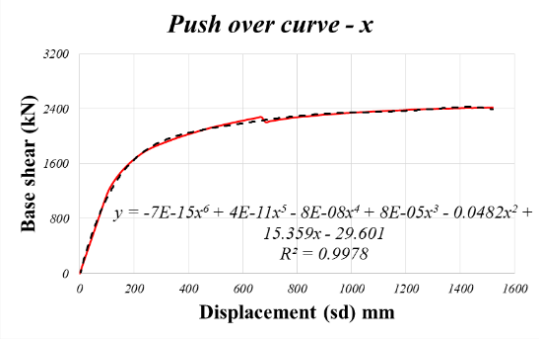

Figure 7.178 Pushover curve of building S6_1.00_DF_BI_IR3_ACCL_X

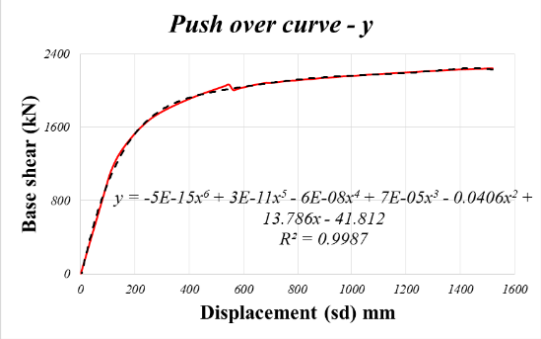

Figure 7.179 Pushover curve of building S6_1.00_DF_BI_IR3_ACCL_Y

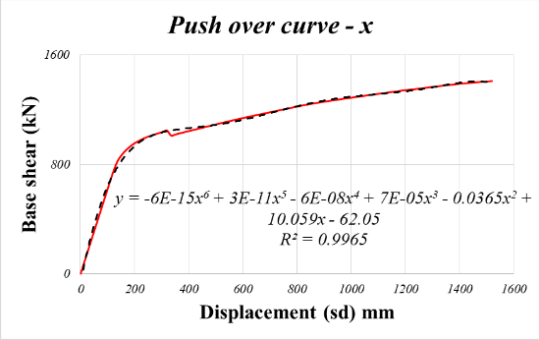

Figure 7.180 Pushover curve of building S6_1.00_DF_BI_IR3_IS_X

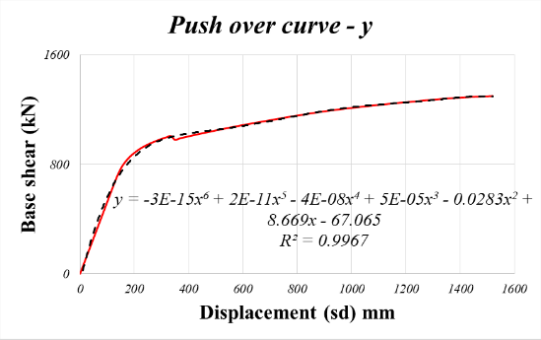

Figure 7.181 Pushover curve of building S6_1.00_DF_BI_IR3_IS_Y

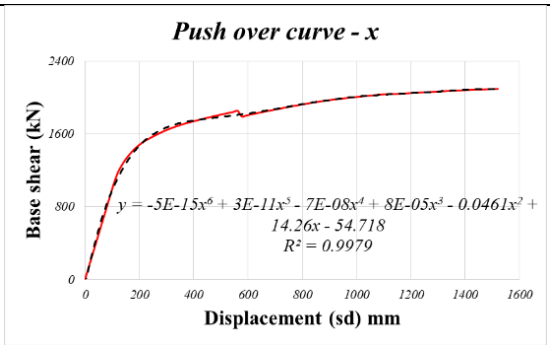

Figure 7.182 Pushover curve of building S6_1.00_DF_BI_IR3_MODE_X

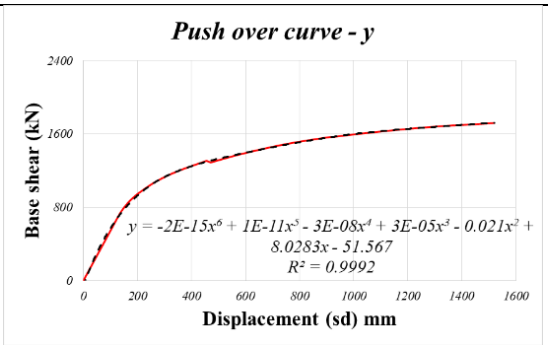

Figure 7.183 Pushover curve of building S6_1.00_DF_BI_IR3_MODE_Y

5.2 Results of proposed methods based on absorbed energy and degradation stiffness

Equation 2 was used to calculate out the energy based damage index, and the energy based damage index calculation results of buildings that used user-defined plastic hinges criteria with different aspect ratios are shown in Table 7.1through Table 7.18. Table 7.19 to Table 7.58be shown the energy based damage index calculation results of buildings used the defaults types of plastic hinges with plan aspect ratio 1.00.

Table 7.1 4- storey building with user defined plastic hinges in X dirn.

(0.5 aspect ratio)

S4_AR_0.5_ACCL_LOAD TYPE_PUSH_X						
Per.lvl.	step no.	Region	Sd (mm)	Drift (%)	DI_E (%)	DI_K (%)
OP	64	A-B	46.08	0.256	0.00	0.00
IO	65	B-IO	46.80	0.260	0.40	49.23
P.P	72	-	51.24	0.285	2.74	49.33
LS	109	IO-LS	78.48	0.436	17.93	50.38
CP	261	LS-CP	187.92	1.044	76.77	56.43
C	323	CP-C-D-E	232.56	1.292	100.00	58.10
S4_AR_0.5_IS_LOAD TYPE_PUSH_X						
Per.lvl.	step no.	Region	Sd (mm)	Drift (%)	DI_E (%)	DI_K (%)
OP	126	A-B	90.72	0.504	0.00	0.00
P.P	94	-	67.70	0.376	0.00	49.47

IO	127	B-IO	91.44	0.508	0.35	49.61
LS	187	IO-LS	134.64	0.748	21.49	50.15
CP	355	LS-CP	255.60	1.420	79.82	55.36
C	414	CP-C-D-E	298.08	1.656	100.00	56.92
S4_AR_0.5_MODE_LOAD TYPE_PUSH_X						
Per.lvl.	step no.	Region	Sd (mm)	Drift (%)	DI_E (%)	DI_K (%)
OP	69	A-B	49.68	0.276	0.00	0.00
P.P	82	-	59.07	0.328	4.82	49.46
IO	70	B-IO	50.40	0.280	0.37	49.29
LS	117	IO-LS	84.24	0.468	17.66	50.58
CP	291	LS-CP	209.52	1.164	79.89	57.43
C	349	CP-C-D-E	251.28	1.396	100.00	58.59

Table 7.2 4- storey building with user defined plastic hinges in Y dirn.

(0.5 aspect ratio)

S4_AR_0.5_ACCL_LOAD TYPE_PUSH_Y						
Per.lvl.	step no.	Region	Sd (mm)	Drift (%)	DI_E (%)	DI_K (%)
OP	70	A-B	50.40	0.280	0.00	0.00
IO	71	B-IO	51.12	0.284	0.22	49.30
P.P	82	-	59.53	0.331	2.81	49.44
LS	120	IO-LS	86.40	0.480	11.93	50.59
CP	289	LS-CP	208.08	1.156	69.68	56.30
C	356	CP-C-D-E	256.32	1.424	100.00	63.34
S4_AR_0.5_IS_LOAD TYPE_PUSH_Y						
Per.lvl.	step no.	Region	Sd (mm)	Drift (%)	DI_E (%)	DI_K (%)
OP	146	A-B	105.12	0.584	0.00	0.00
IO	147	B-IO	105.84	0.588	0.35	49.66
P.P	113	-	81.79	0.454	0.00	49.56
LS	221	IO-LS	159.12	0.884	26.13	50.04
CP	386	LS-CP	277.92	1.544	80.43	53.52

C	449	CP-C-D-E	323.28	1.796	100.00	54.95
S4_AR_0.5_MODE_LOAD TYPE_PUSH_Y						
Per.lvl.	step no.	Region	Sd (mm)	Drift (%)	DI_E (%)	DI_K (%)
OP	86	A-B	61.92	0.344	0.00	0.00
P.P	106	-	76.70	0.426	7.79	49.69
IO	87	B-IO	62.64	0.348	0.38	49.43
LS	129	IO-LS	92.88	0.516	16.29	50.27
CP	292	LS-CP	210.24	1.168	76.59	54.58
C	357	CP-C-D-E	257.04	1.428	100.00	55.86

Table 7.3 4- storey building with user defined plastic hinges in X dirn.

(0.75 aspect ratio)

S4_AR_0.75_ACCL_LOAD TYPE_PUSH_X						
Per.lvl.	step no.	Region	Sd (mm)	Drift (%)	DI_E (%)	DI_K (%)
OP	66	A-B	47.52	0.264	0.00	0.00
IO	67	B-IO	48.24	0.268	0.37	49.25
P.P	71	-	51.31	0.285	1.93	49.31
LS	113	IO-LS	81.36	0.452	17.15	50.57
CP	285	LS-CP	205.20	1.140	78.27	57.10
C	348	CP-C-D-E	250.56	1.392	100.00	58.71
S4_AR_0.75_IS_LOAD TYPE_PUSH_X						
Per.lvl.	step no.	Region	Sd (mm)	Drift (%)	DI_E (%)	DI_K (%)
OP	75	A-B	54.00	0.300	0.00	0.00
IO	76	B-IO	54.72	0.304	0.37	49.34
P.P	88	-	63.98	0.355	5.16	49.55
LS	127	IO-LS	91.44	0.508	19.25	51.05
CP	295	LS-CP	212.40	1.180	79.73	57.66
C	353	CP-C-D-E	254.16	1.412	100.00	59.10
S4_AR_0.75_MODE_LOAD TYPE_PUSH_X						
Per.lvl.	step no.	Region	Sd (mm)	Drift (%)	DI_E (%)	DI_K (%)
OP	71	A-B	51.12	0.284	0.00	0.00

IO	72	B-IO	51.84	0.288	0.37	49.31
P.P	81	-	58.94	0.327	4.00	49.44
LS	123	IO-LS	88.56	0.492	19.08	50.94
CP	293	LS-CP	210.96	1.172	79.84	57.48
C	351	CP-C-D-E	252.72	1.404	100.00	58.94

Table 7.4 4- storey building with user defined plastic hinges in Y dirn.

(0.75 aspect ratio)

S4_AR_0.75_ACCL_LOAD TYPE_PUSH_Y						
Per.lvl.	step no.	Region	Sd (mm)	Drift (%)	DI_E (%)	DI_K (%)
OP	69	A-B	49.68	0.276	0.00	0.00
IO	70	B-IO	50.40	0.280	0.36	49.29
P.P	80	-	57.67	0.320	4.04	49.41
LS	119	IO-LS	85.68	0.476	18.13	50.51
CP	289	LS-CP	208.08	1.156	78.29	56.20
C	352	CP-C-D-E	253.44	1.408	100.00	57.73
S4_AR_0.75_IS_LOAD TYPE_PUSH_Y						
Per.lvl.	step no.	Region	Sd (mm)	Drift (%)	DI_E (%)	DI_K (%)
OP	81	A-B	58.32	0.324	0.00	0.00
IO	82	B-IO	59.04	0.328	0.37	49.39
P.P	103	-	74.63	0.415	8.30	49.69
LS	137	IO-LS	98.64	0.548	20.46	50.78
CP	303	LS-CP	218.16	1.212	79.76	56.28
C	361	CP-C-D-E	259.92	1.444	100.00	57.65
S4_AR_0.75_MODE_LOAD TYPE_PUSH_Y						
Per.lvl.	step no.	Region	Sd (mm)	Drift (%)	DI_E (%)	DI_K (%)
OP	86	A-B	61.92	0.344	0.00	0.00
IO	87	B-IO	62.64	0.348	0.38	49.43
P.P	102	-	73.63	0.409	6.11	49.58
LS	130	IO-LS	93.60	0.520	16.47	50.19
CP	297	LS-CP	213.84	1.188	77.35	54.34
C	361	CP-C-D-E	259.92	1.444	100.00	55.62

Table 7.5 4- storey building with user defined plastic hinges in X dirn.

(1.00 aspect ratio)

S4_AR_1.00_ACCL_LOAD TYPE_PUSH_X						
Per.lvl.	step no.	Region	Sd (mm)	Drift (%)	DI_E (%)	DI_K (%)
OP	66	A-B	47.52	0.264	0.00	0.00
IO	67	B-IO	48.24	0.268	0.36	49.25
P.P	71	-	51.39	0.286	1.93	49.31
LS	114	IO-LS	82.08	0.456	17.11	50.66
CP	293	LS-CP	210.96	1.172	79.16	57.50
C	355	CP-C-D-E	255.60	1.420	100.00	59.05
S4_AR_1.00_IS_LOAD TYPE_PUSH_X						
Per.lvl.	step no.	Region	Sd (mm)	Drift (%)	DI_E (%)	DI_K (%)
OP	111	A-B	79.92	0.444	0.00	0.00
P.P	93	-	67.26	0.374	0.00	49.46
IO	112	B-IO	80.64	0.448	0.34	49.55
LS	170	IO-LS	122.40	0.680	19.72	49.96
CP	357	LS-CP	257.04	1.428	81.23	55.67
C	415	CP-C-D-E	298.80	1.660	100.00	57.18
S4_AR_1.00_MODE_LOAD TYPE_PUSH_X						
Per.lvl.	step no.	Region	Sd (mm)	Drift (%)	DI_E (%)	DI_K (%)
OP	71	A-B	51.12	0.284	0.00	0.00
IO	72	B-IO	51.84	0.288	0.37	49.31
P.P	81	-	58.88	0.327	3.95	49.44
LS	125	IO-LS	90.00	0.500	19.70	51.12
CP	295	LS-CP	212.40	1.180	80.01	57.72
C	353	CP-C-D-E	254.16	1.412	100.00	59.18

Table 7.6 4- storey building with user defined plastic hinges in Y dirn.

(1.00 aspect ratio)

S4_AR_1.00_ACCL_LOAD TYPE_PUSH_Y						
Per.lvl.	step no.	Region	Sd (mm)	Drift (%)	DI_E (%)	DI_K (%)
OP	69	A-B	49.68	0.276	0.00	0.00
IO	70	B-IO	50.40	0.280	0.37	49.29
P.P	78	-	56.31	0.313	3.44	49.39
LS	118	IO-LS	84.96	0.472	18.21	50.49
CP	283	LS-CP	203.76	1.132	78.08	56.23
C	345	CP-C-D-E	248.40	1.380	100.00	57.83
S4_AR_1.00_IS_LOAD TYPE_PUSH_Y						
Per.lvl.	step no.	Region	Sd (mm)	Drift (%)	DI_E (%)	DI_K (%)
OP	124	A-B	89.28	0.496	0.00	0.00
P.P	105	-	75.82	0.421	0.00	49.52
IO	125	B-IO	90.00	0.500	0.32	49.60
LS	203	IO-LS	146.16	0.812	25.22	50.14
CP	382	LS-CP	275.04	1.528	81.07	54.62
C	444	CP-C-D-E	319.68	1.776	100.00	56.08
S4_AR_1.00_MODE_LOAD TYPE_PUSH_Y						
Per.lvl.	step no.	Region	Sd (mm)	Drift (%)	DI_E (%)	DI_K (%)
OP	86	A-B	61.92	0.344	0.00	0.00
IO	87	B-IO	62.64	0.348	0.38	49.43
P.P	98	-	70.82	0.393	4.66	49.52
LS	131	IO-LS	94.32	0.524	16.88	50.16
CP	297	LS-CP	213.84	1.188	77.60	54.28
C	360	CP-C-D-E	259.20	1.440	100.00	55.60

Table 7.7 6- storey building with user defined plastic hinges in X dirn.

(0.5 aspect ratio)

S6_AR_0.5_ACCL_LOAD TYPE_PUSH_X						
Per.lvl.	step no.	Region	Sd (mm)	Drift (%)	DI_E (%)	DI_K (%)
OP	60	A-B	62.40	0.240	0.00	0.00
IO	61	B-IO	63.44	0.244	0.48	42.38
P.P	74	-	77.08	0.296	6.78	49.43
LS	102	IO-LS	106.08	0.408	20.02	50.48
CP	232	LS-CP	241.28	0.928	79.21	55.98
C	280	CP-C-D-E	291.20	1.120	100.00	57.35
S6_AR_0.5_IS_LOAD TYPE_PUSH_X						
Per.lvl.	step no.	Region	Sd (mm)	Drift (%)	DI_E (%)	DI_K (%)
OP	198	A-B	205.92	0.792	0.00	0.00
P.P	99	-	103.45	0.398	0.00	49.50
IO	199	B-IO	206.96	0.796	0.48	49.75
LS	238	IO-LS	247.52	0.952	19.13	49.90
CP	366	LS-CP	380.64	1.464	81.59	51.90
C	403	CP-C-D-E	419.12	1.612	100.00	52.66
S6_AR_0.5_MODE_LOAD TYPE_PUSH_X						
Per.lvl.	step no.	Region	Sd (mm)	Drift (%)	DI_E (%)	DI_K (%)
OP	64	A-B	66.56	0.256	0.00	0.00
IO	65	B-IO	67.60	0.260	0.46	49.23
P.P	84	-	87.65	0.337	9.19	49.62
LS	106	IO-LS	110.24	0.424	18.97	50.49
CP	241	LS-CP	250.64	0.964	77.79	56.19
C	294	CP-C-D-E	305.76	1.176	100.00	57.71

Table 7.8 6- storey building with user defined plastic hinges in Y dirn.

(0.5 aspect ratio)

S6_AR_0.5_ACCL_LOAD TYPE_PUSH_Y						
Per.lvl.	step no.	Region	Sd (mm)	Drift (%)	DI_E (%)	DI_K (%)
OP	66	A-B	68.64	0.264	0.00	0.00
IO	67	B-IO	69.68	0.268	0.45	49.25
P.P	84	-	87.29	0.336	8.12	49.62
LS	112	IO-LS	116.48	0.448	20.69	50.80
CP	248	LS-CP	257.92	0.992	79.37	55.96
C	298	CP-C-D-E	309.92	1.192	100.00	57.21
S6_AR_0.5_IS_LOAD TYPE_PUSH_Y						
Per.lvl.	step no.	Region	Sd (mm)	Drift (%)	DI_E (%)	DI_K (%)
OP	194	A-B	201.76	0.776	0.00	0.00
P.P	119	-	123.55	0.475	0.00	49.58
IO	195	B-IO	202.80	0.780	0.42	49.74
LS	237	IO-LS	246.48	0.948	18.05	49.90
CP	369	LS-CP	383.76	1.476	74.37	51.73
C	428	CP-C-D-E	445.12	1.712	100.00	52.81
S6_AR_0.5_MODE_LOAD TYPE_PUSH_Y						
Per.lvl.	step no.	Region	Sd (mm)	Drift (%)	DI_E (%)	DI_K (%)
OP	79	A-B	82.16	0.316	0.00	0.00
IO	80	B-IO	83.20	0.320	0.46	49.38
P.P	112	-	116.15	0.447	14.98	50.05
LS	121	IO-LS	125.84	0.484	19.22	50.37
CP	254	LS-CP	264.16	1.016	78.17	54.56
C	305	CP-C-D-E	317.20	1.220	100.00	55.66

Table 7.9 6- storey building with user defined plastic hinges in X dirn.

(0.75 aspect ratio)

S6_AR_0.75_ACCL_LOAD TYPE_PUSH_X						
Per.lvl.	step no.	Region	Sd (mm)	Drift (%)	DI_E (%)	DI_K (%)
OP	31	A-B	64.48	0.248	0.00	0.00
IO	32	B-IO	66.56	0.256	0.93	48.44
P.P	37	-	77.19	0.297	5.68	48.76
LS	53	IO-LS	110.24	0.424	20.26	50.30
CP	120	LS-CP	249.60	0.960	79.13	56.12
C	145	CP-C-D-E	301.60	1.160	100.00	57.57
S6_AR_0.75_IS_LOAD TYPE_PUSH_X						
Per.lvl.	step no.	Region	Sd (mm)	Drift (%)	DI_E (%)	DI_K (%)
OP	194	A-B	201.76	0.776	0.00	0.00
P.P	99	-	103.62	0.399	0.00	49.49
IO	195	B-IO	202.80	0.780	0.41	49.74
LS	235	IO-LS	244.40	0.940	17.13	49.89
CP	365	LS-CP	379.60	1.460	72.98	52.00
C	426	CP-C-D-E	443.04	1.704	100.00	53.26
S6_AR_0.75_MODE_LOAD TYPE_PUSH_X						
Per.lvl.	step no.	Region	Sd (mm)	Drift (%)	DI_E (%)	DI_K (%)
OP	167	A-B	173.68	0.668	0.00	0.00
P.P	91	-	94.55	0.364	0.00	49.45
IO	168	B-IO	174.72	0.672	0.25	49.70
LS	211	IO-LS	219.44	0.844	14.15	49.83
CP	321	LS-CP	333.84	1.284	78.67	51.42
C	347	CP-C-D-E	360.88	1.388	100.00	51.93

Table 7.10 6- storey building with user defined plastic hinges in Y dirn.

(0.75 aspect ratio)

S6_AR_0.75_ACCL_LOAD TYPE_PUSH_Y						
Per.lvl.	step no.	Region	Sd (mm)	Drift (%)	DI_E (%)	DI_K (%)
OP	32	A-B	66.56	0.256	0.00	0.00
IO	33	B-IO	68.64	0.264	0.92	48.48
P.P	40	-	84.78	0.326	8.00	48.90
LS	55	IO-LS	114.40	0.440	20.88	50.25
CP	122	LS-CP	253.76	0.976	79.19	55.72
C	147	CP-C-D-E	305.76	1.176	100.00	57.09
S6_AR_0.75_IS_LOAD TYPE_PUSH_Y						
Per.lvl.	step no.	Region	Sd (mm)	Drift (%)	DI_E (%)	DI_K (%)
OP	222	A-B	230.88	0.888	0.00	0.00
P.P	114	-	118.49	0.456	0.00	49.56
IO	223	B-IO	231.92	0.892	0.46	49.78
LS	264	IO-LS	274.56	1.056	19.29	49.89
CP	387	LS-CP	402.48	1.548	76.21	51.45
C	438	CP-C-D-E	455.52	1.752	100.00	52.32
S6_AR_0.75_MODE_LOAD TYPE_PUSH_Y						
Per.lvl.	step no.	Region	Sd (mm)	Drift (%)	DI_E (%)	DI_K (%)
OP	139	A-B	144.56	0.556	0.00	0.00
P.P	116	-	120.86	0.465	0.00	49.57
IO	140	B-IO	145.60	0.560	0.62	49.64
LS	201	IO-LS	209.04	0.804	35.32	49.81
CP	331	LS-CP	344.24	1.324	88.17	50.91
C	377	CP-C-D-E	392.08	1.508	100.00	51.44

Table 7.11 6- storey building with user defined plastic hinges in X dirn.

(1.00 aspect ratio)

S6_AR_1.00_ACCL_LOAD TYPE_PUSH_X						
Per.lvl.	step no.	Region	Sd (mm)	Drift (%)	DI_E (%)	DI_K (%)
OP	31	A-B	64.48	0.248	0.00	0.00
IO	32	B-IO	66.56	0.256	0.89	48.44
P.P	35	-	77.03	0.296	5.34	48.63
LS	53	IO-LS	110.24	0.424	19.30	50.38
CP	123	LS-CP	255.84	0.984	77.82	56.60
C	151	CP-C-D-E	314.08	1.208	100.00	58.24
S6_AR_1.00_IS_LOAD TYPE_PUSH_X						
Per.lvl.	step no.	Region	Sd (mm)	Drift (%)	DI_E (%)	DI_K (%)
OP	18	A-B	37.44	0.144	0.00	0.00
IO	19	B-IO	39.52	0.152	0.93	47.37
LS	39	IO-LS	81.12	0.312	19.47	49.37
P.P	47	-	98.97	0.381	27.33	50.12
CP	103	LS-CP	214.24	0.824	76.76	54.22
C	130	CP-C-D-E	270.40	1.040	100.00	55.94
S6_AR_1.00_MODE_LOAD TYPE_PUSH_X						
Per.lvl.	step no.	Region	Sd (mm)	Drift (%)	DI_E (%)	DI_K (%)
OP	32	A-B	66.56	0.256	0.00	0.00
IO	33	B-IO	68.64	0.264	0.81	48.48
P.P	42	-	87.37	0.336	8.08	49.07
LS	54	IO-LS	112.32	0.432	17.70	50.30
CP	130	LS-CP	270.40	1.040	76.81	56.92
C	161	CP-C-D-E	334.88	1.288	100.00	58.73

Table 7.12 6- storey building with user defined plastic hinges in Y dirn.

(1.00 aspect ratio)

S6_AR_1.00_ACCL_LOAD TYPE_PUSH_Y						
Per.lvl.	step no.	Region	Sd (mm)	Drift (%)	DI_E (%)	DI_K (%)
OP	32	A-B	66.56	0.256	0.00	0.00
IO	33	B-IO	68.64	0.264	0.90	48.48
P.P	39	-	82.96	0.319	7.06	48.84
LS	55	IO-LS	114.40	0.440	20.46	50.27
CP	124	LS-CP	257.92	0.992	79.49	56.18
C	149	CP-C-D-E	309.92	1.192	100.00	57.64
S6_AR_1.00_IS_LOAD TYPE_PUSH_Y						
Per.lvl.	step no.	Region	Sd (mm)	Drift (%)	DI_E (%)	DI_K (%)
OP	21	A-B	43.68	0.168	0.00	0.00
IO	22	B-IO	45.76	0.176	0.87	47.73
LS	46	IO-LS	95.68	0.368	21.55	49.26
P.P	53	-	111.07	0.427	27.87	49.64
CP	113	LS-CP	235.04	0.904	77.88	53.05
C	140	CP-C-D-E	291.20	1.120	100.00	56.53
S6_AR_1.00_MODE_LOAD TYPE_PUSH_Y						
Per.lvl.	step no.	Region	Sd (mm)	Drift (%)	DI_E (%)	DI_K (%)
OP	38	A-B	79.04	0.304	0.00	0.00
IO	39	B-IO	81.12	0.312	0.87	48.72
P.P	52	-	108.51	0.417	12.29	49.27
LS	61	IO-LS	126.88	0.488	19.89	49.85
CP	130	LS-CP	270.40	1.040	77.95	54.21
C	157	CP-C-D-E	326.56	1.256	100.00	55.49

Table 7.13 9- storey building with user defined plastic hinges in X dirn.

(0.5 aspect ratio)

S9_AR_0.5_ACCL_LOAD TYPE_PUSH_X						
Per.lvl.	step no.	Region	Sd (mm)	Drift (%)	DI_E (%)	DI_K (%)
OP	28	A-B	85.12	0.224	0.00	0.00
IO	29	B-IO	88.16	0.232	1.20	48.28
P.P	38	-	115.97	0.305	12.05	48.95
LS	46	IO-LS	139.84	0.368	21.21	49.79
CP	99	LS-CP	300.96	0.792	79.57	55.54
C	119	CP-C-D-E	361.76	0.952	100.00	57.03
S9_AR_0.5_IS_LOAD TYPE_PUSH_X						
Per.lvl.	step no.	Region	Sd (mm)	Drift (%)	DI_E (%)	DI_K (%)
OP	15	A-B	45.60	0.120	0.00	0.00
IO	16	B-IO	48.64	0.128	1.11	46.87
LS	34	IO-LS	103.36	0.272	20.99	48.83
P.P	47	-	144.93	0.381	35.92	49.69
CP	87	LS-CP	264.48	0.696	78.02	53.26
C	108	CP-C-D-E	328.32	0.864	100.00	54.97
S9_AR_0.5_MODE_LOAD TYPE_PUSH_X						
Per.lvl.	step no.	Region	Sd (mm)	Drift (%)	DI_E (%)	DI_K (%)
OP	30	A-B	91.20	0.240	0.00	0.00
IO	31	B-IO	94.24	0.248	1.08	48.39
P.P	43	-	130.95	0.345	14.00	49.21
LS	50	IO-LS	152.00	0.400	21.33	49.96
CP	107	LS-CP	325.28	0.856	79.52	55.93
C	128	CP-C-D-E	389.12	1.024	100.00	57.40

Table 7.14 9- storey building with user defined plastic hinges in Y dirn.

(0.5 aspect ratio)

S9_AR_0.5_ACCL_LOAD TYPE_PUSH_Y						
Per.lvl.	step no.	Region	Sd (mm)	Drift (%)	DI_E (%)	DI_K (%)
OP	30	A-B	91.20	0.240	0.00	0.00
IO	31	B-IO	94.24	0.248	1.08	48.39
P.P	42	-	128.52	0.338	13.17	49.21
LS	49	IO-LS	148.96	0.392	20.29	50.02
CP	107	LS-CP	325.28	0.856	79.00	55.82
C	129	CP-C-D-E	392.16	1.032	100.00	57.23
S9_AR_0.5_IS_LOAD TYPE_PUSH_Y						
Per.lvl.	step no.	Region	Sd (mm)	Drift (%)	DI_E (%)	DI_K (%)
OP	24	A-B	72.96	0.192	0.00	0.00
IO	25	B-IO	76.00	0.200	1.08	48.00
LS	43	IO-LS	130.72	0.344	20.45	49.13
P.P	55	-	168.21	0.443	33.60	49.87
CP	99	LS-CP	300.96	0.792	79.42	53.25
C	119	CP-C-D-E	361.76	0.952	100.00	54.63
S9_AR_0.5_MODE_LOAD TYPE_PUSH_Y						
Per.lvl.	step no.	Region	Sd (mm)	Drift (%)	DI_E (%)	DI_K (%)
OP	36	A-B	109.44	0.288	0.00	0.00
IO	37	B-IO	112.48	0.296	0.99	48.65
P.P	55	-	168.79	0.444	19.30	49.83
LS	57	IO-LS	173.28	0.456	20.75	50.02
CP	118	LS-CP	358.72	0.944	79.42	55.11
C	140	CP-C-D-E	425.60	1.120	100.00	56.34

Table 7.15 9- storey building with user defined plastic hinges in X dirn.

(0.75 aspect ratio)

S9_AR_0.75_ACCL_LOAD TYPE_PUSH_X						
Per.lvl.	step no.	Region	Sd (mm)	Drift (%)	DI_E (%)	DI_K (%)
OP	28	A-B	85.12	0.224	0.00	0.00
IO	29	B-IO	88.16	0.232	1.21	48.28
P.P	38	-	115.51	0.304	11.92	48.99
LS	46	IO-LS	139.84	0.368	21.23	49.90
CP	102	LS-CP	310.08	0.816	80.45	55.88
C	123	CP-C-D-E	373.92	0.984	100.00	57.35
S9_AR_0.75_IS_LOAD TYPE_PUSH_X						
Per.lvl.	step no.	Region	Sd (mm)	Drift (%)	DI_E (%)	DI_K (%)
OP	117	A-B	355.68	0.936	0.00	0.00
P.P	52	-	158.60	0.417	0.00	49.04
IO	118	B-IO	358.72	0.944	0.93	49.58
LS	140	IO-LS	425.60	1.120	21.39	49.68
CP	202	LS-CP	614.08	1.616	79.33	51.23
C	224	CP-C-D-E	680.96	1.792	100.00	52.00
S9_AR_0.75_MODE_LOAD TYPE_PUSH_X						
Per.lvl.	step no.	Region	Sd (mm)	Drift (%)	DI_E (%)	DI_K (%)
OP	30	A-B	91.20	0.240	0.00	0.00
IO	31	B-IO	94.24	0.248	1.08	48.39
P.P	43	-	130.20	0.343	13.66	49.31
LS	50	IO-LS	152.00	0.400	21.18	50.13
CP	109	LS-CP	331.36	0.872	79.70	56.24
C	131	CP-C-D-E	398.24	1.048	100.00	57.70

Table 7.16 9- storey building with user defined plastic hinges in Y dirn.

(0.75 aspect ratio)

S9_AR_0.75_ACCL_LOAD TYPE_PUSH_Y						
Per.lvl.	step no.	Region	Sd (mm)	Drift (%)	DI_E (%)	DI_K (%)
OP	29	A-B	88.16	0.232	0.00	0.00
IO	30	B-IO	91.20	0.240	1.13	48.33
P.P	41	-	124.50	0.328	13.33	49.16
LS	48	IO-LS	145.92	0.384	21.05	49.95
CP	105	LS-CP	319.20	0.840	79.92	55.76
C	126	CP-C-D-E	383.04	1.008	100.00	57.18
S9_AR_0.75_IS_LOAD TYPE_PUSH_Y						
Per.lvl.	step no.	Region	Sd (mm)	Drift (%)	DI_E (%)	DI_K (%)
OP	114	A-B	346.56	0.912	0.00	0.00
P.P	58	-	176.75	0.465	0.00	49.14
IO	115	B-IO	349.60	0.920	0.94	49.57
LS	136	IO-LS	413.44	1.088	20.80	49.70
CP	197	LS-CP	598.88	1.576	78.90	51.16
C	219	CP-C-D-E	665.76	1.752	100.00	51.89
S9_AR_0.75_MODE_LOAD TYPE_PUSH_Y						
Per.lvl.	step no.	Region	Sd (mm)	Drift (%)	DI_E (%)	DI_K (%)
OP	35	A-B	106.40	0.280	0.00	0.00
IO	36	B-IO	109.44	0.288	0.98	48.61
P.P	53	-	162.71	0.428	18.10	49.61
LS	58	IO-LS	176.32	0.464	22.45	50.07
CP	118	LS-CP	358.72	0.944	79.57	55.01
C	140	CP-C-D-E	425.60	1.120	100.00	56.27

Table 7.17 9- storey building with user defined plastic hinges in X dirn.

(1.00 aspect ratio)

S9_AR_1.00_ACCL_LOAD TYPE_PUSH_X						
Per.lvl.	step no.	Region	Sd (mm)	Drift (%)	DI_E (%)	DI_K (%)
OP	29	A-B	88.16	0.232	0.00	0.00
IO	30	B-IO	91.20	0.240	1.56	48.33
P.P	38	-	114.03	0.300	12.89	48.96
LS	48	IO-LS	145.92	0.384	27.61	50.15
CP	111	LS-CP	337.44	0.888	89.07	56.34
C	134	CP-C-D-E	407.36	1.072	100.00	57.71
S9_AR_1.00_IS_LOAD TYPE_PUSH_X						
Per.lvl.	step no.	Region	Sd (mm)	Drift (%)	DI_E (%)	DI_K (%)
OP	111	A-B	337.44	0.888	0.00	0.00
P.P	51	-	155.43	0.409	0.00	49.02
IO	112	B-IO	340.48	0.896	0.90	49.55
LS	132	IO-LS	401.28	1.056	18.97	49.67
CP	195	LS-CP	592.80	1.560	76.23	51.24
C	221	CP-C-D-E	671.84	1.768	100.00	52.17
S9_AR_1.00_MODE_LOAD TYPE_PUSH_X						
Per.lvl.	step no.	Region	Sd (mm)	Drift (%)	DI_E (%)	DI_K (%)
OP	31	A-B	94.24	0.248	0.00	0.00
IO	32	B-IO	97.28	0.256	1.10	48.44
P.P	42	-	128.48	0.338	12.17	49.23
LS	51	IO-LS	155.04	0.408	21.32	50.33
CP	115	LS-CP	349.60	0.920	80.57	56.60
C	140	CP-C-D-E	425.60	1.120	100.00	58.06

Table 7.18 9- storey building with user defined plastic hinges in Y dirn.

(1.00 aspect ratio)

S9_AR_1.00_ACCL_LOAD TYPE_PUSH_Y						
Per.lvl.	step no.	Region	Sd (mm)	Drift (%)	DI_E (%)	DI_K (%)
OP	29	A-B	88.16	0.232	0.00	0.00
IO	30	B-IO	91.20	0.240	1.18	48.33
P.P	40	-	120.44	0.317	12.34	49.08
LS	48	IO-LS	145.92	0.384	21.77	50.00
CP	109	LS-CP	331.36	0.872	81.93	56.04
C	131	CP-C-D-E	398.24	1.048	100.00	57.41
S9_AR_1.00_IS_LOAD TYPE_PUSH_Y						
Per.lvl.	step no.	Region	Sd (mm)	Drift (%)	DI_E (%)	DI_K (%)
OP	122	A-B	370.88	0.976	0.00	0.00
P.P	55	-	168.86	0.444	0.00	49.09
IO	123	B-IO	373.92	0.984	0.89	49.59
LS	147	IO-LS	446.88	1.176	22.41	49.72
CP	210	LS-CP	638.40	1.680	79.17	51.19
C	233	CP-C-D-E	708.32	1.864	100.00	51.93
S9_AR_1.00_MODE_LOAD TYPE_PUSH_Y						
Per.lvl.	step no.	Region	Sd (mm)	Drift (%)	DI_E (%)	DI_K (%)
OP	35	A-B	106.40	0.280	0.00	0.00
IO	36	B-IO	109.44	0.288	0.97	48.61
P.P	51	-	155.10	0.408	15.45	49.51
LS	57	IO-LS	173.28	0.456	21.18	50.07
CP	119	LS-CP	361.76	0.952	79.14	55.14
C	142	CP-C-D-E	431.68	1.136	100.00	56.42

Table 7.19 4- storey regular building of X dirn

S4_AR_1.0_ACCL_LOAD TYPE_PUSH_X						
Per.lvl.	step no.	Region	Sd (mm)	Drift (%)	DI_E (%)	DI_K (%)
OP	4	A-B	28.80	0.160	0.00	0.00
IO	5	B-IO	28.80	0.160	3.44	40.00
LS	14	IO-LS	100.80	0.560	45.60	50.24
CP	21	LS-CP	151.20	0.840	92.33	53.90
C	22	CP-C-D-E	158.40	0.880	100.00	54.32
P.P	5	-	36.00	0.200	3.44	40.00
S4_AR_1.0_IS_LOAD TYPE_PUSH_X						
Per.lvl.	step no.	Region	Sd (mm)	Drift (%)	DI_E (%)	DI_K (%)
OP	3	A-B	21.60	0.120	0.00	0.00
IO	4	B-IO	28.80	0.160	4.06	37.50
LS	13	IO-LS	93.60	0.520	41.76	50.00
CP	25	LS-CP	180.00	1.000	95.36	55.49
C	26	CP-C-D-E	187.20	1.040	100.00	55.79
P.P	5	-	36.00	0.200	8.14	40.21
S4_AR_1.0_MODE_LOAD TYPE_PUSH_X						
Per.lvl.	step no.	Region	Sd (mm)	Drift (%)	DI_E (%)	DI_K (%)
OP	3	A-B	21.60	0.120	0.00	0.00
IO	4	B-IO	28.80	0.160	3.85	37.50
LS	13	IO-LS	93.60	0.520	39.74	49.88
CP	26	LS-CP	187.20	1.040	95.52	55.63
C	27	CP-C-D-E	194.40	1.080	100.00	55.91
P.P	5	-	36.00	0.200	7.73	40.30

Table 7.20 4- storey regular building of Y dirn

S4_AR_1.0_ACCL_LOAD TYPE_PUSH_Y						
Per.lvl.	step no.	Region	Sd (mm)	Drift (%)	DI_E (%)	DI_K (%)
OP	4	A-B	28.80	0.160	0.00	0.00
IO	5	B-IO	36.00	0.200	0.26	40.00
LS	14	IO-LS	100.80	0.560	14.56	50.33
CP	30	LS-CP	216.00	1.200	92.86	57.58
C	31	CP-C-D-E	223.20	1.240	100.00	57.85
P.P	6	-	43.20	0.240	0.79	40.00
S4_AR_1.0_IS_LOAD TYPE_PUSH_Y						
Per.lvl.	step no.	Region	Sd (mm)	Drift (%)	DI_E (%)	DI_K (%)
OP	3	A-B	21.60	0.120	0.00	0.00
IO	4	B-IO	28.80	0.160	4.20	37.50
LS	12	IO-LS	86.40	0.480	38.97	49.66
CP	24	LS-CP	172.80	0.960	95.11	56.14
C	25	CP-C-D-E	180.00	1.000	100.00	56.48
P.P	5	-	36.00	0.200	8.43	40.34
S4_AR_1.0_MODE_LOAD TYPE_PUSH_Y						
Per.lvl.	step no.	Region	Sd (mm)	Drift (%)	DI_E (%)	DI_K (%)
OP	3	A-B	21.60	0.120	0.00	0.00
IO	4	B-IO	28.80	0.160	4.18	37.50
LS	13	IO-LS	93.60	0.520	41.78	49.90
CP	26	LS-CP	187.20	1.040	95.85	56.16
C	27	CP-C-D-E	194.40	1.080	100.00	56.49
P.P	5	-	36.00	0.200	8.37	40.32

Table 7.21 4- storey unidirectional setback with IR1 building case of X dirn

S4_AR_1.0_ACCL_LOAD TYPE_PUSH_X						
Per.lvl.	step no.	Region	Sd (mm)	Drift (%)	DI_E (%)	DI_K (%)
OP	4	A-B	28.80	0.160	0.00	0.00
IO	5	B-IO	36.00	0.200	3.23	40.00
LS	14	IO-LS	100.80	0.560	39.17	50.17
CP	24	LS-CP	172.80	0.960	93.70	55.12
C	25	CP-C-D-E	180.00	1.000	100.00	55.48
P.P	5	-	36.00	0.200	3.23	40.00
S4_AR_1.0_IS_LOAD TYPE_PUSH_X						
Per.lvl.	step no.	Region	Sd (mm)	Drift (%)	DI_E (%)	DI_K (%)
OP	3	A-B	21.60	0.120	0.00	0.00
IO	4	B-IO	28.80	0.160	4.02	37.50
LS	13	IO-LS	93.60	0.520	41.52	49.87
CP	25	LS-CP	180.00	1.000	95.32	55.79
C	26	CP-C-D-E	187.20	1.040	100.00	56.09
P.P	5	-	36.00	0.200	8.06	40.16
S4_AR_1.0_MODE_LOAD TYPE_PUSH_X						
Per.lvl.	step no.	Region	Sd (mm)	Drift (%)	DI_E (%)	DI_K (%)
OP	3	A-B	21.60	0.120	0.00	0.00
IO	4	B-IO	28.80	0.160	3.46	37.50
LS	14	IO-LS	100.80	0.560	41.47	50.32
CP	26	LS-CP	187.20	1.040	95.13	55.92
C	27	CP-C-D-E	194.40	1.080	100.00	56.23
P.P	5	-	36.00	0.200	6.99	40.13

Table 7.22 4- storey unidirectional setback with IR1 building case of Y dirn

S4_AR_1.0_ACCL_LOAD TYPE_PUSH_Y						
Per.lvl.	step no.	Region	Sd (mm)	Drift (%)	DI_E (%)	DI_K (%)
OP	4	A-B	28.80	0.160	0.00	0.00
IO	5	B-IO	36.00	0.200	2.07	40.00
LS	14	IO-LS	100.80	0.560	28.92	50.14
CP	27	LS-CP	194.40	1.080	93.74	55.98
C	28	CP-C-D-E	201.60	1.120	100.00	56.28
P.P	5	-	36.00	0.200	2.07	40.00
S4_AR_1.0_IS_LOAD TYPE_PUSH_Y						
Per.lvl.	step no.	Region	Sd (mm)	Drift (%)	DI_E (%)	DI_K (%)
OP	4	A-B	28.80	0.160	0.00	0.00
IO	5	B-IO	36.00	0.200	6.08	40.00
LS	14	IO-LS	100.80	0.560	53.31	49.92
CP	27	LS-CP	194.40	1.080	97.75	55.79
C	28	CP-C-D-E	201.60	1.120	100.00	56.08
P.P	5	-	36.00	0.200	6.08	40.00
S4_AR_1.0_MODE_LOAD TYPE_PUSH_Y						
Per.lvl.	step no.	Region	Sd (mm)	Drift (%)	DI_E (%)	DI_K (%)
OP	4	A-B	28.80	0.160	0.00	0.00
IO	5	B-IO	36.00	0.200	5.62	40.00
LS	14	IO-LS	100.80	0.560	50.10	49.87
CP	28	LS-CP	201.60	1.120	97.62	55.97
C	29	CP-C-D-E	208.80	1.160	100.00	56.25
P.P	6	-	43.20	0.240	11.10	41.85

Table 7.23 4- storey unidirectional setback with IR2 building case of X dirn

S4_AR_1.0_ACCL_LOAD TYPE_PUSH_X						
Per.lvl.	step no.	Region	Sd (mm)	Drift (%)	DI_E (%)	DI_K (%)
OP	1	A-B	7.20	0.040	0.00	0.00
IO	2	B-IO	14.40	0.080	6.64	25.00
LS	6	IO-LS	43.20	0.240	33.25	48.17
CP	15	LS-CP	108.00	0.600	93.31	61.57
C	16	CP-C-D-E	115.20	0.640	100.00	62.34
P.P	3	-	21.60	0.120	13.29	33.95
S4_AR_1.0_IS_LOAD TYPE_PUSH_X						
Per.lvl.	step no.	Region	Sd (mm)	Drift (%)	DI_E (%)	DI_K (%)
OP	2	A-B	14.40	0.080	0.00	0.00
IO	3	B-IO	21.60	0.120	7.67	34.42
LS	5	IO-LS	36.00	0.200	23.02	44.39
CP	14	LS-CP	100.80	0.560	92.29	61.23
C	15	CP-C-D-E	108.00	0.600	100.00	62.04
P.P	3	-	21.60	0.120	7.67	34.42
S4_AR_1.0_MODE_LOAD TYPE_PUSH_X						
Per.lvl.	step no.	Region	Sd (mm)	Drift (%)	DI_E (%)	DI_K (%)
OP	1	A-B	7.20	0.040	0.00	0.00
IO	2	B-IO	14.40	0.080	6.64	25.00
LS	6	IO-LS	43.20	0.240	33.25	48.44
CP	15	LS-CP	108.00	0.600	93.31	61.81
C	16	CP-C-D-E	115.20	0.640	100.00	62.57
P.P	3	-	21.60	0.120	13.29	33.98

Table 7.24 4- storey unidirectional setback with IR2 building case of Y dirn

S4_AR_1.0_ACCL_LOAD TYPE_PUSH_Y						
Per.lvl.	step no.	Region	Sd (mm)	Drift (%)	DI_E (%)	DI_K (%)
OP	1	A-B	7.20	0.040	0.00	0.00
IO	3	B-IO	21.60	0.120	11.69	33.33
LS	6	IO-LS	43.20	0.240	29.27	45.57
CP	17	LS-CP	122.40	0.680	94.08	60.85
C	18	CP-C-D-E	129.60	0.720	100.00	61.58
P.P	4	-	28.80	0.160	17.55	38.72
S4_AR_1.0_IS_LOAD TYPE_PUSH_Y						
Per.lvl.	step no.	Region	Sd (mm)	Drift (%)	DI_E (%)	DI_K (%)
OP	2	A-B	14.40	0.080	0.00	0.00
IO	3	B-IO	21.60	0.120	5.85	33.44
LS	6	IO-LS	43.20	0.240	23.41	45.32
CP	16	LS-CP	115.20	0.640	82.26	59.85
C	19	CP-C-D-E	136.80	0.760	100.00	61.70
P.P	4	-	28.80	0.160	11.69	38.72
S4_AR_1.0_MODE_LOAD TYPE_PUSH_Y						
Per.lvl.	step no.	Region	Sd (mm)	Drift (%)	DI_E (%)	DI_K (%)
OP	2	A-B	14.40	0.080	0.00	0.00
IO	3	B-IO	21.60	0.120	5.51	33.33
LS	5	IO-LS	36.00	0.200	16.55	42.11
CP	15	LS-CP	108.00	0.600	72.05	57.73
C	20	CP-C-D-E	144.00	0.800	100.00	60.79
P.P	3	-	21.60	0.120	5.51	33.33

Table 7.25 4- storey unidirectional setback with IR3 building case of X dirn

S4_AR_1.0_ACCL_LOAD TYPE_PUSH_X						
Per.lvl.	step no.	Region	Sd (mm)	Drift (%)	DI_E (%)	DI_K (%)
OP	1	A-B	7.20	0.040	0.00	0.00
IO	2	B-IO	14.40	0.080	7.02	25.00
LS	6	IO-LS	43.20	0.240	35.30	44.57
CP	14	LS-CP	100.80	0.560	92.74	54.03
C	15	CP-C-D-E	108.00	0.600	100.00	54.71
P.P	3	-	21.60	0.120	14.07	33.38
S4_AR_1.0_IS_LOAD TYPE_PUSH_X						
Per.lvl.	step no.	Region	Sd (mm)	Drift (%)	DI_E (%)	DI_K (%)
OP	2	A-B	14.40	0.080	0.00	0.00
IO	3	B-IO	21.60	0.120	9.90	33.33
LS	6	IO-LS	43.20	0.240	39.72	44.20
CP	12	LS-CP	79.20	0.440	89.90	48.88
C	13	CP-C-D-E	86.40	0.480	100.00	50.43
P.P	3	-	21.60	0.120	9.90	33.33
S4_AR_1.0_MODE_LOAD TYPE_PUSH_X						
Per.lvl.	step no.	Region	Sd (mm)	Drift (%)	DI_E (%)	DI_K (%)
OP	2	A-B	14.40	0.080	0.00	0.00
IO	3	B-IO	21.60	0.120	7.57	33.33
LS	6	IO-LS	43.20	0.240	30.42	44.33
CP	14	LS-CP	100.80	0.560	92.19	54.04
C	15	CP-C-D-E	108.00	0.600	100.00	54.83
P.P	3	-	21.60	0.120	7.57	33.33

Table 7.26 4- storey unidirectional setback with IR3 building case of Y dirn

S4_AR_1.0_ACCL_LOAD TYPE_PUSH_Y						
Per.lvl.	step no.	Region	Sd (mm)	Drift (%)	DI_E (%)	DI_K (%)
OP	2	A-B	14.40	0.080	0.00	0.00
IO	3	B-IO	21.60	0.120	5.46	33.33
LS	8	IO-LS	57.60	0.320	33.39	46.27
CP	19	LS-CP	131.40	0.730	93.87	54.29
C	20	CP-C-D-E	138.60	0.770	100.00	54.92
P.P	3	-	21.60	0.120	5.46	33.33
S4_AR_1.0_IS_LOAD TYPE_PUSH_Y						
Per.lvl.	step no.	Region	Sd (mm)	Drift (%)	DI_E (%)	DI_K (%)
OP	3	A-B	21.60	0.120	0.00	0.00
IO	4	B-IO	28.80	0.160	5.40	37.50
LS	8	IO-LS	57.60	0.320	27.59	45.92
CP	19	LS-CP	136.80	0.760	93.63	54.98
C	20	CP-C-D-E	144.00	0.800	100.00	55.50
P.P	4	-	28.80	0.160	5.40	37.50
S4_AR_1.0_MODE_LOAD TYPE_PUSH_Y						
Per.lvl.	step no.	Region	Sd (mm)	Drift (%)	DI_E (%)	DI_K (%)
OP	3	A-B	21.60	0.120	0.00	0.00
IO	4	B-IO	28.80	0.160	6.32	37.50
LS	7	IO-LS	50.40	0.280	26.64	43.90
CP	15	LS-CP	108.00	0.600	90.93	51.68
C	16	CP-C-D-E	115.20	0.640	100.00	52.32
P.P	4	-	28.80	0.160	6.32	37.50

Table 7.27 4- storey bi-directional setback with IR2 building case of X dirn

S4_AR_1.0_ACCL_LOAD TYPE_PUSH_X						
Per.lvl.	step no.	Region	Sd (mm)	Drift (%)	DI_E (%)	DI_K (%)
OP	2	A-B	14.40	0.080	0.00	0.00
IO	3	B-IO	21.60	0.120	7.00	33.33
LS	6	IO-LS	43.20	0.240	28.12	44.29
CP	15	LS-CP	108.00	0.600	92.71	54.30
C	16	CP-C-D-E	115.20	0.640	100.00	54.97
P.P	3	-	21.60	0.120	7.00	33.33
S4_AR_1.0_IS_LOAD TYPE_PUSH_X						
Per.lvl.	step no.	Region	Sd (mm)	Drift (%)	DI_E (%)	DI_K (%)
OP	2	A-B	14.40	0.080	0.00	0.00
IO	3	B-IO	21.60	0.120	8.23	33.53
LS	6	IO-LS	43.20	0.240	33.04	44.13
CP	13	LS-CP	93.60	0.520	91.57	58.69
C	14	CP-C-D-E	100.80	0.560	100.00	59.15
P.P	2	-	14.40	0.080	0.00	25.00
S4_AR_1.0_MODE_LOAD TYPE_PUSH_X						
Per.lvl.	step no.	Region	Sd (mm)	Drift (%)	DI_E (%)	DI_K (%)
OP	1	A-B	7.20	0.040	0.00	0.00
IO	2	B-IO	14.40	0.080	12.46	25.00
LS	3	IO-LS	21.60	0.120	24.93	34.73
CP	9	LS-CP	57.60	0.320	87.46	49.13
C	10	CP-C-D-E	64.80	0.360	100.00	51.27
P.P	2	-	14.40	0.080	12.46	25.00

Table 7.28 4- storey bi-directional setback with IR2 building case of Y dirn

S4_AR_1.0_ACCL_LOAD TYPE_PUSH_Y						
Per.lvl.	step no.	Region	Sd (mm)	Drift (%)	DI_E (%)	DI_K (%)
OP	3	A-B	21.60	0.120	0.00	0.00
IO	4	B-IO	28.80	0.160	7.51	37.81
LS	7	IO-LS	50.40	0.280	30.22	45.41
CP	15	LS-CP	108.00	0.600	92.12	53.52
C	16	CP-C-D-E	115.20	0.640	100.00	54.16
P.P	3	-	21.60	0.120	0.00	37.81
S4_AR_1.0_IS_LOAD TYPE_PUSH_Y						
Per.lvl.	step no.	Region	Sd (mm)	Drift (%)	DI_E (%)	DI_K (%)
OP	3	A-B	21.60	0.120	0.00	0.00
IO	4	B-IO	28.80	0.160	5.60	37.66
LS	7	IO-LS	50.40	0.280	22.62	45.13
CP	19	LS-CP	136.80	0.760	93.84	55.23
C	20	CP-C-D-E	144.00	0.800	100.00	55.74
P.P	3	-	21.60	0.120	0.00	33.33
S4_AR_1.0_MODE_LOAD TYPE_PUSH_Y						
Per.lvl.	step no.	Region	Sd (mm)	Drift (%)	DI_E (%)	DI_K (%)
OP	3	A-B	21.60	0.120	0.00	0.00
IO	4	B-IO	28.80	0.160	3.42	37.50
LS	7	IO-LS	50.40	0.280	15.54	44.23
CP	19	LS-CP	136.80	0.760	91.66	53.91
C	20	CP-C-D-E	144.00	0.800	100.00	54.40
P.P	1	-	7.20	0.040	0.00	0.00

Table 7.29 4- storey bi-directional setback with IR3 building case of X dirn

S4_AR_1.0_ACCL_LOAD TYPE_PUSH_X						
Per.lvl.	step no.	Region	Sd (mm)	Drift (%)	DI_E (%)	DI_K (%)
OP	1	A-B	7.20	0.040	0.00	0.00
IO	2	B-IO	14.40	0.080	8.61	25.00
LS	6	IO-LS	43.20	0.240	43.20	44.62
CP	12	LS-CP	82.80	0.460	91.22	51.07
C	13	CP-C-D-E	90.00	0.500	100.00	52.26
P.P	2	-	14.40	0.080	8.61	25.00
S4_AR_1.0_IS_LOAD TYPE_PUSH_X						
Per.lvl.	step no.	Region	Sd (mm)	Drift (%)	DI_E (%)	DI_K (%)
OP	1	A-B	7.20	0.040	0.00	0.00
IO	2	B-IO	14.40	0.080	9.69	25.00
LS	5	IO-LS	36.00	0.200	38.84	42.22
CP	11	LS-CP	73.80	0.410	90.18	51.30
C	12	CP-C-D-E	81.00	0.450	100.00	52.65
P.P	2	-	14.40	0.080	9.69	25.00
S4_AR_1.0_MODE_LOAD TYPE_PUSH_X						
Per.lvl.	step no.	Region	Sd (mm)	Drift (%)	DI_E (%)	DI_K (%)
OP	2	A-B	14.40	0.080	0.00	0.00
IO	3	B-IO	21.60	0.120	9.95	33.33
LS	4	IO-LS	28.80	0.160	19.91	39.21
CP	11	LS-CP	79.20	0.440	89.95	53.77
C	12	CP-C-D-E	86.40	0.480	100.00	54.86
P.P	3	-	21.60	0.120	9.95	33.33

Table 7.30 4- storey bi-directional setback with IR3 building case of Y dirn

S4_AR_1.0_ACCL_LOAD TYPE_PUSH_Y						
Per.lvl.	step no.	Region	Sd (mm)	Drift (%)	DI_E (%)	DI_K (%)
OP	2	A-B	14.40	0.080	0.00	0.00
IO	3	B-IO	21.60	0.120	6.84	33.33
LS	7	IO-LS	50.40	0.280	34.49	45.36
CP	16	LS-CP	109.80	0.610	92.81	52.47
C	17	CP-C-D-E	117.00	0.650	100.00	53.29
P.P	3	-	21.60	0.120	6.84	33.33
S4_AR_1.0_IS_LOAD TYPE_PUSH_Y						
Per.lvl.	step no.	Region	Sd (mm)	Drift (%)	DI_E (%)	DI_K (%)
OP	3	A-B	21.60	0.120	0.00	0.00
IO	4	B-IO	28.80	0.160	6.89	37.50
LS	8	IO-LS	57.60	0.320	34.84	46.04
CP	16	LS-CP	115.20	0.640	92.61	53.60
C	17	CP-C-D-E	122.40	0.680	100.00	54.24
P.P	3	-	21.60	0.120	0.00	33.33
S4_AR_1.0_MODE_LOAD TYPE_PUSH_Y						
Per.lvl.	step no.	Region	Sd (mm)	Drift (%)	DI_E (%)	DI_K (%)
OP	3	A-B	21.60	0.120	0.00	0
IO	4	B-IO	28.80	0.160	6.40	37.50
LS	7	IO-LS	50.40	0.280	25.82	44.29
CP	17	LS-CP	122.40	0.680	93.06	53.95
C	18	CP-C-D-E	129.60	0.720	100.00	54.53
P.P	1	-	7.20	0.040	0.00	25.00

Table 7.31 6- storey regular building of X dirn

S6_AR_1.0_ACCL_LOAD TYPE_PUSH_X						
Per.lvl.	step no.	Region	Sd (mm)	Drift (%)	DI_E (%)	DI_K (%)
OP	6	A-B	62.40	0.240	0.00	0.00
IO	7	B-IO	72.80	0.280	2.61	42.86
LS	21	IO-LS	218.40	0.840	37.54	53.19
CP	49	LS-CP	509.60	1.960	98.07	60.81
C	50	CP-C-D-E	520.00	2.000	100.00	60.98
P.P	8	-	83.20	0.320	5.21	43.94
S6_AR_1.0_IS_LOAD TYPE_PUSH_X						
Per.lvl.	step no.	Region	Sd (mm)	Drift (%)	DI_E (%)	DI_K (%)
OP	6	A-B	62.40	0.240	0.00	0.00
IO	7	B-IO	72.80	0.280	2.32	42.86
LS	23	IO-LS	239.20	0.920	38.60	53.99
CP	51	LS-CP	530.40	2.040	97.98	61.76
C	52	CP-C-D-E	540.80	2.080	100.00	61.92
P.P	9	-	93.60	0.360	6.95	44.72
S6_AR_1.0_MODE_LOAD TYPE_PUSH_X						
Per.lvl.	step no.	Region	Sd (mm)	Drift (%)	DI_E (%)	DI_K (%)
OP	6	A-B	62.40	0.240	0.00	0.00
IO	7	B-IO	72.80	0.280	2.31	42.86
LS	22	IO-LS	228.80	0.880	36.02	53.48
CP	52	LS-CP	540.80	2.080	98.06	61.60
C	53	CP-C-D-E	551.20	2.120	100.00	61.76
P.P	9	-	93.60	0.360	6.91	44.84

Table 7.32 6- storey regular building of Y dirn

S6_AR_1.0_ACCL_LOAD TYPE_PUSH_Y						
Per.lvl.	step no.	Region	Sd (mm)	Drift (%)	DI_E (%)	DI_K (%)
OP	6	A-B	62.40	0.240	0.00	0.00
IO	7	B-IO	72.80	0.280	2.83	42.86
LS	21	IO-LS	218.40	0.840	40.16	53.28
CP	47	LS-CP	488.80	1.880	98.07	60.48
C	48	CP-C-D-E	499.20	1.920	100.00	60.66
P.P	8	-	83.20	0.320	5.64	43.95
S6_AR_1.0_IS_LOAD TYPE_PUSH_Y						
Per.lvl.	step no.	Region	Sd (mm)	Drift (%)	DI_E (%)	DI_K (%)
OP	6	A-B	62.40	0.240	0.00	0.00
IO	7	B-IO	72.80	0.280	2.54	42.86
LS	22	IO-LS	228.80	0.880	39.37	53.87
CP	48	LS-CP	499.20	1.920	97.88	61.49
C	49	CP-C-D-E	509.60	1.960	100.00	61.67
P.P	9	-	93.60	0.360	7.58	44.87
S6_AR_1.0_MODE_LOAD TYPE_PUSH_Y						
Per.lvl.	step no.	Region	Sd (mm)	Drift (%)	DI_E (%)	DI_K (%)
OP	6	A-B	62.40	0.240	0.00	0.00
IO	7	B-IO	72.80	0.280	2.41	42.86
LS	22	IO-LS	228.80	0.880	37.52	53.71
CP	50	LS-CP	520.00	2.000	97.96	61.33
C	51	CP-C-D-E	530.40	2.040	100.00	61.50
P.P	9	-	93.60	0.360	7.20	44.82

Table 7.33 6- storey unidirectional setback with IR1 building case of X dirn

S6_AR_1.0_ACCL_LOAD TYPE_PUSH_X						
Per.lvl.	step no.	Region	Sd (mm)	Drift (%)	DI_E (%)	DI_K (%)
OP	3	A-B	31.20	0.120	0.00	0.00
IO	4	B-IO	41.60	0.160	5.64	37.50
LS	10	IO-LS	104.00	0.400	40.12	48.31
CP	19	LS-CP	197.60	0.760	93.88	54.64
C	20	CP-C-D-E	208.00	0.800	100.00	55.07
P.P	5	-	52.00	0.200	11.31	40.35
S6_AR_1.0_IS_LOAD TYPE_PUSH_X						
Per.lvl.	step no.	Region	Sd (mm)	Drift (%)	DI_E (%)	DI_K (%)
OP	3	A-B	31.20	0.120	0.00	0.00
IO	4	B-IO	41.60	0.160	5.66	37.50
LS	10	IO-LS	104.00	0.400	40.19	48.69
CP	19	LS-CP	197.60	0.760	93.89	54.63
C	20	CP-C-D-E	208.00	0.800	100.00	55.06
P.P	5	-	52.00	0.200	11.34	40.36
S6_AR_1.0_MODE_LOAD TYPE_PUSH_X						
Per.lvl.	step no.	Region	Sd (mm)	Drift (%)	DI_E (%)	DI_K (%)
OP	3	A-B	31.20	0.120	0.00	0.00
IO	4	B-IO	41.60	0.160	5.65	37.50
LS	10	IO-LS	104.00	0.400	40.15	48.31
CP	19	LS-CP	197.60	0.760	93.88	54.62
C	20	CP-C-D-E	208.00	0.800	100.00	55.05
P.P	5	-	52.00	0.200	11.32	40.35

Table 7.34 6- storey unidirectional setback with IR1 building case of Y dirn

S6_AR_1.0_ACCL_LOAD TYPE_PUSH_Y						
Per.lvl.	step no.	Region	Sd (mm)	Drift (%)	DI_E (%)	DI_K (%)
OP	3	A-B	31.20	0.120	0.00	0.00
IO	4	B-IO	41.60	0.160	5.43	37.50
LS	11	IO-LS	114.40	0.440	45.02	49.06
CP	19	LS-CP	197.60	0.760	93.67	54.90
C	20	CP-C-D-E	208.00	0.800	100.00	55.38
P.P	5	-	52.00	0.200	10.92	40.35
S6_AR_1.0_IS_LOAD TYPE_PUSH_Y						
Per.lvl.	step no.	Region	Sd (mm)	Drift (%)	DI_E (%)	DI_K (%)
OP	3	A-B	31.20	0.120	0.00	0.00
IO	4	B-IO	41.60	0.160	5.05	37.50
LS	11	IO-LS	114.40	0.440	42.07	49.06
CP	20	LS-CP	208.00	0.800	93.94	54.90
C	21	CP-C-D-E	218.40	0.840	100.00	55.38
P.P	5	-	52.00	0.200	10.16	40.35
S6_AR_1.0_MODE_LOAD TYPE_PUSH_Y						
Per.lvl.	step no.	Region	Sd (mm)	Drift (%)	DI_E (%)	DI_K (%)
OP	3	A-B	31.20	0.120	0.00	0.00
IO	4	B-IO	41.60	0.160	5.44	37.50
LS	11	IO-LS	114.40	0.440	45.06	49.20
CP	19	LS-CP	197.60	0.760	93.67	54.60
C	20	CP-C-D-E	208.00	0.800	100.00	55.12
P.P	5	-	52.00	0.200	10.93	40.35

Table 7.35 6- storey unidirectional setback with IR2 building case of X dirn

S6_AR_1.0_ACCL_LOAD TYPE_PUSH_X						
Per.lvl.	step no.	Region	Sd (mm)	Drift (%)	DI_E (%)	DI_K (%)
OP	12	A-B	124.80	0.480	0.00	0.00
IO	13	B-IO	135.20	0.520	3.62	46.15
LS	24	IO-LS	249.60	0.960	42.61	48.78
CP	40	LS-CP	416.00	1.600	96.72	53.16
C	41	CP-C-D-E	426.40	1.640	100.00	53.41
P.P	8	-	83.20	0.320	0.00	43.75
S6_AR_1.0_IS_LOAD TYPE_PUSH_X						
Per.lvl.	step no.	Region	Sd (mm)	Drift (%)	DI_E (%)	DI_K (%)
OP	16	A-B	166.40	0.640	0.00	0.00
IO	17	B-IO	176.80	0.680	1.71	47.06
LS	35	IO-LS	364.00	1.400	34.89	50.80
CP	64	LS-CP	665.60	2.560	97.63	57.04
C	65	CP-C-D-E	676.00	2.600	100.00	57.20
P.P	10	-	104.00	0.400	0.00	45.00
S6_AR_1.0_MODE_LOAD TYPE_PUSH_X						
Per.lvl.	step no.	Region	Sd (mm)	Drift (%)	DI_E (%)	DI_K (%)
OP	14	A-B	145.60	0.560	0.00	0.00
IO	15	B-IO	156.00	0.600	4.67	46.67
LS	29	IO-LS	301.60	1.160	58.44	49.54
CP	52	LS-CP	540.80	2.080	99.55	55.08
C	53	CP-C-D-E	551.20	2.120	100.00	55.28
P.P	9	-	93.60	0.360	0.00	44.44

Table 7.36 6- storey unidirectional setback with IR2 building case of Y dirn

S6_AR_1.0_ACCL_LOAD TYPE_PUSH_Y						
Per.lvl.	step no.	Region	Sd (mm)	Drift (%)	DI_E (%)	DI_K (%)
OP	14	A-B	145.60	0.560	0.00	0.00
IO	15	B-IO	156.00	0.600	5.90	46.67
LS	24	IO-LS	249.60	0.960	51.26	48.29
CP	41	LS-CP	426.40	1.640	98.76	52.36
C	42	CP-C-D-E	436.80	1.680	100.00	54.28
P.P	9	-	93.60	0.360	0.00	37.50
S6_AR_1.0_IS_LOAD TYPE_PUSH_Y						
Per.lvl.	step no.	Region	Sd (mm)	Drift (%)	DI_E (%)	DI_K (%)
OP	21	A-B	218.40	0.840	0.00	0.00
IO	22	B-IO	228.80	0.880	2.01	47.73
LS	39	IO-LS	405.60	1.560	36.34	50.23
CP	69	LS-CP	717.60	2.760	97.93	55.86
C	70	CP-C-D-E	728.00	2.800	100.00	56.01
P.P	11	-	114.40	0.440	0.00	45.45
S6_AR_1.0_MODE_LOAD TYPE_PUSH_Y						
Per.lvl.	step no.	Region	Sd (mm)	Drift (%)	DI_E (%)	DI_K (%)
OP	21	A-B	218.40	0.840	0.00	0.00
IO	22	B-IO	228.80	0.880	2.88	47.73
LS	34	IO-LS	353.60	1.360	37.74	48.99
CP	54	LS-CP	561.60	2.160	97.00	51.97
C	55	CP-C-D-E	572.00	2.200	100.00	52.12
P.P	11	-	114.40	0.440	0.00	45.45

Table 7.37 6- storey unidirectional setback with IR3 building case of X dirn

S6_AR_1.0_ACCL_LOAD TYPE_PUSH_X						
Per.lvl.	step no.	Region	Sd (mm)	Drift (%)	DI_E (%)	DI_K (%)
OP	6	A-B	62.40	0.240	0.00	0.00
IO	7	B-IO	72.80	0.280	2.20	42.86
LS	24	IO-LS	249.60	0.960	38.64	54.40
CP	54	LS-CP	561.60	2.160	98.12	62.14
C	55	CP-C-D-E	572.00	2.200	100.00	62.28
P.P	7	-	72.80	0.280	0.00	42.86
S6_AR_1.0_IS_LOAD TYPE_PUSH_X						
Per.lvl.	step no.	Region	Sd (mm)	Drift (%)	DI_E (%)	DI_K (%)
OP	6	A-B	62.40	0.240	0.00	0.00
IO	7	B-IO	72.80	0.280	2.48	42.86
LS	23	IO-LS	239.20	0.920	41.20	54.22
CP	48	LS-CP	499.20	1.920	97.83	61.31
C	49	CP-C-D-E	509.60	1.960	100.00	61.48
P.P	9	-	93.60	0.360	0.00	44.59
S6_AR_1.0_MODE_LOAD TYPE_PUSH_X						
Per.lvl.	step no.	Region	Sd (mm)	Drift (%)	DI_E (%)	DI_K (%)
OP	7	A-B	72.80	0.280	0.00	0.00
IO	8	B-IO	83.20	0.320	2.35	43.75
LS	26	IO-LS	270.40	1.040	43.30	55.36
CP	52	LS-CP	540.80	2.080	98.00	61.86
C	53	CP-C-D-E	551.20	2.120	100.00	62.02
P.P	9	-	93.60	0.360	0.00	44.60

Table 7.38 6- storey unidirectional setback with IR3 building case of Y dirn

S6_AR_1.0_ACCL_LOAD TYPE_PUSH_Y						
Per.lvl.	step no.	Region	Sd (mm)	Drift (%)	DI_E (%)	DI_K (%)
OP	6	A-B	62.40	0.240	0.00	0.00
IO	7	B-IO	72.80	0.280	2.38	42.86
LS	23	IO-LS	239.20	0.920	39.49	52.68
CP	50	LS-CP	520.00	2.000	97.94	59.89
C	51	CP-C-D-E	530.40	2.040	100.00	60.07
P.P	8	-	83.20	0.320	4.75	43.77
S6_AR_1.0_IS_LOAD TYPE_PUSH_Y						
Per.lvl.	step no.	Region	Sd (mm)	Drift (%)	DI_E (%)	DI_K (%)
OP	8	A-B	83.20	0.320	0.00	0.00
IO	9	B-IO	93.60	0.360	2.24	44.44
LS	26	IO-LS	270.40	1.040	39.56	53.66
CP	54	LS-CP	561.60	2.160	97.98	60.63
C	55	CP-C-D-E	572.00	2.200	100.00	60.78
P.P	10	-	104.00	0.400	4.47	45.06
S6_AR_1.0_MODE_LOAD TYPE_PUSH_Y						
Per.lvl.	step no.	Region	Sd (mm)	Drift (%)	DI_E (%)	DI_K (%)
OP	8	A-B	83.20	0.320	0.00	0.00
IO	9	B-IO	93.60	0.360	2.35	44.44
LS	24	IO-LS	249.60	0.960	36.94	51.55
CP	52	LS-CP	540.80	2.080	97.91	58.24
C	53	CP-C-D-E	551.20	2.120	100.00	58.40
P.P	10	-	104.00	0.400	4.70	45.04

Table 7.39 6- storey bi-directional setback with IR1 building case of X dirn

S6_AR_1.0_ACCL_LOAD TYPE_PUSH_X						
Per.lvl.	step no.	Region	Sd (mm)	Drift (%)	DI_E (%)	DI_K (%)
OP	4	A-B	41.60	0.160	0.00	0.00
IO	5	B-IO	52.00	0.200	5.93	40.00
LS	10	IO-LS	104.00	0.400	34.49	47.13
CP	22	LS-CP	228.80	0.880	95.41	49.87
C	23	CP-C-D-E	239.20	0.920	100.00	57.23
P.P	5	-	52.00	0.200	0.00	40.00
S6_AR_1.0_IS_LOAD TYPE_PUSH_X						
Per.lvl.	step no.	Region	Sd (mm)	Drift (%)	DI_E (%)	DI_K (%)
OP	5	A-B	52.00	0.200	0.00	0.00
IO	6	B-IO	62.40	0.240	6.44	41.77
LS	10	IO-LS	104.00	0.400	31.16	47.09
CP	22	LS-CP	228.80	0.880	95.33	56.79
C	23	CP-C-D-E	239.20	0.920	100.00	57.31
P.P	6	-	62.40	0.240	0.00	41.77
S6_AR_1.0_MODE_LOAD TYPE_PUSH_X						
Per.lvl.	step no.	Region	Sd (mm)	Drift (%)	DI_E (%)	DI_K (%)
OP	4	A-B	41.60	0.160	0.00	0.00
IO	5	B-IO	52.00	0.200	6.51	40.00
LS	10	IO-LS	104.00	0.400	37.36	47.13
CP	21	LS-CP	218.40	0.840	95.39	56.23
C	22	CP-C-D-E	228.80	0.880	100.00	56.79
P.P	5	-	52.00	0.200	0.00	40.00

Table 7.40 6- storey bi-directional setback with IR1 building case of Y dirn

S6_AR_1.0_ACCL_LOAD TYPE_PUSH_Y						
Per.lvl.	step no.	Region	Sd (mm)	Drift (%)	DIE (%)	DI_K (%)
OP	5	A-B	52.00	0.200	0.00	0.00
IO	6	B-IO	62.40	0.240	6.45	41.72
LS	11	IO-LS	114.40	0.440	37.11	48.04
CP	22	LS-CP	228.80	0.880	95.34	56.63
C	23	CP-C-D-E	239.20	0.920	100.00	54.80
P.P	5	-	52.00	0.200	0.00	40.00
S6_AR_1.0_IS_LOAD TYPE_PUSH_Y						
Per.lvl.	step no.	Region	Sd (mm)	Drift (%)	DIE (%)	DI_K (%)
OP	5	A-B	52.00	0.200	0.00	0.00
IO	6	B-IO	62.40	0.240	6.64	41.74
LS	10	IO-LS	104.00	0.400	31.94	47.01
CP	22	LS-CP	228.80	0.880	95.53	56.69
C	23	CP-C-D-E	239.20	0.920	100.00	57.21
P.P	5	-	52.00	0.200	0.00	40.00
S6_AR_1.0_MODE_LOAD TYPE_PUSH_Y						
Per.lvl.	step no.	Region	Sd (mm)	Drift (%)	DIE (%)	DI_K (%)
OP	5	A-B	52.00	0.200	0.00	0.00
IO	6	B-IO	62.40	0.240	5.45	41.67
LS	12	IO-LS	124.80	0.480	37.73	47.90
CP	23	LS-CP	239.20	0.920	94.93	55.20
C	24	CP-C-D-E	249.60	0.960	100.00	55.68
P.P	6	-	62.40	0.240	5.45	41.67

Table 7.41 6- storey bi-directional setback with IR2 building case of X dirn

S6_AR_1.0_ACCL_LOAD TYPE_PUSH_X						
Per.lvl.	step no.	Region	Sd (mm)	Drift (%)	DI_E (%)	DI_K (%)
OP	2	A-B	20.80	0.080	0.00	0.00
IO	3	B-IO	31.20	0.120	6.52	33.33
LS	9	IO-LS	93.60	0.360	46.08	48.89
CP	16	LS-CP	166.40	0.640	93.19	54.51
C	17	CP-C-D-E	176.80	0.680	100.00	55.06
P.P	3	-	31.20	0.120	6.52	33.33
S6_AR_1.0_IS_LOAD TYPE_PUSH_X						
Per.lvl.	step no.	Region	Sd (mm)	Drift (%)	DI_E (%)	DI_K (%)
OP	2	A-B	20.80	0.080	0.00	0.00
IO	3	B-IO	31.20	0.120	7.01	33.33
LS	8	IO-LS	83.20	0.320	42.37	47.43
CP	15	LS-CP	156.00	0.600	92.72	54.14
C	16	CP-C-D-E	166.40	0.640	100.00	50.82
P.P	3	-	31.20	0.120	7.01	33.33
S6_AR_1.0_MODE_LOAD TYPE_PUSH_X						
Per.lvl.	step no.	Region	Sd (mm)	Drift (%)	DI_E (%)	DI_K (%)
OP	2	A-B	20.80	0.080	0.00	0.00
IO	3	B-IO	31.20	0.120	7.01	33.33
LS	8	IO-LS	83.20	0.320	42.37	47.42
CP	15	LS-CP	156.00	0.600	92.72	54.11
C	16	CP-C-D-E	166.40	0.640	100.00	54.73
P.P	3	-	31.20	0.120	7.01	33.33

Table 7.42 6- storey bi-directional setback with IR2 building case of Y dirn

S6_AR_1.0_ACCL_LOAD TYPE_PUSH_Y						
Per.lvl.	step no.	Region	Sd (mm)	Drift (%)	DI_E (%)	DI_K (%)
OP	2	A-B	20.80	0.080	0.00	0.00
IO	3	B-IO	31.20	0.120	5.74	33.33
LS	10	IO-LS	104.00	0.400	46.40	49.66
CP	18	LS-CP	187.20	0.720	93.97	55.43
C	19	CP-C-D-E	197.60	0.760	100.00	55.94
P.P	4	-	41.60	0.160	11.49	37.87
S6_AR_1.0_IS_LOAD TYPE_PUSH_Y						
Per.lvl.	step no.	Region	Sd (mm)	Drift (%)	DI_E (%)	DI_K (%)
OP	2	A-B	20.80	0.080	0.00	0.00
IO	3	B-IO	31.20	0.120	5.70	33.33
LS	10	IO-LS	104.00	0.400	46.24	48.98
CP	18	LS-CP	187.20	0.720	93.93	55.16
C	19	CP-C-D-E	197.60	0.760	100.00	55.68
P.P	4	-	41.60	0.160	11.42	37.73
S6_AR_1.0_MODE_LOAD TYPE_PUSH_Y						
Per.lvl.	step no.	Region	Sd (mm)	Drift (%)	DI_E (%)	DI_K (%)
OP	3	A-B	31.20	0.120	0.00	0.00
IO	4	B-IO	41.60	0.160	5.94	37.50
LS	10	IO-LS	104.00	0.400	42.43	48.42
CP	18	LS-CP	187.20	0.720	93.44	54.00
C	19	CP-C-D-E	197.60	0.760	100.00	54.49
P.P	5	-	52.00	0.200	11.91	40.30

Table 7.43 6- storey bi-directional setback with IR3 building case of X dirn

S6_AR_1.0_ACCL_LOAD TYPE_PUSH_X						
Per.lvl.	step no.	Region	Sd (mm)	Drift (%)	DI_E (%)	DI_K (%)
OP	3	A-B	31.20	0.120	0.00	0.00
IO	4	B-IO	41.60	0.160	4.82	37.50
LS	10	IO-LS	104.00	0.400	35.54	47.99
CP	20	LS-CP	208.00	0.800	93.70	54.62
C	21	CP-C-D-E	218.40	0.840	100.00	55.12
P.P	4	-	41.60	0.160	4.82	37.50
S6_AR_1.0_IS_LOAD TYPE_PUSH_X						
Per.lvl.	step no.	Region	Sd (mm)	Drift (%)	DI_E (%)	DI_K (%)
OP	2	A-B	20.80	0.080	0.00	0.00
IO	3	B-IO	31.20	0.120	5.43	33.33
LS	9	IO-LS	93.60	0.360	39.21	47.03
CP	18	LS-CP	187.20	0.720	93.67	53.98
C	19	CP-C-D-E	197.60	0.760	100.00	54.52
P.P	4	-	41.60	0.160	10.92	37.72
S6_AR_1.0_MODE_LOAD TYPE_PUSH_X						
Per.lvl.	step no.	Region	Sd (mm)	Drift (%)	DI_E (%)	DI_K (%)
OP	2	A-B	20.80	0.080	0.00	0.00
IO	3	B-IO	31.20	0.120	6.82	33.33
LS	8	IO-LS	83.20	0.320	41.65	46.62
CP	15	LS-CP	156.00	0.600	92.53	52.90
C	16	CP-C-D-E	166.40	0.640	100.00	53.49
P.P	3	-	31.20	0.120	6.82	33.33

Table 7.44 6- storey bi-directional setback with IR3 building case of Y dirn

S6_AR_1.0_ACCL_LOAD TYPE_PUSH_Y						
Per.lvl.	step no.	Region	Sd (mm)	Drift (%)	DI_E (%)	DI_K (%)
OP	3	A-B	31.20	0.120	0.00	0.00
IO	4	B-IO	41.60	0.160	4.15	37.50
LS	11	IO-LS	114.40	0.440	36.67	48.66
CP	21	LS-CP	218.40	0.840	93.63	54.68
C	22	CP-C-D-E	228.80	0.880	100.00	55.14
P.P	4	-	41.60	0.160	4.15	37.50
S6_AR_1.0_IS_LOAD TYPE_PUSH_Y						
Per.lvl.	step no.	Region	Sd (mm)	Drift (%)	DI_E (%)	DI_K (%)
OP	3	A-B	31.20	0.120	0.00	0.00
IO	4	B-IO	41.60	0.160	10.39	37.50
LS	12	IO-LS	124.80	0.480	73.08	48.83
CP	22	LS-CP	228.80	0.880	100.39	54.57
C	23	CP-C-D-E	239.20	0.920	100.00	54.96
P.P	5	-	52.00	0.200	20.21	40.14
S6_AR_1.0_MODE_LOAD TYPE_PUSH_Y						
Per.lvl.	step no.	Region	Sd (mm)	Drift (%)	DI_E (%)	DI_K (%)
OP	3	A-B	31.20	0.120	0.00	0.00
IO	4	B-IO	41.60	0.160	4.53	37.50
LS	12	IO-LS	124.80	0.480	43.72	49.15
CP	21	LS-CP	218.40	0.840	94.01	54.72
C	22	CP-C-D-E	228.80	0.880	100.00	55.13
P.P	6	-	62.40	0.240	13.84	42.26

Table 7.45 9- storey regular building of X dirn

S9_AR_1.0_ACCL_LOAD TYPE_PUSH_X						
Per.lvl.	step no.	Region	Sd (mm)	Drift (%)	DI_E (%)	DI_K (%)
OP	5	A-B	76.00	0.200	0.00	0.00
IO	6	B-IO	91.20	0.240	3.34	41.67
P.P	8	-	121.60	0.320	9.90	44.05
LS	19	IO-LS	288.80	0.760	43.04	52.90
CP	43	LS-CP	653.60	1.720	98.21	59.99
C	44	CP-C-D-E	668.80	1.760	100.00	60.18
S9_AR_1.0_IS_LOAD TYPE_PUSH_X						
Per.lvl.	step no.	Region	Sd (mm)	Drift (%)	DI_E (%)	DI_K (%)
OP	6	A-B	91.20	0.240	0.00	0.00
IO	7	B-IO	106.40	0.280	2.56	42.86
P.P	9	-	136.80	0.360	7.64	44.81
LS	22	IO-LS	334.40	0.880	39.60	54.22
CP	48	LS-CP	729.60	1.920	97.91	61.57
C	49	CP-C-D-E	744.80	1.960	100.00	61.74
S9_AR_1.0_MODE_LOAD TYPE_PUSH_X						
Per.lvl.	step no.	Region	Sd (mm)	Drift (%)	DI_E (%)	DI_K (%)
OP	6	A-B	91.20	0.240	0.00	0.00
IO	7	B-IO	106.40	0.280	3.31	42.86
P.P	9	-	136.80	0.360	9.81	45.02
LS	20	IO-LS	304.00	0.800	42.40	53.43
CP	46	LS-CP	699.20	1.840	98.43	60.77
C	47	CP-C-D-E	714.40	1.880	100.00	60.95

Table 7.46 9- storey regular building of Y dirn

S9_AR_1.0_ACCL_LOAD TYPE_PUSH_Y						
Per.lvl.	step no.	Region	Sd (mm)	Drift (%)	DI_E (%)	DI_K (%)
OP	5	A-B	76.00	0.200	0.00	0.00
IO	6	B-IO	91.20	0.240	3.50	41.67
LS	19	IO-LS	288.80	0.760	45.01	53.08
CP	41	LS-CP	623.20	1.640	98.10	59.91
C	42	CP-C-D-E	638.40	1.680	100.00	60.11
P.P	8	-	121.60	0.320	10.38	44.13
S9_AR_1.0_IS_LOAD TYPE_PUSH_Y						
Per.lvl.	step no.	Region	Sd (mm)	Drift (%)	DI_E (%)	DI_K (%)
OP	6	A-B	91.20	0.240	0.00	0.00
IO	7	B-IO	106.40	0.280	2.85	42.86
LS	20	IO-LS	304.00	0.800	37.98	53.78
CP	46	LS-CP	699.20	1.840	97.97	61.61
C	47	CP-C-D-E	714.40	1.880	100.00	61.79
P.P	9	-	136.80	0.360	8.48	45.04
S9_AR_1.0_MODE_LOAD TYPE_PUSH_Y						
Per.lvl.	step no.	Region	Sd (mm)	Drift (%)	DI_E (%)	DI_K (%)
OP	6	A-B	91.20	0.240	0.00	0.00
IO	7	B-IO	106.40	0.280	2.89	42.86
LS	20	IO-LS	304.00	0.800	39.19	53.49
CP	43	LS-CP	653.60	1.720	97.63	60.61
C	44	CP-C-D-E	668.80	1.760	100.00	60.79
P.P	9	-	136.80	0.360	8.63	45.00

Table 7.47 9- storey unidirectional setback with IR1 building case of X dirn

S9_AR_1.0_ACCL_LOAD TYPE_PUSH_X						
Per.lvl.	step no.	Region	Sd (mm)	Drift (%)	DI_E (%)	DI_K (%)
P.P	8	-	121.60	0.320	0.00	43.75
OP	16	A-B	243.20	0.640	0.00	0.00
IO	17	B-IO	258.40	0.680	3.08	47.06
LS	29	IO-LS	440.80	1.160	40.82	48.87
CP	46	LS-CP	699.20	1.840	96.63	52.34
C	47	CP-C-D-E	714.40	1.880	100.00	52.53
S9_AR_1.0_IS_LOAD TYPE_PUSH_X						
Per.lvl.	step no.	Region	Sd (mm)	Drift (%)	DI_E (%)	DI_K (%)
P.P	10	-	152.00	0.400	0.00	45.00
OP	23	A-B	349.60	0.920	0.00	0.00
IO	24	B-IO	364.80	0.960	5.23	47.92
LS	38	IO-LS	577.60	1.520	78.84	50.14
CP	41	LS-CP	623.20	1.640	94.70	50.78
C	42	CP-C-D-E	638.40	1.680	100.00	50.99
S9_AR_1.0_MODE_LOAD TYPE_PUSH_X						
Per.lvl.	step no.	Region	Sd (mm)	Drift (%)	DI_E (%)	DI_K (%)
P.P	9	-	136.80	0.360	0.00	44.44
OP	20	A-B	304.00	0.800	0.00	0.00
IO	21	B-IO	319.20	0.840	2.96	47.62
LS	33	IO-LS	501.60	1.320	38.80	49.33
CP	52	LS-CP	790.40	2.080	96.90	53.16
C	53	CP-C-D-E	805.60	2.120	100.00	53.34

Table 7.48 9- storey unidirectional setback with IR1 building case of Y dirn

S9_AR_1.0_ACCL_LOAD TYPE_PUSH_Y						
Per.lvl.	step no.	Region	Sd (mm)	Drift (%)	DI_E (%)	DI_K (%)
OP	18	A-B	273.60	0.720	0.00	0.00
IO	19	B-IO	288.80	0.760	3.15	47.37
LS	31	IO-LS	471.20	1.240	41.32	48.99
CP	48	LS-CP	729.60	1.920	96.69	52.34
C	49	CP-C-D-E	744.80	1.960	100.00	52.53
P.P	9	-	136.80	0.360	0.00	44.44
S9_AR_1.0_IS_LOAD TYPE_PUSH_Y						
Per.lvl.	step no.	Region	Sd (mm)	Drift (%)	DI_E (%)	DI_K (%)
OP	25	A-B	380.00	1.000	0.00	0.00
IO	26	B-IO	395.20	1.040	2.41	48.08
LS	40	IO-LS	608.00	1.600	36.34	50.04
CP	65	LS-CP	988.00	2.600	97.54	54.65
C	66	CP-C-D-E	1003.20	2.640	100.00	54.81
P.P	11	-	167.20	0.440	0.00	45.45
S9_AR_1.0_MODE_LOAD TYPE_PUSH_Y						
Per.lvl.	step no.	Region	Sd (mm)	Drift (%)	DI_E (%)	DI_K (%)
OP	23	A-B	349.60	0.920	0.00	0.00
IO	24	B-IO	364.80	0.960	2.81	47.92
LS	37	IO-LS	562.40	1.480	39.62	49.17
CP	57	LS-CP	866.40	2.280	97.10	52.14
C	58	CP-C-D-E	881.60	2.320	100.00	52.28
P.P	11	-	167.20	0.440	0.00	45.45

Table 7.49 9- storey unidirectional setback with IR2 building case of X dirn

S9_AR_1.0_ACCL_LOAD TYPE_PUSH_X						
Per.lvl.	step no.	Region	Sd (mm)	Drift (%)	DI_E (%)	DI_K (%)
OP	5	A-B	76.00	0.200	0.00	0.00
IO	6	B-IO	91.20	0.240	3.65	41.67
LS	19	IO-LS	288.80	0.760	45.57	52.96
CP	45	LS-CP	684.00	1.800	98.77	60.63
C	46	CP-C-D-E	699.20	1.840	100.00	60.82
P.P	7	-	106.40	0.280	7.24	42.95
S9_AR_1.0_IS_LOAD TYPE_PUSH_X						
Per.lvl.	step no.	Region	Sd (mm)	Drift (%)	DI_E (%)	DI_K (%)
OP	6	A-B	91.20	0.240	0.00	0.00
IO	7	B-IO	106.40	0.280	2.40	42.86
LS	22	IO-LS	334.40	0.880	37.45	54.44
CP	50	LS-CP	760.00	2.000	97.96	62.44
C	51	CP-C-D-E	775.20	2.040	100.00	62.60
P.P	9	-	136.80	0.360	7.18	44.75
S9_AR_1.0_MODE_LOAD TYPE_PUSH_X						
Per.lvl.	step no.	Region	Sd (mm)	Drift (%)	DI_E (%)	DI_K (%)
OP	18	A-B	273.60	0.720	0.00	0.00
IO	19	B-IO	288.80	0.760	2.74	47.37
LS	32	IO-LS	486.40	1.280	38.97	49.36
CP	52	LS-CP	790.40	2.080	97.02	53.56
C	53	CP-C-D-E	805.60	2.120	100.00	53.74
P.P	9	-	136.80	0.360	0.00	44.44

Table 7.50 9- storey unidirectional setback with IR2 building case of Y dirn

S9_AR_1.0_ACCL_LOAD TYPE_PUSH_Y						
Per.lvl.	step no.	Region	Sd (mm)	Drift (%)	DI_E (%)	DI_K (%)
OP	6	A-B	91.20	0.240	0.00	0.00
IO	7	B-IO	106.40	0.280	3.03	42.86
LS	19	IO-LS	288.80	0.760	37.96	52.45
CP	42	LS-CP	638.40	1.680	97.62	59.57
C	43	CP-C-D-E	653.60	1.720	100.00	59.76
P.P	8	-	121.60	0.320	6.04	43.95
S9_AR_1.0_IS_LOAD TYPE_PUSH_Y						
Per.lvl.	step no.	Region	Sd (mm)	Drift (%)	DI_E (%)	DI_K (%)
OP	7	A-B	106.40	0.280	0.00	0.00
IO	8	B-IO	121.60	0.320	2.43	43.75
LS	22	IO-LS	334.40	0.880	35.66	53.32
CP	50	LS-CP	760.00	2.000	97.88	61.18
C	51	CP-C-D-E	775.20	2.040	100.00	61.35
P.P	10	-	152.00	0.400	7.26	45.37
S9_AR_1.0_MODE_LOAD TYPE_PUSH_Y						
Per.lvl.	step no.	Region	Sd (mm)	Drift (%)	DI_E (%)	DI_K (%)
OP	24	A-B	364.80	0.960	0.00	0.00
IO	25	B-IO	380.00	1.000	4.29	48.00
LS	39	IO-LS	592.80	1.560	64.88	49.23
CP	46	LS-CP	699.20	1.840	95.59	50.10
C	47	CP-C-D-E	714.40	1.880	100.00	50.23
P.P	11	-	167.20	0.440	0.00	45.45

Table 7.51 9- storey unidirectional setback with IR3 building case of X dirn

S9_AR_1.0_ACCL_LOAD TYPE_PUSH_X						
Per.lvl.	step no.	Region	Sd (mm)	Drift (%)	DI_E (%)	DI_K (%)
OP	5	A-B	76.00	0.200	0.00	0.00
IO	6	B-IO	91.20	0.240	2.91	41.67
LS	20	IO-LS	304.00	0.800	40.75	53.43
CP	47	LS-CP	714.40	1.880	98.26	61.16
C	48	CP-C-D-E	729.60	1.920	100.00	61.34
P.P	7	-	106.40	0.280	5.80	42.95
S9_AR_1.0_IS_LOAD TYPE_PUSH_X						
Per.lvl.	step no.	Region	Sd (mm)	Drift (%)	DI_E (%)	DI_K (%)
OP	7	A-B	106.40	0.280	0.00	0.00
IO	8	B-IO	121.60	0.320	2.33	43.75
LS	23	IO-LS	349.60	0.920	36.43	54.68
CP	52	LS-CP	790.40	2.080	97.98	62.81
C	53	CP-C-D-E	805.60	2.120	100.00	62.96
P.P	9	-	136.80	0.360	4.65	44.63
S9_AR_1.0_MODE_LOAD TYPE_PUSH_X						
Per.lvl.	step no.	Region	Sd (mm)	Drift (%)	DI_E (%)	DI_K (%)
OP	6	A-B	91.20	0.240	0.00	0.00
IO	7	B-IO	106.40	0.280	2.53	42.86
LS	22	IO-LS	334.40	0.880	38.57	54.34
CP	51	LS-CP	775.20	2.040	98.18	62.19
C	52	CP-C-D-E	790.40	2.080	100.00	62.36
P.P	8	-	121.60	0.320	5.04	43.89

Table 7.52 9- storey unidirectional setback with IR3 building case of Y dirn

S9_AR_1.0_ACCL_LOAD TYPE_PUSH_Y						
Per.lvl.	step no.	Region	Sd (mm)	Drift (%)	DI_E (%)	DI_K (%)
OP	6	A-B	91.20	0.240	0.00	0.00
IO	7	B-IO	106.40	0.280	2.94	42.86
LS	19	IO-LS	288.80	0.760	37.19	52.05
CP	42	LS-CP	638.40	1.680	97.53	59.27
C	43	CP-C-D-E	653.60	1.720	100.00	59.47
P.P	8	-	121.60	0.320	5.87	43.89
S9_AR_1.0_IS_LOAD TYPE_PUSH_Y						
Per.lvl.	step no.	Region	Sd (mm)	Drift (%)	DI_E (%)	DI_K (%)
OP	7	A-B	106.40	0.280	0.00	0.00
IO	8	B-IO	121.60	0.320	2.36	43.75
LS	24	IO-LS	364.80	0.960	39.25	53.65
CP	51	LS-CP	775.20	2.040	97.91	60.95
C	52	CP-C-D-E	790.40	2.080	100.00	61.12
P.P	10	-	152.00	0.400	7.06	45.24
S9_AR_1.0_MODE_LOAD TYPE_PUSH_Y						
Per.lvl.	step no.	Region	Sd (mm)	Drift (%)	DI_E (%)	DI_K (%)
OP	7	A-B	106.40	0.280	0.00	0.00
IO	8	B-IO	121.60	0.320	2.74	43.75
LS	22	IO-LS	334.40	0.880	40.14	51.56
CP	45	LS-CP	684.00	1.800	97.61	57.55
C	46	CP-C-D-E	699.20	1.840	100.00	57.73
P.P	10	-	152.00	0.400	8.20	45.23

Table 7.53 9- storey bi-directional setback with IR1 building case of X dirn

S9_AR_1.0_ACCL_LOAD TYPE_PUSH_X						
Per.lvl.	step no.	Region	Sd (mm)	Drift (%)	DI_E (%)	DI_K (%)
OP	5	A-B	76.00	0.200	0.00	0.00
IO	6	B-IO	91.20	0.240	6.62	41.67
P.P	7	-	106.40	0.280	13.15	42.95
LS	19	IO-LS	288.80	0.760	84.29	53.02
CP	21	LS-CP	319.20	0.840	94.85	53.98
C	22	CP-C-D-E	334.40	0.880	100.00	54.42
S9_AR_1.0_IS_LOAD TYPE_PUSH_X						
Per.lvl.	step no.	Region	Sd (mm)	Drift (%)	DI_E (%)	DI_K (%)
OP	6	A-B	91.20	0.240	0.00	0.00
IO	7	B-IO	106.40	0.280	2.78	42.86
P.P	9	-	136.80	0.360	8.28	44.99
LS	21	IO-LS	319.20	0.840	39.27	53.96
CP	49	LS-CP	744.80	1.960	98.24	61.78
C	50	CP-C-D-E	760.00	2.000	100.00	61.96
S9_AR_1.0_MODE_LOAD TYPE_PUSH_X						
Per.lvl.	step no.	Region	Sd (mm)	Drift (%)	DI_E (%)	DI_K (%)
OP	5	A-B	76.00	0.200	0.00	0.00
IO	6	B-IO	91.20	0.240	3.73	41.67
P.P	9	-	136.80	0.360	14.57	45.31
LS	17	IO-LS	258.40	0.680	40.74	51.95
CP	43	LS-CP	653.60	1.720	98.60	60.44
C	44	CP-C-D-E	668.80	1.760	100.00	60.65

Table 7.54 9- storey bi-directional setback with IR1 building case of Y dirn

S9_AR_1.0_ACCL_LOAD TYPE_PUSH_Y						
Per.lvl.	step no.	Region	Sd (mm)	Drift (%)	DI_E (%)	DI_K (%)
OP	5	A-B	76.00	0.200	0.00	0.00
IO	6	B-IO	91.20	0.240	3.97	41.67
LS	19	IO-LS	288.80	0.760	51.08	53.03
CP	35	LS-CP	532.00	1.400	97.52	58.57
C	36	CP-C-D-E	547.20	1.440	100.00	58.82
P.P	8	-	121.60	0.320	11.77	44.13
S9_AR_1.0_IS_LOAD TYPE_PUSH_Y						
Per.lvl.	step no.	Region	Sd (mm)	Drift (%)	DI_E (%)	DI_K (%)
OP	6	A-B	91.20	0.240	0.00	0.00
IO	7	B-IO	106.40	0.280	2.56	42.86
LS	21	IO-LS	319.20	0.840	37.22	53.87
CP	48	LS-CP	729.60	1.920	97.91	61.80
C	49	CP-C-D-E	744.80	1.960	100.00	61.97
P.P	9	-	136.80	0.360	7.65	44.87
S9_AR_1.0_MODE_LOAD TYPE_PUSH_Y						
Per.lvl.	step no.	Region	Sd (mm)	Drift (%)	DI_E (%)	DI_K (%)
OP	6	A-B	91.20	0.240	0.00	0.00
IO	7	B-IO	106.40	0.280	3.51	42.86
LS	21	IO-LS	319.20	0.840	51.38	52.84
CP	35	LS-CP	532.00	1.400	96.84	57.70
C	36	CP-C-D-E	547.20	1.440	100.00	57.93
P.P	8	-	121.60	0.320	7.01	43.81

Table 7.55 9- storey bi-directional setback with IR2 building case of X dirn

S9_AR_1.0_ACCL_LOAD TYPE_PUSH_X						
Per.lvl.	step no.	Region	Sd (mm)	Drift (%)	DI_E (%)	DI_K (%)
OP	5	A-B	76.00	0.200	0.00	0.00
IO	6	B-IO	91.20	0.240	3.96	41.67
LS	18	IO-LS	273.60	0.720	45.68	52.52
CP	44	LS-CP	668.80	1.760	98.96	60.61
C	45	CP-C-D-E	684.00	1.800	100.00	60.81
P.P	7	-	106.40	0.280	7.85	43.00
S9_AR_1.0_IS_LOAD TYPE_PUSH_X						
Per.lvl.	step no.	Region	Sd (mm)	Drift (%)	DI_E (%)	DI_K (%)
OP	6	A-B	91.20	0.240	0.00	0.00
IO	7	B-IO	106.40	0.280	2.41	42.86
LS	21	IO-LS	319.20	0.840	35.21	53.80
CP	50	LS-CP	760.00	2.000	97.96	62.45
C	51	CP-C-D-E	775.20	2.040	100.00	62.61
P.P	9	-	136.80	0.360	7.19	44.88
S9_AR_1.0_MODE_LOAD TYPE_PUSH_X						
Per.lvl.	step no.	Region	Sd (mm)	Drift (%)	DI_E (%)	DI_K (%)
OP	5	A-B	76.00	0.200	0.00	0.00
IO	6	B-IO	91.20	0.240	3.02	41.67
LS	17	IO-LS	258.40	0.680	34.86	51.85
CP	42	LS-CP	638.40	1.680	97.76	60.59
C	43	CP-C-D-E	653.60	1.720	100.00	60.81
P.P	10	-	152.00	0.400	14.89	46.32

Table 7.56 9- storey bi-directional setback with IR2 building case of Y dirn

S9_AR_1.0_ACCL_LOAD TYPE_PUSH_Y						
Per.lvl.	step no.	Region	Sd (mm)	Drift (%)	DI_E (%)	DI_K (%)
OP	5	A-B	76.00	0.200	0.00	0.00
IO	6	B-IO	91.20	0.240	2.98	41.67
LS	18	IO-LS	273.60	0.720	37.23	52.21
CP	42	LS-CP	638.40	1.680	97.71	60.08
C	43	CP-C-D-E	653.60	1.720	100.00	60.28
P.P	7	-	106.40	0.280	5.93	42.94
S9_AR_1.0_IS_LOAD TYPE_PUSH_Y						
Per.lvl.	step no.	Region	Sd (mm)	Drift (%)	DI_E (%)	DI_K (%)
OP	7	A-B	106.40	0.280	0.00	0.00
IO	8	B-IO	121.60	0.320	2.38	43.75
LS	22	IO-LS	334.40	0.880	34.95	53.80
CP	51	LS-CP	775.20	2.040	97.94	61.96
C	52	CP-C-D-E	790.40	2.080	100.00	62.12
P.P	10	-	152.00	0.400	7.12	45.46
S9_AR_1.0_MODE_LOAD TYPE_PUSH_Y						
Per.lvl.	step no.	Region	Sd (mm)	Drift (%)	DI_E (%)	DI_K (%)
OP	7	A-B	106.40	0.280	0.00	0.00
IO	8	B-IO	121.60	0.320	2.84	43.75
LS	21	IO-LS	319.20	0.840	39.09	51.65
CP	43	LS-CP	653.60	1.720	97.44	58.04
C	44	CP-C-D-E	668.80	1.760	100.00	58.23
P.P	3	-	45.60	0.120	0.00	33.33

Table 7.57 9- storey bi-directional setback with IR3 building case of X dirn

S9_AR_1.0_ACCL_LOAD TYPE_PUSH_X						
Per.lvl.	step no.	Region	Sd (mm)	Drift (%)	DI_E (%)	DI_K (%)
OP	5	A-B	76.00	0.200	0.00	0.00
IO	6	B-IO	91.20	0.240	2.92	41.67
LS	18	IO-LS	273.60	0.720	36.08	52.32
CP	45	LS-CP	684.00	1.800	98.04	60.87
C	46	CP-C-D-E	699.20	1.840	100.00	61.07
P.P	7	-	106.40	0.280	5.82	42.97
S9_AR_1.0_IS_LOAD TYPE_PUSH_X						
Per.lvl.	step no.	Region	Sd (mm)	Drift (%)	DI_E (%)	DI_K (%)
OP	6	A-B	91.20	0.240	0.00	0.00
IO	7	B-IO	106.40	0.280	2.30	42.86
LS	23	IO-LS	349.60	0.920	38.37	54.65
CP	51	LS-CP	775.20	2.040	97.96	62.67
C	52	CP-C-D-E	790.40	2.080	100.00	62.82
P.P	9	-	136.80	0.360	6.89	44.61
S9_AR_1.0_MODE_LOAD TYPE_PUSH_X						
Per.lvl.	step no.	Region	Sd (mm)	Drift (%)	DI_E (%)	DI_K (%)
OP	6	A-B	91.20	0.240	0.00	0.00
IO	7	B-IO	106.40	0.280	2.65	42.86
LS	19	IO-LS	288.80	0.760	33.67	52.64
CP	46	LS-CP	699.20	1.840	97.78	61.55
C	47	CP-C-D-E	714.40	1.880	100.00	61.75
P.P	10	-	152.00	0.400	10.55	45.87

Table 7.58 9- storey bi-directional setback with IR3 building case of Y dirn

S9_AR_1.0_ACCL_LOAD TYPE_PUSH_Y						
Per.lvl.	step no.	Region	Sd (mm)	Drift (%)	DI_E (%)	DI_K (%)
OP	5	A-B	76.00	0.200	0.00	0.00
IO	6	B-IO	91.20	0.240	2.72	41.67
LS	19	IO-LS	288.80	0.760	36.79	52.22
CP	45	LS-CP	684.00	1.800	97.84	60.34
C	46	CP-C-D-E	699.20	1.840	100.00	60.54
P.P	7	-	106.40	0.280	5.42	42.87
S9_AR_1.0_IS_LOAD TYPE_PUSH_Y						
Per.lvl.	step no.	Region	Sd (mm)	Drift (%)	DI_E (%)	DI_K (%)
OP	7	A-B	106.40	0.280	0.00	0.00
IO	8	B-IO	121.60	0.320	2.14	43.75
LS	26	IO-LS	395.20	1.040	39.99	54.69
CP	55	LS-CP	836.00	2.200	98.06	62.11
C	56	CP-C-D-E	851.20	2.240	100.00	62.26
P.P	10	-	152.00	0.400	6.42	45.13
S9_AR_1.0_MODE_LOAD TYPE_PUSH_Y						
Per.lvl.	step no.	Region	Sd (mm)	Drift (%)	DI_E (%)	DI_K (%)
OP	7	A-B	106.40	0.280	0.00	0.00
IO	8	B-IO	121.60	0.320	2.62	43.75
LS	21	IO-LS	319.20	0.840	36.15	51.29
CP	46	LS-CP	699.20	1.840	97.62	58.27
C	47	CP-C-D-E	714.40	1.880	100.00	58.45
P.P	1	-	15.20	0.040	0.00	0.00

In 4-storey buildings with an aspect ratio (AR) of 0.5, the drift limit at the performance point is between 0.285% and 0.376% in the x direction and between 0.331% and 0.454% in the y direction for all three load conditions. In the x direction, the energy-based DI ranged from 0% to 4.82% and from 0% to 7.80% in the y direction. Drift is about the same in plan aspect ratios of 0.75 and 1.00 as it is in 0.5 AR. However, the energy-based DI

ranges have changed to 1.93% to 5.16% and 0% to 3.95% in the x direction and 4.04% to 8.30% and 0% to 4.66% in the y direction for plan aspect ratios of 0.75 and 1.00, respectively.

In a 6-storey building with an aspect ratio (AR) of 0.5, the drift limit at the performance point is found to be 0.296% to 0.398% in the x direction and 0.336% to 0.475% in the y direction for all three loads. In the x direction, the energy-based DI increases from 0% to 9.19%, and in the y direction, it ranges from 0% to 14.98%. The drift is almost the same in aspect ratios (AR) 0.75 and 1.00 as it is in 0.5 AR, but the energy-based DI range for AR 0.75 and 1.00 has been changed to 0% to 5.68% and 5.34% to 27.33% in the x direction and 0% to 8% and 7.06% to 27.87% in the y direction, respectively.

The drift limit at the performance point is shown for both a 6-storey building and a 9-storey building with all aspect ratios and for all three load cases. But with 0.5 AR, the energy-based DI range in the x and y directions changes to 12.05% to 35.92% and 13.17% to 33.60%, respectively. For aspect ratios of 0.75 and 1.00, the energy-based DI range is changed to 0% to 13.66% and 0% to 12.89% in the x direction and 0% to 18.10% and 0% to 15.34% in the y direction.

In all circumstances, a performance point is reached that is well within the damage control range (DCR) level's drift limit. When the stiffness damage index is expanded by roughly 50%, the performance point is obtained in all cases (in accordance as per Figure 7.1 and Figure 7.2 buildings), as indicated in Table 7.59 and Table 7.60. The majority of the results are nearly identical, but some diverge. It is possible that this is related to the usage of a single engineering demand parameter (energy). When the stiffness of the building decreased as a result of the pushover analysis, it experienced more damage. There is not a significant change in drift range for any load pattern as the building's height increases. The mode types of load patterns have a larger drift when compared to the acceleration and IS 1893-2016 type of load. Damage is estimated using the first hysteretic cycle for various energies and initial and secant stiffness at various performance levels. Both DIs are validated using nonlinear static analysis methods proposed by Powell and Allahabadi (1988) [51] and Zameeruddin and K. Sanghle (2020) [3] and their values are shown in Table 7.59and Table 7.60.The minimum and maximum drift limits are mentioned in Table 7.61; they are well within the prescribed limits shown in Table 5.2.

Table 7.59 Damage indices at performance point

Sr. No.	Building designation	Lateral loading type	Sd (mm)	Di_E (%) Proposed	Di_D (%) P&A (1988) Existing	Di_K (%) Proposed	Di_V (%) Z&K (2020) Existing
1	S4_0.5_UD_X	Accl.	51.24	2.87	2.76	49.33	51.62
2		IS-1893	67.70	0.00	0.00	49.47	49.29
3		Mode-2	59.07	4.82	4.66	49.46	57.77
4	S4_0.5_UD_Y	Accl.	59.53	5.73	4.44	49.44	51.26
5		IS-1893	81.79	0.00	0.00	49.56	45.62
6		Mode-1	76.70	7.80	7.57	49.69	52.92
7	S4_0.75_UD_X	Accl.	51.31	1.93	1.86	49.31	50.31
8		IS-1893	63.98	5.16	4.99	49.55	61.81
9		Mode-2	58.94	4.00	3.88	49.44	57.17
10	S4_0.75_UD_Y	Accl.	57.67	4.04	3.92	49.41	50.86
11		IS-1893	74.63	8.30	8.09	49.69	61.07
12		Mode-1	73.63	6.11	5.92	49.58	50.43
13	S4_1.00_UD_X	Accl.	51.39	1.93	1.86	49.31	50.87
14		IS-1893	67.26	0.00	0.00	49.46	49.91
15		Mode-2	58.88	3.95	3.82	49.44	58.18
16	S4_1.00_UD_Y	Accl.	56.31	3.44	3.34	49.39	51.43
17		IS-1893	75.82	0.00	0.00	49.52	47.36
18		Mode-1	70.82	4.66	4.51	49.52	49.40
19	S6_0.5_UD_X	Accl.	77.08	6.78	6.42	49.43	55.34
20		IS-1893	103.45	0.00	0.00	49.50	35.63
21		Mode-2	87.65	9.19	8.82	49.62	61.14
22	S6_0.5_UD_Y	Accl.	87.29	8.12	7.73	49.62	56.67
23		IS-1893	123.55	0.00	0.00	49.58	40.48
24		Mode-1	116.15	14.98	14.46	50.05	60.29

25	S6_0.75_UD_X	Accl.	77.19	5.68	5.36	48.76	55.32
26		IS-1893	103.62	0.00	0.00	49.49	35.73
27		Mode-2	94.55	0.00	0.00	49.45	34.84
28	S6_0.75_UD_Y	Accl.	84.78	8.00	7.62	48.90	55.80
29		IS-1893	118.49	0.00	0.00	49.56	36.19
30		Mode-1	12s0.86	0.00	0.00	49.57	37.33
31	S6_1.00_UD_X	Accl.	77.03	5.34	5.03	48.63	54.64
32		IS-1893	98.97	27.33	26.41	50.12	61.82
33		Mode-2	87.37	8.08	7.75	49.07	61.48
34	S6_1.00_UD_Y	Accl.	82.96	7.06	6.74	48.84	57.23
35		IS-1893	111.07	27.87	27.23	49.64	60.16
36		Mode-1	108.51	12.29	11.91	49.27	57.64
37	S9_0.5_UD_X	Accl.	115.97	12.05	11.15	48.95	64.68
38		IS 1893	144.93	35.92	35.13	49.69	71.30
39		Mode-2	130.95	14.00	13.34	49.21	68.98
40	S9_0.5_UD_Y	Accl.	128.52	13.17	12.40	49.21	64.54
41		IS 1893	168.21	33.60	32.98	49.87	71.55
42		Mode-1	168.79	19.30	18.77	49.83	67.91
43	S9_0.75_UD_X	Accl.	115.51	11.92	10.52	48.99	63.65
44		IS 1893	158.60	0.00	0.00	49.04	31.63
45		Mode-2	130.20	13.66	12.70	49.31	67.85
46	S9_0.75_UD_Y	Accl.	124.50	13.33	12.33	49.16	65.01
47		IS 1893	176.75	0.00	0.00	49.14	35.42
48		Mode-1	162.71	18.10	17.64	49.61	66.89
49	S9_1.00_UD_X	Accl.	114.03	12.89	8.10	48.96	60.01
50		IS 1893	155.43	0.00	0.00	49.02	31.95
51		Mode-2	128.48	12.17	10.33	49.23	64.21
52	S9_1.00_UD_Y	Accl.	120.44	12.34	10.41	49.08	62.39
53		IS 1893	168.86	0.00	0.00	49.09	31.78

54		Mode-1	155.10	15.45	14.97	49.51	64.91

Table 7.60 Damage indices at performance point for 9- storey building

Sr. No.	Storey_ Reg./IR_DF_ Dir. n	Lateral loading type	Sd (mm)	Drift (%)	Di E (%) Proposed	Di K (%) Proposed	Di D (%) P&A (1988) Existing	Di V (%) Z&K (2020) Existing
1	S9_Reg_DF_X	Accl.	121.60	0.320	9.90	44.05	7.69	52.69
2		IS 1893	136.80	0.360	7.64	44.81	6.98	61.35
3		Mode-2	136.80	0.360	9.81	45.02	7.32	58.61
4	S9_Reg_DF_X	Accl.	121.60	0.320	10.38	44.13	8.11	54.57
5		IS 1893	136.80	0.360	8.48	45.04	7.32	63.45
6		Mode-1	136.80	0.360	8.63	45.00	7.89	60.21
7	S9_UNI_ IR1_DF_X	Accl.	121.60	0.320	0.00	43.75	0.00	23.72
8		IS 1893	152.00	0.400	0.00	45.00	0.00	30.27
9		Mode-2	136.80	0.360	0.00	44.44	0.00	25.70
10	S9_UNI_ IR1_DF_Y	Accl.	136.80	0.360	0.00	44.44	0.00	25.99
11		IS 1893	167.20	0.440	0.00	45.45	0.00	29.36
12		Mode-1	167.20	0.440	0.00	45.45	0.00	26.11
13	S9_UNI_ IR2_DF_X	Accl.	106.40	0.280	7.24	42.95	4.88	49.12
14		IS 1893	136.80	0.360	7.18	44.75	6.67	64.43
15		Mode-2	136.80	0.360	0.00	44.44	0.00	26.71
16	S9_UNI_ IR2_DF_Y	Accl.	121.60	0.320	6.04	43.95	5.41	52.14
17		IS 1893	152.00	0.400	7.26	45.37	6.82	62.83
18		Mode-1	167.20	0.440	0.00	45.45	0.00	26.44
19	S9_UNI_ IR3_DF_X	Accl.	106.40	0.280	5.80	42.95	4.65	49.26
20		IS 1893	136.80	0.360	4.65	44.63	4.35	64.89
21		Mode-2	121.60	0.320	5.04	43.89	4.35	57.03
22	S9_UNI_ IR3_DF_Y	Accl.	121.60	0.320	5.87	43.89	5.41	50.99
23		IS 1893	152.00	0.400	7.06	45.24	6.67	61.25

24		Mode-1	152.00	0.400	8.20	45.23	7.69	49.77
25	S9_BI_ IR1_DF_X	Accl.	106.40	0.280	13.15	42.95	11.76	58.10
26		IS 1893	136.80	0.360	8.28	44.99	6.23	61.90
27		Mode-2	136.80	0.360	14.57	45.31	10.26	59.59
28	S9_BI_ IR1_DF_Y	Accl.	121.60	0.320	11.77	44.13	9.68	56.63
29		IS 1893	136.80	0.360	7.65	44.87	6.98	62.85
30		Mode-1	121.60	0.320	7.01	43.81	6.67	52.97
31	S9_BI_ IR2_DF_X	Accl.	106.40	0.280	7.85	43.00	5.00	49.88
32		IS 1893	136.80	0.360	7.19	44.88	6.67	63.64
33		Mode-2	152.00	0.400	14.89	46.32	13.16	66.20
34	S9_BI_ IR2_DF_Y	Accl.	106.40	0.280	5.93	42.94	5.26	49.00
35		IS 1893	152.00	0.400	7.12	45.46	6.67	65.54
36		Mode-1	45.60	0.120	0.00	33.33	0.00	12.65
37	S9_BI_ IR3_DF_X	Accl.	106.40	0.280	5.82	42.97	4.88	50.61
38		IS 1893	136.80	0.360	6.89	44.61	6.52	64.94
39		Mode-2	152.00	0.400	10.55	45.87	9.76	68.41
40	S9_BI_ IR3_DF_Y	Accl.	106.40	0.280	5.42	42.87	4.88	47.89
41		IS 1893	152.00	0.400	6.42	45.13	6.12	63.68
42		Mode-1	15.20	0.040	0.00	0.00	0.00	0.00

Table 7.61 Different minimum to maximum ranges at performance point

Building type & Setback type	Storey	Drift range %		EBDI range %		SBDI range %	
		X direction	Y direction	X direction	Y direction	X direction	Y direction
Regular	4	0.200	0.200	3.44-8.14	0.79-8.47	40.0-40.3	40.0-40.3
Irreg_Uni_IR1		0.200	0.20-0.24	3.23-8.06	2.07-11.1	40.0-40.2	40.0-41.9
Irreg_Uni_IR2		0.120	0.12-0.16	7.67-13.3	5.51-17.6	34.0-34.3	33.4-38.8

Irreg_Uni_IR3		0.120	0.12-0.16	9.90-14.1	5.40-5.46	33.3-33.4	33.3-37.5
Irreg_BI_IR2		0.08-0.12	0.04-0.12	0.00-12.5	0.00	25.0-33.3	0.00-37.8
Irreg_BI_IR3		0.08-0.12	0.04-0.12	8.61-9.95	0.00-6.84	25.0-33.3	25.0-33.3
Regular	6	0.32-0.36	0.32-0.36	5.21-6.95	5.64-7.58	43.9-44.7	43.9-44.8
Irreg_IR1		0.20	0.20	11.31-11.34	10.16-10.92	40.3	40.3
Irreg_IR2		0.32-0.40	0.36-0.44	0.00	0.00	43.7-45.0	37.5-45.4
Irreg_IR3		0.28-0.36	0.32-0.40	2.20-7.43	4.47-4.75	42.8-44.6	43.7-45.1
Irreg_BI_IR1		0.2-0.24	0.2-0.24	5.93-6.51	0.00-5.45	40.0-41.8	40.0-41.7
Irreg_BI_IR2		0.12	0.16-0.20	6.52-7.01	11.42-11.91	33.3	37.8-40.3
Irreg_BI_IR3		0.12-0.16	0.16-0.24	4.82-10.92	4.15-20.21	33.3-37.7	37.5-42.3
Regular	9	0.32-0.36	0.32-0.36	7.64-9.90	8.48-10.38	44.0-45.0	44.1-45.0
Irreg_IR1		0.32-0.40	0.36-0.44	0.00	0.00	43.7-45.0	44.4-45.4
Irreg_IR2		0.28-0.36	0.32-0.44	0.00-7.24	0.00-7.26	42.9-44.7	43.9-45.4
Irreg_IR3		0.28-0.36	0.32-0.40	4.65-5.80	5.87-8.20	42.9-44.6	43.9-45.2
Irreg_BI_IR1		0.28-0.36	0.32-0.36	8.28-14.57	7.01-11.77	42.9-45.3	43.8-44.8
Irreg_BI_IR2		0.28-0.40	0.12-0.40	7.19-14.89	0.00-7.12	43.0-46.3	33.3-45.5
Irreg_BI_IR3		0.28-0.40	0.04-0.40	5.82-10.55	0.00-6.42	42.9-45.8	0.00-45.1

Table 7.62 Pushover result for S4_AR_0.5_UNI_IR1_UD_ Accl_X building case

Step no.	Disp. (mm)	Base Shear (kN)	Number of hinges in particular range of performance levels							
			A-B	B-IO	IO-LS	LS-CP	CP-C	C-D	D-E	Beyond E
0	0	0	308	0	0	0	0	0	0	0
1	0.720	10.124	308	0	0	0	0	0	0	0
65	46.80	658.084	307	1	0	0	0	0	0	0
109	78.48	959.858	267	39	2	0	0	0	0	0
261	187.92	1309.105	200	30	77	1	0	0	0	0
323	232.56	1389.947	195	12	63	37	0	0	1	0
530	381.60	1571.625	193	8	20	4	0	0	82	1

Table 7.63 EBDI calculation for S4_AR_0.5_UNI_IR1_UD_ Accl_X

Step no.	Disp. (mm)	Base Shear (kN)	Per. level	Region	Drift (%)	Area under curve (kN-m)	Energy based damage index (%)	Remarks
0	0	0	-	-	0.000	-	-	Total 308 hinges
1	0.72	10.124	OP	A-B	0.004	0.037	0.00	First step of Elastic range
64	46.08	647.959	OP	A-B	0.256	2.376	0.00	Last step of Elastic range
65	46.80	658.084	IO	B-IO	0.260	2.413	0.40	First hinge formation
72	51.87	722.406	P.P	IO-LS	0.288	2.639	2.87	P.P @ IO-LS
109	78.48	959.858	LS	IO-LS	0.436	4.021	17.93	Hinge @ IO-LS
261	187.92	1309.105	CP	LS-CP	1.044	9.418	76.77	Hinge @ LS-CP
323	232.56	1389.947	C	CP-C-D-E	1.292	11.55	100.00	Hinge @ D-E

Table 7.64 SBDI calculation for S4_AR_0.5_UNI_IR1_UD_ Accl_X building case

Step no. (1)	Drift (%) (2)	Stiffness (kN) (3)	Cumulative base shear, $\sum K_o \times d_c$ (kN) (4)	Sum. of base shear, $\sum V$ (kN) (5)	Ratio of col.5/ col.4 (%) (6)	Stiffness based damage index (%) (7)	Remarks
1	0.004	14061.11	10.124	10.124	1.00	0.00	First step of Elastic range
65	0.260	14061.62	42775.417	21716.760	50.77	49.23	First hinge formation
72	0.288	13935.30	52640.575	26583.315	50.67	49.33	P.P @ IO-LS
109	0.436	12230.60	117713.407	58406.346	49.62	50.38	Hinge @ IO-LS
261	1.044	6966.28	541622.700	235964.161	43.57	56.43	Hinge @ LS-CP
323	1.292	5976.72	763074.193	319764.867	41.90	58.10	Hinge @ D-E

Table 7.65 Damage indices at performance levels on curve of S4_AR_0.5_UNI_IR1_UD_Accl_X building case

Performance level	Sd (mm)	Drift (%)	Di_E (%)	Di_K (%)	$Di_{P\&A}$ (1988) (%)	$Di_{Z\&K}$ (2020) (%)
OP	46.080	0.256	0.00	0.00	0.00	0.00
IO	46.800	0.260	0.40	49.23	0.39	46.96
P.P	51.236	0.285	2.87	49.33	2.76	51.62
LS	78.480	0.436	17.93	50.38	17.37	68.83
CP	187.920	1.044	76.77	56.43	76.07	94.14
C	232.560	1.292	100.00	58.10	100.00	100.00

Di_E = Energy based damage index, Di_k = Stiffness based damage index

$Di_{P\&A}$ = Powell & Allahabadi's deformation based damage index (1988) [51]

$Di_{Z\&K}$ = Zameeruddin & K. Sanghle's strength based damage index (2020) [3]

The results of a building's pushover analysis for the S4_0.5_UNI_ IR1_UD_ Acceleration-X case are shown in Table 7.62.

Table ***7.63***and Table 7.64show examples of the methods used to calculate the EBDI and SBDI for the S4_0.5_UNI_IR1_UD_ Acceleration load type of building at different performance levels. Table 7.65indicates the manner in which the damage index results at different performance levels. Table 7.66displays the results of a building's pushover analysis for the S9_1.00_BI_ IR1_DF_ Acceleration-X case. Table 7.67 and Table 7.68present EBDI and SBDI calculation examples for the S9_1.00_BI_IR1_DF_ Acceleration load type building at various performance levels. Table 7.69 illustrates the way the damage index is affected by varying performance levels for 9-storey building.

Table 7.66 Pushover result for S9_AR_1.00_BI_IR1_DF_ Accl_X building case

Step no.	Disp. (mm)	Base Shear (kN)	Number of hinges in particular range of performance levels							
			A-B	B-IO	IO-LS	LS-CP	CP-C	C-D	D-E	Beyond E
0	0	0	1162	0	0	0	0	0	0	0
1	15.2	163.66	1162	0	0	0	0	0	0	0
6	106.4	1127.78	1076	86	0	0	0	0	0	0
19	288.8	1735.72	883	245	34	0	0	0	0	0
22	334.4	1822.94	851	221	89	0	1	0	0	0
44	668.8	2141.52	772	141	231	0	6	10	2	0
0	0	0	1162	0	0	0	0	0	0	0

Table 7.67 EBDI calculation for S9_AR_1.00_BI_IR1_DF_ Accl_X building case

Step no.	Disp. (mm)	Base Shear (kN)	Per. level	Region	Drift (%)	Area under curve (kN-m)	Energy based damage index (%)	Remarks
0	0	0	-	-	0.000	-	-	Total 1162 hinges
1	15.2	163.66	OP	A-B	0.040	0.246	0.00	First step of Elastic range
5	76.0	818.38	OP	A-B	0.200	1.197	0.00	Last step of Elastic range
6	91.2	982.05	IO	B-IO	0.240	1.427	6.62	Hinge formation B-IO
7	106.4	1127.78	P.P	IO-LS	0.280	1.654	13.15	P.P @ IO-LS
19	288.8	1735.72	LS	IO-LS	0.760	4.124	84.29	Hinge @ IO-LS
21	319.2	1794.52	CP	LS-CP	0.840	4.490	94.85	Hinge @ LS-CP
22	334.4	1822.94	C	CP-C-D-E	0.880	4.467	100	Hinge @ CP-C-D-E

Table 7.68 SBDI calculation for S9_AR_1.00_BI_IR1_DF_ Accl_X building case

Step no. (1)	Drift (%) (2)	Stiffness (kN) (3)	Cumulative base shear, $\sum K_o \times d_c$ (kN) (4)	Sum. of base shear, $\sum V$ (kN) (5)	Ratio of col.5/ col.4 (%) (6)	Stiffness based damage index (%) (7)	Remarks
1	0.040	10768.09	163.675	163.375	100.00	0.00	First step of Elastic range
6	0.240	10768.09	5892.300	3437.175	58.33	41.67	Hinge formation B-IO
7	0.280	10599.43	8002.129	4564.954	56.05	43.95	P.P @ IO-LS
19	0.760	6010.11	48442.298	22758.266	46.98	53.02	Hinge @ IO-LS
21	0.840	5621.93	57189.539	26318.055	46.02	53.98	Hinge @ LS-CP
22	0.880	5451.36	61735.785	28140.989	45.58	54.42	Hinge @ D-E

Table 7.69 Damage indices at performance levels on curve of S9_AR_1.00_BI_IR1_DF_Accl_X building case

Performance level	Sd (mm)	Drift (%)	Di_E (%)	Di_K (%)	$Di_{P\&A}$ (1988) (%)	$Di_{Z\&K}$ (2020) (%)
OP	76.00	0.200	0.00	0.00	0.00	0.00
IO	91.20	0.240	6.62	41.67	5.88	49.32
P.P	106.4	0.280	13.15	43.95	11.76	58.10
LS	288.8	0.760	84.29	53.02	82.35	94.74
CP	319.2	0.840	94.85	53.98	94.12	98.29
C	334.4	0.880	100	54.42	100	100

Di_E = Energy based damage index, Di_k = Stiffness based damage index

$Di_{P\&A}$ = Powell & Allahabadi's deformation based damage index (1988) [51]

$Di_{Z\&K}$ = Zameeruddin & K. Sanghle's strength based damage index (2020) [3]

5.3 Results of proposed methods based on drift/displacement using NLSA

A mathematical model based on nonlinear regression analysis is developed to predict potential damage. This application demonstrates the applicability of nonlinear regression in a variety of domains, particularly in situations where linear models cannot convey the relationships between variables. In this study, the drift criterion was applied to the results of pushover analysis to estimate the structural damage caused to irregular buildings. To create a damage index based on drift, we use equation 7 to derive the modified Park-Ang damage index [33]. Therefore, two distinct formulas have been provided using the database that has been developed and the multi-variable nonlinear regression analysis to assess the amount of damage caused to setback types of irregular buildings. The total drift of a building subjected to lateral force can be calculated using the formula in equation 8.The "irregularity index" is a variable also used for determining the step-back irregularity, also known as the setback irregularity, of a building. The Table 6.2 data collection has been used to formulate the drift based damage index equation 9 and 10.Parameters used ($Ø_b$ and $Ø_s$) in the sample calculation of the irregularity index are shown in Table 7.70.InTable 7.71, the results of the drift-based damage index are provided at the performance point for

all of the buildings. The error % that occurs when comparing the drift-based damage index to the modified version of Park and Ang's damage model is displayed in Figure 7.184 through Figure 7.189. The comparison results of drift based DI for 4-storey buildings are displayed in Figure 7.190 and Figure 7.191. The comparison results of all DIs for 4-storey buildings are displayed in Figure 7.192 to Figure 7.197. The comparison results of all DIs for 4-storey buildings are also shown in Table 7.72.

Table 7.70 Sample calculation of irregularity index for 4- storey building case

Model	Load	n_b-1	ns-1	L1	L2	L3	L4	L5	H1	H2	H3	H4	Ø b	Ø s
S4_0.50_ UD_X	**Accl.**	3	4	20	10	10	10	10	18	14	14	14	1.10	1.25
	IS	3	4	20	10	10	10	10	18	14	14	14	1.10	1.25
	Mode	3	4	20	10	10	10	10	18	14	14	14	1.10	1.25
S4_0.50_ UD_Y	**Accl.**	1	4	10	10	10	10	10	18	18	18	18	1.00	1.00
	IS	1	4	10	10	10	10	10	18	18	18	18	1.00	1.00
	Mode	1	4	10	10	10	10	10	18	18	18	18	1.00	1.00
S4_0.75_ UD_X	**Accl.**	3	4	20	10	10	10	10	18	14	14	14	1.10	1.25
	IS	3	4	20	10	10	10	10	18	14	14	14	1.10	1.25
	Mode	3	4	20	10	10	10	10	18	14	14	14	1.10	1.25
S4_0.75_ UD_Y	**Accl.**	2	4	15	15	15	15	15	18	18	18	18	1.00	1.00
	IS	2	4	15	15	15	15	15	18	18	18	18	1.00	1.00
	Mode	2	4	15	15	15	15	15	18	18	18	18	1.00	1.00
S4_1.00_ UD_X	**Accl.**	3	4	20	10	10	10	10	18	14	14	14	1.10	1.25
	IS	3	4	20	10	10	10	10	18	14	14	14	1.10	1.25
	Mode	3	4	20	10	10	10	10	18	14	14	14	1.10	1.25
0_ UD	**Accl.**	3	4	20	20	20	20	20	18	18	18	18	1.00	1.00

	IS	3	4	20	20	20	20	20	18	18	18	18	1.00	1.00
	Mode	3	4	20	20	20	20	20	18	18	18	18	1.00	1.00

Table 7.71 Drift based damage results using NLSA

Sr. No.	Model Designation	Load type	Measured DI (%) Modified P & A	Estimated DI (%) Equation-DBDI	Error (%)
1	S4_0.50_UD_X	Accl.	2.765	3.421	19.2
2		IS	0.000	1.291	100.0
3		Mode	4.657	3.804	-22.4
4	S4_0.50_UD_Y	Accl.	4.435	4.344	-2.1
5		IS	0.000	1.317	100.0
6		Mode	7.572	6.517	-16.2
7	S4_0.75_UD_X	Accl.	1.864	2.045	8.8
8		IS	4.988	4.134	-20.6
9		Mode	3.879	3.679	-5.4
10	S4_0.75_UD_Y	Accl.	3.919	4.649	15.7
11		IS	8.090	7.135	-13.4
12		Mode	5.916	5.760	-2.7
13	S4_1.00_UD_X	Accl.	1.862	2.928	36.4
14		IS	0.000	1.421	100.0
15		Mode	3.819	3.649	-4.7
16	S4_1.00_UD_Y	Accl.	3.337	4.370	23.6

17		IS	0.000	2.490	100.0
18		Mode	4.512	4.749	5.0
19	S6_0.50_UD_X	Accl.	6.417	6.178	-3.9
20		IS	0.000	0.642	100.0
21		Mode	8.815	7.801	-13.0
22	S6_0.50_UD_Y	Accl.	7.730	7.951	2.8
23		IS	0.000	0.086	100.0
24		Mode	14.460	15.850	8.8
25	S6_0.75_UD_X	Accl.	5.361	5.326	-0.6
26		IS	0.000	0.644	100.0
27		Mode	0.000	0.617	100.0
28	S6_0.75_UD_Y	Accl.	7.617	7.566	-0.7
29		IS	0.000	0.957	100.0
30		Mode	0.000	1.133	100.0
31	S6_1.00_UD_X	Accl.	5.028	5.064	0.7
32		IS	26.413	20.124	-31.2
33		Mode	7.755	6.962	-11.4
34	S6_1.00_UD_Y	Accl.	6.741	6.670	-1.1
35		IS	27.227	21.212	-28.4
36		Mode	11.906	10.694	-11.3
37	S9_0.50_UD_X	Accl.	11.152	12.244	8.9
38		IS	35.134	35.430	0.8
39		Mode	13.342	14.574	8.5

40	S9_0.50_UD_Y	Accl.	12.402	7.283	-70.3
41		IS	32.982	38.588	14.5
42		Mode	18.772	18.158	-3.4
43	S9_0.75_UD_X	Accl.	10.521	11.503	8.5
44		IS	0.000	-1.363	100.0
45		Mode	12.700	13.828	8.2
46	S9_0.75_UD_Y	Accl.	12.325	13.491	8.6
47		IS	0.000	0.000	100.0
48		Mode	17.642	20.730	14.9
49	S9_1.00_UD_X	Accl.	8.105	8.643	6.2
50		IS	0.000	0.000	100.0
51		Mode	10.332	11.042	6.4
52	S9_1.00_UD_Y	Accl.	10.410	11.277	7.7
53		IS	0.000	-1.047	100.0
54		Mode	14.971	16.497	9.3
55	S4_1.00_DF_X_ REG	Accl.	5.556	6.492	14.4
56		IS	8.696	8.162	-6.5
57		Mode	8.333	7.970	-4.6
58	S4_1.00_DF_Y_ REG	Accl.	7.407	7.184	-3.1
59		IS	9.091	8.370	-8.6
60		Mode	8.332	7.969	-4.5
61	S4_1.00_DF_X_ UNI_IR1	Accl.	4.762	5.195	8.3

62		IS	8.696	7.289	-19.3
63		Mode	8.333	7.098	-17.4
64	S4_1.00_DF_Y _UNI_IR1	Accl.	4.167	5.748	27.5
65		IS	4.167	5.748	27.5
66		Mode	8.000	7.499	-6.7
67	S4_1.00_DF_X_ UNI_IR2	Accl.	13.334	10.004	-33.3
68		IS	7.693	7.076	-8.7
69		Mode	13.334	10.004	-33.3
70	S4_1.00_DF_Y__UNI_IR2	Accl.	17.648	12.771	-38.2
71		IS	11.765	9.893	-18.9
72		Mode	5.556	6.492	14.4
73	S4_1.00_DF_X_ UNI__IR3	Accl.	14.286	11.293	-26.5
74		IS	10.000	9.105	-9.8
75		Mode	7.693	7.889	2.5
76	S4_1.00_DF_Y_ UNI_IR3	Accl.	5.797	6.621	12.4
77		IS	5.882	6.797	13.5
78		Mode	7.692	7.761	0.9
79	S4_1.00_DF_X_ BI_IR2	Accl.	7.143	6.783	-5.3
80		IS	0.000	2.468	100.0
81		Mode	12.501	9.096	-37.4
82	S4_1.00_DF_Y_ BI_IR2	Accl.	0.000	2.955	100.0
83		IS	0.000	2.955	100.0
84		Mode	0.000	1.524	100.0

85	S4_1.00_DF_X_ BI__IR3	Accl.	8.696	7.936	-9.6
86		IS	9.757	8.494	-14.9
87		Mode	10.001	9.105	-9.8
88	S4_1.00_DF_Y_ BI_IR3	Accl.	7.018	7.530	6.8
89		IS	0.000	3.769	100.0
90		Mode	0.000	2.343	100.0
91	S6_1.00_DF_X_ REG	Accl.	4.545	4.901	7.3
92		IS	6.522	6.288	-3.7
93		Mode	6.383	6.177	-3.3
94	S6_1.00_DF_Y_ REG	Accl.	4.762	5.075	6.2
95		IS	6.977	6.653	-4.9
96		Mode	6.667	6.404	-4.1
97	S6_1.00_DF_X_ UNI_IR1	Accl.	11.765	11.229	-4.8
98		IS	11.765	11.229	-4.8
99		Mode	11.765	11.229	-4.8
100	S6_1.00_DF_Y _UNI_IR1	Accl.	11.765	11.636	-1.1
101		IS	11.111	11.124	0.1
102		Mode	11.765	11.636	-1.1
103	S6_1.00_DF_X_ UNI_IR2	Accl.	0.000	0.827	100.0
104		IS	0.000	0.650	100.0
105		Mode	0.000	0.625	100.0
106	S6_1.00_DF_Y_ UNI_IR2	Accl.	0.000	1.039	100.0

107		IS	0.000	1.416	100.0
108		Mode	0.000	1.416	100.0
109	S6_1.00_DF_X_ UNI__IR3	Accl.	2.041	3.048	33.0
110		IS	6.977	6.481	-7.6
111		Mode	4.348	4.370	0.5
112	S6_1.00_DF_Y_ UNI_IR3	Accl.	4.444	4.820	7.8
113		IS	4.255	4.493	5.3
114		Mode	4.444	4.645	4.3
115	S6_1.00_DF_X_ BI_IR1	Accl.	5.263	6.056	13.1
116		IS	5.556	5.995	7.3
117		Mode	5.556	6.291	11.7
118	S6_1.00_DF_Y _BI_IR1	Accl.	0.000	1.817	100.0
119		IS	0.000	1.817	100.0
120		Mode	5.263	5.759	8.6
121	S6_1.00_DF_X_ BI_IR2	Accl.	6.667	7.151	6.8
122		IS	7.143	7.533	5.2
123		Mode	7.143	7.533	5.2
124	S6_1.00_DF_Y_ BI_IR2	Accl.	11.765	11.326	-3.9
125		IS	11.765	11.326	-3.9
126		Mode	12.500	11.767	-6.2
127	S6_1.00_DF_X_ BI__IR3	Accl.	5.556	6.673	16.7
128		IS	11.765	11.610	-1.3
129		Mode	7.143	7.818	8.6

130	S6_1.00_DF_Y_ BI_IR3	Accl.	5.263	6.438	18.2
131		IS	10.000	10.088	0.9
132		Mode	15.790	14.267	-10.7
133	S9_1.00_DF_X_ REG	Accl.	7.692	8.000	3.8
134		IS	6.977	6.939	-0.5
135		Mode	7.317	7.348	0.4
136	S9_1.00_DF_Y_ REG	Accl.	8.108	8.500	4.6
137		IS	7.317	7.348	0.4
138		Mode	7.895	8.043	1.8
139	S9_1.00_DF_X_ UNI_IR1	Accl.	0.000	0.000	100.0
140		IS	0.000	0.000	100.0
141		Mode	0.000	0.000	100.0
142	S9_1.00_DF_Y _UNI_IR1	Accl.	0.000	0.000	100.0
143		IS	0.000	0.000	100.0
144		Mode	0.000	0.000	100.0
145	S9_1.00_DF_X_ UNI_IR2	Accl.	4.878	4.944	1.3
146		IS	6.667	6.568	-1.5
147		Mode	0.000	0.000	100.0
148	S9_1.00_DF_Y_ UNI_IR2	Accl.	5.405	5.245	-3.1
149		IS	6.818	6.774	-0.7
150		Mode	0.000	0.000	100.0
151	S9_1.00_DF_X_	Accl.	4.651	4.734	1.8

152	UNI__IR3	IS	4.348	3.834	-13.4
153		Mode	4.348	4.036	-7.7
154	S9_1.00_DF_Y_ UNI_IR3	Accl.	5.405	5.245	-3.1
155		IS	6.667	6.591	-1.1
156		Mode	7.692	7.826	1.7
157	S9_1.00_DF_X_ BI_IR1	Accl.	11.765	13.189	10.8
158		IS	6.818	6.739	-1.2
159		Mode	10.256	10.863	5.6
160	S9_1.00_DF_Y _BI_IR1	Accl.	9.677	10.373	6.7
161		IS	6.977	6.930	-0.7
162		Mode	6.667	6.758	1.4
163	S9_1.00_DF_X_ BI_IR2	Accl.	5.000	5.091	1.8
164		IS	6.667	6.568	-1.5
165		Mode	13.158	14.338	8.2
166	S9_1.00_DF_Y_ BI_IR2	Accl.	5.263	5.409	2.7
167		IS	6.667	6.593	-1.1
168		Mode	0.000	0.000	100.0
169	S9_1.00_DF_X_ BI__IR3	Accl.	4.878	5.008	2.6
170		IS	6.522	6.457	-1.0
171		Mode	9.756	10.365	5.9
172	S9_1.00_DF_Y_ BI_IR3	Accl.	4.878	5.008	2.6
173		IS	6.122	6.000	-2.0
174		Mode	0.000	0.000	100.0

Table 7.72 Comparison results of three DIs using NLSA

Sr. No.	Model Designation	Load type	Di_E (%) Proposed	Di_D (%) Proposed	Di_k (%) Proposed
1	S4_0.50_UD_X	Accl.	2.870	3.421	49.33
2		IS	0.000	1.291	49.47
3		Mode	4.820	3.804	49.46
4	S4_0.50_UD_Y	Accl.	5.730	4.344	49.44
5		IS	0.000	1.317	49.56
6		Mode	7.800	6.517	49.69
7	S4_0.75_UD_X	Accl.	1.930	2.045	49.31
8		IS	5.160	4.134	49.55
9		Mode	4.000	3.679	49.44
10	S4_0.75_UD_Y	Accl.	4.040	4.649	49.41
11		IS	8.300	7.135	49.69
12		Mode	6.110	5.76	49.58
13	S4_1.00_UD_X	Accl.	1.930	2.928	49.31
14		IS	0.000	1.421	49.46
15		Mode	3.950	3.649	49.44
16	S4_1.00_UD_Y	Accl.	3.440	4.37	49.39
17		IS	0.000	2.49	49.52
18		Mode	4.660	4.749	49.52
19	S6_0.50_UD_X	Accl.	6.780	6.178	49.43
20		IS	0.000	0.642	49.5

21		Mode	9.190	7.801	49.62
22	S6_0.50_UD_Y	Accl.	8.120	7.951	49.62
23		IS	0.000	0.086	49.58
24		Mode	14.980	15.85	50.05
25	S6_0.75_UD_X	Accl.	5.680	5.326	48.76
26		IS	0.000	0.644	49.49
27		Mode	0.000	0.617	49.45
28	S6_0.75_UD_Y	Accl.	8.000	7.566	48.9
29		IS	0.000	0.957	49.56
30		Mode	0.000	1.133	49.57
31	S6_1.00_UD_X	Accl.	5.340	5.064	48.63
32		IS	27.330	20.124	50.12
33		Mode	8.080	6.962	49.07
34	S6_1.00_UD_Y	Accl.	7.060	6.67	48.84
35		IS	27.870	21.212	49.64
36		Mode	12.290	10.694	49.27
37	S9_0.50_UD_X	Accl.	12.050	12.244	48.95
38		IS	35.920	35.43	49.69
39		Mode	14.000	14.574	49.21
40	S9_0.50_UD_Y	Accl.	13.170	7.283	49.21
41		IS	33.600	38.588	49.87
42		Mode	19.300	18.158	49.83
43	S9_0.75_UD_X	Accl.	11.920	11.503	48.99

44		IS	0.000	-1.363	49.04
45		Mode	13.660	13.828	49.31
46	S9_0.75_UD_Y	Accl.	13.330	13.491	49.16
47		IS	0.000	0	49.14
48		Mode	18.100	20.73	49.61
49	S9_1.00_UD_X	Accl.	12.890	8.643	48.96
50		IS	0.000	0	49.02
51		Mode	12.170	11.042	49.23
52	S9_1.00_UD_Y	Accl.	12.340	11.277	49.08
53		IS	0.000	-1.047	49.09
54		Mode	15.450	16.497	49.51

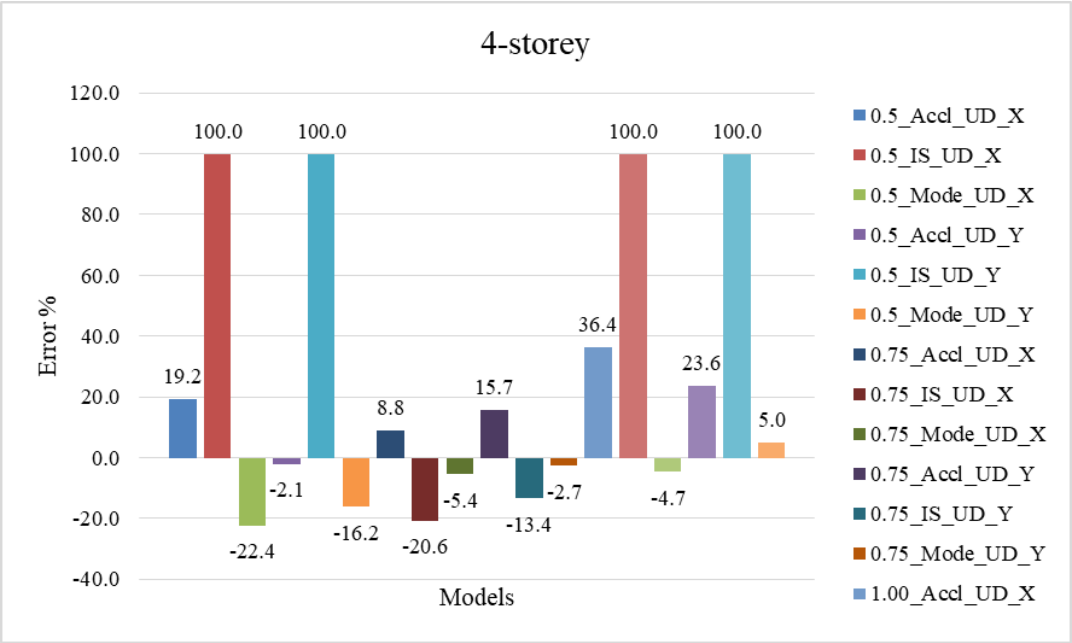

Figure 7.184 Error % of drift based damage index for 4- storey (UD plastic hinge)

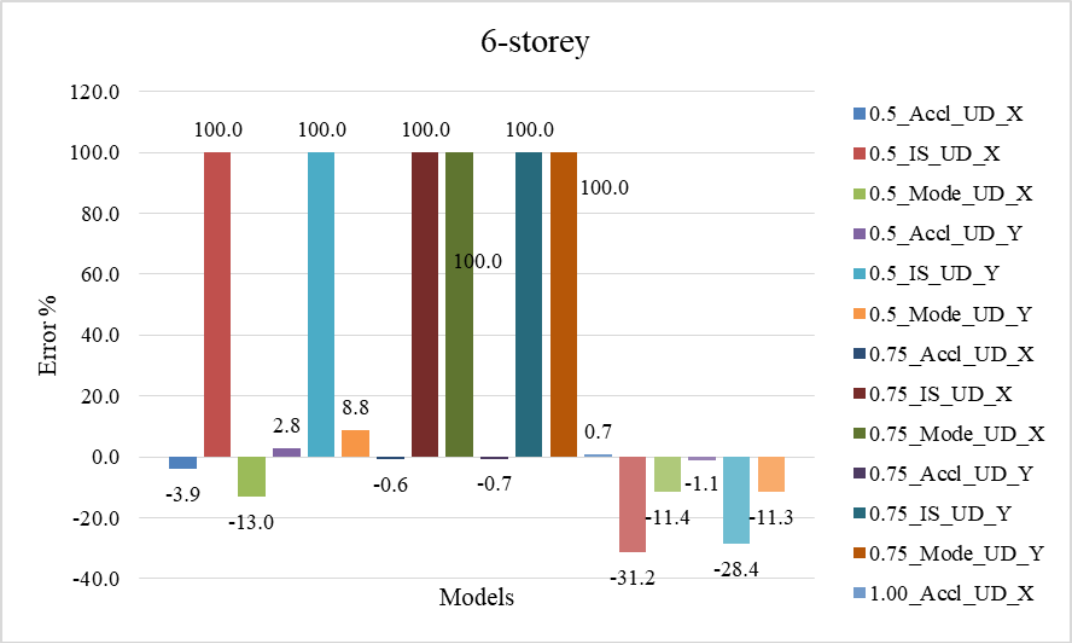

Figure 7.185 Error % of drift based damage index for 6- storey (UD plastic hinge)

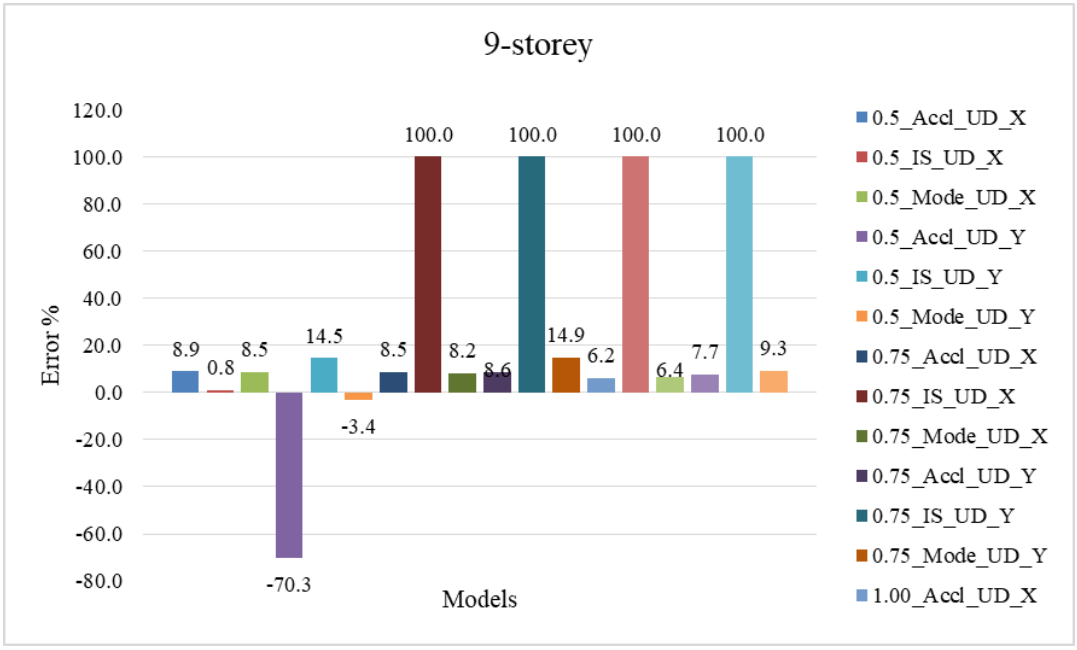

Figure 7.186 Error % of drift based damage index for 9- storey (UD plastic hinge)

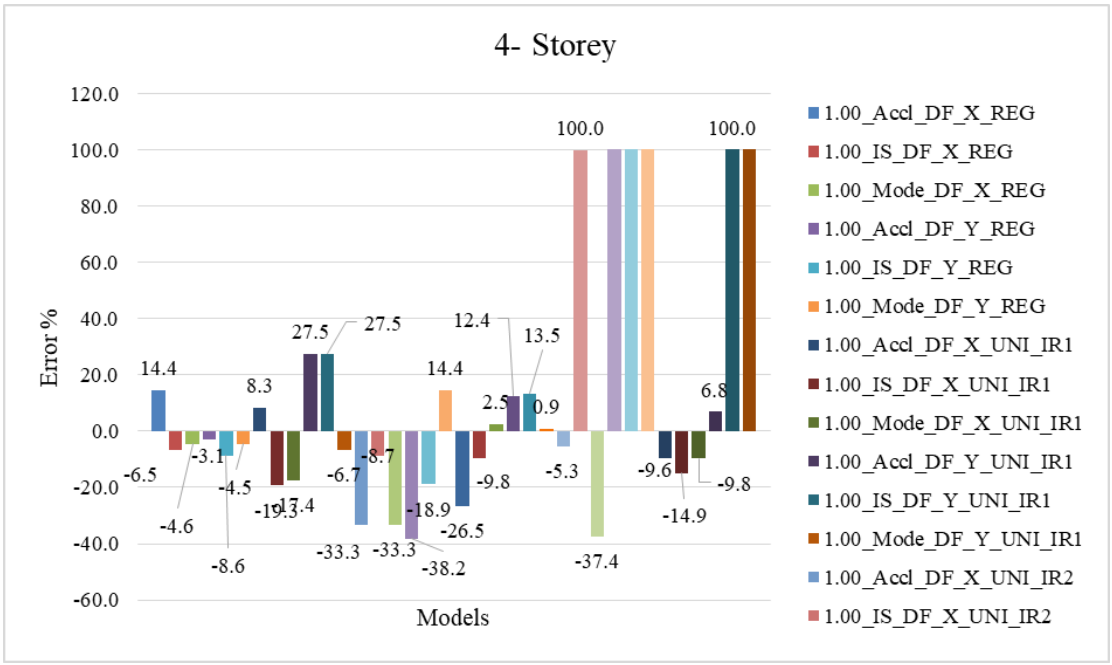

Figure 7.187 Error % of drift based damage index for 4- storey (DF plastic hinge)

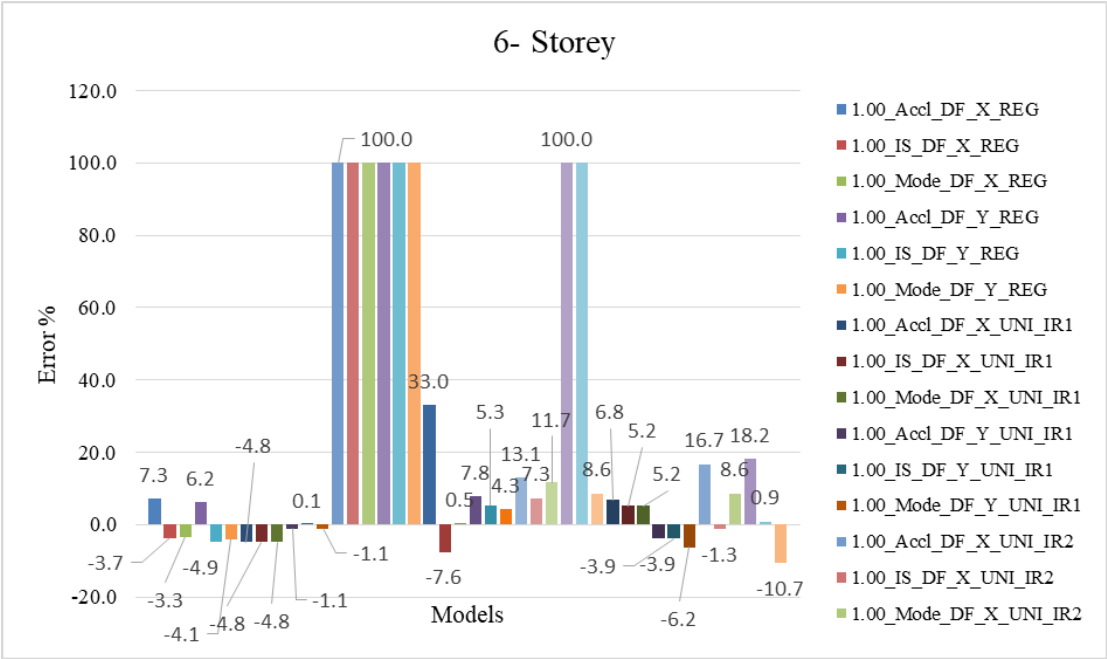

Figure 7.188 Error % of drift based damage index for 6- storey (DF plastic hinge)

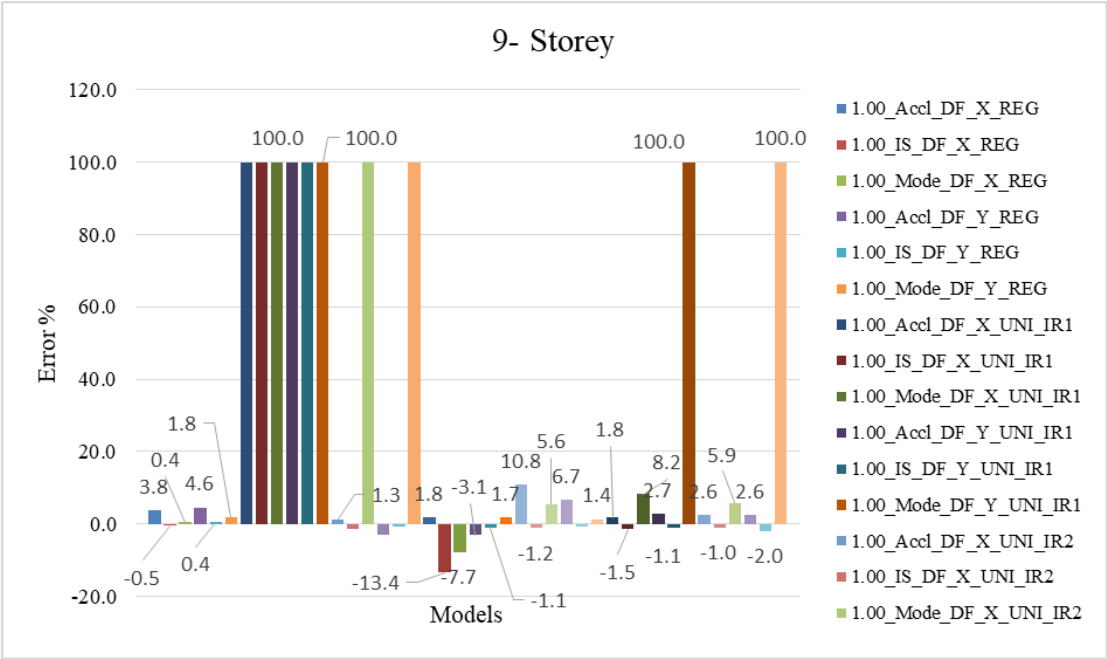

Figure 7.189 Error % of drift based damage index for 9- storey (DF plastic hinge)

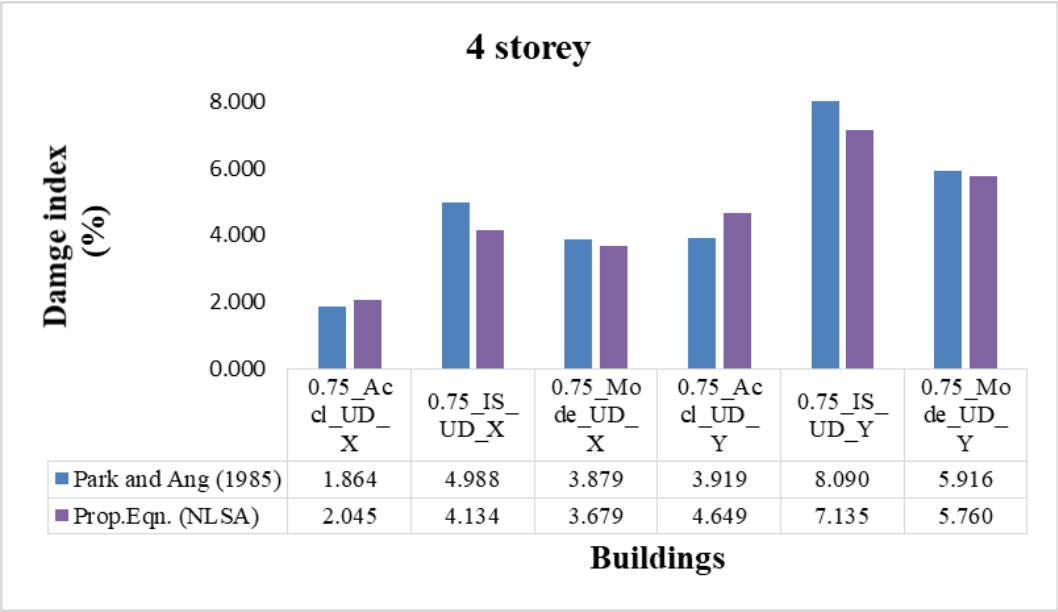

Figure 7.190 Comparison results of drift based DI for 4- storey (UD plastic hinge)

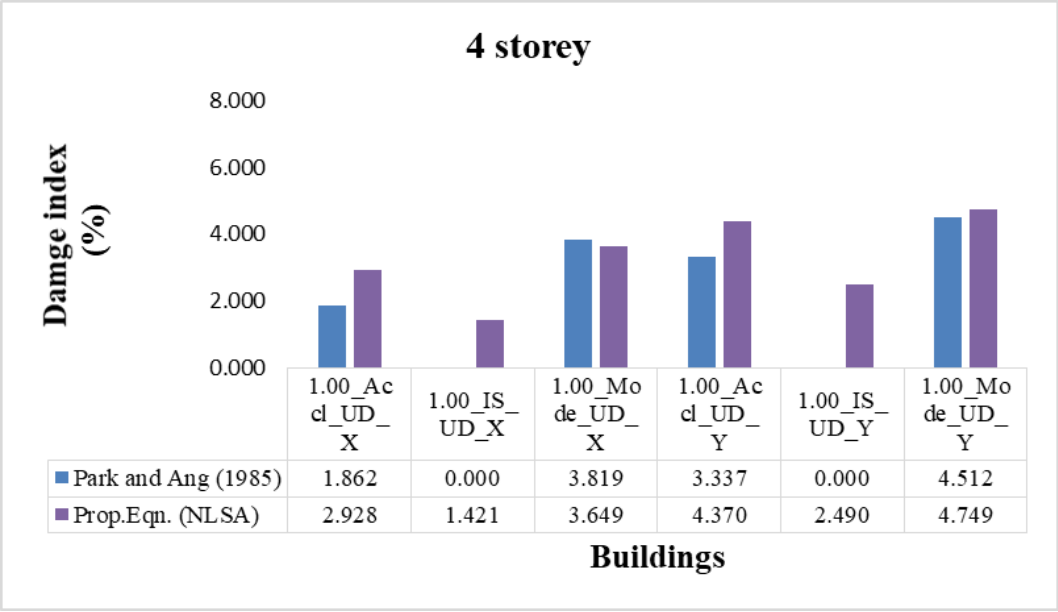

Figure 7.191 Comparison results of drift based DI for 4- storey (UD plastic hinge)

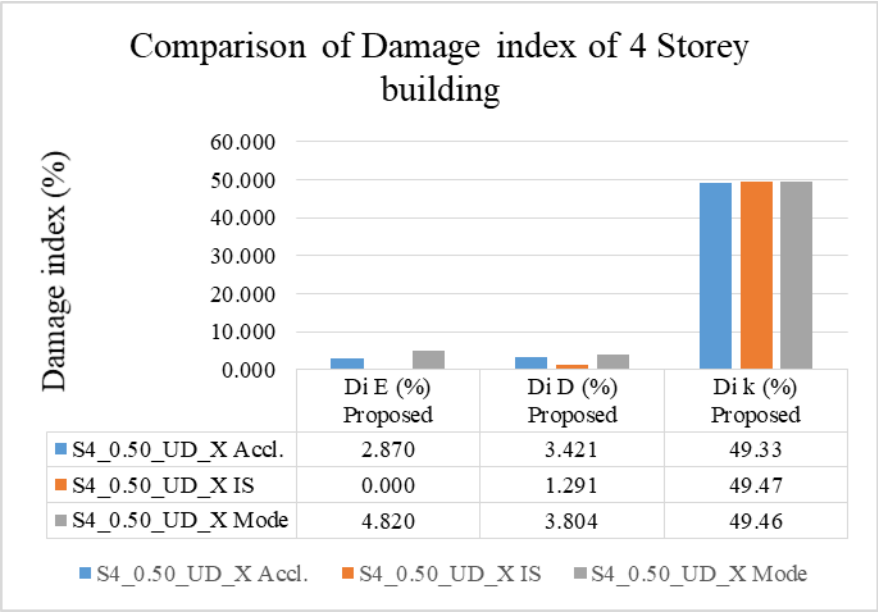

Figure 7.192 Comparison of DIs of 4 storey buildings for 0.5 AR of X direction

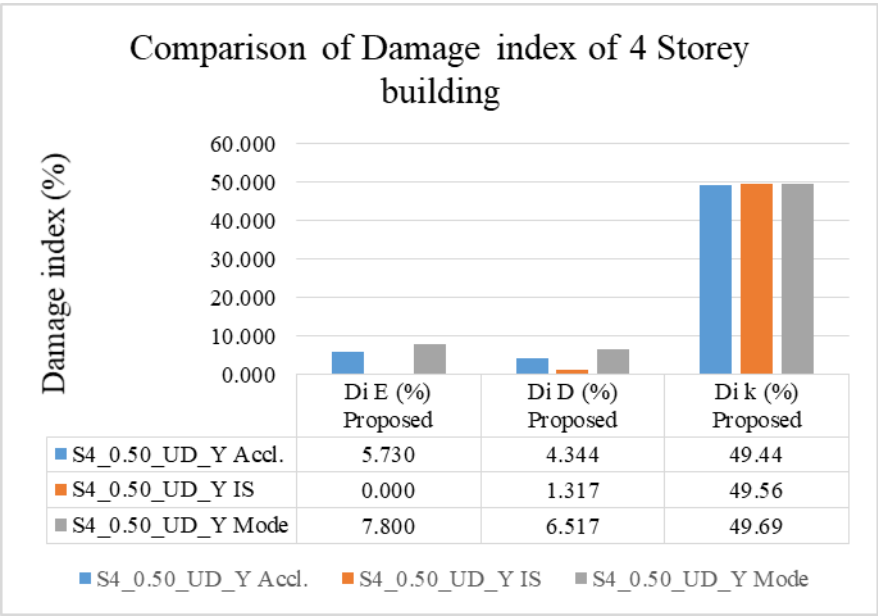

Figure 7.193 Comparison of DIs of 4 storey buildings for 0.5 AR of Y direction

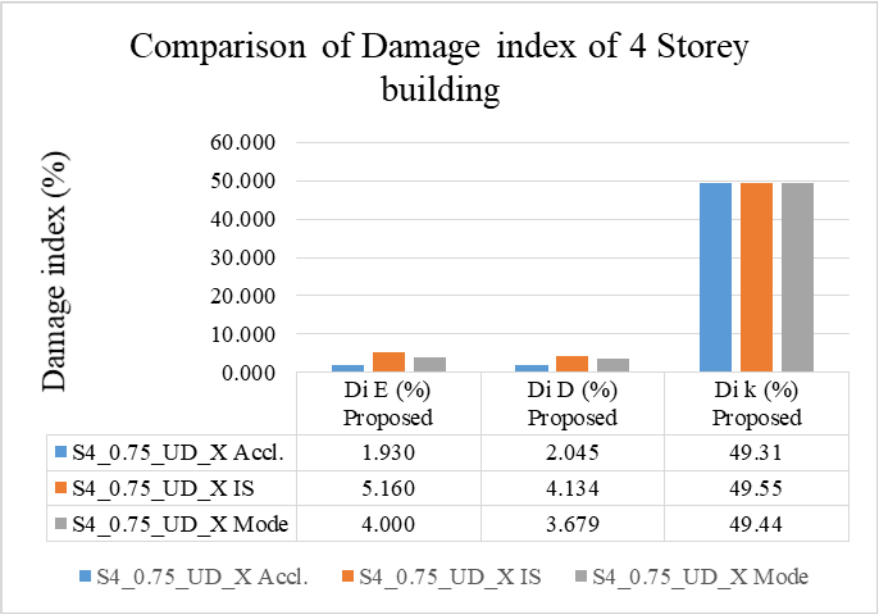

Figure 7.194 Comparison of DIs of 4 storey buildings for 0.75 AR of X direction

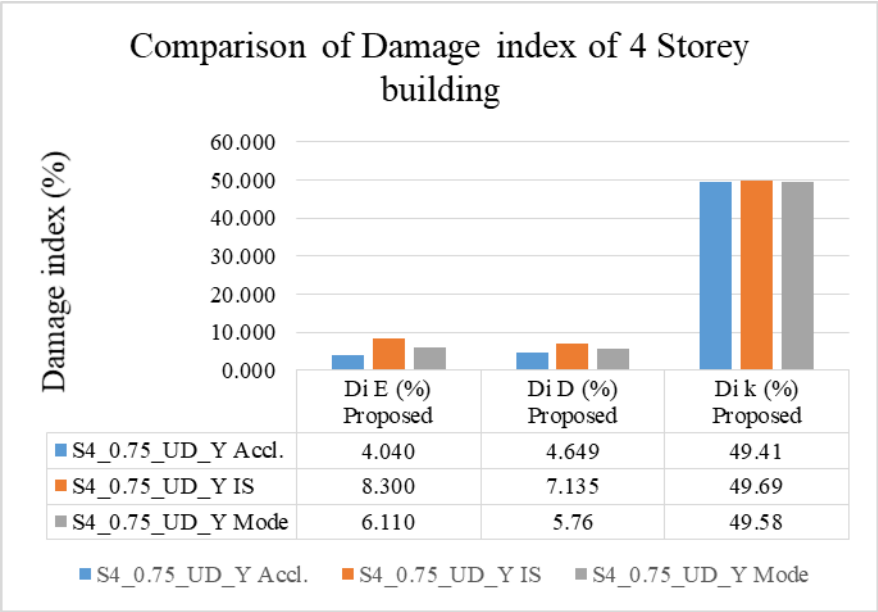

Figure 7.195 Comparison of DIs of 4 storey buildings for 0.75 AR of Y direction

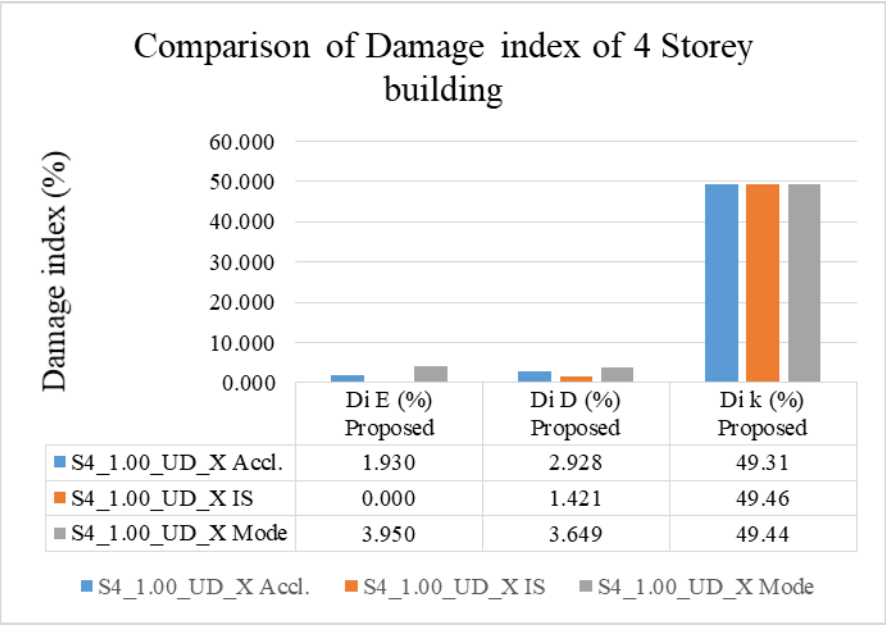

Figure 7.196 Comparison of DIs of 4 storey buildings for 1.00 AR of X direction

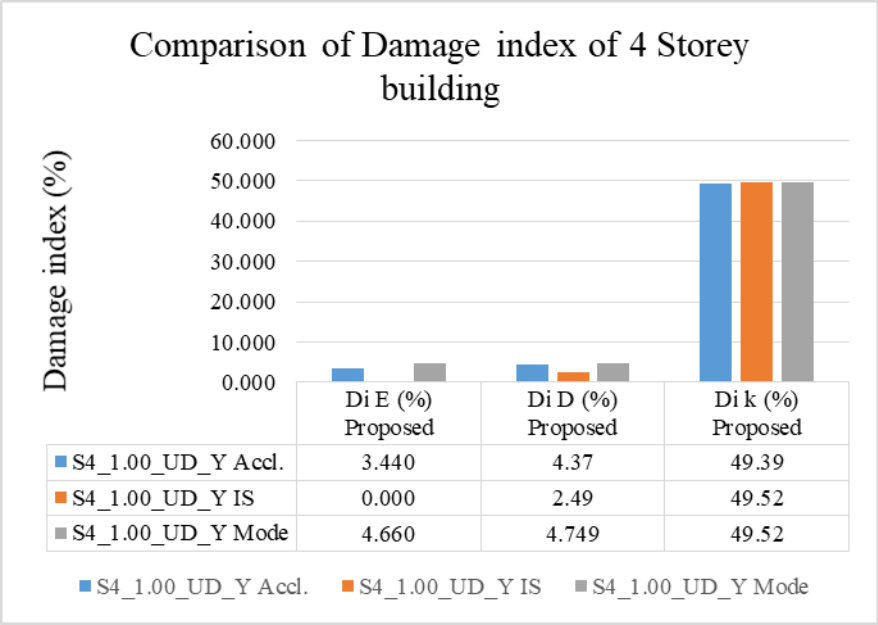

Figure 7.197 Comparison of DIs of 4 storey buildings for 1.00 AR of Y direction

5.4 Results of proposed methods based on drift/displacement using NLDA

Several factors, such as the building's type, dynamic features, plastic displacement, and design variables, influence the level of damage calculated from the nonlinear time history results for a vertically irregular building. It's an enormous task to consider every detail that has to be considered. In this study, a mathematical model is created using nonlinear regression analysis to estimate the level of damage to an irregularly shaped three-dimensional reinforced concrete building. In order to develop a fundamental model that can also be applied, a few of the factors, such as the previously stated irregularity indices, the fundamental period (T), and the overall drift (OD), can be assumed to be independent variables. This will allow the basic model to be designed. Select a subset of earthquake records that is typical of the complete set and that covers a wide range of ground motion features, such as the different ground motion directions, the frequency content, and the intensities.

This subset should also be chosen carefully. As can be seen in Table 6.3, this investigation made use of a total of eight distinct data sets regarding ground motion. When doing research on nonlinear dynamic analysis, a total of 58 unique RC building types are taken into consideration as part of the investigation. Each building's lateral load characteristics are determined by utilising one of the eight time histories that are discussed below. Following the completion of the nonlinear dynamic analysis, a total of 464 results were created as a consequence of this, and the average value of displacement and drift was utilised for the purpose of conducting the regression analysis. Nonlinear dynamic analysis is produced based on the time history illustrated in Figure 6.8 to Figure 6.23. After analysis, the top node displacement value is displayed in Table 7.73. The results of the drift-based damage index at the maximum lateral displacement for all of the buildings are presented in Figure 7.198 to Figure 7.206 indicate the error% that occurs when comparing the drift-based damage index to the power equation of Habibi's (2016) damage index [6]. Figure 7.207 to Figure 7.214 present the comparative results of the drift-based DI for each of the buildings.

Table 7.73 Lateral displacements using results of NLDA

Sr. No.	Model Designation	Lateral displacement (mm)								
		TH1	TH2	TH3	TH4	TH5	TH6	TH7	TH8	Avg.
1	S4_0.50_UD_X	97.57	200.84	35.74	15.84	139.30	55.93	381.40	266.49	149.13
2	S4_0.50_UD_Y	96.03	205.05	35.60	17.96	137.09	63.01	394.00	254.00	150.34
3	S4_0.75_UD_X	97.56	200.45	35.69	15.84	139.47	56.37	381.50	267.29	149.27
4	S4_0.75_UD_Y	95.43	205.15	35.04	17.24	139.44	62.00	390.10	253.70	149.76
5	S4_1.00_UD_X	97.55	200.28	35.66	15.84	139.55	56.57	381.60	267.64	149.33
6	S4_1.00_UD_Y	95.96	204.84	34.30	16.80	139.82	59.77	387.10	255.85	149.30
7	S6_0.50_UD_X	109.48	200.60	36.16	22.68	132.08	77.18	404.10	261.60	155.48
8	S6_0.50_UD_Y	120.40	202.67	45.70	27.50	129.00	91.69	419.50	280.40	164.08
9	S6_0.75_UD_X	109.60	200.64	36.26	22.67	132.11	77.63	404.10	261.82	155.60
10	S6_0.75_UD_Y	119.77	202.67	42.57	26.29	129.70	81.21	417.30	282.13	162.70
11	S6_1.00_UD_X	109.68	200.65	36.33	22.71	132.10	77.90	404.20	262.10	155.70
12	S6_1.00_UD_Y	117.67	201.81	41.07	25.30	130.50	78.81	434.80	281.70	163.95
13	S9_0.50_UD_X	135.00	228.10	46.48	36.18	140.30	83.81	470.80	335.90	184.57

14	S9_0.50_UD_Y	174.40	254.00	69.65	56.20	138.10	116.67	515.30	372.60	212.11
15	S9_0.75_UD_X	137.50	228.80	47.33	36.68	140.60	84.53	472.40	336.30	185.51
16	S9_0.75_UD_Y	165.40	245.10	62.25	48.77	142.20	96.83	498.40	361.60	202.56
17	S9_1.00_UD_X	123.80	230.30	42.92	35.69	136.20	82.06	463.00	334.60	181.07
18	S9_1.00_UD_Y	143.90	236.50	51.90	41.42	144.70	87.31	480.80	343.30	191.22
19	S4_1.00_DF_X _ REG	95.75	198.70	29.41	16.08	135.00	43.65	360.60	257.10	142.03
20	S4_1.00_DF_Y _ REG	95.76	198.90	28.86	16.52	136.30	45.29	364.10	259.70	143.17
21	S4_1.00_DF_X _ UNI_IR1	126.67	235.70	29.30	37.96	133.50	40.37	352.10	253.40	151.12
22	S4_1.00_DF_Y _UNI_IR1	235.70	343.60	197.20	177.90	256.50	193.10	469.10	349.50	277.82
23	S4_1.00_DF_X _ UNI_IR2	94.01	197.77	29.71	11.10	127.80	37.28	349.20	244.20	136.38
24	S4_1.00_DF_Y __UNI_IR2	94.58	198.00	28.68	12.31	127.50	43.64	351.70	243.80	137.52
25	S4_1.00_DF_X _ UNI__IR3	94.13	198.00	28.91	11.21	127.70	36.21	351.10	244.60	136.48
26	S4_1.00_DF_Y _ UNI_IR3	94.68	198.00	29.13	12.51	127.40	44.76	352.30	243.30	137.76
27	S4_1.00_DF_X _ BI_IR2	94.30	198.00	28.80	11.03	127.80	34.91	349.50	243.80	136.01

28	S4_1.00_DF_Y _ BI_IR2	94.29	198.00	29.20	10.90	127.90	36.04	349.90	243.90	136.26
29	S4_1.00_DF_X _ BI__IR3	94.10	197.77	29.31	10.88	127.80	40.95	348.40	242.80	136.50
30	S4_1.00_DF_Y _ BI_IR3	94.05	197.77	29.59	10.95	127.80	40.13	347.10	243.30	136.33
31	S6_1.00_DF_X _ REG	112.80	202.60	43.27	24.90	128.80	77.75	410.00	279.70	159.97
32	S6_1.00_DF_Y _ REG	112.10	200.90	44.69	24.43	131.80	80.60	409.80	277.50	160.22
33	S6_1.00_DF_X _ UNI_IR1	94.52	201.70	31.02	31.45	131.30	45.74	377.70	247.30	145.09
34	S6_1.00_DF_Y _UNI_IR1	224.80	314.60	159.10	143.00	257.90	157.10	484.70	341.40	260.32
35	S6_1.00_DF_X _ UNI_IR2	110.90	202.70	35.85	24.24	132.70	67.14	393.60	264.10	153.90
36	S6_1.00_DF_Y _ UNI_IR2	113.60	200.50	37.25	24.15	130.70	81.17	408.50	269.60	158.18
37	S6_1.00_DF_X _UNI_IR3	110.70	204.70	35.53	24.80	133.60	58.12	391.10	285.80	155.54
38	S6_1.00_DF_Y _ UNI_IR3	110.50	201.40	36.57	24.62	133.30	84.22	405.90	261.80	157.28
39	S6_1.00_DF_X _ BI_IR1	97.67	203.90	36.90	16.29	128.20	60.74	386.20	264.70	149.32
40	S6_1.00_DF_Y _BI_IR1	95.33	202.70	36.33	16.12	128.10	54.94	383.90	269.10	148.31
41	S6_1.00_DF_X _ BI_IR2	199.10	324.10	165.90	170.80	277.60	164.50	461.80	313.10	259.61

42	S6_1.00_DF_Y _ BI_IR2	152.80	243.00	74.10	70.89	176.00	74.82	368.40	286.90	180.86
43	S6_1.00_DF_X _ BI__IR3	100.10	200.60	33.76	17.44	145.30	52.54	373.50	261.60	148.10
44	S6_1.00_DF_Y _ BI_IR3	99.44	200.00	33.97	14.25	142.40	53.55	375.90	263.30	147.85
45	S9_1.00_DF_X _ REG	151.70	233.10	53.93	40.98	139.50	102.20	481.90	355.30	194.82
46	S9_1.00_DF_Y _ REG	157.70	237.60	58.14	44.84	136.90	91.29	491.40	346.67	195.56
47	S9_1.00_DF_X _ UNI_IR1	124.20	230.20	42.92	35.65	136.40	82.10	463.30	336.00	181.34
48	S9_1.00_DF_Y _UNI_IR1	144.10	236.50	51.18	41.43	144.80	87.36	480.50	346.80	191.58
49	S9_1.00_DF_X _ UNI_IR2	115.00	227.80	43.20	36.08	130.70	86.61	451.30	327.60	177.28
50	S9_1.00_DF_Y _ UNI_IR2	125.70	239.60	47.92	38.19	138.90	86.14	475.55	342.90	186.86
51	S9_1.00_DF_X _ UNI_IR3	118.20	221.30	46.42	32.48	134.80	103.80	441.70	318.90	177.2
52	S9_1.00_DF_Y _ UNI_IR3	118.70	238.10	48.09	37.34	134.60	86.67	467.00	338.60	183.63
53	S9_1.00_DF_X _ BI_IR1	115.20	232.60	43.55	37.79	134.30	80.27	459.20	336.10	179.87
54	S9_1.00_DF_Y _BI_IR1	120.50	233.34	44.08	37.83	135.90	81.97	465.40	336.67	181.96
55	S9_1.00_DF_X _ BI_IR2	123.10	229.90	53.76	34.41	133.20	114.20	438.90	322.30	181.22

56	S9_1.00_DF_Y _ BI_IR2	122.50	230.10	50.48	37.23	130.60	108.40	446.30	326.70	181.53
57	S9_1.00_DF_X _ BI__IR3	131.30	224.90	55.18	29.39	134.00	102.50	418.80	307.40	175.43
58	S9_1.00_DF_Y _ BI_IR3	130.60	224.10	53.45	30.38	133.40	96.05	426.30	299.90	174.27

Table 7.74 Drift based damage results using NLDA

Sr. No.	Model Designation	Load type	Measured DI (%) Habibi 2016, power equation-11	Estimated DI (%) Equation-12	Error (%)
1	S4_0.50_UD_X	TH	2.495	2.488	0.006
2	S4_0.50_UD_Y	TH	2.988	2.956	-0.261
3	S4_0.75_UD_X	TH	2.496	2.489	-0.304
4	S4_0.75_UD_Y	TH	2.499	2.472	-0.586
5	S4_1.00_UD_X	TH	2.497	2.490	0.315
6	S4_1.00_UD_Y	TH	2.201	2.174	-0.169
7	S6_0.50_UD_X	TH	2.719	2.705	-0.467
8	S6_0.50_UD_Y	TH	3.504	3.483	-0.529
9	S6_0.75_UD_X	TH	2.721	2.706	0.514
10	S6_0.75_UD_Y	TH	2.914	2.894	0.140
11	S6_1.00_UD_X	TH	2.722	2.707	-0.793
12	S6_1.00_UD_Y	TH	2.585	2.556	-0.833
13	S9_0.50_UD_X	TH	3.254	3.241	-0.837

14	S9_0.50_UD_Y	TH	4.564	4.588	-0.785
15	S9_0.75_UD_X	TH	3.266	3.253	-0.580
16	S9_0.75_UD_Y	TH	3.706	3.706	-0.629
17	S9_1.00_UD_X	TH	3.211	3.196	-0.480
18	S9_1.00_UD_Y	TH	3.142	3.129	-0.630
19	S4_1.00_DF_X_ REG	TH	2.125	2.089	-0.723
20	S4_1.00_DF_Y_ REG	TH	2.137	2.102	-0.746
21	S4_1.00_DF_X_ UNI_IR1	TH	2.518	2.513	-0.654
22	S4_1.00_DF_Y _UNI_IR1	TH	3.393	3.495	-0.358
23	S4_1.00_DF_X_ UNI_IR2	TH	2.333	2.376	-0.793
24	S4_1.00_DF_Y__UNI_IR2	TH	2.078	2.036	-0.825
25	S4_1.00_DF_X_ UNI__IR3	TH	2.313	2.586	-0.757
26	S4_1.00_DF_Y_ UNI_IR3	TH	2.081	2.039	-0.684
27	S4_1.00_DF_X_ BI_IR2	TH	2.328	2.371	-0.638
28	S4_1.00_DF_Y_ BI_IR2	TH	2.331	2.374	0.000
29	S4_1.00_DF_X_ BI__IR3	TH	2.313	2.586	-0.727
30	S4_1.00_DF_Y_ BI_IR3	TH	2.311	2.584	0.104
31	S6_1.00_DF_X_ REG	TH	2.542	2.510	-0.568
32	S6_1.00_DF_Y_ REG	TH	2.544	2.513	-0.590
33	S6_1.00_DF_X_ UNI_IR1	TH	2.591	2.570	-0.782
34	S6_1.00_DF_Y_UNI_IR1	TH	3.569	3.568	-0.691
35	S6_1.00_DF_X_ UNI_IR2	TH	2.700	2.685	0.000
36	S6_1.00_DF_Y_ UNI_IR2	TH	2.522	2.490	0.000

37	S6_1.00_DF_X_UNI_IR3	TH	2.702	2.721	-0.389
38	S6_1.00_DF_Y_ UNI_IR3	TH	2.512	2.479	-0.434
39	S6_1.00_DF_X_ BI_IR1	TH	2.644	2.626	-0.519
40	S6_1.00_DF_Y _BI_IR1	TH	2.631	2.613	0.490
41	S6_1.00_DF_X_ BI_IR2	TH	3.877	3.893	-0.443
42	S6_1.00_DF_Y_ BI_IR2	TH	3.013	3.014	-0.749
43	S6_1.00_DF_X_ BI__IR3	TH	2.612	2.621	-0.679
44	S6_1.00_DF_Y_ BI_IR3	TH	2.608	2.618	-0.747
45	S9_1.00_DF_X_ REG	TH	3.183	3.172	-0.567
46	S9_1.00_DF_Y_ REG	TH	3.192	3.181	-0.591
47	S9_1.00_DF_X_ UNI_IR1	TH	3.215	3.199	0.000
48	S9_1.00_DF_Y_UNI_IR1	TH	3.146	3.133	0.000
49	S9_1.00_DF_X_ UNI_IR2	TH	3.159	3.165	-0.178
50	S9_1.00_DF_Y_ UNI_IR2	TH	3.092	3.075	-0.245
51	S9_1.00_DF_X_ UNI_IR3	TH	3.152	3.169	-0.288
52	S9_1.00_DF_Y_ UNI_IR3	TH	3.055	3.034	-0.539
53	S9_1.00_DF_X_ BI_IR1	TH	3.196	3.180	-0.669
54	S9_1.00_DF_Y _BI_IR1	TH	3.222	3.207	-0.587
55	S9_1.00_DF_X_ BI_IR2	TH	3.208	3.218	-0.611
56	S9_1.00_DF_Y_ BI_IR2	TH	3.212	3.222	-0.190
57	S9_1.00_DF_X_ BI__IR3	TH	3.130	3.145	-0.554
58	S9_1.00_DF_Y_ BI_IR3	TH	3.116	3.128	-0.147

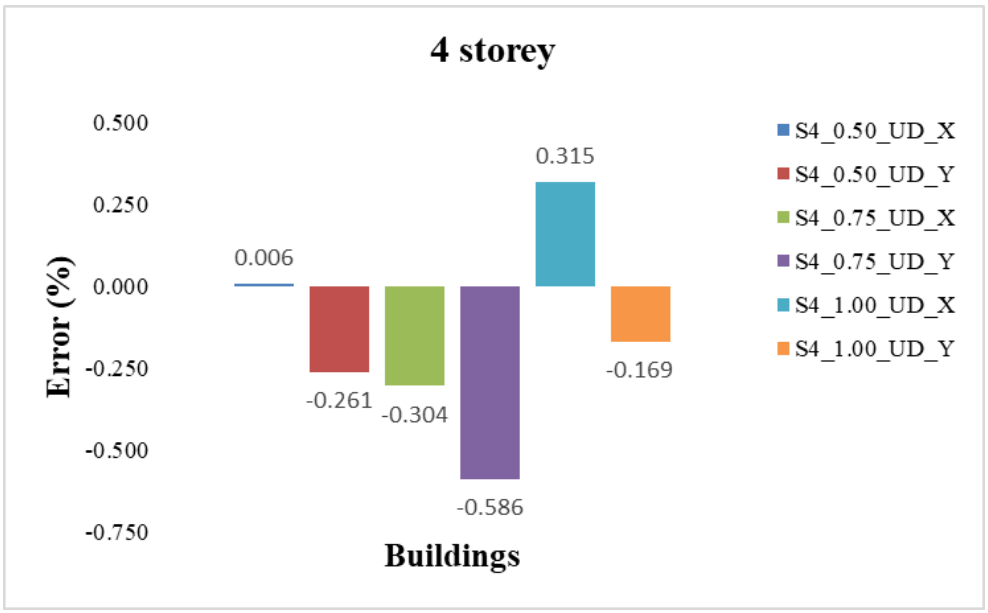

Figure 7.198 Error % of DBDI using NLDA for 4- storey (UD plastic hinge)

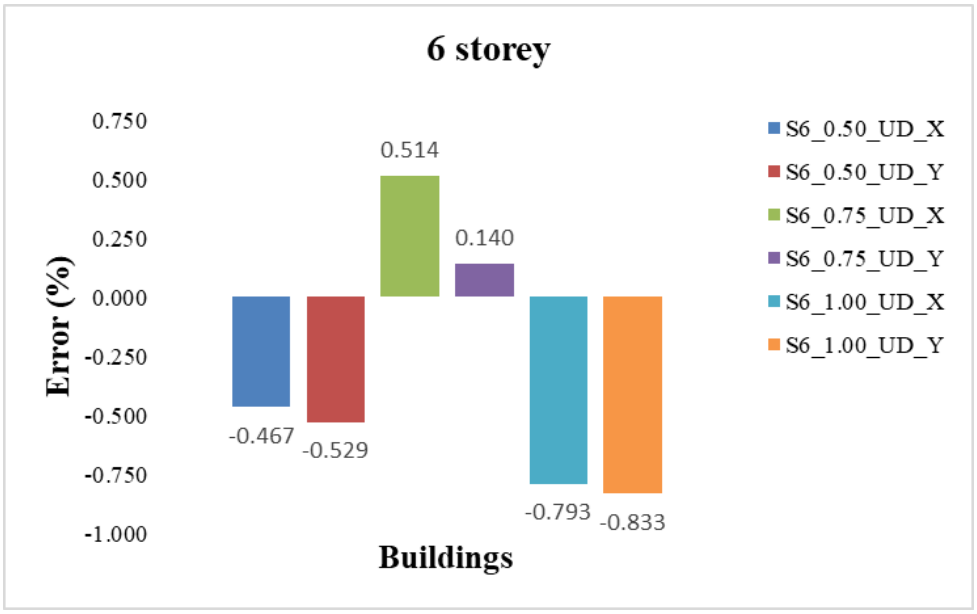

Figure 7.199 Error % of DBDI using NLDA for 6- storey (UD plastic hinge)

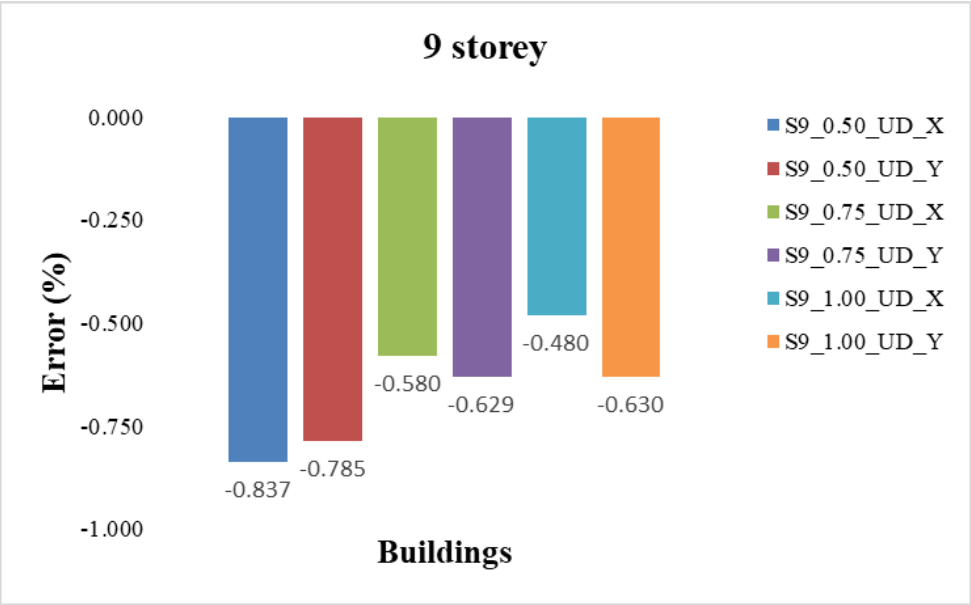

Figure 7.200 Error % of DBDI using NLDA for 9- storey (UD plastic hinge)

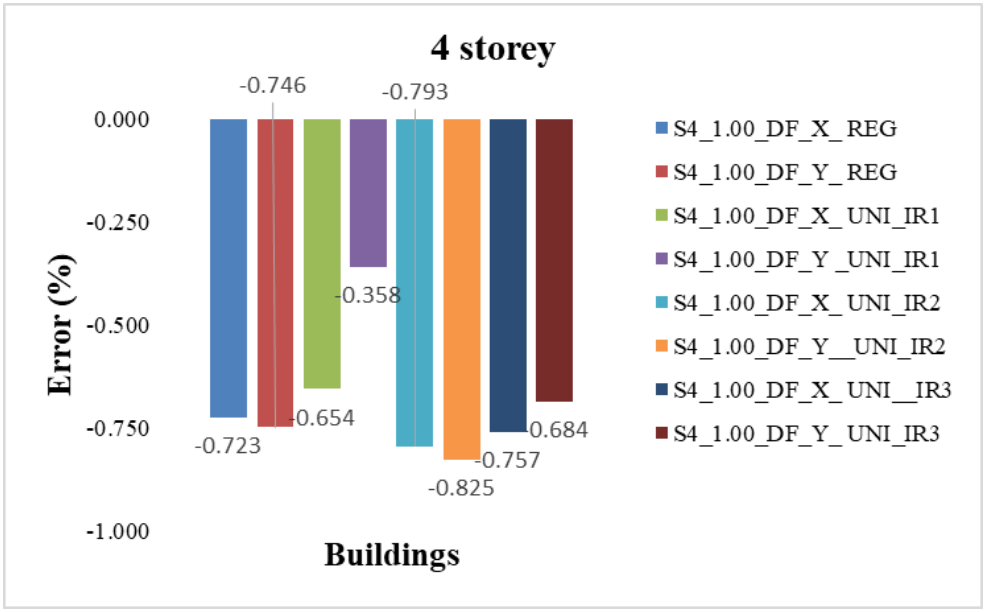

Figure 7.201 Error % of DBDI using NLDA for 4- storey (DF plastic hinge) _1

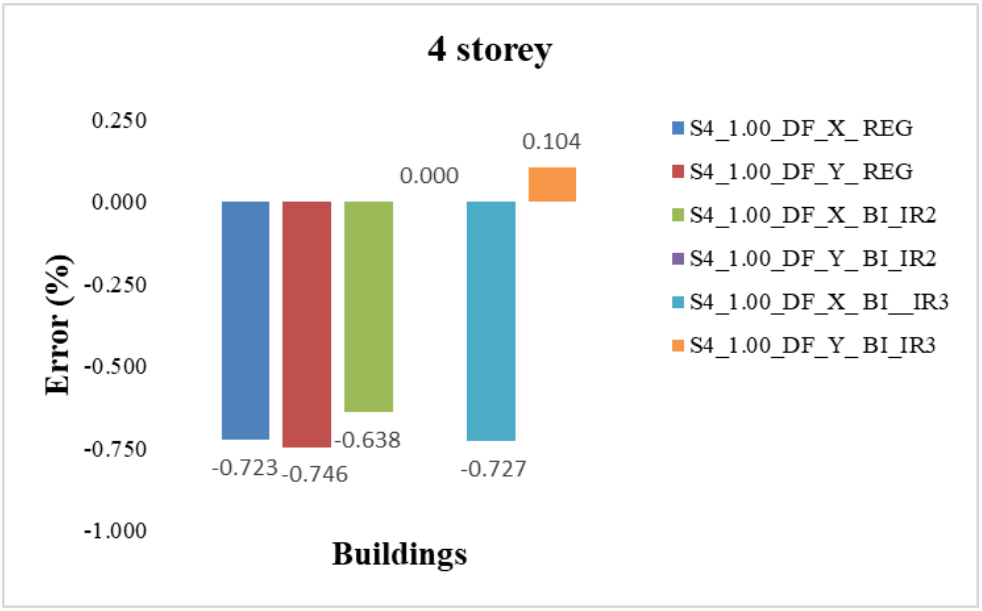

Figure 7.202 Error % of DBDI using NLDA for 4- storey (DF plastic hinge) _2

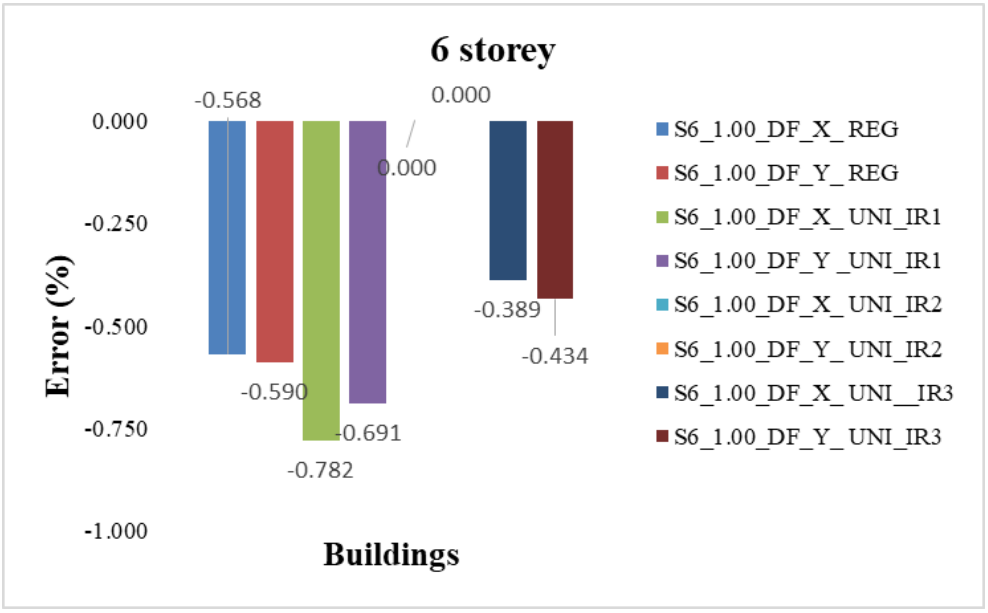

Figure 7.203 Error % of DBDI using NLDA for 6- storey (DF plastic hinge) _1

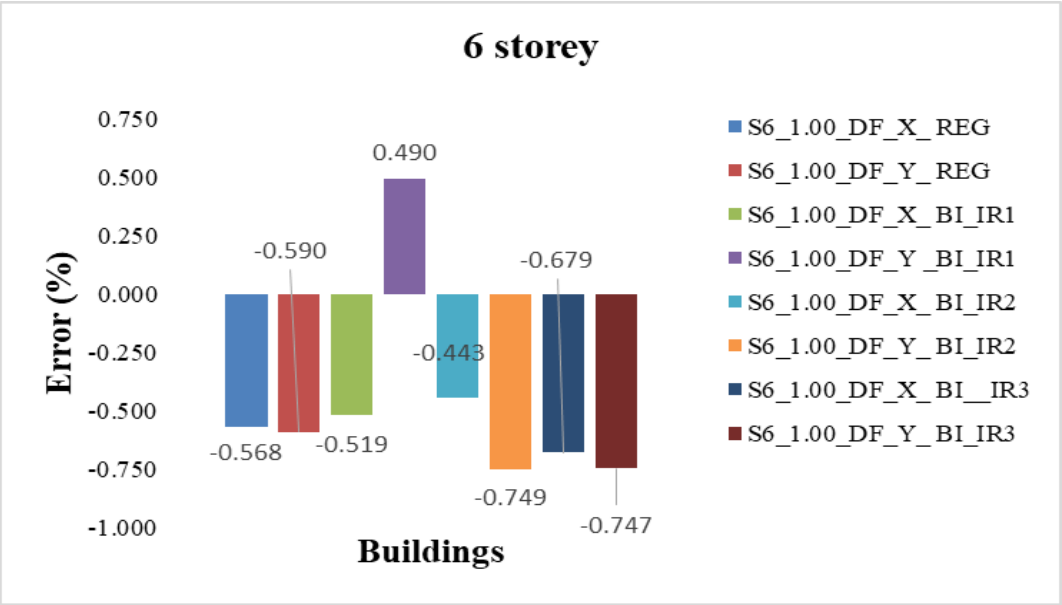

Figure 7.204 Error % of DBDI using NLDA for 6- storey (DF plastic hinge) _2

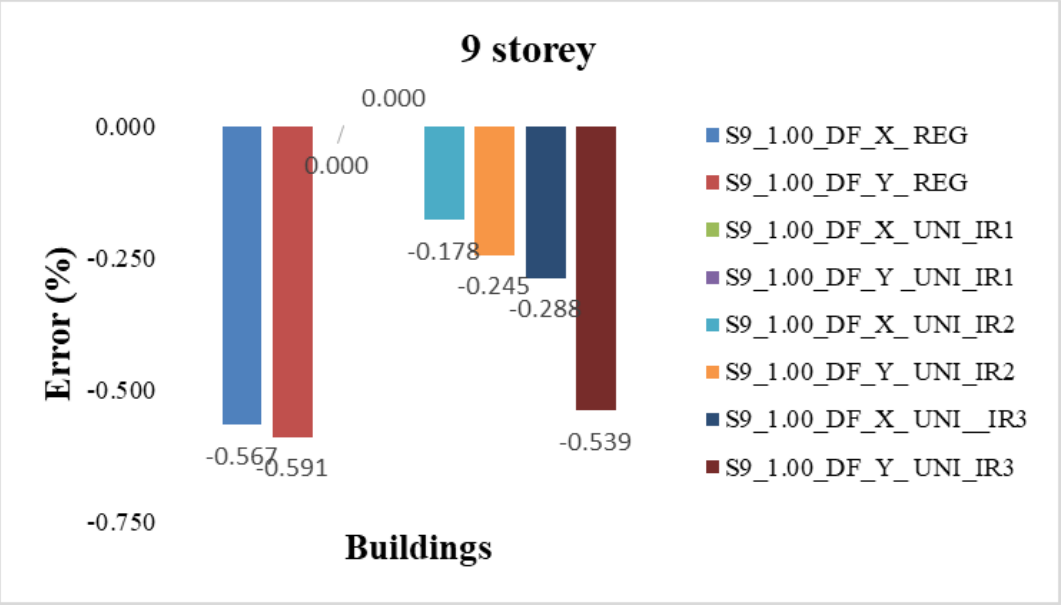

Figure 7.205 Error % of DBDI using NLDA for 9- storey (DF plastic hinge) _1

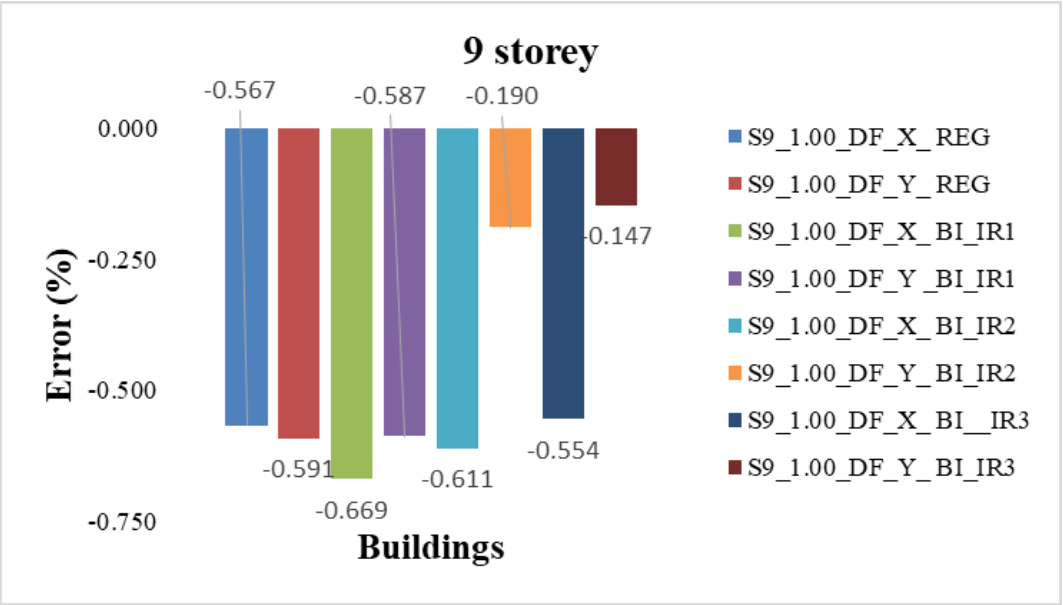

Figure 7.206 Error % of DBDI using NLDA for 9- storey (DF plastic hinge) _2

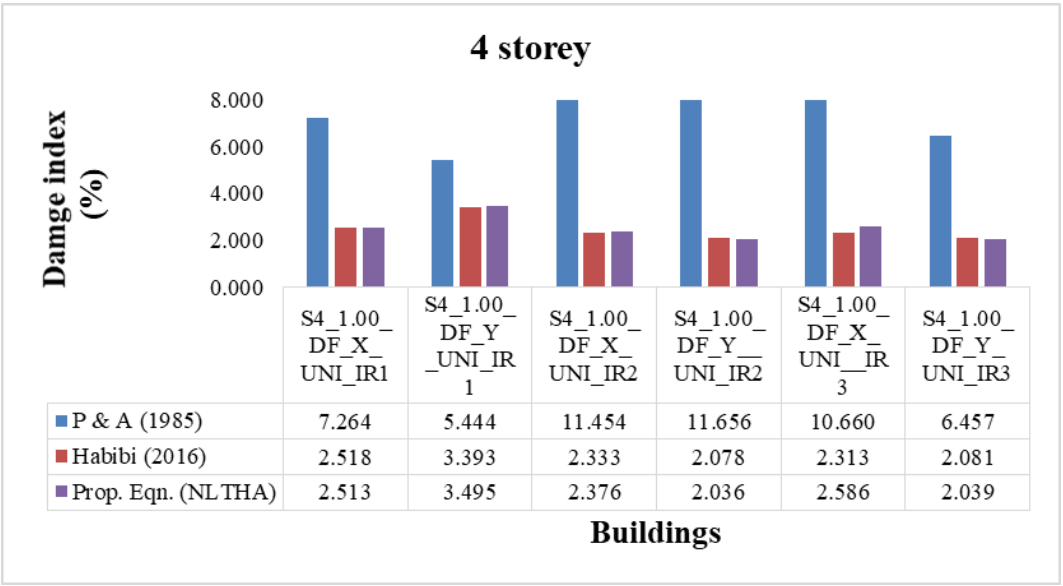

	S4_1.00_ DF_X_ UNI_IR1	S4_1.00_ DF_Y _UNI_IR 1	S4_1.00_ DF_X_ UNI_IR2	S4_1.00_ DF_Y__ UNI_IR2	S4_1.00_ DF_X_ UNI__IR 3	S4_1.00_ DF_Y_ UNI_IR3
P & A (1985)	7.264	5.444	11.454	11.656	10.660	6.457
Habibi (2016)	2.518	3.393	2.333	2.078	2.313	2.081
Prop. Eqn. (NLTHA)	2.513	3.495	2.376	2.036	2.586	2.039

Figure 7.207 Comparison results of DBDI using NLDA for 4- storey (DF plastic hinge) _1

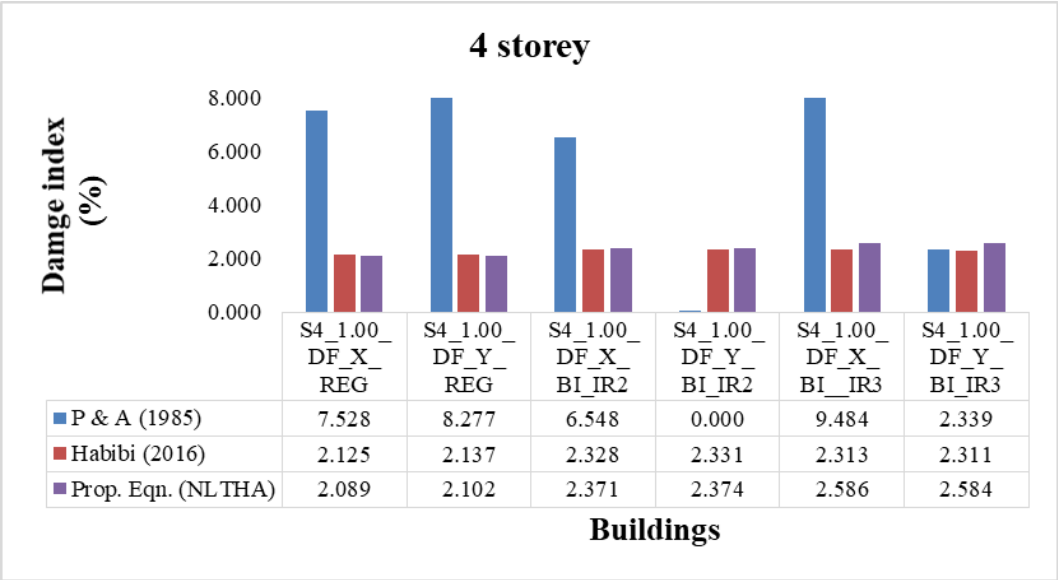

Figure 7.208 Comparison results of DBDI using NLDA for 4- storey (DF plastic hinge) _2

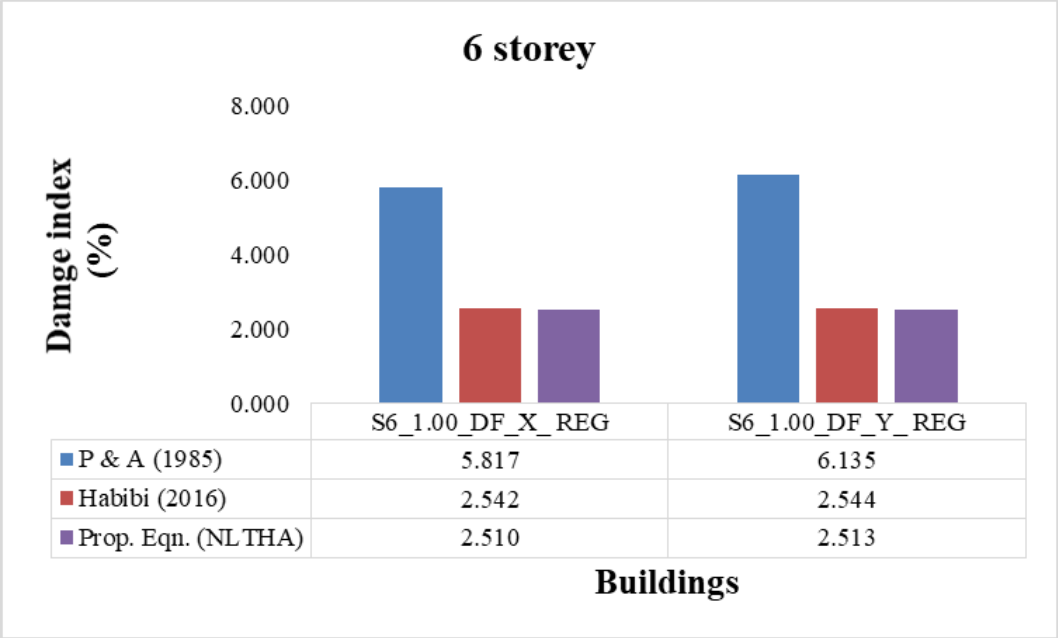

Figure 7.209 Comparison results of DBDI using NLDA for 6- storey (DF plastic hinge) _1

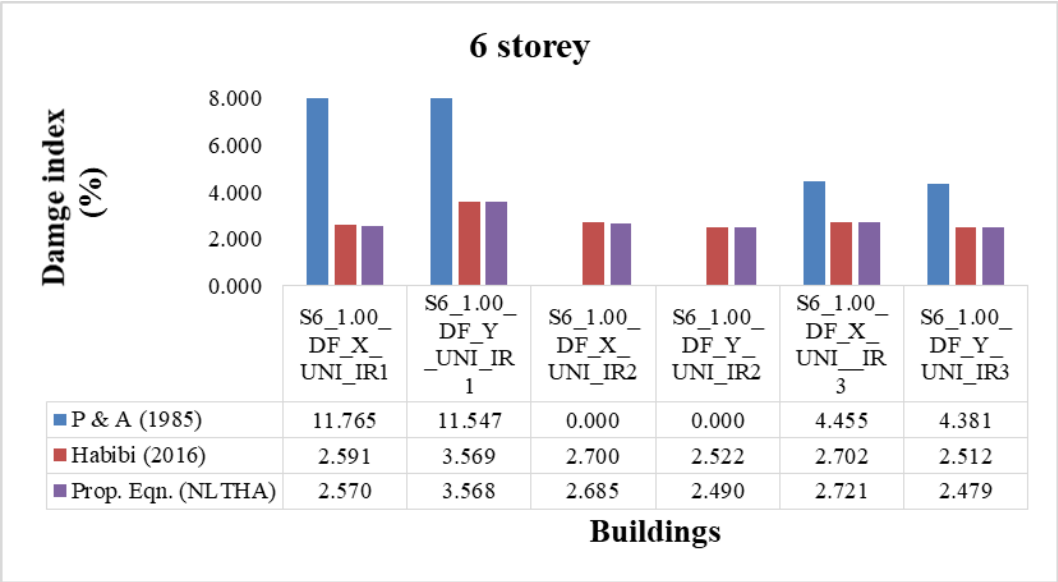

Figure 7.210 Comparison results of DBDI using NLDA for 6- storey (DF plastic hinge) _2

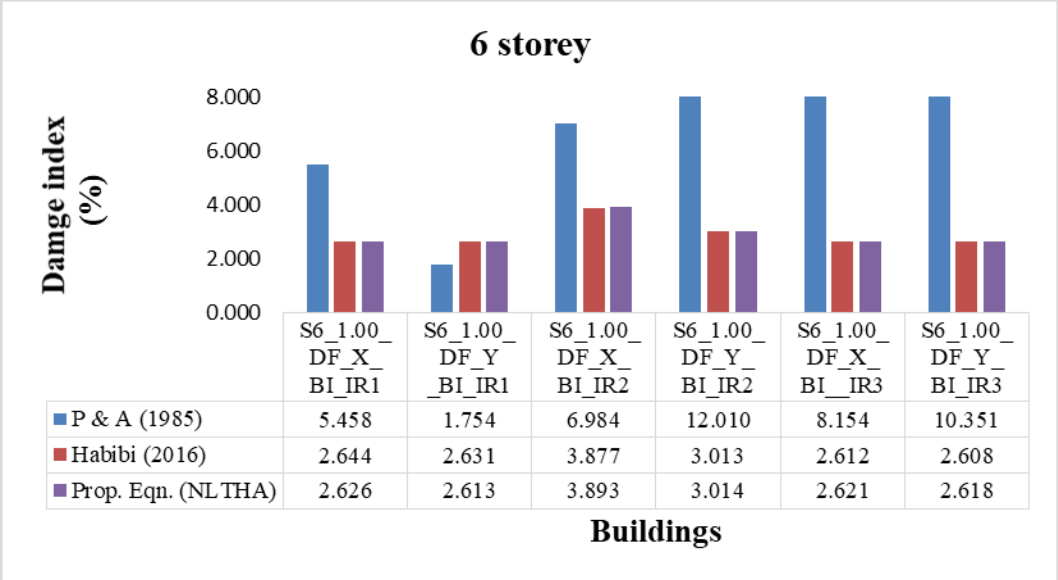

Figure 7.211 Comparison results of DBDI using NLDA for 6- storey (DF plastic hinge) _3

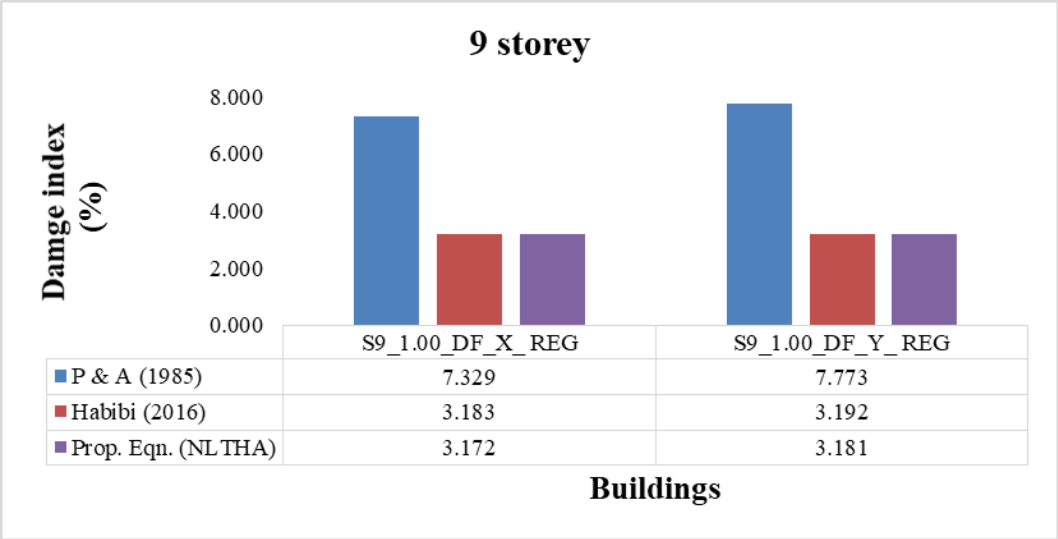

Figure 7.212 Comparison results of DBDI using NLDA for 9- storey (DF plastic hinge) _1

Figure 7.213 Comparison results of DBDI using NLDA for 9- storey (DF plastic hinge) _2

Figure 7.214 Comparison results of DBDI using NLDA for 9- storey (DF plastic hinge) _3

5.5 Validation the results of proposed method based on drift/displacement using NLDA

The proposed DIs have been applied to 5-, 7-, and 8-story regular and vertically irregular RC buildings with unidirectional and bidirectional setbacks, as shown in Figure 7.215 and Figure 7.217. The heights of the foundation and the remaining floors are, respectively, 2 metres and 4 metres. The building's plan geometry, loadings, and material grades are all evaluated in the same manner as they are for buildings with 5, 7, and 8 stories.

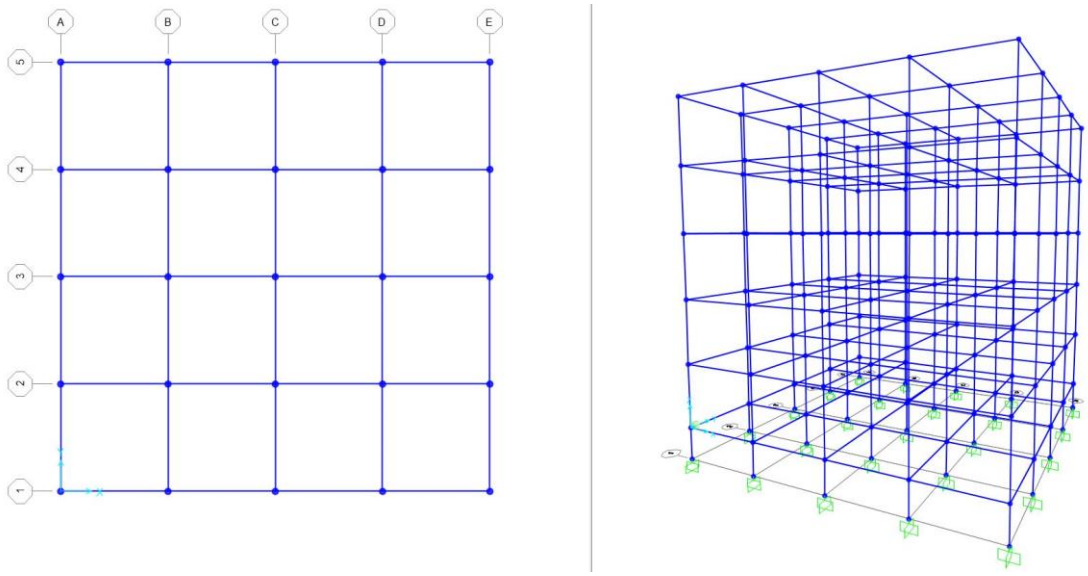

Figure 7.215 5- storey regular building's plan and elevation

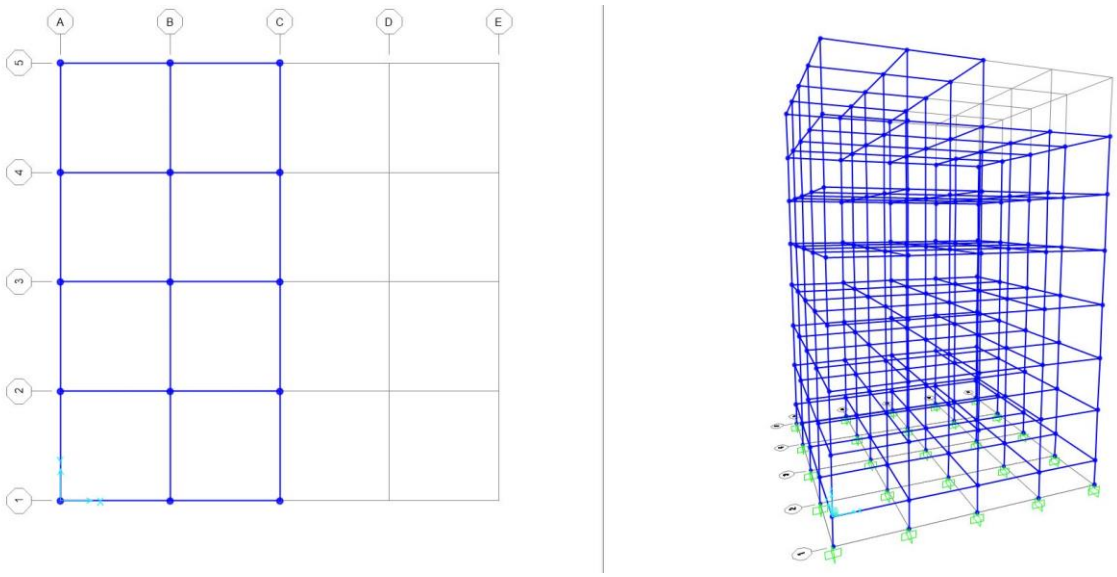

Figure 7.216 7- storey unidirectional setback building's plan and elevation

For the purpose of computing DIs, parametric analyses were carried out, and within these analyses were incorporated three distinct monotonic loadings, two distinct setback directions, and the two distinct storey irregularities. For the purpose of nonlinear dynamic analysis, the 5 storey with regular, 7 storey unidirectional IR1 type, and 9 story buildings bidirectional IR 2 types of building geometry have been taken into consideration. The selection process for the validation set samples has been designed to ensure that they accurately represent the frames being researched.

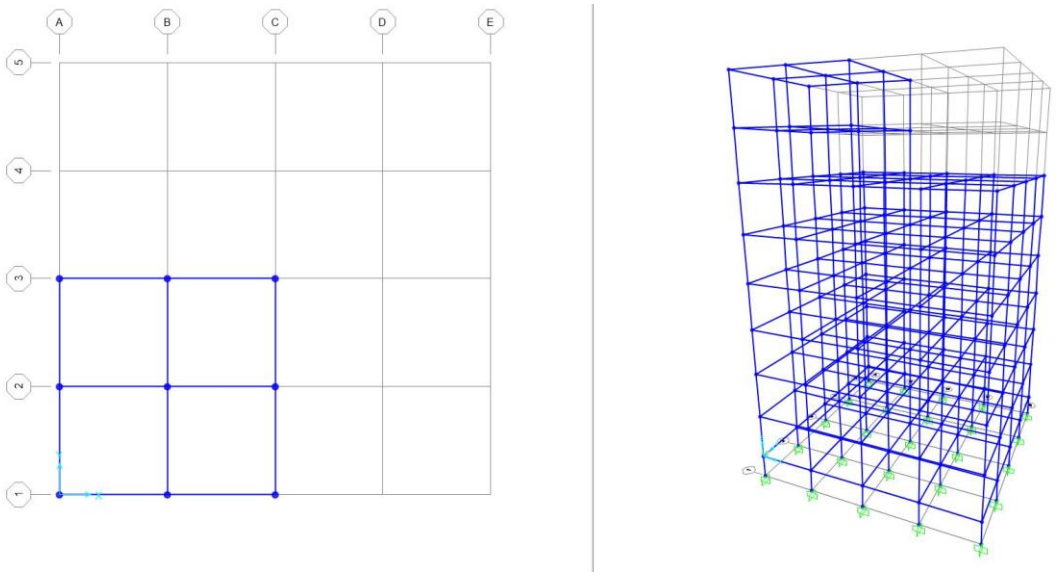

Figure 7.217 8- storey bidirectional setback building's plan and elevation

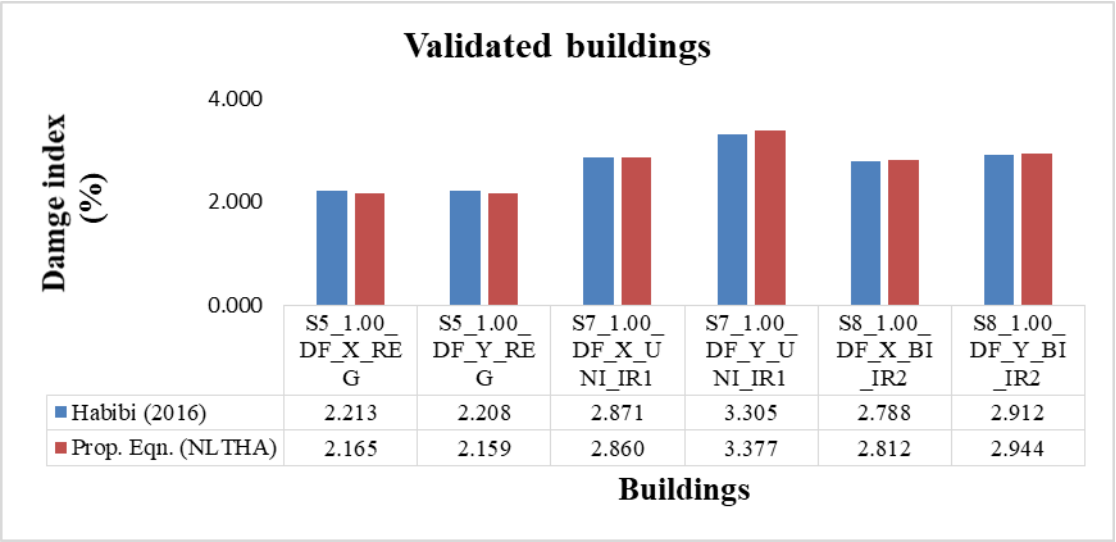

Figure 7.218 Comparison results of DBDI using NLDA

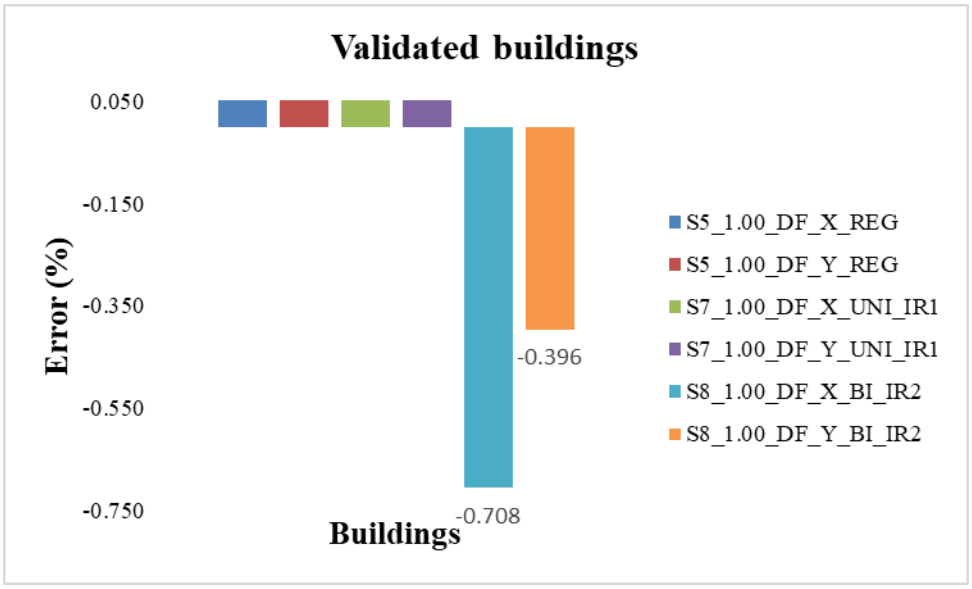

Figure 7.219 Error % of DBDI using NLDA

It was assumed that the concrete possessed a compressive strength of 25 MPa, whereas the steel exhibited yield strength of 410 MPa. Each floor has a height of 4.0 metres, and each bay inside the frames has a length of 5 metres. A comprehensive study using inelastic static and dynamic time history were conducted on all of the sample buildings. The damage formulae were utilised to determine the extent of damage to the frames, and the outcomes were afterwards compared to those obtained from an examination of inelastic damage. Figure 7.218 and Figure 7.219are shown validated buildings (Storey 5, 7 and 8 Buildings) results.

CHAPTER 6 CONCLUSIONS

6.1 Conclusion

The seismic performance of RC buildings with regular and vertical irregular configurations was designed using linear static and dynamic analysis based on the Indian seismic codes. After that, a nonlinear static analysis was performed on them, during which three unique monotonic loadings were applied to them. There have been numerous attempts made to measure seismic damage indices. The vast majority of them, depended on either regular or irregular 2D frames, neither of which responded very well to unexpected seismic forces. The present study, which is based on three-dimensional vertically irregular buildings, indicates that torsion is responsible for the unexpected nonlinear response, and that the building is more susceptible to damage as a result of torsion. The following are some conclusions that can be drawn from this study:

It has been demonstrated that all three DI methods are capable of precisely forecasting the damage that will be caused to 3D irregular buildings, and it has also been demonstrated that the results of estimations of such buildings are acceptable. Damage evaluation at the point of performance required to make use of each of the three types of monotonic load patterns. This is because the load pattern is the most significant variable in absorbed energy and stiffness deterioration. When it comes to calculating damages, damage indices can be computed to any point on the pushover curve. It is possible to make damage estimates for irregular buildings at any point along the curve, which is not only more convenient but also more efficient. These estimates may be created for both existing and proposed buildings. The proposed stiffness damage index is able to determine the extent of the damage while nonetheless maintaining the level of performance that was planned for it. This is accomplished by taking in the cumulative consequences of deteriorating stiffness and any and all nonlinear responses at each stage of the pushover, both of which were neglected by earlier damage estimates. This allows for a better estimation of the amount of damage caused.

The results of the pushover curve indicate that the drift is almost never more than an exceedingly slight deviance from the standards that are already in place. The force-based design technique that is offered by the Indian seismic code appears to be effective when it is used for standard frame structures. However, when it is applied to irregular frames that have setbacks along their height, it is not able to meet the regulations for the

life safety performance level. Particularly susceptible were short buildings that had either unidirectional or bidirectional setbacks; as a result, more attention was required to ensure the users' safety in such buildings. In addition, a nonlinear static and dynamic time-history analysis was performed on all of the 3D RC buildings derived from the variety of parametric studies in order to establish a reliable database for the development of the suggested method. In order to determine the damage index, a number of parameters were included in nonlinear assessments of many buildings. The range of the energy-based damage index for life safety performance level is around 20% to 65%. In terms of stiffness, the damage index can be anywhere from 45% to 65%, while in terms of drift/displacement, it can be anywhere from 1% to 2%.

In order to determine the associations that exist between total drift, fundamental period, and irregularity indices, a multivariate nonlinear regression analysis was carried out. This research produced two useful equations: based on two nonlinear analyses methods and derived the quadratic polynomial equation. It was demonstrated that each of the proposed functions are capable of making accurate estimations of damage at various critical locations of the RC buildings. All the damage index methods had been evaluated with existing damage indices and found to have high degrees of accuracy after being validated by those studies. The majority of the irregularly configured buildings that were built were not able to withstand earthquakes and eventually fell. It would appear that the criteria found in regulations 1893-2016 need to be added in order to facilitate a more accurate damage estimation using different demand parameters of the seismic behaviour shown by buildings that feature vertical irregularities.

The main limitation of the three methods which have been proposed by the nonlinear static analysis are assumption of static monotonic loading, simplification of dynamic effects of an earthquake loads which are dynamic in nature, little bit not trustworthy while considering the tall buildings and p delta effects. However Pushover analysis is still a useful method for quickly determining out the extent to which a building is going to buckle up in a seismic event as well as whether vulnerable it is to lateral loads. Researchers should be competent with regard to how they use it and combine it with additional resources and techniques for a full earthquake evaluation.

6.2 Original contribution by the thesis

The use of a performance-based seismic design philosophy was employed in the process of generating damage estimates for the vertically irregular RC buildings. For the purpose of damage assessment, empirical formulas that take into account variables such as energy, stiffness, and drift have been developed. These formulas are developed through the application of the results of nonlinear analysis. Before putting the final decisions on the design of a structure, practitioners can use this damage index to make an assessment of the potential damage on a scale ranging from 0 to 1, and based on the values practitioners can be modify the structural to get an appropriate degree of damage. It is also possible to decide on a target performance level for the RC structures.

6.3 Future recommendations

The following specific recommendations are offered for additional research in this field:

1) The method that has been proposed can be used for belongings other than building structures and can compute the damage index at foundation levels. Additionally, further studies can be expanded in order to make use of soil structure interactions.
2) The results of a nonlinear static analysis are more dependent on the monotonic loads that are applied to the structures; the scope of this research can be widened to include the application of a variety of different forms of lateral loads that can be used in a way that is both more practical and accurate.
3) The use of scaled ground motions can be employed for the purpose of performing experiments, and the outcomes of these experiments can be validated by the application of a drift-based damage index.
4) The case studies can be performed using nonlinear static analysis on different types of horizontal and torsional irregular buildings. The findings should be compared with nonlinear dynamic assessments for numerous intensities in order to evaluate the effectiveness of the approach for varying degrees of structural inelasticity using various engineering demand parameters such as ductility, strength, hysteric energy, stiffness, drift etc.

References

[1] M. Zameeruddin and K. K. Sangle, “Review on Recent developments in the performance-based seismic design of reinforced concrete structures,” *Structures*, vol. 6, pp. 119–133, 2016, doi: 10.1016/j.istruc.2016.03.001.

[2] A. Sil, G. Das, and P. Hait, “Characteristics of FBD and DDBD techniques for SMRF buildings designed for seismic zone-V in India,” *J. Build. Pathol. Rehabil.*, vol. 4, no. 1, 2019, doi: 10.1007/s41024-018-0040-6.

[3] M. Zameeruddin and K. K. Sangle, “Damage assessment of reinforced concrete moment resisting frames using performance-based seismic evaluation procedure,” *J. King Saud Univ. - Eng. Sci.*, vol. 33, no. 4, pp. 227–239, 2021, doi: 10.1016/j.jksues.2020.04.010.

[4] A. Vimala, R. P. Kumar, and C. V. R. Murty, “Expended energy based damage assessment of RC bare frame using nonlinear pushover analysis,” *Indian Concr. J.*, vol. 91, no. 10, pp. 47–56, 2017.

[5] K. Rama Raju, A. Cinitha, P. Kamatchi, and N. R. Iyer, “Estimation of enhanced design base shear for strengthening the existing RC buildings designed as per IS codes prior to is: 1893 -2002 by seismic coefficient method,” *J. Inst. Eng. Civ. Eng. Div.*, vol. 90, no. AUGUST, pp. 9–13, 2009.

[6] A. Habibi and K. Asadi, “Development of Drift-Based Damage Index for Reinforced Concrete Moment Resisting Frames with Setback,” *Int. J. Civ. Eng.*, vol. 15, no. 4, pp. 487–498, 2017, doi: 10.1007/s40999-016-0085-3.

[7] G. J. O’Reilly and G. M. Calvi, “Conceptual seismic design in performance-based earthquake engineering,” *Earthq. Eng. Struct. Dyn.*, vol. 48, no. 4, pp. 389–411, 2019, doi: 10.1002/eqe.3141.

[8] A. Cinitha, P. K. Umesha, N. R Iyer, and N. Lakshmanan, “Performance-based Seismic Evaluation of RC Framed Building,” *J. Inst. Eng. Ser. A*, vol. 96, no. 4, pp. 285–294, 2015, doi: 10.1007/s40030-015-0129-8.

[9] A. D’Ambrisi and M. Mezzi, “An energy-based approach for nonlinear static analysis of structures,” *Bull. Earthq. Eng.*, vol. 13, no. 5, pp. 1513–1530, 2015, doi: 10.1007/s10518-014-9673-2.

[10] P. R. Kovela, “Nonlinear Pushover Analysis for Performance Based Engineering Design – A Review,” *Int. J. Res. Appl. Sci. Eng. Technol.*, vol. V, no. III, pp. 1293–1300, 2017, doi: 10.22214/ijraset.2017.3239.

[11] D. Khan and A. Rawat, “Nonlinear Seismic Analysis of Masonry Infill RC Buildings with Eccentric Bracings at Soft Storey Level,” *Procedia Eng.*, vol. 161, pp. 9–17, 2016, doi: 10.1016/j.proeng.2016.08.490.

[12] S. K. Prajapati and J. A. Amin, “Seismic assessment of RC frame building designed using gross and cracked section as per Indian standards,” *Asian J. Civ. Eng.*, vol. 20, no. 6, pp. 821–836, 2019, doi: 10.1007/s42107-019-00147-9.

[13] Bureau of Indian Standards, “IS 1893:Part-I-2016 Criteria for Earthquake resistant design of structures,Part 1:General Provisions and buildings,” *Bur. Indian Stand. New Delhi*, vol. 1893, no. December, pp. 1–44, 2016.

[14] M. Zameeruddin and K. K. Sangle, “Study of NSPs and NTH Analyses of RCMRFs,” *Int. J. Mod. Trends Eng. Res.*, vol. 40, no. 2349, pp. 443–449, 2016.

[15] O. Merter, T. Ucar, and M. Duzgun, “Determination of earthquake safety of RC frame structures using an energy-based approach,” *Comput. Concr.*, vol. 19, no. 6, pp. 689–699, 2017, doi: 10.12989/cac.2017.19.6.689.

[16] O. Merter and T. Ucar, “Energy-based design base shear for rc frames considering global failure mechanism and reduced hysteretic behavior,” *Struct. Eng. Mech.*, vol. 63, no. 1, pp. 23–35, 2017, doi: 10.12989/sem.2017.63.1.023.

[17] Y. Wang, Z. Liu, W. Yang, Y. Hu, and Y. Chen, “Damage index of reinforced concrete members based on the energy dissipation capability degradation,” *Struct. Des. Tall Spec. Build.*, vol. 29, no. 2, pp. 1–20, 2020, doi: 10.1002/tal.1695.

[18] L. Halder and S. Paul, “Seismic Damage Evaluation of Gravity Load Designed Low Rise RC Building Using Non-linear Static Method,” *Procedia Eng.*, vol. 144, pp. 1373–1380, 2016, doi: 10.1016/j.proeng.2016.05.167.

[19] H. He, M. Cong, and Y. Lv, “Earthquake damage assessment for RC structures based on fuzzy sets,” *Math. Probl. Eng.*, vol. 2013, 2013, doi: 10.1155/2013/254865.

[20] M. V Mohod, “Pushover Analysis of Structures with Plan Irregularity,” *IOSR J.*

Mech. Civ. Eng. e-ISSN, vol. 12, no. 4, pp. 46–55, 2015, doi: 10.9790/1684-12474655.

[21] P. Hait, A. Sil, and S. Choudhury, “Damage Assessment of Reinforced Concrete-Framed Building Considering Multiple Demand Parameters in Indian Codal Provisions,” *Iran. J. Sci. Technol. - Trans. Civ. Eng.*, vol. 44, no. 0123456789, pp. 121–139, 2020, doi: 10.1007/s40996-020-00380-2.

[22] A. Ghobarah, H. Abou-Elfath, and A. Biddah, “Response-based damage assessment of structures,” *Earthq. Eng. Struct. Dyn.*, vol. 28, no. 1, pp. 79–104, 1999, doi: 10.1002/(SICI)1096-9845(199901)28:1<79::AID-EQE805>3.0.CO;2-J.

[23] K. Arjomandi, H. Estekanchi, and A. Vafai, “Correlation between structural performance levels and damage indexes in steel frames subjected to earthquakes,” *Sci. Iran.*, vol. 16, no. 2 A, pp. 147–155, 2009.

[24] E. Erduran and A. Yakut, “Drift based damage functions for reinforced concrete columns,” *Comput. Struct.*, vol. 82, no. 2–3, pp. 121–130, 2004, doi: 10.1016/j.compstruc.2003.10.003.

[25] S. A. Diaz, L. G. Pujades, A. H. Barbat, Y. F. Vargas, and D. A. Hidalgo-Leiva, “Energy damage index based on capacity and response spectra,” *Eng. Struct.*, vol. 152, pp. 424–436, 2017, doi: 10.1016/j.engstruct.2017.09.019.

[26] P. Hait, A. Sil, and S. Choudhury, “Damage assessment of reinforced concrete buildings considering irregularities,” *Int. J. Eng. Trans. A Basics*, vol. 32, no. 10, pp. 1388–1394, 2019, doi: 10.5829/ije.2019.32.10a.08.

[27] R. C M, B. Narayan K S, S. B V, and V. Reddy D, “Effect of Irregular Configurations on Seismic Vulnerability of RC Buildings,” *Archit. Res.*, vol. 2, no. 3, pp. 20–26, 2012, doi: 10.5923/j.arch.20120203.01.

[28] G. Özmen, K. Girgin, and Y. Durgun, “Torsional irregularity in multi-story structures,” *Int. J. Adv. Struct. Eng.*, vol. 6, no. 4, pp. 121–131, 2014, doi: 10.1007/s40091-014-0070-5.

[29] S. B. Naik, “International Journal of Modern Trends in Engineering and Research Seismic Performance Evaluation of Reinforced Concrete Frames with Irregular Elevations using Nonlinear Static Pushover Analysis,” no. 2349, pp. 2–4, 2015.

[30] M. Cosic and S. Brcic, “The development of controlled damage mechanisms-based design method for nonlinear static pushover analysis,” *Facta Univ. - Ser. Archit. Civ. Eng.*, vol. 12, no. 1, pp. 25–40, 2014, doi: 10.2298/fuace1401025c.

[31] D. P. Soni and B. B. Mistry, “Qualitative review of seismic response of vertically irregular building frames,” *ISET J. Earthq. Technol.*, vol. 43, no. 4, pp. 121–132, 2006.

[32] T. I. Maulana, B. Enkhtengis, and T. Saito, “Proposal of damage index ratio for low- to mid-rise reinforced concrete moment-resisting frame with setback subjected to uniaxial seismic loading,” *Appl. Sci.*, vol. 11, no. 15, 2021, doi: 10.3390/app11156754.

[33] Y. Park and A. H. -S. Ang, “Mechanistic Seismic Damage Model for Reinforced Concrete,” *J. Struct. Eng.*, vol. 111, no. 4, pp. 722–739, 1985, doi: 10.1061/(asce)0733-9445(1985)111:4(722).

[34] P. Hait, A. Sil, and S. Choudhury, “Seismic damage assessment and prediction using artificial neural network of RC building considering irregularities,” *J. Struct. Integr. Maint.*, vol. 5, no. 1, pp. 51–69, 2020, doi: 10.1080/24705314.2019.1692167.

[35] A. Behtani *et al.*, “Residual Force Method for damage identification in a laminated composite plate with different boundary conditions,” *Frat. ed Integrita Strutt.*, vol. 15, no. 59, pp. 35–48, 2021, doi: 10.3221/IGF-ESIS.59.03.

[36] S. Tiachacht, S. Khatir, C. Le Thanh, R. V. Rao, S. Mirjalili, and M. Abdel Wahab, “Inverse problem for dynamic structural health monitoring based on slime mould algorithm,” *Eng. Comput.*, vol. 38, no. 0123456789, pp. 2205–2228, 2022, doi: 10.1007/s00366-021-01378-8.

[37] S. Khatir, S. Tiachacht, B. Benaissa, C. Le Thanh, R. Capozucca, and M. Abdel Wahab, “Damage Identification in Frame Structure Based on Inverse Analysis,” *Lect. Notes Civ. Eng.*, vol. 204, no. January, pp. 197–211, 2022, doi: 10.1007/978-981-16-7216-3_15.

[38] A. R. Habibi, M. Izadpanah, and A. Yazdani, “Inelastic damage analysis of RCMRFs using pushover method,” *Iran. J. Sci. Technol. - Trans. Civ. Eng.*, vol. 37, no. C2, pp. 345–352, 2013.

[39] J. Bai and J. Ou, “Earthquake-resistant design of buckling-restrained braced RC moment frames using performance-based plastic design method,” *Eng. Struct.*, vol. 107, pp. 66–79, 2016, doi: 10.1016/j.engstruct.2015.10.048.

[40] M. Reza Banihashemi, A. R. Mirzagoltabar, and H. R. Tavakoli, “Development of the performance based plastic design for steel moment resistant frame,” *Int. J. Steel Struct.*, vol. 15, no. 1, pp. 51–62, 2015, doi: 10.1007/s13296-015-3004-6.

[41] A. Vimala and R. P. Kumar, “Displacement Based Damage Estimation of RC Bare Frame Subjected to Earthquake Loads : A Case Study on 4 Storey Building,” *Proc 15h World Conf. Earthq. Eng.*, 2012.

[42] S. Gumpertz, S. Francisco, and S. Engineering, “C a m f,” *J. Struct. Eng.*, vol. 127, no. September, pp. 1045–1053, 2001.

[43] P. Haldar and Y. Singh, “Seismic performance and vulnerability of Indian code designed RC frame buildings,” *ISET J. Earthq. Technol.*, vol. 46, no. 1, pp. 29–45, 2009, [Online]. Available: http://home.iitk.ac.in/~vinaykg/Iset502.pdf.

[44] A. J. Kappos and S. Stefanidou, “A deformation-based seismic design method for 3D R/C irregular buildings using inelastic dynamic analysis,” *Bull. Earthq. Eng.*, vol. 8, no. 4, pp. 875–895, 2010, doi: 10.1007/s10518-009-9170-1.

[45] T. Ucar and O. Merter, “Derivation of energy-based base shear force coefficient considering hysteretic behavior and P-delta effects,” *Earthq. Eng. Eng. Vib.*, vol. 17, no. 1, pp. 149–163, 2018, doi: 10.1007/s11803-018-0431-3.

[46] M. Jinjie, S. Qingxuan, and Z. Qi, “Method of Performance Based Seismic Evaluation for,” *14 World Conf. Earthq. Eng.*, no. 2001, 2008.

[47] IS 1893 (Part 1):2002, “7.11 Deformations,” *Earthq. Resist. Des. Struct.*, vol. 1893, no. June, p. 27, 2002, [Online]. Available: http://rahat.up.nic.in/sdmplan/Earthquake/AnnexureI-V/AnnexureI_Bldg. Earthquake.pdf.

[48] M. Bhavan, B. Shah, and Z. Marg, “Ductile Detailing of Reinforced Concrete Structures Subjected To Seismic Forces-Code of Practice B U R E a U O F I N D I a N S T a N D a R D S,” *Is*, vol. 13920, no. 2, pp. 2002–2005, 1993.

[49] P. Giannakouras and C. Zeris, “Seismic performance of irregular RC frames

designed according to the DDBD approach," *Eng. Struct.*, vol. 182, no. January 2018, pp. 427–445, 2019, doi: 10.1016/j.engstruct.2018.12.058.

[50] A. J. Kappos, "Seismic damage indices for RC buildings: evaluation of concepts and procedures," *Prog. Struct. Eng. Mater.*, vol. 1, no. 1, pp. 78–87, 1997, doi: 10.1002/pse.2260010113.

[51] G. H. Powell and R. Allahabadi, "Seismic damage prediction by deterministic methods: Concepts and procedures," *Earthq. Eng. Struct. Dyn.*, vol. 16, no. 5, pp. 719–734, 1988, doi: 10.1002/eqe.4290160507.

[52] P. Rajeev and K. K. Wijesundara, "Energy-based damage index for concentrically braced steel structure using continuous wavelet transform," *J. Constr. Steel Res.*, vol. 103, pp. 241–250, 2014, doi: 10.1016/j.jcsr.2014.09.011.

[53] R. L. N. Ditao, "A modified seismic damage model with double variables for reinforced concrete structures," *Earthq. Eng. Eng. Vib.*, vol. 16, no. 4, pp. 44–54, 1996.

[54] B. M. S. L. Roufaiel and C. Meyer, "in recorded history occurred in the Mississippi valley near New Madrid , Missouri in the winter of 1811-12 . This immense event consisted of ba- sically three shocks with approximately four-week intervals , of which the third shock probably was the larges," vol. 113, no. 3, pp. 445–457, 1987.

[55] B. E. Dipasquale, J. Ju, A. Askar, and A. S. Qakmak, "s = isr- Z PA," vol. 116, no. 5, pp. 1440–1456, 1990.

[56] M. Z. M. Saleemuddin and K. K. Sangle, "Seismic damage assessment of reinforced concrete structure using non-linear static analyses," *KSCE J. Civ. Eng.*, vol. 21, no. 4, pp. 1319–1330, 2017, doi: 10.1007/s12205-016-0541-2.

[57] T. L. Karavasilis, N. Bazeos, and D. E. Beskos, "Seismic response of plane steel MRF with setbacks: Estimation of inelastic deformation demands," *J. Constr. Steel Res.*, vol. 64, no. 6, pp. 644–654, 2008, doi: 10.1016/j.jcsr.2007.12.002.

[58] Bureau of Indian Standards, "Plain and Reinforced Concrete - Codeofpractice," *Concrete*, vol. 2000, no. July 2000, 2005.

List of Publications

Journal Papers

1. Paper published on, Damage estimation of low to medium rise reinforced concrete buildings considering vertical irregularity, *Journal of Materials and Engineering Structures*, volume 10, No. 1, 2023, 51-68, ISSN: 2170-127X. (Web of Science)
2. Paper published on, Development of Absorbed Energy and Stiffness-Based Damage Index for Vertical Irregular Buildings, *International Journal of Engineering Trends and Technology*, volume 70, Issue 8, 375-386, August 2022, ISSN: 2231 –5381. https://doi.org/10.14445/22315381/IJETT-V70I8P238 (Scopus)
3. Paper accepted on, Seismic Damage Estimation of Unidirectional Setback Type of 3D Irregular Buildings, *Journal of The Maharaja Sayajirao University of Baroda*, ISSN: 0025-0422. (UGC approved)

Conference Papers

4. Paper presented on "Seismic damage assessment of RC vertical irregular buildings using push over analysis", *International Multidisciplinary Engineering Conference (IMEC'22)*, organized by Sankalchand Patel College of Engineering, Visanagar, 04-06 August 2022, International Conference, ISBN: 978-93-5680-184-4.